AD 667846

SHOCK-RESISTANT WELLS

R. W. Anderson
K. Hove

AGBABIAN – JACOBSEN ASSOCIATES
Los Angeles, California

Contracts

NBy-62212
N 62399-67-0017

REPORT NO. CR 68.007

August 1967

U.S. NAVAL CIVIL ENGINEERING LABORATORY
Port Hueneme, California

DISTRIBUTION OF THIS DOCUMENT IS UNLIMITED

SHOCK-RESISTANT WELLS

R. W. Anderson
K. Hove

AGBABIAN – JACOBSEN ASSOCIATES
Los Angeles, California

Contracts

NBy-62212
N 62399-67-0017

REPORT NO. CR 68.007

August 1967

U. S. NAVAL CIVIL ENGINEERING LABORATORY
Port Hueneme, California

AGBABIAN-JACOBSEN ASSOCIATES

FOREWORD

This report was prepared by Agbabian-Jacobsen Associates, Los Angeles, California, under Contracts NBy-62212 and N62399-67-C-0017. The principal contributors to the study were R. W. Anderson, R. J. Brandt, R. D. Ewing, C. Fechtman, and K. Hove. R. W. Anderson and K. Hove prepared the written text.

Inclusive dates of research were June 1966 through August 1967.

The Program Monitor for this study was Mr. John A. Norbutas of the U. S. Naval Civil Engineering Laboratory.

ABSTRACT

A study is presented of water wells for shelter facilities, which will functionally survive the critical effects associated with the detonation of nuclear weapons. Overpressure, weapon yield, well depth, and soil properties are varied in order to determine siting and hardness limitations of the well concepts studied.

Two basic well casing environments are investigated: (1) direct encasement in soil (integral concept), and (2) encasement in a gel medium for shock isolation (gel-isolated concept). Well depths of 50 to 1,600 ft, overpressures up to 300 psi, and weapon yields up to 20 megatons are used in the study. The dynamic behavior of the well casing, the discharge pipe, and the pump unit is investigated for the different well concepts and weapon effects.

The integral well concept is analyzed as an equivalent static problem by using propagating wave fronts. Shock spectra analysis and the normal mode method are used to analyze the gel-isolated concepts.

(This page intentionally left blank.)

CONTENTS

CONTENTS (Continued)

CONTENTS (Continued)

CONTENTS (Continued)

AGBABIAN-JACOBSEN ASSOCIATES

LIST OF FIGURES

AGBABIAN-JACOBSEN ASSOCIATES

LIST OF FIGURES (Continued)

LIST OF FIGURES (Continued)

LIST OF TABLES

LIST OF TABLES (Continued)

NOTATION

A - Maximum response acceleration, also static matrix

A_m - Metal area of casing cross section

C - Seismic velocity, subsurface stress wave front velocity

C_p - Subsurface stress wave peak pressure velocity

C_o - Cohesive strength of soil

D - Casing outside diameter, also maximum response displacement

D_p^+ - Positive phase duration of surface overpressure

G - Acceleration of gravity, also shear modulus

H - Horizontal displacement

V - Vertical displacement

$\Delta H/\Delta Z$ - Slope of the horizontal displacement versus depth curve

$\beta = H/V$ - Ratio of horizontal to vertical displacement

E Elastic modulus of steel, (taken as 3×10^7 psi)

E_b - Bulk modulus of water, (taken as 3×10^5 psi)

f, f_z, f_Z - Drag stress exerted between soil and casing during relative axial motion; the total shear strength of the soil; or the frequency

I - Moment of inertia of casing

K - Bulk modulus

$k_m = M_p/M_c$ - Ratio of soil modulus under overpressure to the seismic modulus, ρC^2

k_o - Ratio (P_H/P_Z) of horizontal to vertical soil pressure under overpressure loading

k_p - Ratio of permanent to peak soil deformation under overpressure loading

L - Length of casing

NOTATION (Continued)

M - Bending moment in casing

M_c - Seismic modulus of soil, ρC^2

M_p - Soil modulus at peak stress, also effective modulus

P_s - Decayed surface overpressure after shock front passage

P_{so} - Peak surface overpressure

P_z - Vertical overpressure at depth Z

P_h - Horizontal overpressure at depth Z

P_{zp} - Peak attenuated subsurface overpressure

Q - Total drag force on a strip of unit circumferential width extending the full length of the casing

S - Section modulus, in^3, also elasticity matrix

t_n - Time when surface shock front reaches the depth Z_n

t_m - Metal thickness of casing

T_B - Bottom-most target point of casing considered for displacement, stress, etc.

T_N - The N^{th} target point from the top of the casing

$S\Big|_N^{N+1}$ - Total horizontal shear acting on casing between target points N and $N+1$

U - Free air shock front

W - Weapon yield (megatons)

Z - Depth below surface

Z_1, Z_2, Z_3 --- Z_N - The vertical distances between each target point and the next lower target point, as Z_N and Z_{N+1}

Z_n - Pre-selected depth (of a series) of stress wave front used in determination of t_n and stress wave profile at t_n

Z_{TN} - Depth below surface of target point T_N

NOTATION (Continued)

α, α_z - Spatial attenuation factor for peak overpressure (versus depth, yield, and peak surface overpressure)

ΔZ - Finite increment of depth

V_B, H_B - Absolute vertical and horizontal displacements of bottom target point of casing

V - Maximum pseudo velocity

σ_a - Bending stress

σ_a - Axial compressive stress due to downdrag forces

σ_b - Bending stress

σ_{af} - Axial compressive stress, as computed by the friction method

σ_{as} - Axial compressive stress, as computed by the strain method

$\sigma_s \Big|_N^{N+1}$ - Shear stress as a function of rate of change of bending stress between target points N and N+1

ϕ - Angle of internal friction in soil, also the model matrix

ρ - Mass density of soil

α, Γ - Participation factors

ε - Strain, in./in.

η - Longitudinal strain, in./in.

γ - Shear strain, in./in.

τ - Shear stress, psi (general)

μ - Coefficient of friction (general)

NOTE: Other notations are defined where they are used.

SECTION 1

INTRODUCTION

1.1 OBJECTIVES

The purpose of this study is to develop design criteria for water wells for shelter facilities, which will functionally survive the critical effects associated with the detonation of nuclear weapons.

1.2 STATEMENT OF PROBLEM

The specific problems in this study are to:

a. determine by analysis the stresses induced in well casings due to weapons effects for a number of assumed soils and soil-layer profiles

b. develop shockproof water well concepts for different shock environments

c. develop the necessary criteria for design of shockproof wells.

1.3 SCOPE OF STUDY

The scope of study is to evaluate proposed shockproof well concepts for their survivability under nuclear weapons ground-shock environments. The different concepts are shown schematically in Figures 1.1, 1.2 and 1.3. Figure 1.1 shows Concept "A", the integral concept, where the lower part of the well casing is grouted in with the surrounding soil and the upper part is exposed directly to the soil. Concept "A" utilizes conventional water well construction. Figure 1.2 shows Concept "B", the gel isolated concept, where the well casing is isolated from the surrounding soil by a gel or a similar shock reducing medium. The casing is grouted at the bottom and supported at the top by a spring vertically and by a conductor casing horizontally. Figure 1.3 shows Concept "C" which is basically the same as Concept "B" except there is no vertical support at the top of the casing.

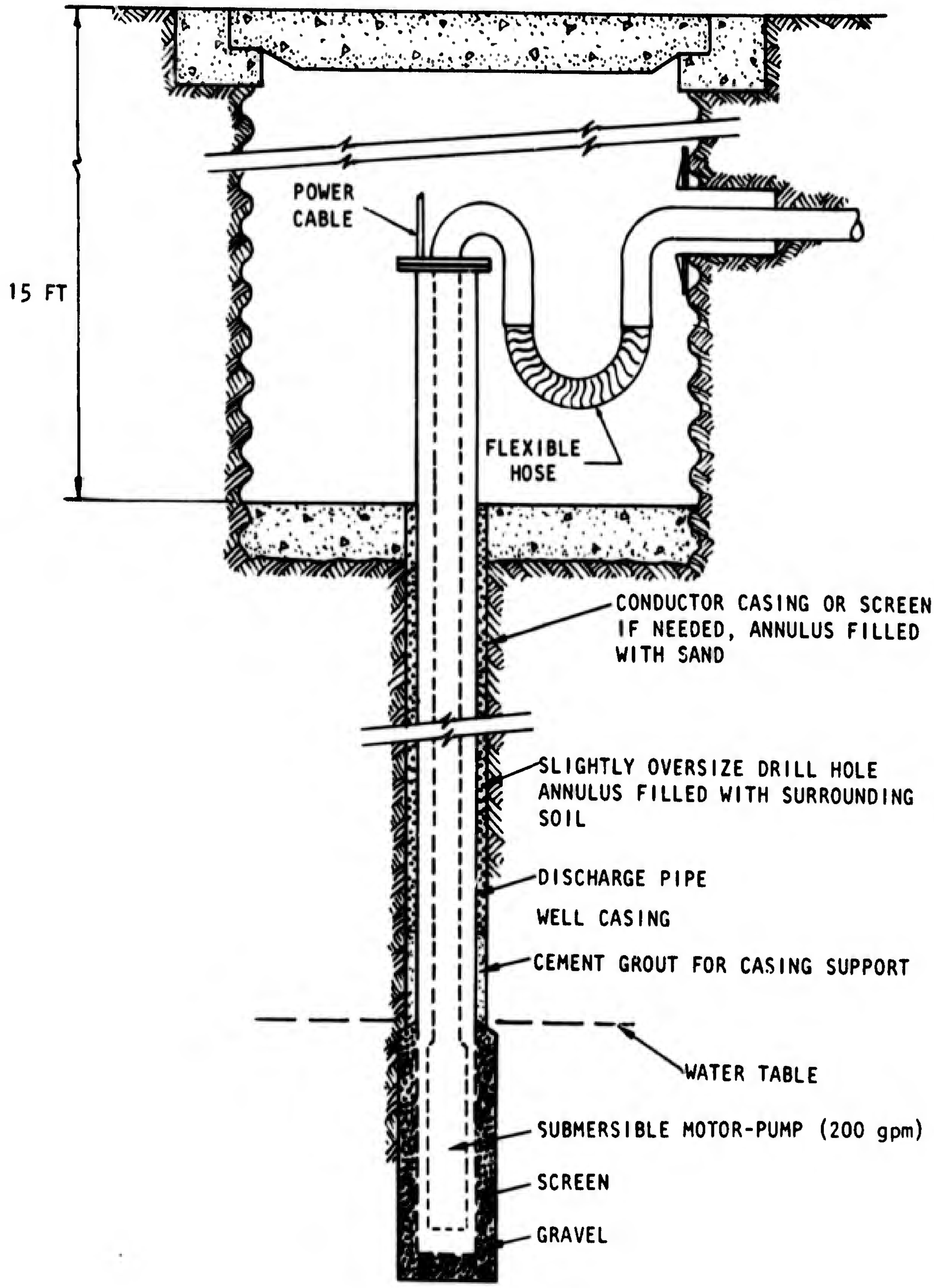

FIGURE 1.1 SHOCK-RESISTANT DEEP WATER WELL INTEGRAL CONCEPT "A"

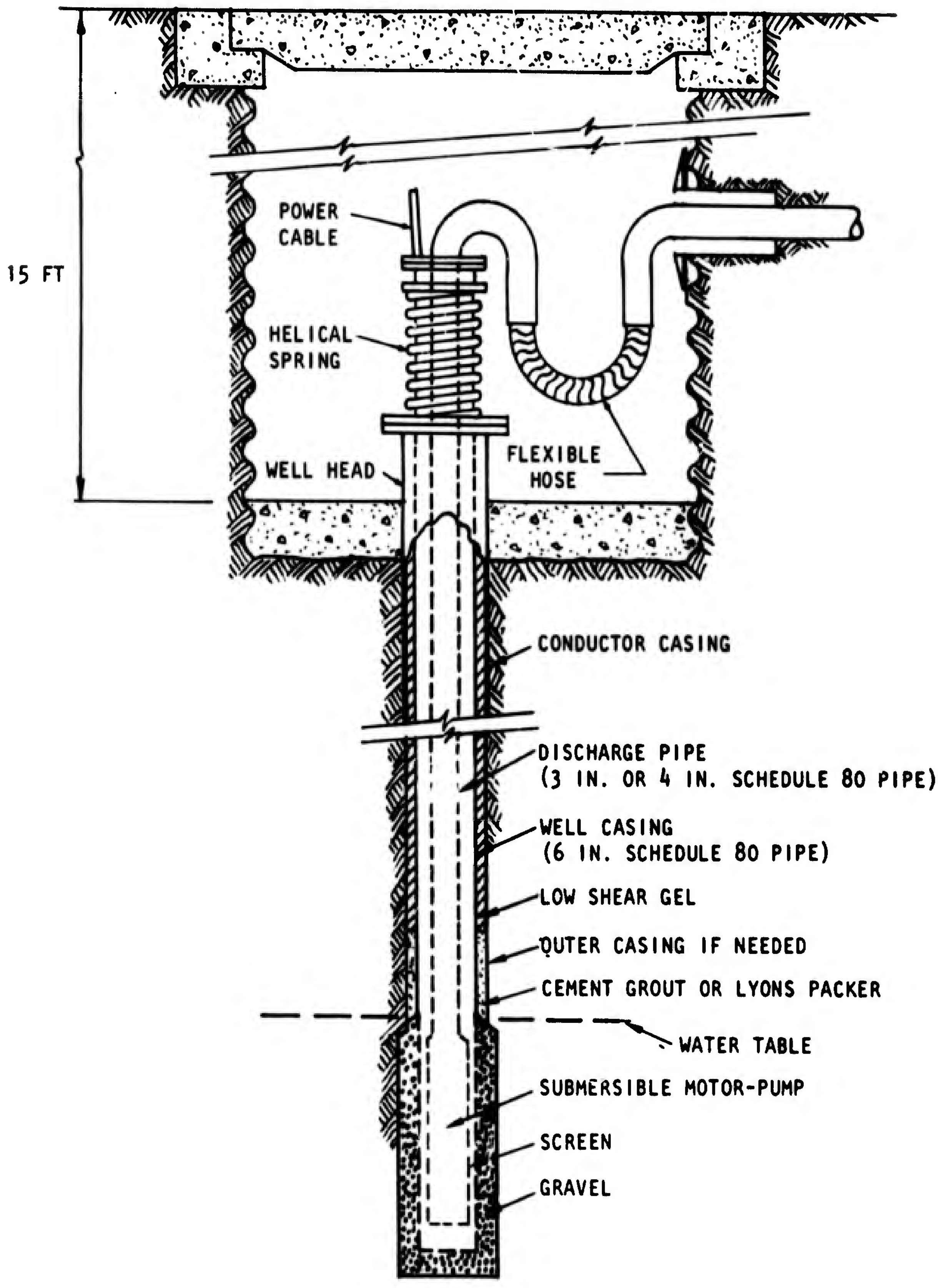

FIGURE 1.2 SHOCK-RESISTANT DEEP WATER WELL GEL-ISOLATED CONCEPT "B"

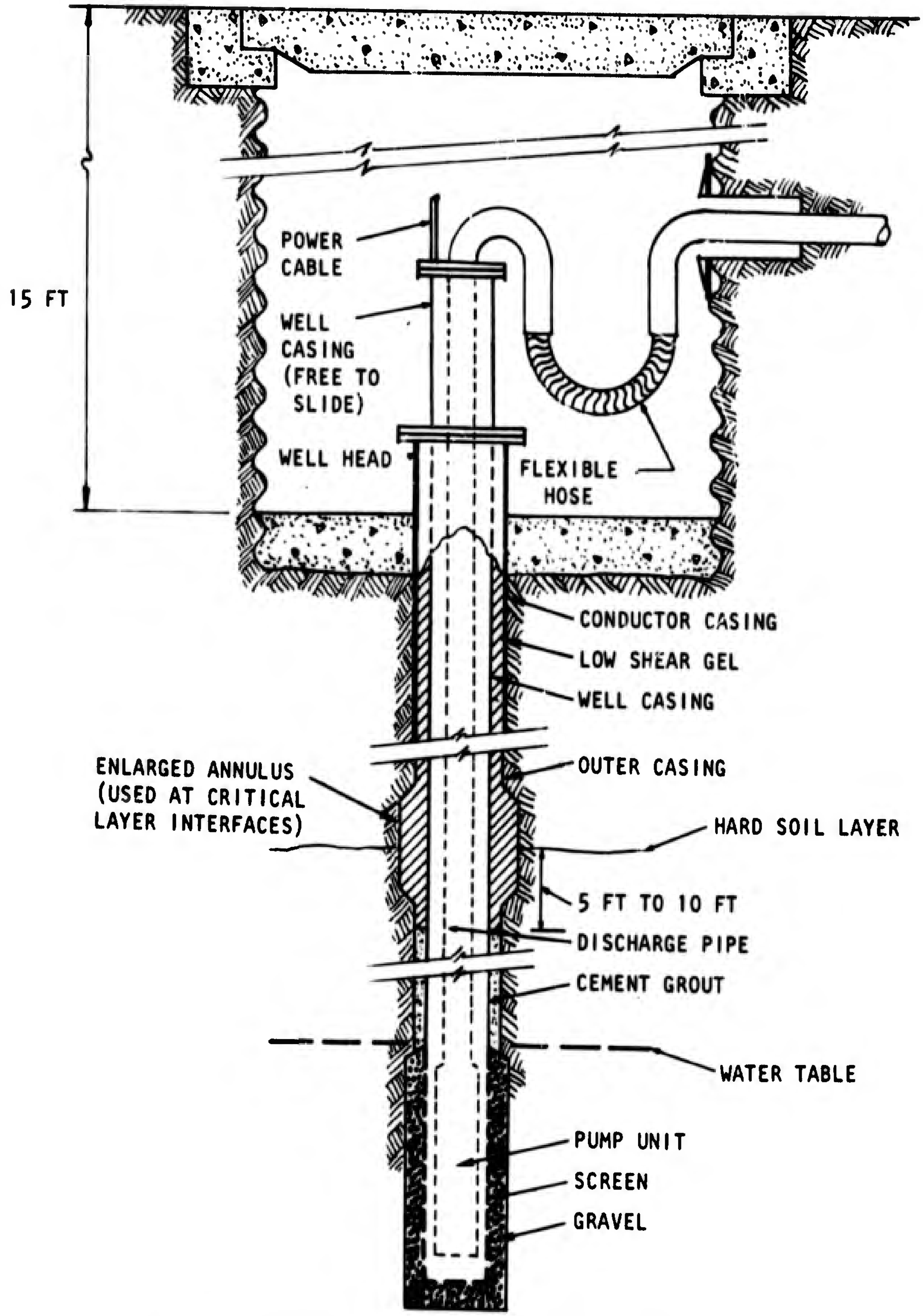

FIGURE 1.3 SHOCK-RESISTANT DEEP WATER WELL
GEL-ISOLATED CONCEPT "C"

This report is the result of studies carried out under two separate contracts. In Navy Contract No. NBy-62212, a parametric study was performed using Concept "A". The primary purpose of this study was to determine the ground shock environment for a range of overpressures, weapon yields and soil profiles. Well casings of different lengths and diameters were considered. In Navy Contract No. N62399-67-0017, these studies were extended to additional cases, and the response characteristics of well Concepts "B" and "C" were determined.

(This page intentionally left blank.)

SECTION 2

BASIS FOR STUDY

2.1 STUDY CRITERIA

The basic criteria utilized for the conduct of this study generally follow the requirements outlined in Section 1.3. Simplifying assumptions which approximate the physical nature of the problem were made to reduce the complexities of the analysis. These are discussed in Section 2.3.

Weapon yields, overpressures, well-configurations, and soil profiles were selected as representative values for arriving at general criteria. The soil profiles, shown in Figures 2.1, 2.2, and 2.3, represent a wide variation of soil combinations from which critical conditions can be concluded.

2.2 PARAMETRIC VARIATIONS

The number of parametric variations is dependent on the

1. Weapon yields
2. Overpressures
3. Casing lengths
4. Soil Profiles

The effect of different weapon yields is to produce different time rates of overpressure decay at the surface and different rates of spatial attenuation below the surface for each of the overpressures considered. Also different yields will produce different travel times for the shock wave from ground zero to a specified overpressure location. Since soil properties, specifically the seismic velocity, the soil's effective modulus, and the ratios of permanent to peak strains (see Appendix A), are influenced by the location of the water table, the elevation of the water table was varied in order to change the properties of the profiles. In the calculations of soil deformations and displacements which are used as the basis for the determination of the stresses in the well casing of Concept "A", a total of 84 discrete combinations of criteria, or input data, was considered in the analysis.

(Text continued on Page 11)

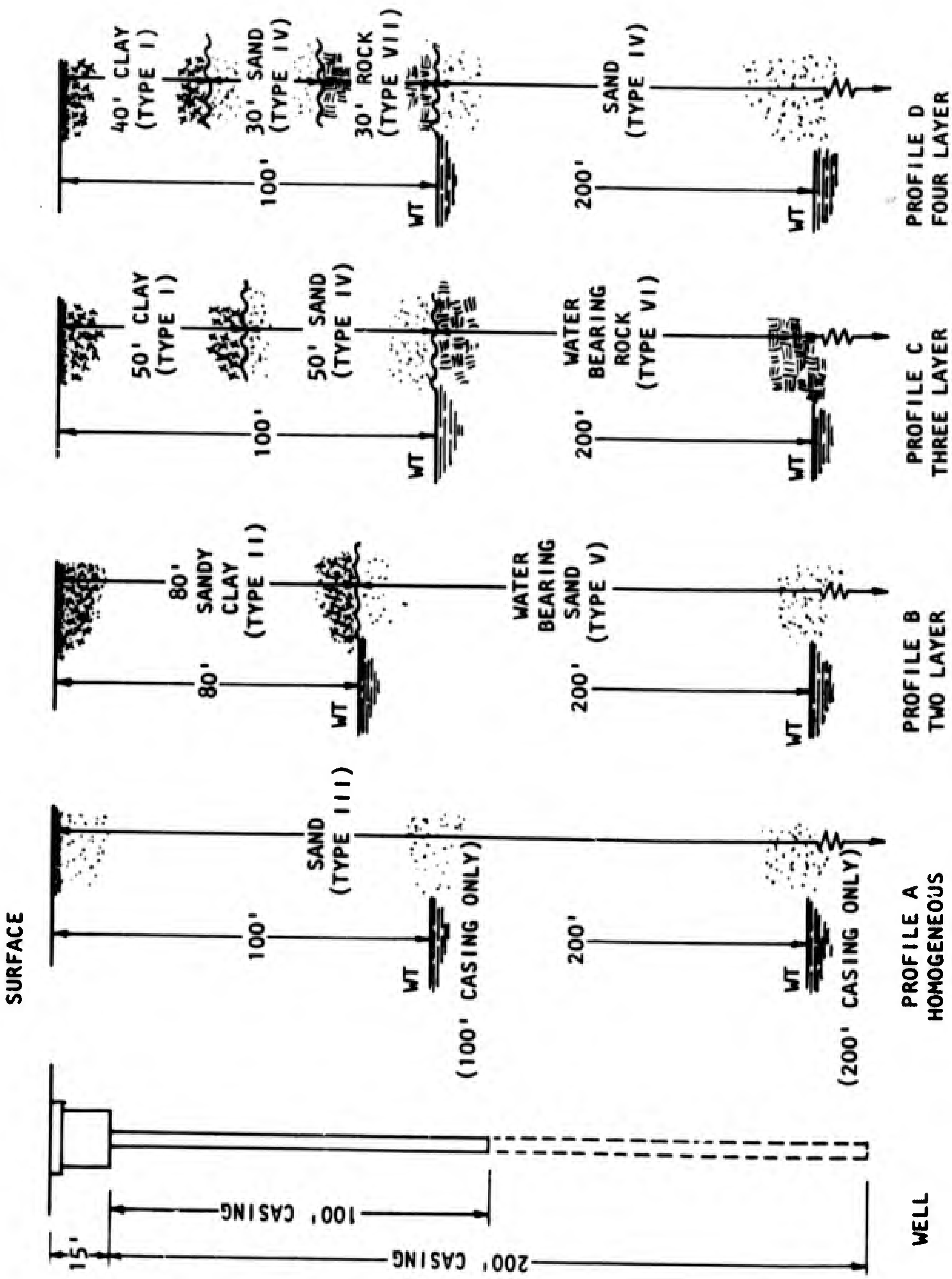

FIGURE 2.1 SOIL PROFILES (REFER TO TABLE A-2, APPENDIX A, FOR SOIL PROPERTIES)

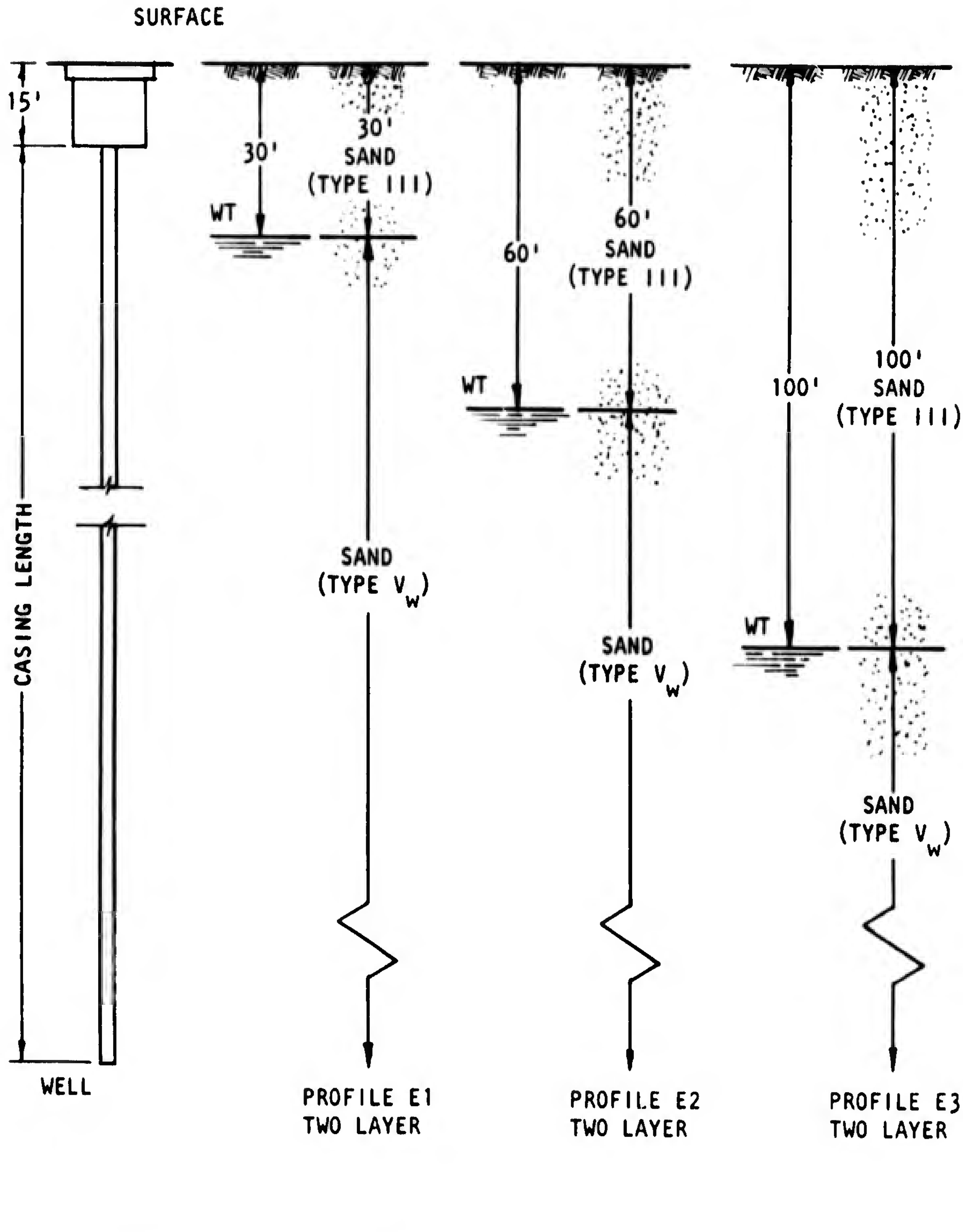

FIGURE 2.2 SOIL PROFILES (REFER TO TABLE A-2, APPENDIX A FOR SOIL PROPERTIES)

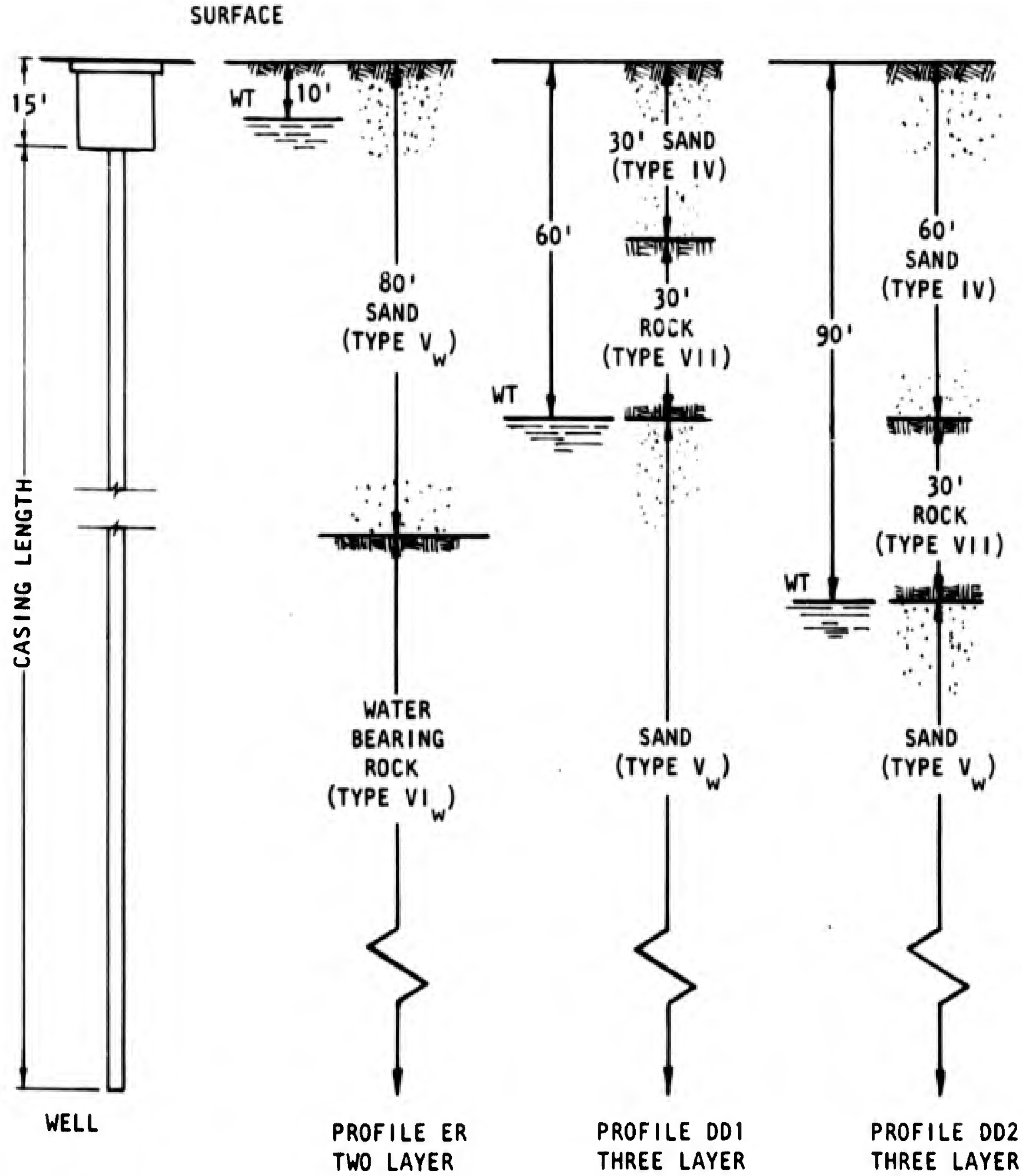

FIGURE 2.3 SOIL PROFILES (REFER TO TABLE A-2, APPENDIX A FOR SOIL PROPERTIES)

The effects of the thickness and diameter of the well casing on the bending and on the axial stresses were included in 64 of the above mentioned combinations. For the remaining 20 combinations the thickness and diameter were held constant and other parameters were varied. One additional case was investigated for the shock effects of the scheduled 500 ton TNT test at the Watching Hill Blast Range of the Suffield Experiment Station, Ralston, Alberta, Canada. (See Section 9.) For the gel-isolated concept a total of 20 combinations was considered, including two cases covering the scheduled 500 ton TNT test. Soil properties used in the investigation of the effects of the TNT test were taken from References 33 to 35.

The primary purpose of the soil profiles E1, E2, and E3, shown in Figure 2.2, was to investigate how the bending stresses in the well casing vary with the elevation of the water table. The soil-layering, dry sand (III), and wet sand (V), represent a critical soil layer combination as far as bending of the casing is concerned. The soil profiles ER, DD1 and DD2 shown in Figure 2.3 are designed to produce outrunning conditions (see Appendix C) for the free-field shock spectra analysis.

2.3 ANALYSIS

2.3.1 Method of Approach

The analyses and criteria are limited to the well casing and its requirements. Other elements of a well, i.e., well head details, pumps and discharge pipe, piping runs, power connections, and motor are analyzed dynamically to the extent necessary to develop feasible concepts. Technical considerations of these details are utilized only with respect to providing estimated boundary conditions for the solution of the displacement equations.

The rigorous treatment of a cylindrical shell of a small diameter embedded in a half-space is extremely complicated if the entire problem is approached from a comprehensive free-field soil-structure interaction viewpoint. It is however, amenable to analysis for the purpose of this study if a more direct and simpler approach is adopted.

2.3.2 Assumptions and Limitations

The methods adopted in this study are based on generally accepted engineering approximations. The free-field motions at the well site may be determined by calculating the deformations of the soil in the immediate vicinity of the well casing without resorting to solutions describing the time-history of stresses through the half-space. For the small casing diameters under consideration it may be assumed that the cylindrical diameters remain unchanged and undeformed by the shock wave engulfing the casing. For the integral concept (Concept "A") it is further assumed that the horizontal displacement of the casing generally follows the computed free-field soil displacement. For the gel-isolated concepts, (Concept "B" and "C") the dynamic response of the casing is analyzed using free-field shock spectra.

The axial loading and stresses in the casings due to vertical soil displacements are estimated by neglecting any end load or static pressure effect. Axial casing load and stress computations are thus based entirely on weapons effects induced soil stresses and displacements, and only the portion of the casing engulfed by the pressure wave is considered. It is also assumed that, within the length of casing so loaded, the unit drag force transferred from soil to casing is equal to the dynamic shear strength of the adjacent soil. An investigation of the buckling stability of the casing indicates that the critical buckling stresses are well above yield stress. This is due primarily to soil restraint and the ratio of casing diameter to wall thickness.

Solutions for the stresses in the casings are based on the representation of the casing as a "column of soil". For those cases considering layered soils (i.e., sand overlaying firm rock) it is assumed that no relative motion occurs at the point of layer interface (i.e., no slip). This can be shown to be a rational approach because of the magnitude of the shear resisting forces existing at the overburden depths indicated and for the overpressures that are considered. It is recognized that oil well casing failures (Reference 8) have indicated that it is quite possible to experience layer slippage under the influence of earthquake forces. It appears, however, that this is a combination of mechanical and geological circumstances, neither of which has been assumed present for the soil profiles under consideration. In the cases described in Reference 8 all measured slippages occurred in incompetent shale beds. In addition, the area of most severe damage is defined as a general subsidence area (probably due to the pumping operations). These factors have contributed to a unique problem of slippage occurring in generally poorly cemented oil bearing shales, under mechanical subsidence which creates tensile loads and thereby reducing (or elminating) the compressive loads necessary to develop horizontal frictional resistance.

Implicit in the assumption of no relative motion at the interface of soil layers is the presence of a zone of influence for the distribution of computed displacements above and below this interface. For a specific case, this distribution can be calculated or estimated on the basis of the physical properties of the two materials. For the purposes of this study the zone is assumed to extend two feet above and below the interfaces in all cases.

This approach will result in critical bending and shear stresses at or in the vicinity of the layer interfaces. These results will be conservative for normally available pipe if the relative effect of the pipe's beam strength and stiffness in relation to the soil stiffness and strength is considered in the zone of influence. That is, the "softer" soils at the interfaces will not be able to force sharp bending or shear in the pipe due to failure of the soil by local shear. The shear strength of the soil must therefore be considered. Reference 6 provides a simplified method for computing bearing capacity based on local shear failure. Using this method, it can be shown that a local shear failure will occur when the strain induced soil loading reaches a value of approximately 3,000 pounds per inch of casing length at the layer interface. This loading will be reached at a strain of approximately 0.5 percent for a granular soil.

2.3.3 Outline of Procedures

The stress analysis in this study follows procedures which are tailored to provide solutions by use of the computer.

2.3.3.1 Integral Well Concept. The procedure for the integral well casing (Concept "A") is outlined as follows:

a. Evaluate the surface overpressure time characteristics, the surface overpressure attenuation with depth factor, and the critical times of arrival at a given depth of the wave front and the stress peak.

b. Determine the vertical soil stress profiles.

c. Calculate the down drag forces on the casing and the resulting axial compressive stresses in the casing.

d. Calculate the relative vertical and horizontal soil displacements as functions of the stress profiles, soil properties, layering, time, and depth.

e. Calculate bending and shear stresses.

f. Determine the maximum combined stresses in the casings.

2.3.3.2 Gel-Isolated Concept. The procedure for the gel-isolated casing (Concepts "B" and "C") is outlined as follows:

a. Evaluate the surface overpressure-time characteristics and the surface overpressure attenuation with depth factor.

b. Evaluate the peak free-field ground motion intensities (accelerations, velocities, and displacements) induced by the air blast.

c. Compute critical arrival times at the ground surface at target distances from ground zero and determine the shock condition (outrunning or superseismic).

d. Compute the peak free-field random ground motion intensities.

e. Compute shock spectra from the results of (b) and (d).

f. Determ..ne the dynamic response of the well system and evaluate the maximum stresses.

(This page intentionally left blank.)

SECTION 3

CONCLUSIONS AND RECOMMENDATIONS

3.1 INTEGRAL CONCEPT

The results of the study have shown that it is feasibile to design hardened well casings to a depth of 1600 feet for the physical soil properties assumed, for weapon yields up to 20 megaton, and for overpressures up to 100 psi. However, where there is a large difference in the stiffness of two layers in a soil profile a thicker casing, or an enlarged annulus, should be provided through the layer interface in order to present excessive bending and shear stresses. Stresses in the discharge pipe are also less than the maximum permitted values.

An overpressure of 300 psi may produce destructive stresses at critical layer interfaces of soft soil and rock since the combined stresses that occur in the casing greatly exceed the allowable dynamic yield strength of the steel. However, steel is a ductile material and should be able to accommodate large plastic strains without imparing the survivability of the well system. Also, the dynamic stresses developed in the discharge pipe exceed the yield stress of the material and may result in failure of the well system.

It was shown that a selective siting can significantly reduce the imposed stresses in the well casing. A soil profile with a high soil modulus that gradually increases with depth without large abrupt changes is desired.

A gel-isolated system is recommended for well installations where the overpressure level will exceed 100 psi.

3.2 GEL-ISOLATED CONCEPT

It has been shown that a gel-isolated well casing can be designed to any depth in the soil profiles assumed and for the maximum weapon effects environment prescribed for this study. It is felt that the soil profiles investigated are fairly representative of the sites in which water wells would be used. Weapon yields up to 20 megatons and overpressures up to 300 psi were used in this study. Stresses or deformations were found to be within allowable limits for both superseismic and outrunning conditions.

At sites where very hard soil profiles occur, the gel isolation should be at least 70 feet deep. For very deep wells the gel isolation need not go deeper than 400 feet for any soil profile since the soil layers at this depth or deeper are generally very stiff.

For soil profiles that border between superseismic and ourtunning conditions (for example, Profiles E1 is outrunning at 100 psi but superseismic at 300 psi), Concept "C" shown in Figure 2.3 should be used for the well design.

In order to protect the pump from high, free field, accelerations the well should be at least 60 feet deep for an overpressure of 300 psi.

The recommended well bore diameter for the 6-inch casing is 10 inches, but an enlarged annulus should always be provided through critical soil layer interfaces. At sites where the loss of the gel may be suspected, an outer casing or a technique that would prevent the loss of the gel should be employed.

Expansion joints or other devices that permit excessive axial moment between the well casing and the discharge pipe should not be used as this may cause a failure of the power cable due to the relative displacement.

All welds, couplings and connections should be designed to develop the full strength of the piping in which they are used.

SECTION 4

RESULTS

4.1 SUMMARY

This section of the report summarizes the results of the analysis used in the investigation of critical stress conditions for well components in both the integral and gel-isolated concepts.

Stresses in the integral well casing and discharge pipe are summarized in Section 4.2. These were determined by utilizing the method of stress analysis discussed in Section 6.0 and Appendix B following the procedure outlined in Section 2.3.3.1. The results indicated that the maximum bending stress always occurs at a layer interface or at the water table in the case of a homogeneous soil. High axial stresses may be developed all along the casing. However, well casings located in soft soil layers will develop higher axial stresses than casings located in stiff layers.

The dynamic stress analysis of the well casing, discharge pipe and submersible pump are summarized in Section 4.3 for the gel-isolated concept. The method of analysis is discussed in Section 7.0 and Appendix D following the procedures outlined in Section 2.3.3.2. The development of shock spectra required for the dynamic response analysis followed the procedures described in Appendix C. It was found that stresses resulting from the dynamic response of the gel-isolated well system are not excessive for the parameters used in the analysis.

4.2 RESULTS - INTEGRAL WELL CONCEPT

4.2.1 Introduction

Two methods were considered in the investigation of axial stresses in the integral well casing imposed by the relative displacements between the soil and casing. These are referred to as the "friction method" and the "strain method" and are described in Section 6.2. The first 64 cases defined in Table 4.1 are analyzed by the friction method only. The remaining 20 cases are analyzed using both the friction and the strain methods.

(Text continued on Page 23)

TABLE 4.1 CASING HEAD DISPLACEMENT SUMMARY - INTEGRAL CONCEPT

SER. No.	CASE NUMBER* SOIL PROFILE	CASING LENGTH (ft)	YIELD (MT)	P_{so} (psi)	VERTICAL DISPLACEMENT (in.) REL.**	ABS.	HORIZONTAL DISPLACEMENT (in.) REL.**	ABS.	RESIDUAL HORIZON. DISPL. (in.)
1	A	100	1	15	0.34	0.42	0.17	0.19	<0.01
2		200	1	15	0.61	0.71	0.30	0.33	<0.01
3		100	20	15	0.37	0.49	0.18	0.22	<0.01
4		200	20	15	0.73	0.87	0.36	0.40	<0.01
5		100	1	50	1.35	1.55	0.52	0.61	<0.01
6		200	1	50	2.19	2.44	1.67	1.71	0.01
7		100	20	50	1.63	2.18	1.19	1.33	<0.01
8		200	20	50	3.04	3.65	2.25	2.35	0.03
9		100	1	100	2.87	3.37	2.11	2.15	0.03
10		200	1	100	4.53	4.63	3.35	3.42	0.05
11		100	20	100	3.70	4.90	2.67	2.93	0.04
12		200	20	100	6.64	7.88	4.90	5.10	0.07
13		100	1	300	9.45	10.74	3.93	4.17	0.1
14		200	1	300	14.25	14.82	5.96	6.15	0.15
15		100	20	300	13.17	17.21	5.48	6.59	0.14
16		200	20	300	22.42	26.10	9.37	10.27	0.24
17	B	100	1	15	0.16	0.17	0.08	0.08	<0.01
18		200	1	15	0.19	0.20	0.09	0.1	<0.01
19		100	20	15	0.18	0.20	0.09	0.09	<0.01
20		200	20	15	0.21	0.24	0.10	0.11	<0.01
21		100	1	50	0.78	0.81	0.39	0.4	<0.01
22		200	1	50	0.86	0.86	0.43	0.43	<0.01
23		100	20	50	0.91	1.03	0.45	0.48	<0.01
24		200	20	50	1.03	1.15	0.51	0.55	<0.01
25		100	1	100	1.87	1.92	1.38	2.02	0.02
26		200	1	100	2.00	2.02	1.45	1.45	0.03
27		100	20	100	2.28	2.47	1.68	1.73	0.03
28		200	20	100	2.54	2.66	1.81	1.92	0.03
29		100	1	300	7.29	7.61	5.39	5.5	0.16
30		200	1	300	7.72	7.78	4.74	4.76	0.14
31		100	20	300	9.74	10.17	7.20	7.34	0.23
32		200	20	300	10.60	10.75	6.50	6.55	0.21

*, **SEE FOOTNOTES ON PAGE 22

TABLE 4.1 (CONTINUED)

SER. No.	CASE NUMBER* SOIL PROFILE	CASING LENGTH (ft)	YIELD (MT)	P_{so} (psi)	VERTICAL DISPLACEMENT (in.) REL.**	ABS.	HORIZONTAL DISPLACEMENT (in.) REL.**	ABS.	RESIDUAL HORIZON. DISPL. (in.)
33	C	100	1	15	0.11	0.11	0.05	0.05	<0.01
34		200	1	15	0.11	0.12	0.05	0.06	<0.01
35		100	20	15	0.12	0.13	0.06	0.06	<0.01
36		200	20	15	0.12	0.13	0.06	0.06	<0.01
37		100	1	50	0.49	0.49	0.24	0.25	<0.01
38		200	1	50	0.50	0.50	0.25	0.25	<0.01
39		100	20	50	0.57	0.59	0.28	0.29	<0.01
40		200	20	50	0.59	0.6	0.29	0.29	<0.01
41		100	1	100	1.12	1.13	0.73	0.74	0.01
42		200	1	100	1.14	1.14	0.74	0.74	0.01
43		100	20	100	1.39	1.43	0.92	0.93	0.01
44		200	20	100	1.43	1.44	0.93	0.93	0.01
45		100	1	300	4.32	4.42	2.75	2.77	0.07
46		200	1	300	4.37	4.37	2.76	2.77	0.07
47		100	20	300	5.74	5.84	3.68	3.72	0.11
48		200	20	300	5.84	5.89	3.71	3.72	0.11
49	D	100	1	15	0.08	0.19	0.04	0.07	<0.01
50		200	1	15	0.21	0.26	0.08	0.1	<0.01
51		100	20	15	0.09	0.23	0.04	0.09	<0.01
52		200	20	15	0.22	0.3	0.09	0.12	<0.01
53		100	1	50	0.35	0.77	0.17	0.3	<0.01
54		200	1	50	0.79	0.99	0.26	0.33	<0.01
55		100	20	50	0.42	1.09	0.20	0.42	<0.01
56		200	20	50	1.05	1.42	0.41	0.52	<0.01
57		100	1	100	0.83	1.52	0.52	0.64	<0.01
58		200	1	100	1.61	1.91	0.72	0.88	0.01
59		100	20	100	0.99	2.26	0.62	1.01	<0.01
60		200	20	100	2.34	3.07	1.03	1.25	0.01
61		100	1	300	3.25	4.83	1.99	2.04	0.06
62		200	1	300	5.23	6.08	2.37	2.52	0.07
63		100	20	300	4.17	8.34	2.54	3.57	0.08
64		200	20	300	8.26	10.60	3.67	4.31	0.11

*, **SEE FOOTNOTES ON PAGE 22

TABLE 4.1 (CONTINUED)

SER. NO.	CASE NUMBER*				VERTICAL DISPLACEMENT (in.)		HORIZONTAL DISPLACEMENT (in.)		RESIDUAL HORIZON. DISPL. (in.)
	SOIL PROFILE	CASING LENGTH (ft)	YIELD (MT)	P_{so} (psi)	REL.**	ABS.	REL.**	ABS.	
65	A	50	20	50	0.74	0.94	0.58	.71	<0.01
66	A	50	20	100	1.79	2.17	1.34	1.63	0.02
67	A	50	20	300	6.65	6.80	2.72	2.95	0.07
68	A	600	20	50	6.34	6.35	4.74	4.74	<0.01
69	A	600	20	100	12.60	12.82	9.44	9.44	0.07
70	A	600	20	300	41.5	41.5	17.3	17.4	0.27
71	B	50	20	50	0.68	1.07	0.34	0.60	<0.01
72	B	50	20	100	1.72	2.94	1.29	2.20	0.02
73	B	400	20	100	2.77	2.77	1.84	1.83	<0.01
74	B	400	20	300	10.60	10.60	6.26	6.26	0.23
75	D	600	20	50	2.92	3.27	1.46	1.63	0.01
76	D	600	20	100	5.90	6.55	2.98	3.31	0.05
77	D	1600	20	15	1.31	1.31	0.65	0.65	<0.01
78	D	1600	20	50	5.60	5.60	2.80	2.80	0.17
79	D	400	20	300	14.00	14.00	10.10	10.12	0.17
80	E1	100	20	100	0.84	0.86	0.55	0.55	<0.01
81	E1	100	20	300	3.14	3.16	1.46	1.46	0.04
82	E2	100	20	100	2.12	2.12	1.54	1.54	<0.01
83	E3	200	20	300	8.06	8.08	3.97	3.97	0.10
84	E3	200	20	300	13.73	14.0	6.75	6.75	0.15

*Case numbers referenced in the report are designated by the soil profile, casing length, weapon yield, and overpressure. For example, Case A-50-20-50 indicates a well casing 50 feet long installed at a site corresponding to Profile A soil conditions and located at the 50 psi overpressure range for a 20 megaton nuclear weapon.

**Relative displacements refer to the casing head displacements relative to the bottom of the casing.

4.2.2 Vertical Stress Profile

The vertical soil stress profile for the various loading conditions and for specific times after shock front arrival were computed in the manner described in Appendix B. They were based on the principles of one-dimensional wave front propagation in a soil medium and resulted in free-field stresses and displacements.

In reviewing the maximum combined casing stresses (as shown in Table 4.2) with the computer time-history printout data (not included in this report), the following observations were noted.

For short casing lengths (approximately 150 feet), the wave front entirely engulfed the full length of the casing before peak combined stresses were reached. For the longer casings the peak combined stresses were reached when the wave front toe had reached a depth of 200 to 600 feet depending on the soil's stiffness.

In the case of the two and three layer soil profiles the influences of the bending stress at the upper interface caused in most cases the induced peak combined stress at that elevation.

4.2.3 Displacements

The maximum absolute vertical an' horizontal displacements, residual displacements, and displacements relative to the bottom of the casings, at the casing head are given in Table 4.2 for all cases investigated. It was found by review of the computer printout data that, in general, the values of peak displacement at maximum stress are very nearly equal to the peak value of relative displacement. This is accounted for by the fact that the displacements are cumulative, and, although the top (which experiences the maximum displacement) is rebounding the reduction in displacement is negligible until the surface overpressure approaches very small values. The tables listing the displacements show larger absolute displacements for deeper wells than

(Text continued on Page 30)

TABLE 4.2 WELL CASING STRESS SUMMARY (INTEGRAL CONCEPT)

(a) Soil Profile A

CASE SERIAL NO.*	BENDING STRESS: DEPTH IN FEET AT CRITICAL STRESS**	BENDING STRESS: MAX. σ_b' (Kips/In.^{3})	σ_bMAX. (= σ_b' R) Kips/In^2, CASING SIZE AND R (In.): 4 / 2.25	5 / 2.78	6 / 3.31	8 / 4.31	AXIAL COMPRESSIVE STRESS: DEPTH IN FEET AT CRITICAL STRESS**	MAX. σ_a' (Kips/In.)	σ_aMAX. (= σ_a' D/A) Kips/In^2, CASING SIZE (in.) AND D/A (SCH. 80): 4 / 1.02	5 / .910	6 / .789	8 / .675	COMBINED COMPRESSIVE STRESS: DEPTH IN FEET AT CRITICAL STRESS**	σ_cMAX. (= σ_b + σ_a) (Kips/In^2 SCH. 80), CASING SIZE (in.): 4	5	6	8
1	100	0.15	0.34	0.42	0.50	0.65	68	3.79	3.87	3.45	2.99	2.56	68	3.87	3.45	2.99	2.56
2	195	0.13	0.29	0.36	0.43	0.56	116	6.57	7.70	5.98	5.18	4.44	116	6.71	5.99	5.18	4.44
3	100	0.17	0.38	0.47	0.56	0.73	68	4.16	4.25	3.79	3.28	2.81	68	4.25	3.79	3.28	2.81
4	195	0.16	0.36	0.45	0.53	0.69	118	7.78	7.94	7.08	6.14	5.26	118	7.94	7.08	6.14	5.26
5	100	1.02	2.30	2.84	3.38	4.40	68	10.7	10.9	9.74	8.44	7.23	68	11.0	9.78	8.48	7.31
6	195	0.79	1.78	2.20	2.62	3.41	118	17.3	17.7	15.8	13.6	11.7	118	17.6	15.7	13.6	11.7
7	100	1.23	2.77	3.42	4.07	5.30	68	12.9	13.2	11.7	10.2	8.72	68	13.1	11.7	10.2	8.82
8	195	1.09	2.45	3.03	3.61	4.70	120	22.9	23.4	20.9	18.1	15.5	120	23.3	20.8	18.0	15.5
9	100	2.21	4.97	6.15	7.32	9.53	70	18.6	19.0	16.9	14.7	12.6	70	19.1	17.0	14.8	14.8
10	195	1.57	3.53	4.37	5.20	6.77	122	28.8	29.4	26.2	22.7	19.5	122	29.4	26.2	22.7	19.5
11	100	2.86	6.44	7.96	9.47	12.3	70	23.8	24.3	21.7	18.8	16.1	70	24.3	21.7	18.8	19.0
12	195	2.44	5.49	6.79	8.08	10.5	122	40.5	41.3	36.9	31.9	27.4	122	41.4	36.9	32.0	27.4
13	100	3.45	7.76	9.60	11.4	14.9	70	44.8	45.7	40.8	35.3	30.3	70	45.8	40.9	35.5	30.5
14	195	2.22	5.00	6.18	7.35	9.57	120	65.7	67.0	59.8	51.8	44.4	120	67.1	59.9	51.9	44.5
15	100	5.03	11.3	14.0	16.7	21.7	68	61.4	62.7	55.9	48.4	41.5	68	62.8	56.1	48.6	41.7
16	195	3.94	8.87	11.0	13.1	17.0	124	99.1	101.	90.2	78.2	67.0	124	101.	90.3	78.3	67.1

*Refer to Table 4.1 for Case Serial Number descriptions.
**Depth below the surface at which the maximum stress occurs as indicated by the friction method.

TABLE 4.2 WELL CASING STRESS SUMMARY (INTEGRAL CONCEPT)

(b) Soil Profile B

CASE SERIAL NO.	BENDING STRESS: DEPTH IN FEET AT CRITICAL STRESS	BENDING STRESS: MAX. σ_b' $\left(\frac{Kips}{In.^3}\right)$	σ_b MAX. (= σ_b' R) Kips/In^2, CASING SIZE AND R (In.): 4 / 2.25	5 / 2.78	6 / 3.31	8 / 4.31	AXIAL COMPRESSIVE STRESS: DEPTH IN FEET AT CRITICAL STRESS	AXIAL: MAX. σ_a' $\left(\frac{Kips}{In.}\right)$	σ_a MAX. (= σ_a' D/A) Kips/In^2, CASING SIZE (in.) AND D/A (SCH. 80): 4 / 1.02	5 / .910	6 / .789	8 / .675	COMBINED COMPRESSIVE STRESS: DEPTH IN FEET AT CRITICAL STRESS	σ_c MAX. (= σ_b + σ_a) (Kips/In^2 SCH. 80), CASING SIZE (in.): 4	5	6	8
17	80	0.11	0.25	0.31	0.36	0.47	52	17.0	17.3	15.5	13.4	11.5	52	17.3	15.4	13.4	11.5
18	80	0.10	0.23	0.28	0.33	0.43	60	21.2	21.6	19.3	16.7	14.3	60	21.6	19.3	16.7	14.3
19	80	0.13	0.29	0.36	0.43	0.56	52	17.4	17.8	15.8	13.7	11.8	52	17.7	15.8	13.7	11.8
20	80	0.11	0.25	0.31	0.36	0.47	62	22.3	22.8	20.3	17.6	15.1	62	22.7	20.3	17.6	15.1
21	80	0.56	1.26	1.56	1.86	2.42	58	22.1	22.6	20.1	17.4	14.9	58	22.5	20.1	17.4	14.9
22	80	0.51	1.15	1.42	1.69	2.20	78	33.1	33.8	30.1	26.1	22.4	80	34.6	31.3	27.5	24.2
23	80	0.67	1.51	1.86	2.22	2.89	58	23.3	23.8	21.2	18.4	15.7	58	23.8	21.2	18.4	15.8
24	80	0.61	1.37	1.70	2.02	2.63	90	38.3	39.1	34.9	30.2	25.9	90	39.1	34.9	30.2	26.5
25	80	2.04	4.59	5.67	6.76	8.80	64	28.7	29.3	26.1	22.6	19.4	64	29.3	26.2	22.7	21.5
26	80	1.94	4.37	5.40	6.43	8.37	100	48.0	49.0	43.7	37.9	32.4	100	49.0	43.7	37.9	34.7
27	80	2.60	5.85	7.23	8.61	11.2	66	31.9	32.6	29.0	25.2	21.6	66	32.5	29.0	26.5	26.5
28	80	2.46	5.54	6.84	8.15	10.6	112	58.6	59.8	53.4	46.2	39.6	112	59.8	53.4	46.2	39.6
29	80	7.51	16.9	20.9	24.9	32.4	78	50.7	51.7	46.2	40.0	34.3	80	66.7	65.3	63.4	65.3
30	80	5.90	13.3	16.4	19.5	25.4	120	102.	104.	92.9	80.4	68.9	120	104.	93.0	80.6	69.0
31	80	11.0	24.8	30.6	36.4	47.4	80	61.7	63.0	56.2	48.7	41.7	30	87.3	86.3	84.6	88.5
32	80	8.70	19.6	24.2	28.8	37.5	122	132.	135.	120.	104.	89.2	122	135.	120.	104.	89.2

TABLE 4.2 WELL CASING STRESS SUMMARY (INTEGRAL CONCEPT)

(c) Soil Profile C

CASE SERIAL NO.	BENDING STRESS						AXIAL COMPRESSIVE STRESS						COMBINED COMPRESSIVE STRESS				
	DEPTH IN FEET AT CRITICAL STRESS	MAX. σ'_b $\left(\frac{Kips}{In.^3}\right)$	σ_b MAX. (= σ'_b R) Kips/In^2 — CASING SIZE AND R (In.)				DEPTH IN FEET AT CRITICAL STRESS	MAX. σ'_a $\left(\frac{Kips}{In.}\right)$	σ_a MAX. (= σ'_a D/A) Kips/In^2 — CASING SIZE (in.) AND D/A (SCH. 80)				DEPTH IN FEET AT CRITICAL STRESS	σ_c MAX. (= $\sigma_b + \sigma_a$) (Kips/In^2 SCH. 80) — CASING SIZE (in.)			
			4 2.25	5 2.78	6 3.31	8 4.31			4 1.02	5 .910	6 .789	8 .675		4	5	6	8
33	100	0.08	0.18	0.22	0.27	0.35	36	15.1	15.4	13.7	11.9	10.2	36	15.4	13.7	11.9	10.2
34	100	0.08	0.18	0.22	0.27	0.35	36	15.8	16.1	14.4	12.5	10.7	36	16.2	14.4	12.5	10.7
35	100	0.09	0.20	0.25	0.30	0.39	36	15.4	15.7	14.0	12.1	10.4	36	15.8	14.1	12.2	10.4
36	100	0.09	0.20	0.25	0.30	0.39	36	15.8	16.1	14.4	12.5	10.7	36	16.2	14.4	12.5	10.7
37	100	0.32	0.72	0.89	1.06	1.38	40	19.0	19.4	17.3	15.0	12.8	40	19.4	17.3	14.5	12.8
38	100	0.32	0.72	0.89	1.06	1.38	42	20.6	21.0	18.8	16.2	13.9	42	21.0	18.7	16.2	13.9
39	100	0.39	0.88	1.09	1.29	1.68	42	20.1	20.5	18.3	15.9	13.6	42	20.6	18.3	15.9	13.6
40	100	0.38	0.86	1.06	1.26	1.64	44	22.2	22.7	20.2	17.5	15.0	44	22.6	20.2	17.5	15.0
41	100	1.05	2.36	2.92	3.48	4.53	46	23.8	24.3	21.7	18.8	16.1	46	24.2	21.6	19.1	17.1
42	100	1.04	2.34	2.89	3.45	4.49	50	26.9	27.4	24.5	21.2	18.2	50	28.6	25.9	22.8	20.3
43	100	1.36	3.06	3.78	4.51	5.87	50	26.4	26.9	24.0	20.8	17.8	50	28.4	25.8	22.9	20.6
44	100	1.35	3.04	3.76	4.47	5.82	58	30.0	30.6	27.3	23.7	20.3	58	30.6	27.3	23.7	21.0
45	100	3.46	7.79	9.62	11.5	14.9	64	42.2	43.1	38.4	33.3	28.5	64	43.1	38.5	33.4	28.7
46	100	3.44	7.74	9.57	11.4	14.8	72	48.8	49.8	44.4	38.5	33.0	72	49.9	44.5	38.6	33.1
47	100	4.89	11.0	13.6	16.2	21.1	66	49.6	50.6	45.2	39.1	33.5	66	50.7	45.3	39.2	33.7
48	100	4.88	11.0	13.6	16.2	21.0	76	59.5	60.7	54.2	46.9	40.2	74	60.8	54.3	47.1	40.4

TABLE 4.2 WELL CASING STRESS SUMMARY (INTEGRAL CONCEPT)

(d) Soil Profile D

CASE SERIAL NO.	BENDING STRESS						AXIAL COMPRESSIVE STRESS						COMBINED COMPRESSIVE STRESS				
	DEPTH IN FEET AT CRITICAL STRESS	MAX. σ_b' (Kips/In.^{3})	σ_bMAX. (= σ_b' R) Kips/In^2 CASING SIZE AND R (In.)				DEPTH IN FEET AT CRITICAL STRESS	MAX. σ_a' (Kips/In.)	σ_aMAX. (= σ_a' D/A) Kips/In^2 CASING SIZE (in.) AND D/A (SCH. 80)				DEPTH IN FEET AT CRITICAL STRESS	σ_cMAX. (= σ_b + σ_a) (Kips/In^2 SCH. 80) CASING SIZE (in.)			
			4	5	6	8			4	5	6	8		4	5	6	8
			2.25	2.78	3.31	4.31			1.02	.910	.789	.675					
49	70	0.08	0.18	0.22	0.27	0.35	30	11.1	11.3	10.1	8.75	7.50	30	11.3	10.1	8.74	7.49
50	70	0.08	0.18	0.22	0.27	0.35	34	14.3	14.6	13.0	11.3	9.67	34	14.5	13.0	11.2	9.63
51	70	0.09	0.20	0.25	0.30	0.39	30	11.1	11.3	10.1	8.75	7.50	30	11.3	10.1	8.74	7.49
52	70	0.09	0.20	0.25	0.30	0.39	36	15.3	15.6	13.9	12.1	10.3	36	15.6	13.9	12.0	10.3
53	70	0.34	0.77	0.95	1.13	1.47	36	15.5	15.8	14.1	12.2	10.5	36	15.8	14.1	12.2	10.5
54	70	0.34	0.77	0.95	1.13	1.47	64	23.5	24.0	21.4	18.5	15.9	64	24.0	21.4	18.7	16.5
55	70	0.41	0.92	1.14	1.36	1.77	38	16.1	16.4	14.7	12.7	10.9	38	16.4	14.6	12.7	10.9
56	70	0.41	0.92	1.14	1.36	1.77	100	27.5	28.1	25.0	21.7	18.6	100	28.6	25.7	22.5	19.7
57	70	1.17	2.63	3.25	3.88	5.05	44	20.1	20.5	18.3	15.9	13.6	40	20.6	18.8	16.7	15.1
58	70	1.17	2.63	3.25	3.88	5.05	110	32.9	33.6	30.0	26.0	22.2	110	33.5	29.9	26.5	24.1
59	70	1.41	3.17	3.92	4.67	6.08	48	22.8	23.3	20.8	18.0	15.4	48	23.3	20.8	18.0	15.7
60	70	1.43	3.22	3.98	4.74	6.17	120	42.3	43.2	38.5	33.4	28.6	120	43.2	38.5	33.4	28.6
61	70	3.96	8.91	11.0	13.1	17.1	58	36.7	37.5	33.4	28.9	24.8	58	37.5	33.5	31.6	32.8
62	70	3.86	8.69	10.7	12.8	16.6	130	61.9	63.2	56.4	48.8	41.8	130	63.2	56.4	49.4	48.0
63	70	5.31	11.9	14.8	17.6	22.9	60	45.0	45.9	41.0	35.5	30.4	70	46.2	44.9	43.2	44.1
64	70	5.31	11.9	14.8	17.6	22.9	135	90.7	92.6	82.6	71.5	61.3	135	92.7	82.7	71.7	62.5

TABLE 4.2 WELL CASING STRESS SUMMARY (INTEGRAL CONCEPT)*

(e) Soil Profiles A and B

SER. NO.	CASE NO. SOIL-L-W-P_{so}	BENDING STRESS DEPTH (ft)	BENDING STRESS σ_b max (ksi)	METHOD†	AXIAL STRESS DEPTH (ft)	AXIAL STRESS σ_a max (ksi)	COMBINED STRESS DEPTH (ft)	COMBINED STRESS σ_c max (ksi)	SHEAR STRESS DEPTH (ft)	SHEAR STRESS σ_s (ksi)
65	A-50-20-50	50	7.0	F	42	5.5	50	10.9	50	3.9
				S	34	47.9				
66	A-50-20-100	50	16.4	F	42	10.4	50	23.6	50	9.0
				S	25	117.7				
67	A-50-20-300	50	37.9	F	43	28.1	50	57.7	50	20.8
				S	43	42.2				
68	A-600-20-50	600	1.32	F	309	39.0			600	0.25
				S	219	31.5	219	32.0		
69	A-600-20-100	600	2.70	F	321	64.3			600	0.50
				S	288	61.5	288	62.0		
70	A-600-20-300	600	3.7	F	327	144.5	327	144.8	600	0.67
				S	327	180.				
71	B-50-20-50	50	0.19	F	40	11.3	40	11.3	50	0.07
				S	50	33.4				
72	B-50-20-100	50	0.62	F	41	13.6	41	13.6	50	0.24
				S	30	90.0				
73	B-400-20-100	80	7.9	F	185	64.0			80	2.2
				S	80	34.5	80	42.4		
74	B-400-20-300	80	28.5	F	201	142.5			80	7.9
				S	80	54.8	80	83.3		

*Stresses are based on a 6-inch diameter, Schedule 80, casing size.

†Notations "F" and "S" indicate friction method and strain method respectively.

AGBABIAN-JACOBSEN ASSOCIATES

TABLE 4.2 WELL CASING STRESS SUMMARY (INTEGRAL CONCEPT)*

(f) Soil Profiles D and E

SER. NO.	CASE NO. SOIL-L-W-P_{so}	BENDING STRESS		METHOD†	AXIAL STRESS		COMBINED STRESS		SHEAR STRESS	
		DEPTH (ft)	$\sigma_{b\,max}$ (ksi)		DEPTH (ft)	$\sigma_{a\,max}$ (ksi)	DEPTH (ft)	$\sigma_{c\,max}$ (ksi)	DEPTH (ft)	σ_s (ksi)
75	D-600-20-50	70	1.35	F	258	48.3			20	0.4
				S	50	18.6	50	19.0		
76	D-600-20-100	70	4.70	F	285	74.1			70	1.1
				S	104	37.2	104	38.0		
77	D-1600-20-15	70	0.30	F	439	37.9			70	<0.1
				S	50	4.2	50	4.4		
78	D-1600-20-50	70	1.35	F	567	74.2			70	0.2
				S	50	18.6	50	19.0		
79	D-400-20-300	70	17.5	F	215	124.0			70	4.8
				S	193	118.0	193	119.0		
80	E1-100-20-100	30	24.2	F	66	23.8			30	13.5
				S	30	6.3	30	30.5		
81	E1-100-20-300	30	64.2	F	64	64.6			30	35.7
				S	33	22.5	30	87.2		
82	E2-100-20-100	60	22.9	F	67	21.0			60	12.7
				S	60	17.9	60	40.5		
83	E2-100-20-300	60	56.0	F	67	58.0			60	31.1
				S	60	49.8	60	105.8		
84	E3-200-20-300	100	50.0	F	114	100.0			100	27.5
				S	100	85.0	100	132.0		

*Stresses are based on a 6-inch diameter, schedule 80, casing size.
†Notations "F" and "S" indicate friction method and strain method respectively.

displacements for deeper wells than for shallower wells subjected to the same overpressures and yields. Since calculated absolute displacements depend on the assumed penetration depth of the wave front, the true maximum absolute displacements of a certain soil profile will be more closely approximated by the results obtained for the deeper wells. However, a shallow water table will produce a stiffer profile, thereby resulting in smaller displacements than calculated for a deep water table.

The residual displacement values are of interest in determining the permanent translation of casing and well head following nuclear detonation. However, for purposes of shock resistant design, the values of interest are the maximum values of hoirzontal and vertical displacement and the vertical displacements at the well head relative to the casing. The latter value can be determined by calculating the difference between the maximum displacement at the well head relative to the displacement of the point on the casing where the strain in the soil is equal to the strain in the casing. This point is usually at the top of the upper hard layer of the soil profile. For design purposes the depth of this point should not be taken less than 70 to 80 feet even though the top of the hard layer may be closer to the surface.

4.2.4 Stresses

In this section σ_{af} is refered to as the axial stress in the well casing as computed by the friction method, and σ_{as} as the axial stress computed by the strain method. These two methods are fully described in Section 6. Table 4.2 summarizes critical casing stresses due to bending and axial downdrag loads for various casing diameters and indicates the depth at which the critical stress occurs. In determining the combined compressive stress (compressive bending stress plus axial stress), the computer program print-outs were used to select the depth at which the critical combined stress occurred. Tables 4.2(e) and 4.2(f) lists axial stresses for both σ_{af} and σ_{as}; however the combined stress is listed for the governing condition only. The bending and shear stresses are the same for both methods.

4.2.4.1 Bending Stresses (Refer to Table 4.2 and Figures 4.1 and 4.2). In the determination of the maximum bending stresses it can be seen that the magnitude of the stresses is a direct function of the casing size and the maximum relative horizontal displacement. Thus the maximum bending stress in the casing will occur at the interface of the two soil layers where the difference in elastic, or seismic, properties is the largest. As the critical layer interface is moved up toward the surface the relative horizontal displacement at the interface will increase, and consequently the bending stress will increase. This is indicated for the soil profiles A, E_1, E_2, and E_3 in Figures 4.1 and 4.2. For short casings where the axial stress is relatively small, the bending stress may govern the combined stress as indicated by the dip in the combined stress curves shown for the homogeneous soil (Profile A) in Figure 4.1. For the homogeneous soil the maximum bending stress always occurs at the water table which is assumed as 15 to 20 feet above the bottom of the casing. See Figures 2.1 through 2.3.

For the 6-inch casing considered and for the soil profiles E_1, E_2 and E_3, which represent extreme soil layer combinations as far as the differential horizontal displacement at the layer-interface is concerned, the bending stress at a layer interface 30 feet deep may reach a value of σ_b = 24,200 psi for an overpressure of 100 psi, and a value of σ_b = 64,200 psi for an overpressure of 300 psi (see Figure 4.2). For a soft soil and rock layer-interface, bending stresses somewhat higher than those indicated by the E profiles may be expected.

These analyses show that extremely high bending stresses may occur in profiles with sharp layer-interfaces subjected to an overpressure of 300 psi. Consequently, where this may be expected provisions should be made to reduce the effects of large differential horizontal displacements.

For an overpressure of 100 psi all the cases investigated give bending stresses within allowable limits.

(Text continued on Page 34)

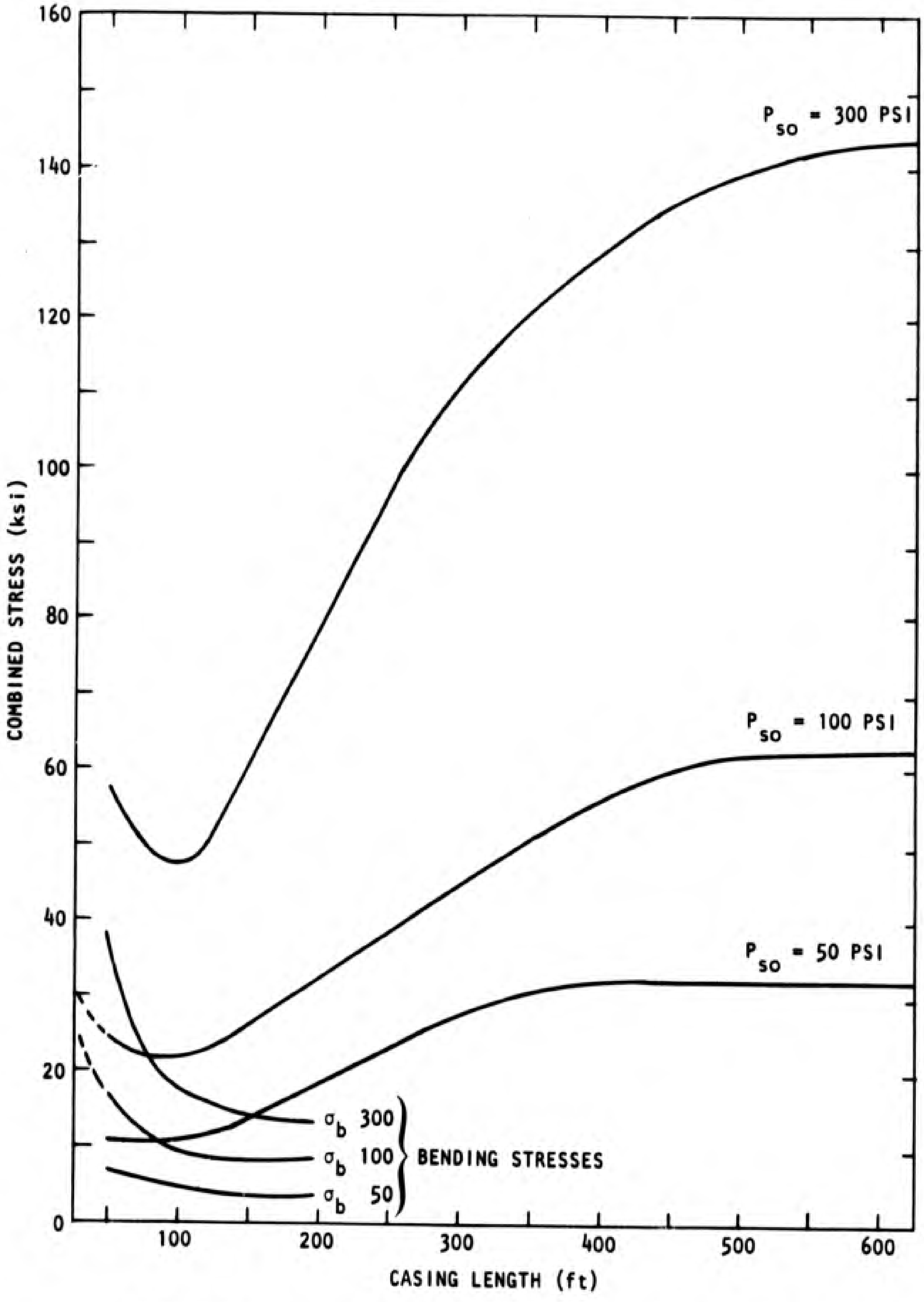

FIGURE 4.1 MAXIMUM STRESS VERSUS CASING LENGTH, PROFILE A

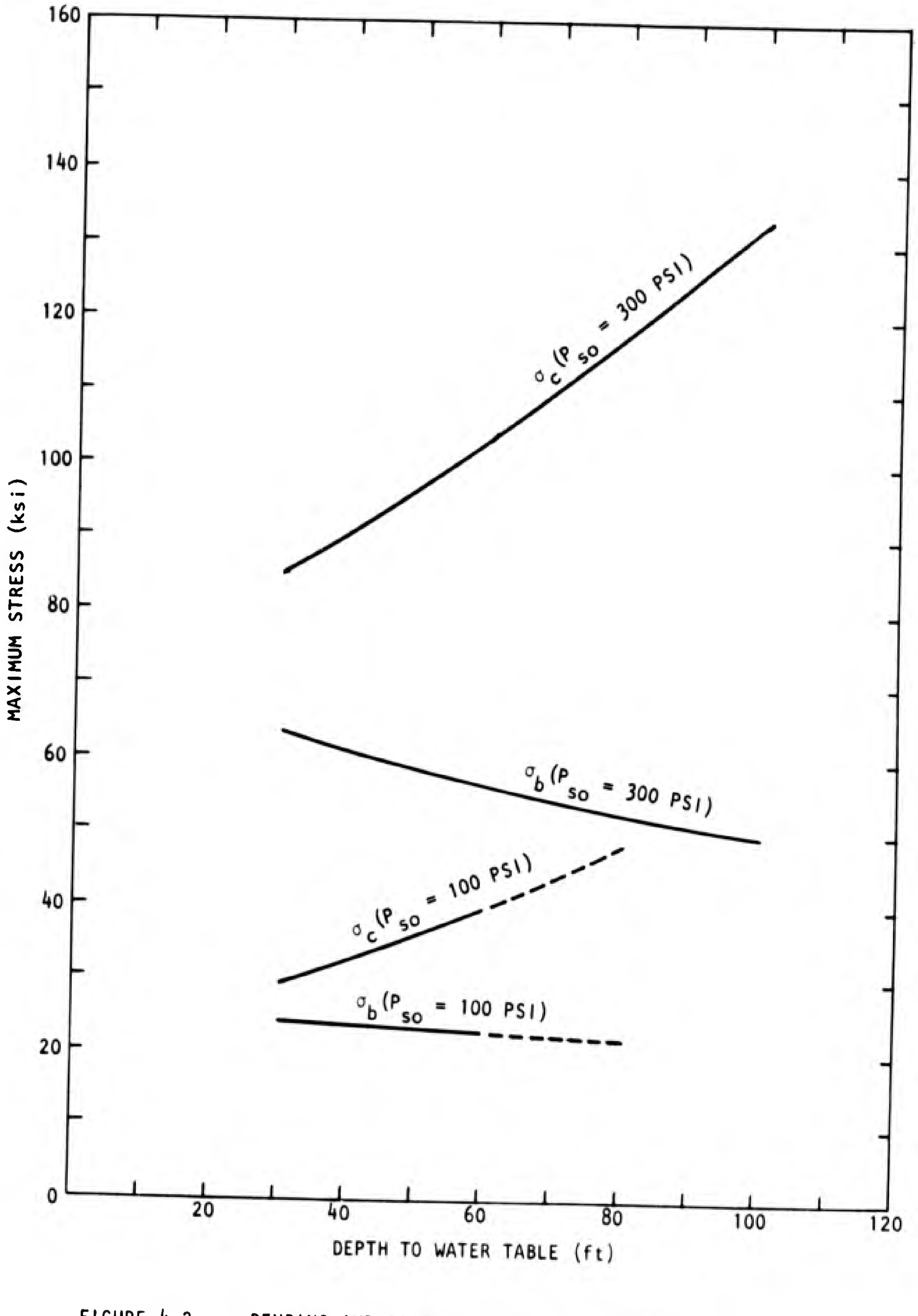

FIGURE 4.2 BENDING AND COMBINED STRESS AT WATER TABLE VERSUS DEPTH OF WATER TABLE FOR PROFILE E

4.2.4.2 Shear Stresses. The maximum shear stress in the casing occurs at the point of maximum change in bending stress. The maximum shear stress for 100 psi overpressure occurred in Case E1-100-20-100, where σ_s = 13,000 psi at 30 feet depth. (See Table 4.2(f).) This is within allowable values.

For an overpressure of 30 psi the shear stress is equal to σ_s = 35,700 psi at the water table of 30 feet depth, Case E1-100-20-300. When the water table is lowered to a 100 feet depth the shear stress becomes equal to σ_s = 27,500 psi, Case E3-200-20-300. These are shown in Table 4.2(f).

The cases investigated show no critical shear stresses for an overpressure of 100 psi. However, a critical soil profile and an overpressure of 300 psi result in destructive shear stresses.

4.2.3.2 Axial Stresses (Refer to Table 4.2 and Figures 4.1 and 4.2). A review of the computed data shows that the largest stresses are due to axial loads. Furthermore, Tables 4.2(e) and 4.2(f) show that the axial stresses in the shorter casing, 50 to 100 feet, are larger by the friction method. Also for the softer soil profiles (Profile A) the friction method governs the axial stresses for casing lengths up to 500 feet at an overpressure of 100 psi. For an overpressure of 300 psi the friction method may govern the axial stress in casing lengths up to 600-700 feet as indicated by Figure 4.1.

For casings located in stiffer soil profiles the strain governs the axial stresses, as shown in Tables 4.2(e) and 4.2(f).

4.2.4.4 Combined Stresses. Table 4.2 has been prepared to illustrate the magnitude and the location of maximum bending and maximum axial stress. The summation of stresses for combined stress has been computed at the depth which yields the maximum combined stress, generally this will occur close to the top of the first hard soil layer. For the higher overpressure of 300 psi, this may not be so. Figures 4.1 through 4.5 show how the maximum combined stress varies with casing length for overpressures of 50 psi, 100 psi and 300 psi for the

(Text continued on Page 38)

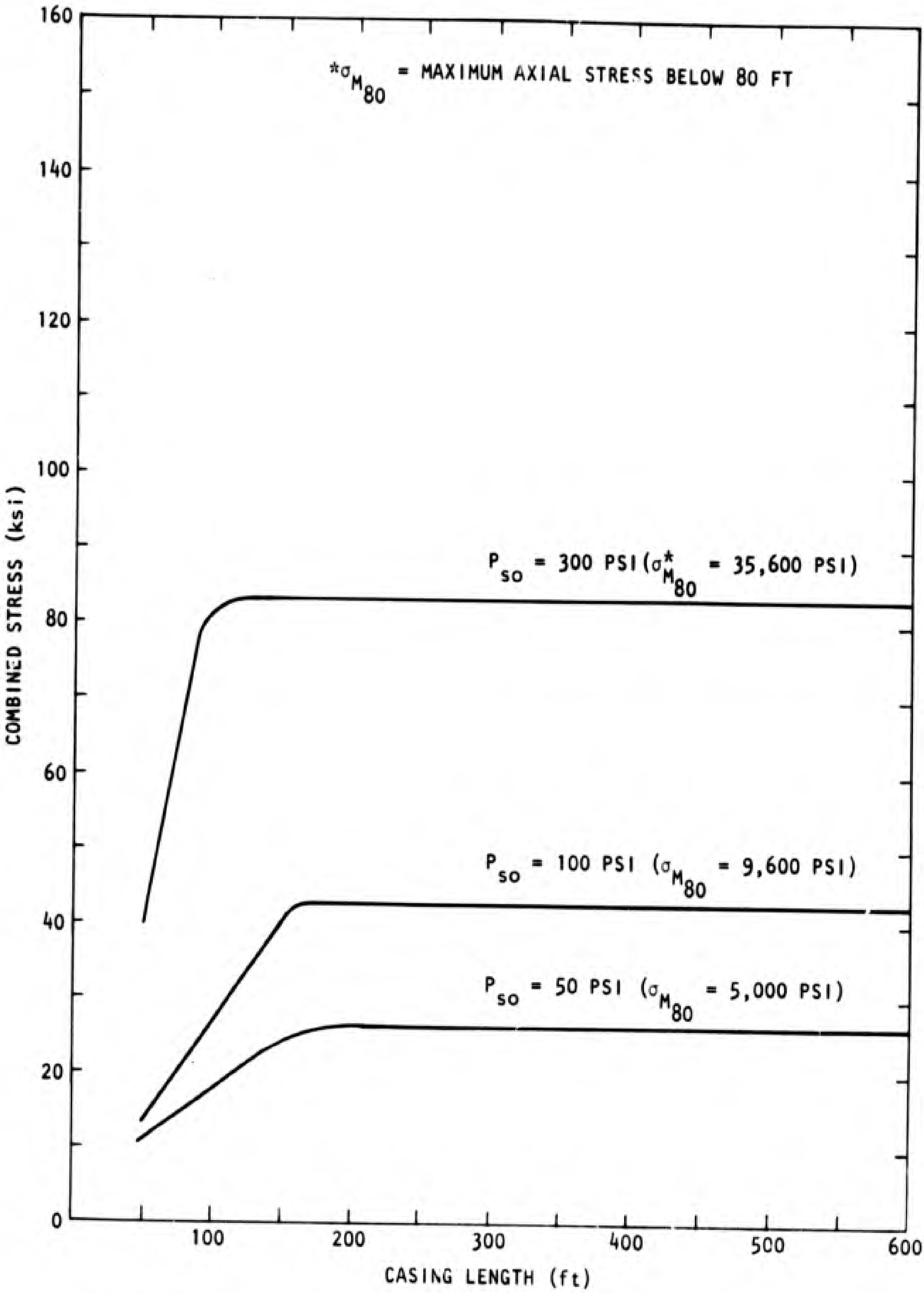

FIGURE 4.3 MAXIMUM STRESS VERSUS CASING LENGTH, PROFILE B

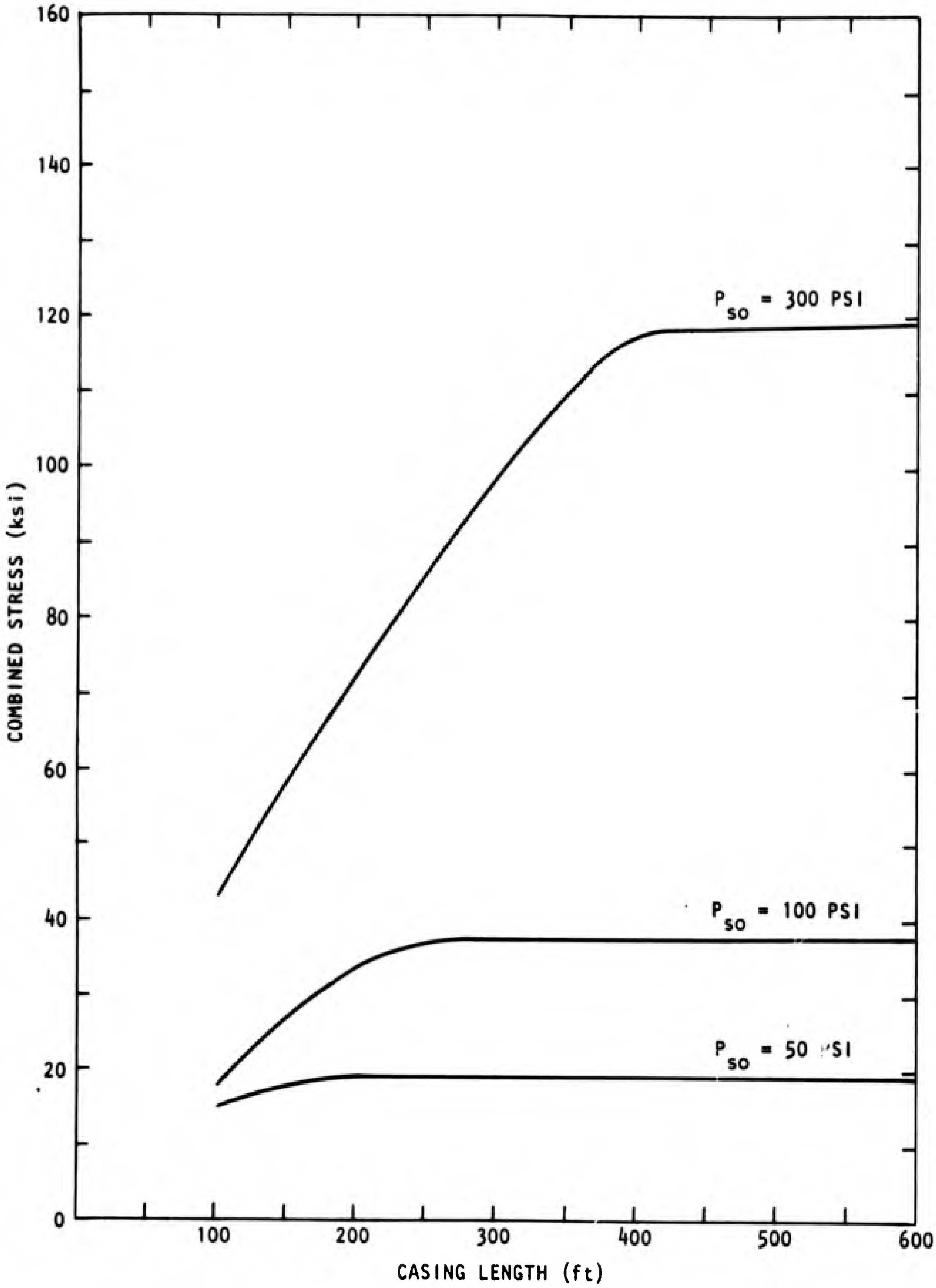

FIGURE 4.4 MAXIMUM STRESS VERSUS CASING LENGTH, PROFILE D

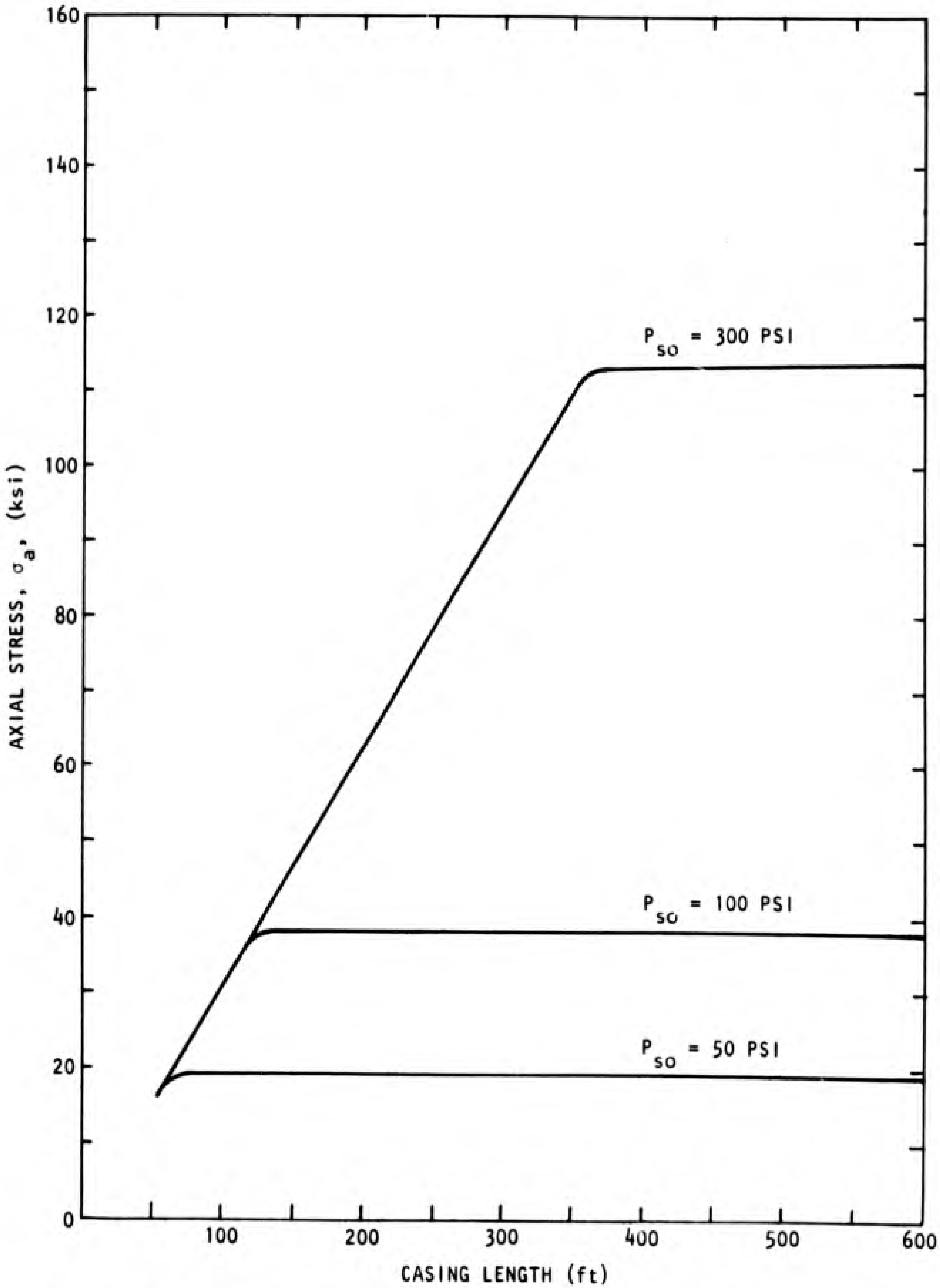

FIGURE 4.5 MAXIMUM AXIAL STRESS VERSUS CASING LENGTH, CLAY (TYPE I)

different soil profiles. It is seen that at a certain casing length and overpressure the maximum combined stress becomes a constant. This is the casing length at which the strain method and the friction method give approximately the same stress.

Table 4.3 shows the casing length L at which the maximum combined stress σ_c(max) becomes a constant. The length and maximum combined compressive stresses are tabulated for three overpressures and four soil profiles.

TABLE 4.3 MAXIMUM COMBINED STRESSES VERSUS CASING LENGTH AND OVERPRESSURE FOR 20-MT WEAPON YIELD

OVERPRESSURE (psi)	PROFILE A		PROFILE B		PROFILE D		CLAY I	
	L (ft)	$\sigma_{c\,max}$ (ksi)	L (ft)	$\sigma_{c\,max}$ (ksi)	L (ft)	$\sigma_{c\,max}$ (ksi)	L (ft)	$\sigma_{c\,max}$ (ksi)
50	400	33	160	27	200	19	70	19
100	500	62	160	43	250	38	130	38
300	600	144	100-160	83	450	119	370	114

The table shows further that the maximum combined axial stresses caused by overpressures up to 100 psi and weapon yields up to 20 megatons, are within allowable limits for all soil-layer combinations.

For an overpressure of 300 psi the combined stresses developed in the casing exceed the allowable dynamic yield strength for steel; however, in the evaluation of stresses in the well casing, an indicated elastic stress of 144 ksi will cause a plastic strain of only 2.4 times the yield strain of a steel with a 60 ksi dyanmic yield strength. This should not be destructive in this design.

4.2.4.5 <u>Axial Stress Versus Soil Pressure and Effective Modulus</u>. Figure 4.6 gives the relation between the allowable axial dynamic stress and vertical soil pressure versus the effective modulus. This figure is based upon the strain-stress relationship discussed in Section 6.2(b), and it only indicates

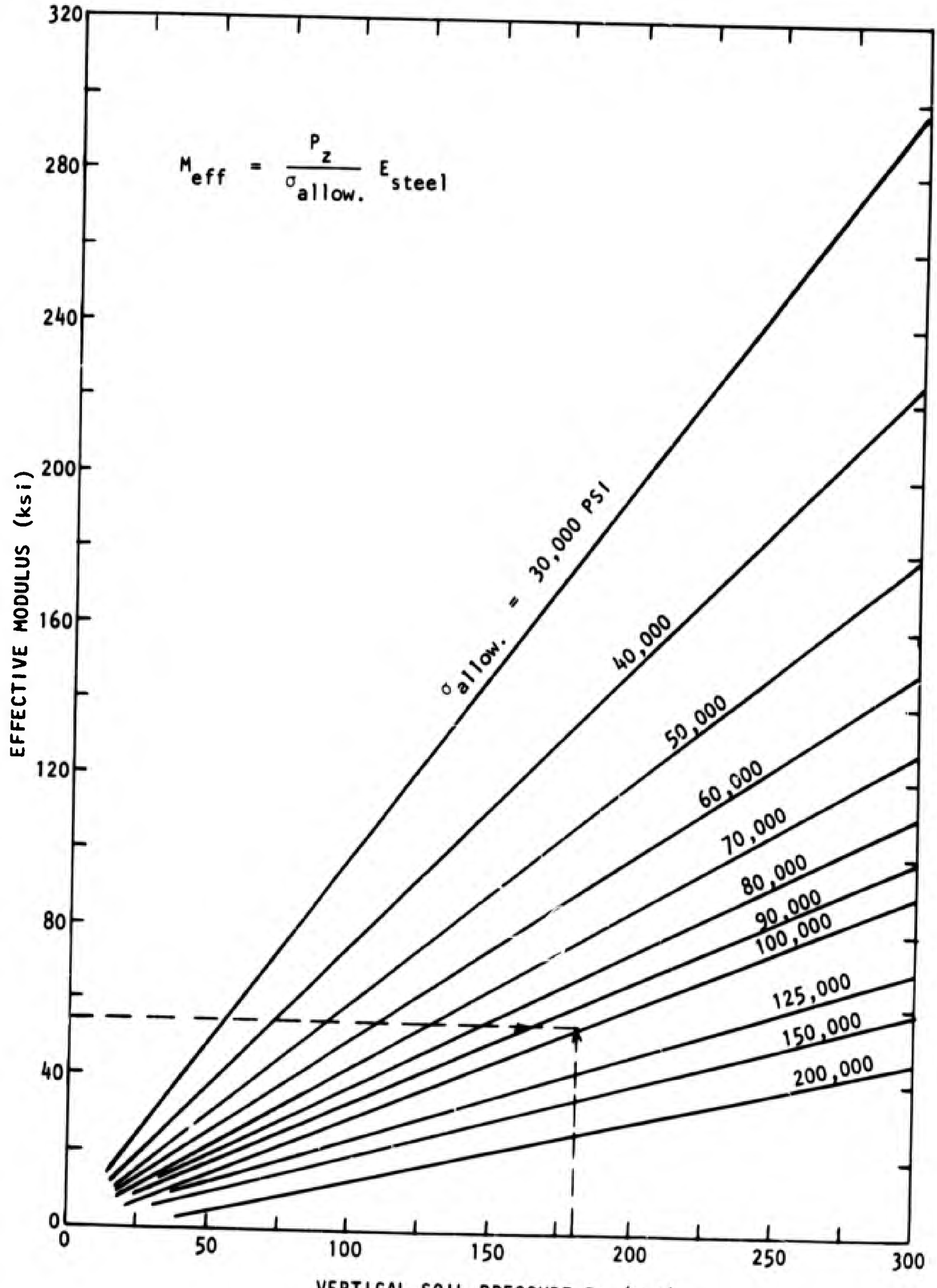

FIGURE 4.6 DYNAMIC AXIAL STRESS AND VERTICAL SOIL PRESSURE VERSUS EFFECTIVE MODULUS

the maximum expected axial stress in the casing caused by a certain vertical soil pressure p_z and an effective modulus. The vertical soil pressure and the effective modulus are found as outlined in Appendix B.

As an example, at a point on the casing where the effective modulus M = 55 ksi and the vertical soil pressure p_z = 180 psi, the absolute maximum axial stress would be 100,000 psi. This graph is only intended as a guide in approximating casing stresses and evaluating the variation in stress with soil pressure and effective modulus.

4.2.5 Stresses in Discharge Pipe

The static and dynamic stresses in the discharge pipe for the integral well are listed in Table 6.1 for 100 psi and 300 psi overpressure. The maximum stresses caused by 100 psi and 300 psi overpressure are listed in Table 4.4 for three lengths of discharge pipe. The different soil profiles yield about the same vertical free-field accelerations, thus the stress in the discharge pipe will be approximately the same for all soil profiles.

TABLE 4.4 DYNAMIC STRESS IN DISCHARGE PIPE

LENGTH OF DISCHARGE PIPE (ft)	STRESS (ksi)	
	P_{so} = 100 psi	P_{so} = 300 psi
65	13.3	43.9
215	17.3	67.0
1615	24.2	76.0

The dynamic stress in the upper part of the well casing due to the response of the discharge pipe will be approximately half that of the discharge pipe. The stresses due to downdrag in this part of the casing are small.

4.3 RESULTS - GEL-ISOLATED CONCEPT

4.3.1 Summary

The dynamic stress analyses of the well casing (6-in. Schedule 80 pipe), the discharge pipe (4-in. Schedule 80 pipe), and other parts of the gel-isolated well system do not indicate any destructive stresses. The maximum bending stresses occur in the upper part of the casing and may reach a value of approximately 48.6 ksi for an overpressure of 300 psi and a weapon yield of 20 megatons. The bending stresses occurring below a depth of approximately 50 feet are negligible. The axial stresses reach a value of approximately 17.5 ksi in the upper part of the casing, thus the maximum combined stress may reach a value of 66 ksi as an upper bound.

For an overpressure of 100 psi and a weapon yield of 20 megaton the maximum bending stress in the casing is 16.6 ksi and the axial stresses are 3.5 ksi. The maximum combined stress may approach 21 ksi as an upper bound.

4.3.2 Shock Spectra Results

The free-field shock spectra for 20 selected cases are summarized in Tables 4.5 through 4.9, and the shock spectras are shown in Appendix C. The tabulated values represent the peak vertical and horizontal motions for the air blast induced motions combined with the random motion.

All the cases analyzed for the soil profiles A, B, and E2 resulted in superseismic conditions. The stiff saturated sand (V) layer in the soil profile E1 caused outrunning condition at the 100 psi overpressure, but not for a 300 psi overpressure. The rock layer in the profiles DD1 and DD2 caused outrunning conditions at the target station for all the cases analyzed.

4.3.3 Displacements

The free-field displacements indicated for the soil profiles A and B by the shock spectra analysis agree with those obtained for the integral analysis.

(Text continued on Page 47)

TABLE 4.5 SHOCK SPECTRA DATA FOR FREE-FIELD VERTICAL AND HORIZONTAL MOTION

	CASE Soil-L-W-P_{so}	TARGET DEPTH (FT)	ACCELE-RATION (G_s)	VELOCITY (IPS)	DISPLACE-MENT (IN.)	RANGE OF RESONANCE MAX. DISPLACE-MENT	RANGE OF RESONANCE FREQUENCY (CPS)
VERTICAL	A-50-20-100	10 30 60	57 21 9	81 78 46	5.0 4.3 3.7	6.4 5.5 4.7	1-3 1-3 0-2
VERTICAL	A-50-20-300	10 30 60	152 52 23	281 262 151	16.2 14.0 12.0	20.6 17.8 15.1	1-3 1-3 0-2
VERTICAL	A-1600-20-100	10 800 1600	57 1 1	81 24 15	8.2 3.8 0.4	10.4 4.8 .5	0-2 0-1 2-6
VERTICAL	A-1600-20-300	10 800 1600	153 2 1	279 51 30	26.1 7.6 0.92	33.3 9.5 1.16	0-2 0-1 1-5
HORIZONTAL	A-50-20-100	10 30 60	57 21 9	54 52 31	2.0 1.7 1.6	2.4 2.1 1.9	1-6 2-6 1-4
HORIZONTAL	A-50-20-300	10 30 60	152 52 23	188 175 101	6.4 5.5 5.0	7.8 6.8 6.1	2-6 2-7 1-4
HORIZONTAL	A-1600-20-100	10 800 1600	57 1 1	54 16 10	3.2 1.60 0.16	4.0 1.9 0.19	1-4 0-2 3-12
HORIZONTAL	A-1600-20-300	10 800 1600	153 2 1	187 34 20	10.3 3.2 0.39	12.7 3.8 0.47	1-4 1-2 3-10

SUPER-SEISMIC CONDITION AT TARGET STATION FOR ALL CASES

TABLE 4.6 SHOCK SPECTRA DATA FOR FREE-FIELD VERTICAL MOTION

CASE Soil-L-W-P_{so}	TARGET DEPTH (FT)	ACCELERATION (G_s)	VELOCITY (IPS)	DISPLACEMENT (IN.)	RANGE OF RESONANCE: MAX. DISPLACEMENT	RANGE OF RESONANCE: FREQUENCY (CPS)
B-50-20-100	10 30 60	46 16 14	71 69 78	3.0 2.2 1.0	3.8 2.6 1.2	0-1 0-1 0-1
B-50-20-300	10 30 60	125 43 34	262 246 271	12.3 8.0 4.0	15.6 9.5 4.5	0-1 0-1 0-1
B-200-20-100	10 70 200	46 7 2	71 65 21	3.0 .91 .34	3.8 1.16 .43	1-4 3-13 2-9
B-200-20-300	10 70 200	125 17 4	262 219 60	12.3 3.3 .8	15.6 4.2 1.0	1-4 3-12 3-12
B-1600-20-100	10 800 1600	46 1. .08	71 7 4	3.0 .47 .08	3.8 .59 .10	1-4 1-2 2-8
B-1600-20-300	10 800 1600	126 1 0.1	263 14 8	12.4 .9 .2	15.8 1.2 .25	1-4 1-2 2-7

SUPER-SEISMIC CONDITION AT TARGET STATION FOR ALL CASES

TABLE 4.7 SHOCK SPECTRA DATA FOR FREE-FIELD HORIZONTAL MOTION

CASE Soil-L-W-P_{so}	TARGET DEPTH (FT)	ACCELE-RATION (G_s)	VELOCITY (IPS)	DISPLACE-MENT (IN.)	RANGE OF RESONANCE MAX. DISPLACE-MENT	RANGE OF RESONANCE FREQUENCY (CPS)
B-50-20-100	10 30 60	46 16 14	48 46 52	1.2 .7 .4	1.46 .8 .5	1-3 1-3 1-3
B-50-20-300	10 30 60	125 43 34	176 165 181	4.8 2.9 1.4	6.0 3.4 1.7	1-3 1-3 1-3
B-200-20-100	10 70 200	46 7 2	48 43 14	1.2 .36 .14	1.46 .44 .17	2-8 6-25 5-18
B-200-20-300	10 70 200	125 17 4	175 146 40	4.8 1.3 .33	6.0 1.6 .40	2-8 6-23 6-24
B-1600-20-100	10 800 1600	46 1. .08	48 4 3	1.2 .20 .03	1.47 .24 .04	2-8 1-4 4-17
B-1600-20-300	10 800 1600	126 1. 0.12	176 9 6	4.9 .39 .08	6.0 .47 .1	2-8 1-5 3-13

SUPER-SEISMIC CONDITION AT TARGET STATION FOR ALL CASES

TABLE 4.8 SHOCK SPECTRA DATA FOR FREE-FIELD VERTICAL MOTION

CASE Soil-L-W-P_{so}	TARGET DEPTH (FT)	ACCELERATION (G's)	VELOCITY (IPS)	DISPLACEMENT (IN)	RANGE OF RESONANCE	
					MAXIMUM DISPLACEMENT	FREQUENCY (CPS)
E1-200-1-300 Superseismic	10	145	264	3.90	4.96	3-12
	30	17	80	1.40	1.78	3-10
	75	9	41	1.37	1.73	1-5
	160	4	28	1.21	1.52	1-4
E2-200-1-300 Superseismic	10	145	264	7.72	9.82	2-6
	30	47	227	4.97	6.36	2-8
	75	6	41	1.38	1.74	1-5
	160	3	28	1.21	1.52	1-4
E1-200-20-100 Outrunning	10	88	94	2.11	2.59	2-8
	30	11	32	1.34	1.65	1-4
	75	7	21	1.40	1.69	1-2
	160	4	19	1.22	1.48	1-2
E1-200-20-300 Superseismic	10	152	278	4.64	5.90	3-11
	30	19	92	3.22	4.09	1-5
	75	11	54	3.16	3.98	1-3
	160	6	45	2.78	3.51	1-2
ER-200-20-300 Outrunning	10	84	116	.86	1.06	6-24
	30	30	60	.85	.79	4-17
	75	25	68	.59	.72	4-18
	160	5	15	.53	.64	1-5
DD1-200-20-100 Outrunning	15	53	57	1.58	1.94	2-6
	35	3	5	1.35	1.66	0-1
	75	11	21	1.47	1.77	1-2
	160	5	19	1.29	1.56	1-2
DD1-200-20-300 Outrunning	15	141	195	4.39	5.41	2-8
	35	6	16	3.77	4.64	0-1
	75	26	68	4.11	4.96	1-3
	160	12	56	3.65	4.40	1-2
DD2-200-20-300 Outrunning	15	141	195	4.59	5.65	2-8
	35	62	183	2.91	3.58	3-11
	75	5	19	3.91	4.72	0-1
	160	10	56	3.57	4.31	1-2
CANADA -50 Superseismic	10	20	62	.89	1.13	3-12
	23	2	16	.15	.18	5-19
	40	1	8	.13	.16	2-10
	70	1	5	.09	.11	2-8
	100	0	3	.06	.08	2-9
CANADA -100 Superseismic	10	19	104	1.44	1.83	3-13
	23	4	31	.41	.52	3-13
	40	2	15	.36	.45	2-6
	70	1	9	.24	.31	1-6
	100	1	6	.16	.21	1-6

TABLE 4.9 SHOCK SPECTRA DATA FOR FREE-FIELD HORIZONTAL MOTION

CASE Soil-L-W-P_{so}	TARGET DEPTH (FT)	ACCELERATION (G's)	VELOCITY (IPS)	DISPLACEMENT (IN)	RANGE OF RESONANCE: MAXIMUM DISPLACEMENT	RANGE OF RESONANCE: FREQUENCY (CPS)
E1-200-1-300 Superseismic	10	145	177	1.54	1.84	6-24
	30	17	54	.58	.68	5-21
	75	9	27	.58	.69	2-9
	160	4	18	.51	.61	2-7
E2-200-1-300 Superseismic	10	145	177	3.04	3.74	3-12
	30	47	152	1.95	2.41	4-16
	75	6	27	.58	.70	2-9
	160	3	18	.51	.61	2-7
E1-200-20-100 Outrunning	10	88	63	1.02	1.19	4-16
	30	11	22	.65	.76	2-9
	75	7	14	.76	.85	1-5
	160	4	12	.66	.74	1-5
E1-200-20-300 Superseismic	10	152	186	1.83	2.25	5-21
	30	19	62	1.27	1.56	3-10
	75	11	36	1.33	1.60	1-5
	160	6	30	1.17	1.41	1-5
ER-200-20-300 Outrunning	10	84	77	.42	.48	12-48
	30	30	40	.31	.36	8-33
	75	25	45	.32	.36	9-35
	160	5	10	.29	.32	2-9
DD1-200-20-100 Outrunning	15	53	38	.77	.89	3-13
	35	3	3	.66	.76	0-1
	75	11	14	.79	.89	1-4
	160	5	12	.70	.79	4
DD1-200-20-300 Outrunning	15	141	130	2.14	2.48	[illegible]-16
	35	6	11	1.84	2.13	0-2
	75	26	45	2.22	2.50	1-5
	160	12	37	1.97	2.22	1-5
DD2-200-20-300 Outrunning	15	141	130	2.23	2.59	4-15
	35	62	122	1.41	1.64	6-23
	75	5	12	2.11	2.38	0-1
	160	10	37	1.93	2.17	1-5
CANADA -50 Superseismic	10	20	41	.35	.43	6-25
	23	2	10	.06	.07	10-38
	40	1	5	.05	.06	5-19
	70	1	3	.04	.05	4-16
	100	0	2	.03	.03	4-18
CANADA -100 Superseismic	10	19	70	.57	.70	6-26
	23	4	21	.16	.20	7-27
	40	2	10	.15	.18	3-13
	70	1	6	.10	.12	3-11
	100	1	4	.07	.08	3-12

For soil profiles where superseismic conditions will occur the initial displacement of the target will be downward. The maximum downward displacement of the well head floor is 30 to 40 inches as indicated by the Case A-1600-20-300. This value is unrealistic as a 1600 feet deep soil layer with soil properties corresponding to dry sand (III) is not likely. A value of 15 to 20 inches for the downward displacement is closer to the maximum that may be developed by similar weapon effects. Where outrunning conditions can be developed the initial displacement of the targets will be upward. The maximum upward displacement of the well head floor as indicated by the Case DD2-200-20-300, Table 4.8, may reach a value of 5 to 6 inches.

4.3.4 Accelerations and Velocities

The maximum values of the free-field accelerations and velocities at different target depths are tabulated in the Tables 4.5 through 4.9 for all the cases investigated. The horizontal and vertical accelerations at a 10 foot depth produced by a 300 psi overpressure varies from 125 to 152 g's for both superseismic and outrunning conditions. For an overpressure of 100 psi the accelerations at a 10 foot depth varies from 50 to 60 g's. However, Case E1-200-20-100 (outrunning) yields a value of 88 g's at the 10 foot depth.

Figures 4.7 and 4.8 show the variation of average maximum horizontal acceleration with depth for the profiles A and B. At 50 foot depth the average accelerations for 300 and 100 psi overpressure are 30 and 10 g's respectively. Therefore any horizontal response analysis of the well casing below this depth was not considered necessary.

4.3.5 Casing Stresses

All the stress values given in this subsection refer to a 6-inch Schedule 80 well casing and a 4-inch Schedule 80 discharge pipe.

4.3.5.1 Bending Stresses. The bending stresses given in Table 4.10 were found as described in Subsection 7.4.2, and the method of analysis is given

(Text continued on Page 51)

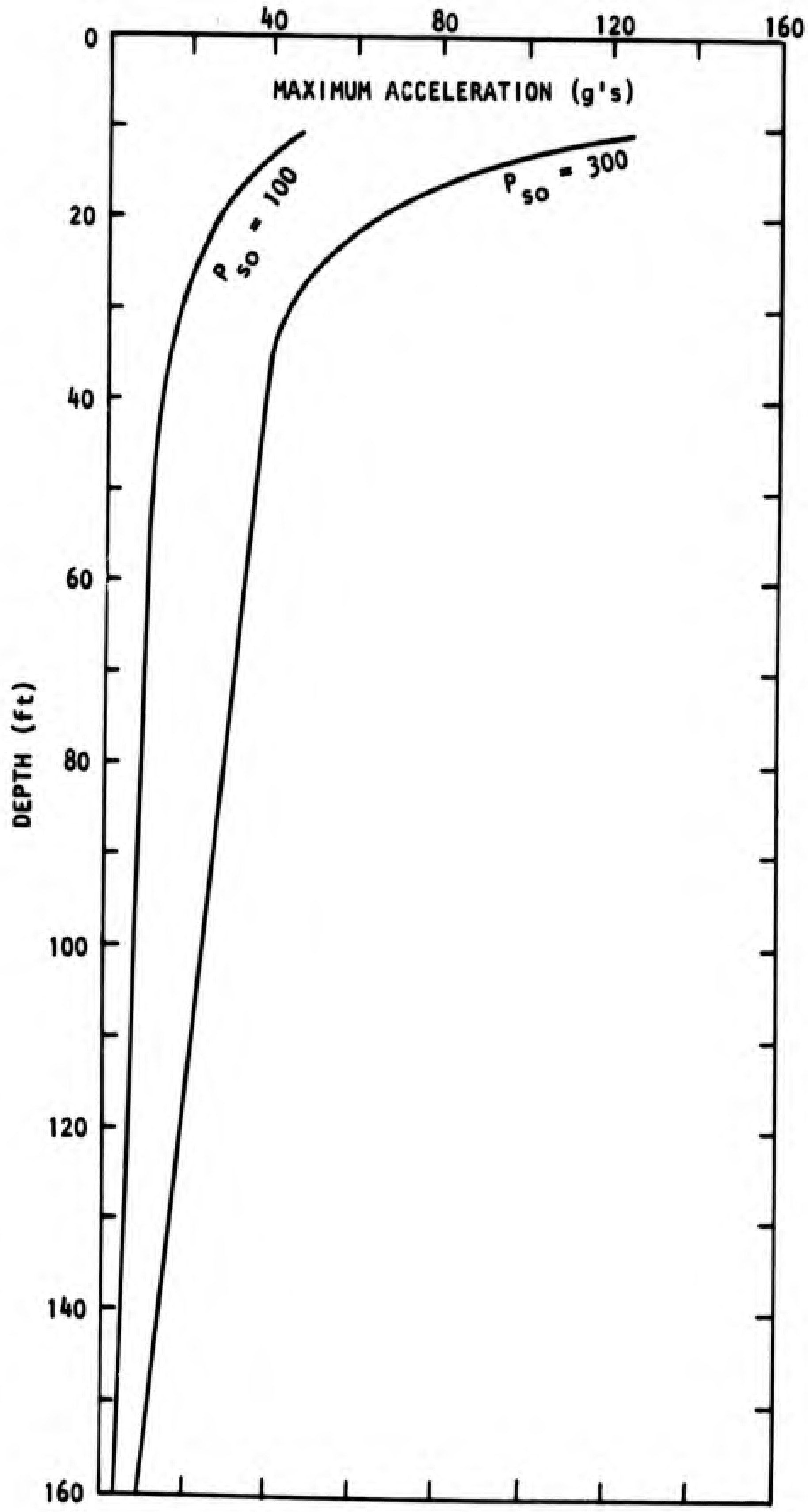

FIGURE 4.7 MAXIMUM HORIZONTAL ACCELERATION VERSUS DEPTH SOIL PROFILE A

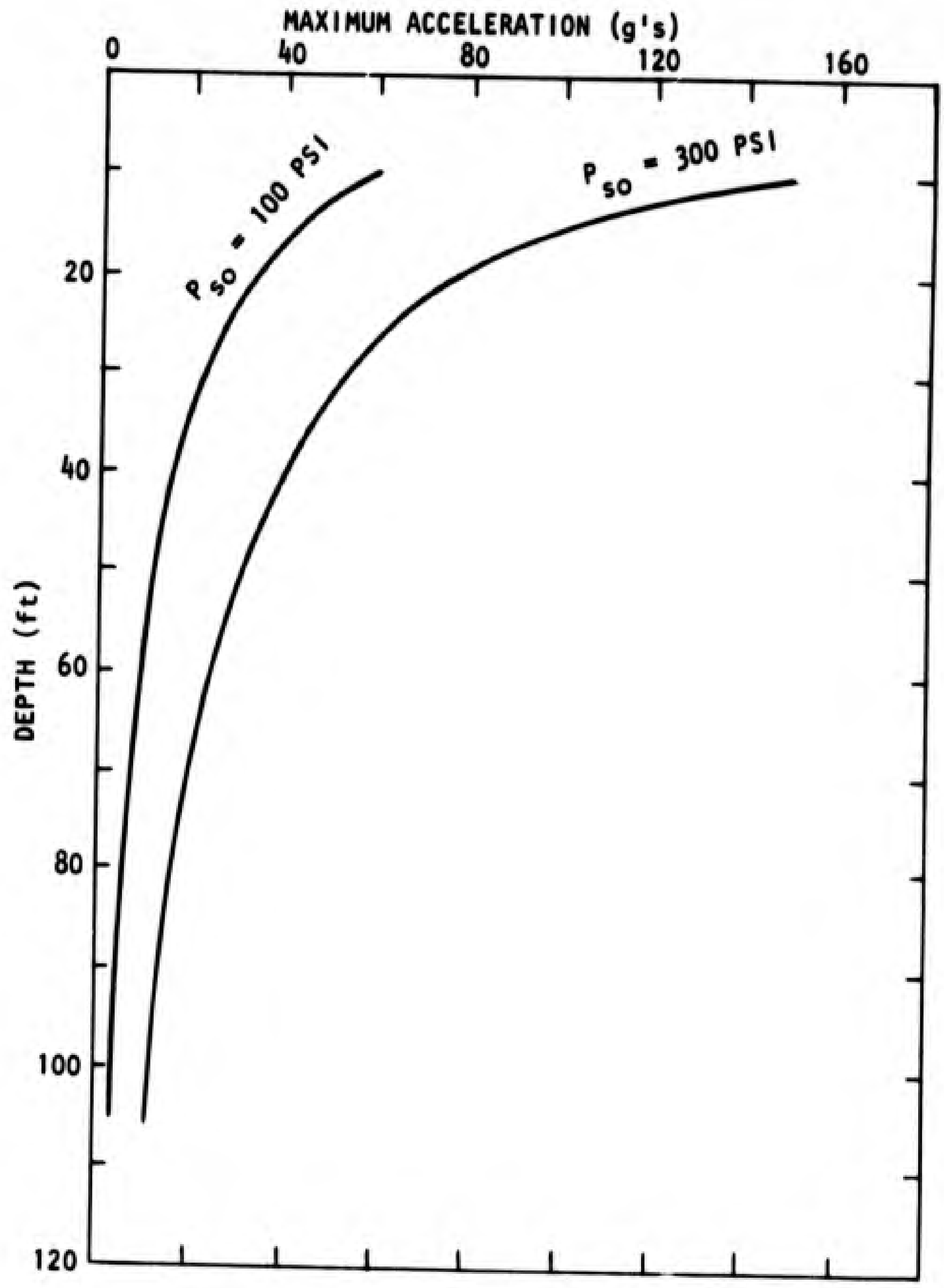

FIGURE 4.8 MAXIMUM HORIZONTAL ACCELERATION VERSUS DEPTH SOIL PROFILE B

TABLE 4.10 MAXIMUM STRESSES IN GEL-ISOLATED SYSTEM

CASE SOIL-L-W-P_{so}	SHOCK VELOCITY CONDITION	WELL CASING F_a DOWNDRAG (ksi)	WELL CASING F_a DYNAMIC (ksi)	WELL CASING F_b DYNAMIC (ksi)	WELL CASING $F_{comb} = F_a + F_b$ DYNAMIC (ksi)	DISCHARGE PIPE F_{comb} (Static + Dynamic) (ksi)
A-50-20-100	Superseismic	1.0	4.8	15.8	20.6	5.2
A-1600-20-100	Superseismic	9.2	7.3	15.8	18.2	16.0
A-50-20-300	Superseismic	1.0	12.3	44.0	56.3	12.8
A-1600-20-300	Superseismic	9.2	6.0	44.0	50.0	10.0
B-50-20-100	Superseismic	1.0	4.2	16.0	20.2	6.4
B-200-20-100	Superseismic	3.0	3.8	16.0	19.8	5.1
B-1600-20-100	Superseismic	3.0	2.3	16.0	18.3	5.6
B-50-20-300	Superseismic	1.0	13.7	48.6	62.3	13.1
B-100-20-300	Superseismic	1.2	17.5	48.6	66.1	17.9
B-200-20-300	Superseismic	3.0	6.6	48.6	55.2	7.6
B-1600-20-300	Superseismic	3.0	4.6	48.6	53.2	11.2
E1-200-1-300	Superseismic	3.0	4.1	37.0	41.1	6.4
E2-200-1-300	Superseismic	3.0	3.5	45.0	48.5	4.0
E1-200-20-100	Outrunning	3.0	3.5	16.6	19.9	4.0
E1-200-20-300	Superseismic	3.0	4.8	40.0	44.8	5.3
ER-200-20-300	Outrunning	3.0	8.0	35.0	43.0	12.3
DD1-200-20-100	Outrunning	3.0	4.1	10.3	14.5	6.4
DD1-200-20-300	Outrunning	3.0	9.3	37.0	46.3	14.3
DD2-200-20-300	Outrunning	3.0	4.0	45.0	49.0	4.5
CANADA-50	Superseismic	2.0	3.8	7.0	10.8	
CANADA-100	Superseismic	2.0	3.8	7.0	10.8	

in Appendix D. These stresses are considered to be on the conservative side, and only the cases that yield the highest stresses are listed. The contributions from the higher modes was considered and was found to be very small.

The soil profiles A and B and an overpressure of 300 psi caused bending stresses approaching 50 ksi in the uppermost part of the casing. The harder soil profiles E and DD indicated smaller stresses, 40 to 45 ksi. For an overpressure of 100 psi the highest bending stresses were found to be 16 to 17 ksi for both the softer and the harder soil profiles. Below a depth of 30 feet the bending stresses will be relatively small.

4.3.5.2 Axial Stresses (Refer to Table 4.10). The axial stresses were obtained as described in Subsection 7.4.3, and the method of analysis is given in Appendix D. Soil profiles A and B yield the largest axial stresses. The shorter well casings experience the highest stresses. A 50 foot casing subjected to a 300 psi overpressure may experience an axial stress of 14 ksi. The deeper wells will experience very small axial stresses since the free-field accelerations below a depth of 150 to 200 feet are attenuated appreciably. Only the two first modes were used in the stress calculations, as the higher modes are of little importance.

4.3.5.3 Downdrag Stresses. The downdrag stresses listed in Table 4.10 are based on a ratio $R_g = 20$ (R_g = ratio of dynamic shear strength of gel to static shear strength of gel, see Section 7.4.4). The listed values are the stresses developed at the top of the cement grouting. No downdrag stresses will be developed at the top of the casing where the maximum bending stresses occur.

4.3.5.4 Combined Stresses. The maximum combined stresses are developed in the upper 20 to 30 feet of the casing and consist of a combination of the dynamic bending and axial stresses. The maximum combined stress was found to be 66 ksi for Case B-100-20-300. All other cases investigated for 300 psi overpressure yielded somewhat smaller values. For the cases where outrunning conditions occurred the combined stress approached 50 ksi. The cases investigated for an overpressure of 100 psi yielded a combined stress of approximately 21 ksi.

At the top of the cement grouting the maximum combined casing stress is the sum of the downdrag stress, the dynamic axial stress, and, in the case of the outrunning condition, the static stress due to the dead load of the casing. It is seen from Table 4.10 that the combined stress at the top of the cement grouting will not reach critical values.

4.3.5.5 Stresses in Discharge Pipe (Refer to Table 4.10). The stresses developed in the discharge pipe are taken as the sum of the dynamic stress and the static stress. No critical values were found for the stresses developed in the discharge pipe for the gel-isolated well concept. The contributions from the higher modes are small and can be neglected.

SECTION 5

MATERIAL AND COMPONENT PROPERTIES

5.1 INTRODUCTION

This section summarizes the results of an evaluation of the physical and material properties of the gel and the characteristics of the mechanical components which make up the proposed well concepts (see Figure 1.1 to 1.3). The properties are used in the survivability analysis of the well concepts.

5.2 GEL

The gel-isolated well concept utilizes a gel material in the annulus between the casing and the walls of the well bore to reduce axial down-drag forces on the casing resulting from vertical ground motion. The gel is typical of the material used in the oil well industry to prevent damage from subsidence and/or corrosion and to facilitate casing recovery when a well is abandoned.

5.2.1 Gel Formation

The basic structure of a gel material depends on the stability of a colloidal dispersion. Colloids are defined as matter in a fine state of subdivision and compare in size with large molecules or groups of molecules. Gels are formed from colloidal solutions (below 10 percent concentration) by reducing the solubility of the colloidal material to an extent sufficient to enable the particles to link together. This results in a gel structure in which the colloidal particles form a connected skeleton interpenetrated by the dispersing liquid as shown in Figure 5.1, taken from Reference 10.

Gels can be formed in various ways. One method is spontaneous swelling of a substance when brought into contact with a solvent. Another method is similar to the coagulation process; except that in a gel formation the particles set to a coherent structure before large aggregates can be formed which could settle under the influences of gravity.

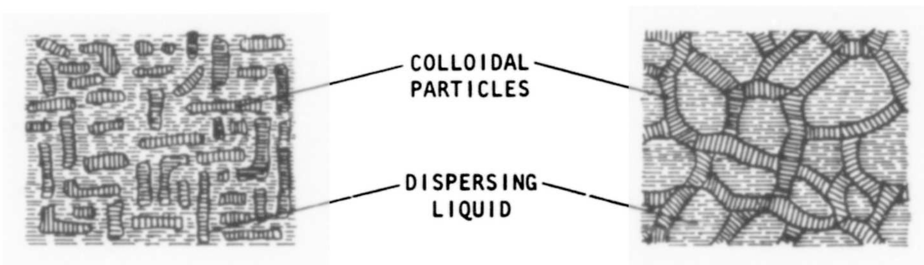

(a) COLLOIDAL DISPERSION

(b) GEL STRUCTURE - COLLOIDAL PARTICLES FORM CONNECTED STRUCTURE

FIGURE 5.1 FORMATION OF GEL

Gels can be identified as rigid, elastic and thixotropic according to their structural properties. Thixotropy can be defined as a "process of softening caused by remolding, followed by a time-dependent return to the original harder state." Thixotropic gels are those that can pass into colloidal solutions as the result of mechanical agitation. Certain clays, such as bentonite, tend to form thixotropic gels. The types of gels associated with oil well drilling are normally formed by the coagulation process described above and are classified as thixotropic. Pastes are concentrated dispersions of fine solid particles in a liquid continuum. There is no sharp distinction between gels and pastes. Pastes include many materials common in engineering practice such as putty, paints, clays, dough and drilling muds.

Gels that are normally used for well packing are either of the oil-base or water-base type in which the formulation can vary the consistency from a heavy fluid to a stiff jello-like substance. The oil-base is usually preferred over the water-base in oil well application since it is more stable, is water-insoluble and there is less chance of loss by seepage into the soil. However, its use with a water well is not recommended because of the chance that the water supply may become unpotable due to a petroleum taste in the water. This may not be objectionable in the operation of a hardened facility where the primary purpose of the well is to provide cooling water. However, the possibility of contaminating a public water supply must also be considered.

The water-base gels are safe to use in conjunction with a water well, but are susceptible to dilution or erosion by ground water, especially in the case of flowing water as might occur in a perched water table that is penetrated by the well. In addition, the water-base gels tend to diffuse into the soil media and the gel can dry out and harden in the vicinity of the well bore. This would reduce its effectiveness as a low shear strength material.

5.2.2 Density and Stiffness

Oil-base gels are made from oil, chemicals and chemical compounds combined to impart specific properties as required to protect the casing. A weigh material is included in the formulation to give the gel a weight slightly greater than salt water, or enough to confine any water to their respective formations. The density of an oil-base gel will normally average about 70 pounds per cubic foot.

In addition to density control, the gels are designed to generate sufficient shear strength to support material that might slough from the walls of the well bore. It has been found that a shear strength of approximately 1/2 pound per square foot will suspend the material and prevent it from sinking to the bottom of the hole.*

5.2.3 Shear Strength

The thixotropic characteristics of gels make them an ideal material for use in well drilling to prevent hole sloughing and provide lubricating qualities which reduce friction to a minimum. Results of laboratory tests for the shear strength of gels indicate shear strengths of from 0.40 lbs per sq ft to 4.75 lbs per sq ft depending on the type of gel and its

---

*Calada Materials Company, Long Beach, California formulation. This corresponds to 0.0028 to 0.033 lb per sq in., but the average value probably falls nearer to the lower bound. The gel formulations of interest in this study will favor the lower shear strengths.

An interesting comparison of shear strengths determined in the laboratory with available field experience in oil well casing recovery can be made from information contained in References 12 and 13.

a. Reference 12 reports that a drag force of 40,000 pounds in excess of the calculated weight of the casing was required to recover 8,450 ft of 7-inch casing installed with an oil-base pack extending over a length of 3,350 ft. Assuming the shear stress acting on the casing was uniform over the depth of the pack, a shear stress of 6 lbs per sq ft was required to overcome the drag force.

b. Reference 13 reports on another installation in which a drag force of 40,000 lbs in excess of the casing weight was required to lift 10,600 ft of 5-½-inch casing packed for 9,570 ft. This corresponds to a unit shear force of 2.9 lbs per sq ft.

The shear strengths estimated in both laboratory tests and oil well casing recovery operations are for static loading conditions. In addition, when attempting to recover casings, experience has shown that the casing must be "worked" to break the gel strength over the depth of the casing. Simply taking a strain on the pipe breaks the bond near the surface first and, considering the tensile strength of the casing, it may be impossible to break the gel to the depth at which the casing is free without failing the casing. The tendency of gel to stick to the casing wall is probably similar to the build-up of skin friction with time that has been experienced with piles driven into soft clay. It is believed that this increased cohesion is assisted by thixotropic hardening. Prior to pulling on the casing, it is first "worked", either with the draw bar of the drilling rig or by use of hydraulic jacks. Casings may be "worked" for 10 to 12 hours in some extreme cases. After "working", the casing is then sheared by explosives just above the cement seal or at the location where it has been determined that the casing is free. Using explosives to cut the casing also helps break down the shear strength of the gel. Experience has shown that once the first section of casing is out of the hole, the drag force drops off and only a force equal to the casing weight is required. This could result from the thixotropic characteristic of the gel in which mechanical agitation from withdrawing the casing causes the gel to pass into a colloidal solution.

Information on tests of the dynamic shear strengths of gels could not be determined from the manufacturers surveyed.* However, it is believed that the shear strength would be increased under dynamic loading. This can be demonstrated by trying to pull out a stick from a soft clay by using a quick tug or jerk. It is usually found that a slow steady pull will be more effective in overcoming the skin friction. This was also demonstrated by using actual samples of gels that were borrowed from the NCEL for use during the study. The effect of dynamic loading was very pronounced in a very stiff oil-base gel in which a glass rod was embedded. It was impossible to pull the rod out by a quick jerk due to fingers slipping; but there was no difficulty in pulling the rod out by a slow and steady pull. This was also observed to lesser degrees with the thinner gels. The sample that appeared to have the lowest shear strength was a water-base gel formulated by Calada Materials Company and identified as a 7 percent gel mixture (7 percent Bentonite by weight in water).

It is recommended that tests be made to determine the shear strength of gels based on dynamic loading. The tests should not be difficult to conduct and are ideally suited to shock test equipment available at the NCEL.

5.2.4 Modulus of Elasticity

The fact that liquid flows immediately under even a very small shear stress does not exclude the possibility of elastic forces in the liquid structure. The molecules in a liquid, as in an elastic solid, vibrate under stress about the equilibrium position before jumping to a new position. Because of the high fluidity of a liquid, the elastic response has no chance to be

*Oil Base, Inc., Houston, Texas
Calada Materials Co., Long Beach, California
International Materials and Chemical Corporation, Long Beach, California

effective under normal conditions, but elastic behavior can be observed if the time is very short (order of microseconds). With increasing viscosity of the liquid, the elastic response to shear stress becomes more significant; finally at very high viscosity, as in a pitch, it is more predominant than the flow.

The ratio of stress to strain is a constant characteristic of a material and is called modulus of elasticity. Since there are three main types of stress, (tension, compression and shear), there are three corresponding moduli of elasticity.

a. Tension - Young's Modulus, E

$$E = \frac{\sigma_t}{\varepsilon_t} \qquad \left(\frac{\text{tensile stress}}{\text{longitudinal strain}}\right)$$

b. Compression - Modulus of Compressibility or Bulk Modulus, K

$$K = \frac{\sigma}{\Delta v/v_o} \qquad \left(\frac{\text{hydrostatic pressure}}{\text{relative change in volume}}\right)$$

c. Shear - Modulus of Rigidity or Shear Modulus, G

$$G = \frac{\tau}{\gamma} \qquad \left(\frac{\text{shear stress}}{\text{shear strain}}\right)$$

Young's modulus is related to the bulk modulus K and the modulus of rigidity G by the relation:

$$\frac{1}{E} = \frac{1}{9K} + \frac{1}{3G}$$

For most soft materials as gels, pastes and putties, K is very large compared to G, and it follows that E = 3G. Such materials are regarded as incompressible because they do not compress to the extent to which they change their shape under the stress employed. For liquids which cannot sustain any pressure but a hydrostatic one for any length of time, the bulk modulus K is the only elastic modulus to be considered.

Representative bulk moduli are shown below for several liquids.

Liquid	Bulk Modulus, psi
Water	300,000
Oil	275,000
Glycerol	650,000

For comparison, the modulus of soil can vary from about 150,000 to 1×10^6 psi, while for rock, the values exceed 3×10^6 psi. The bulk modulus for the gels would approximate those for water or oil.

5.2.5 Viscosity

A second proportionality factor in the mechanics of viscous fluids is the coefficient of viscosity. Absolute or dynamic viscosity η is the resistance offered by a fluid to relative motion of its parts and is defined as a function of the time rate of internal slipping or distortion:

$$\eta = \frac{\tau}{d\gamma/dt}$$

where

τ = shear stress

$\frac{d\gamma}{dt}$ = rate of shear strain.

Fluids that follow the above equation are termed Newtonian liquids. They are shown in Figure 5.2 as a straight line similar to the stress-strain diagram for solids. The viscosity is a constant characteristic for each material, just as modulus of elasticity is a characteristic elastic constant for an elastic solid. Table 5.1 indicates typical values for the viscosity of some liquids and solids and compares these with an estimate of gel viscosity obtained from Calada Materials Company.

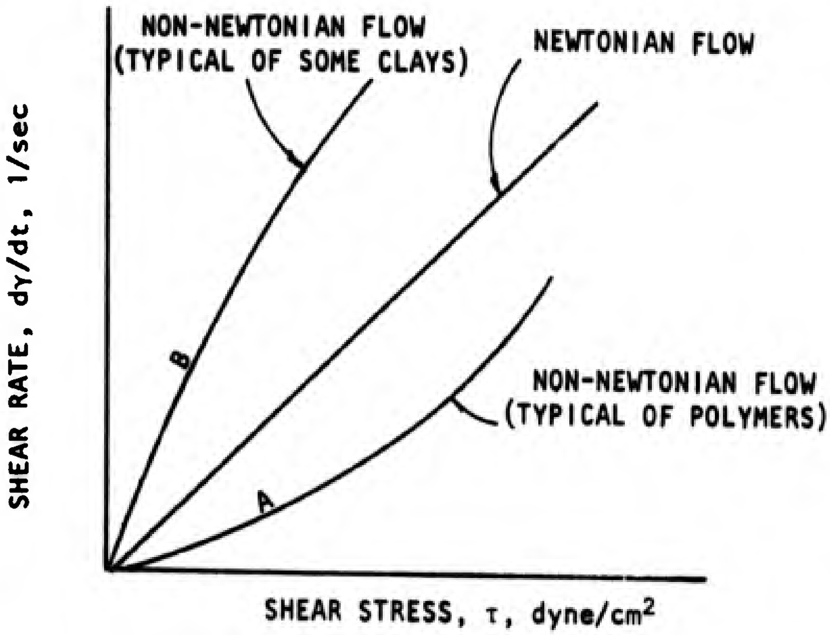

FIGURE 5.2 SHEAR RATE VERSUS STRESS FOR FLUIDS

If a material obeying Hook's law is deformed, the work expended in the deformation is completely conserved as strain work. When the load is released, the material will return to its original condition. In a Newtonian liquid the work done on the material is always expended and never recovered, resulting in a continuous flow. All work is dissipated and converted into heat.

TABLE 5.1 COMPARISON OF VISCOSITY

MATERIAL	TEMPERATURE (°C)	VISCOSITY (centipoises)
Water	14	1.17
Drilling Mud	-	15
Gel (colloidal solution)	-	100
Oil, light	15.6	100
Oil, heavy	15.6	600
Glycerin	14.3	1400
Wax	8	4.7×10^6
Pitch	15	1.3×10^{10}

The introduction of solid particles into a Newtonian liquid results in an increase of its viscosity. The increased viscosity is determined by the concentration of colloidal suspensions, how they interact with the solvent and the nature and surface characteristics of the particles.

In some liquids the viscosity is not constant but varies with the rate of shear or shear stress. These materials are referred to as non-Newtonian liquids. Figure 5.2 indicates this type of flow. The shape of Curve A shows that the viscosity of these materials decreases as the shearing rate or shearing stress increases. Curve B indicates a type of flow which is just the opposite. The increase in viscosity as the shear rate increases, as illustrated by Curve B, is representative of some clays and sands, and is believed to be the result of stiffening and hardening of the material when subjected to shearing action.

The increased resistance of the gel to rapid displacement is not only a function of its dynamic shear strength but also of its viscosity, which is comparable to the viscous resistance of liquids against rapid displacement.

5.2.6 Conclusions

The preceding discussions of viscosity, moduli of elasticity, general behavior of thixotropic materials, etc., was an attempt to establish a criterion for the dynamic shear strength of gel materials since this type of information is not available from the industry. It is thought that by relating the gels to known properties of other materials, an estimate of the required strengths could be made. Only very crude estimates can be made, however, and laboratory testing of the gels will be necessary to determine the required properties.

It is recommended that a water-base gel formulation be used for the application being considered. The formulation should be as fluid as possible when considering the limitations imposed by density requirements and need to support material that might slough from the surface of the well bore. Representative gel samples that meet these requirements should then be tested in the laboratory for static and dynamic strength characteristics, including resistance to pull-out.

5.3 SUBMERSIBLE PUMPS

5.3.1 Description

A submersible pump combines the pump and motor in a single unit containing everything but the controls. The unit is located at the bottom of the well with a discharge pipe and power cable leading to the surface. The pump is supported at the well head housing by the discharge pipe. The submersible pump is more efficient than any other pump since all power is used to lift water.

A series of impellers is normally used to raise the water which enters the pump through screened ports above the motor. Figure 5.3 shows the basic construction for two types of submersible pumps which are representative of several manufacturers. The units are made up of a pump section connected to a submersible motor to form an integral unit.

5.3.2 Pump

Usually the pump is a multi-stage centrifugal electric pump consisting of a series of stages keyed to a pump shaft. Each stage consists of an impeller and diffuser. A sufficient number of stages are used in each pump to generate the required head and discharge pressure. The basic difference between pump manufacturers is in the method of connecting the stages together and in the material used for construction.

Figure 5.3(a) shows a design in which the pump stages are fully encased in a housing which is constructed of seamless steel tubing. In Figure 5.3(b), the stages are bolted together and a separate housing is not used.

The diffusers and impellers are normally one piece bronze castings. The pump shaft is stainless steel.

5.3.3 Motor

The elctric motor is usually a squirrel cage induction motor. Some motors use an oil as a lubricant and insulator, some use water for this

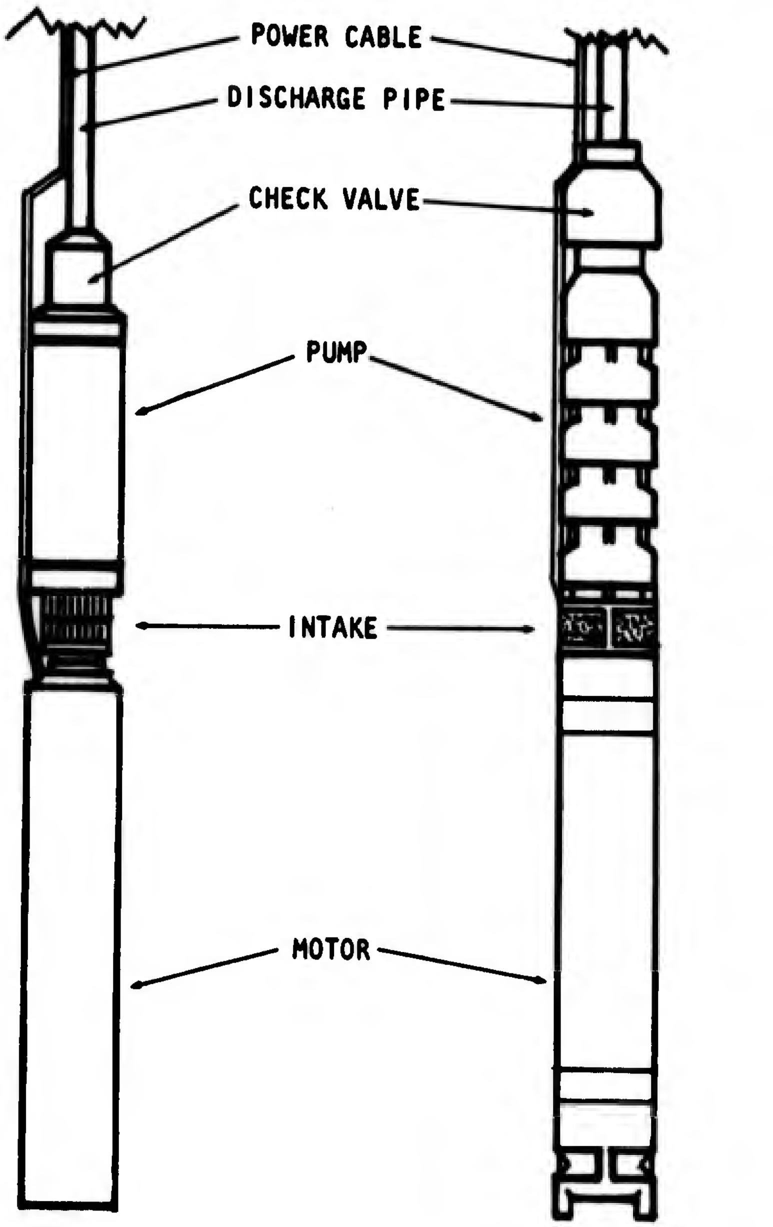

(a) REDA PUMP CO.
LAYNE & BOWLER, INC.
PEERLESS PUMP

(b) U.S. PUMPS
JOHNSTON PUMP CO.

FIGURE 5.3 SUBMERSIBLE PUMPS

purpose. A stainless steel shaft and outer housing is common to many motor manufacturers. Thrust and guide bearings are an important component in the design of the motor and probably the most sensitive part of the motor in resisting ground shock effects. Fortunately, however, bearings are designed for high reliability and are tested under large thrusts and shock conditions. In the case of oil-filled motors, the seal at the shaft is also an important design feature. A pump unit using a flexible shaft coupling between the pump and the motor may be advantageous.

5.3.4 Assembly

The pump and motor are bolted together in the final assembly of the pump. This connection will have to resist tension loads due to axial ground shock accelerations plus possible bending stresses. Conventional mounting details usually specify four 1/2-inch bolts which provide resistance in tension of approximately 20,000 pounds. This should be adequate in resisting the ground motions anticipated for the worse condition.

Table 5.2 summarizes typical pump and motor sizes and weights for submersible pumps manufactured by Reda Pump Company and shows the required diameter of the discharge pipe. At well depths of 200 ft and greater, it will be necessary to reduce the 200 gpm capacity specified as criteria if standard water well pumps are utilized. Special pump designs (such as oil well pumps) are available if greater capacities are needed.

5.3.5 Cable

The power cable for use with the pumping unit is normally a three conductor cable. Each conductor is protected by moisture-resisting rubber insulation then twisted together and enclosed in a tough protective, overall jacket. Armored cable is covered with interlocking galvanized steel armor. Monel armored cable is also available. As noted in Figure 5.3, the cable runs up on the outside of the pump housing and then up alongside the discharge pipe. The cable is tied to the housing and discharge pipe at frequent intervals. Since there is only limited space between the pump unit and the well casing, it is possible that the cable could be crushed as the result of ground motion.

TABLE 5.2

SUBMERSIBLE PUMP CHARACTERISTICS*

WELL DEPTH (ft)	HEAD (ft)	DISCHARGE (gpm)	PUMP POWER (hp)	DISCHARGE PIPE DIAMETER (in.)	LENGTH OF MOTOR (in.)	LENGTH OF PUMP (in.)	TOTAL LENGTH (in.)	TOTAL WEIGHT (lb)	PUMP DIAMETER (in.)	MOTOR DIAMETER (in.)
65	70	245	15	4	52	57	109	528	$5\frac{1}{8}$	$5\frac{7}{16}$
115	125	205	15	4	52	57	109	528	$5\frac{1}{8}$	$5\frac{7}{16}$
215	230	172	20	4	64	75	139	643	$5\frac{1}{8}$	$5\frac{7}{16}$
615	660	150	40	3	97	118	215	1050	$5\frac{1}{3}$	$5\frac{7}{16}$
1615	1735	52	40	3	97	123	220	981	$5\frac{1}{8}$	$5\frac{7}{16}$

*Based on data obtained from Reda Pump Company

Concepts for protecting the cable are discussed in Section 6.4. It is recommended that a stainless steel armored cable be used for added protection.

5.3.6 Sensitivity to Shock

Very little information is available on the shock resistance of submersible pumps except for experience gained in the field as the result of earthquakes and accidentally dropping pumps.

In the case of major earthquakes, it has been found that a casing may have been bent so badly that the pump couldn't be removed, but there was no apparent damage to the pump and it continued to operate satisfactorily.

Reda pumps have been dropped accidentally 300 feet down a casing but were still operable. The only damage was crumpling of the motor housing at the bottom of the pump. This part of the motor houses the oil reservoir and pressure equalizer and is not a critical part of the motor.

Longitudinal bending of the pump assembly due to ground motions could cause the shaft to bind depending on the magnitude of the relative deflections. Elastic transient deflections are not a problem since the pump assembly usually experiences large deflections when they are up-ended and placed in the well. However, permanent longitudinal distortions could fail the unit.

In summary, a submersible pump of the type shown in Figure 5.3(a) which utilizes a heavy-walled exterior housing is recommended for use in a shockproof well design.

SECTION 6

CASING ANALYSIS OF THE INTEGRAL WELL CONCEPT

6.1 WELL CASING INSTALLATION ASSUMPTIONS

The method of analysis of the axial drag loading on the casing is based on the following assumptions.

a. The casing will be installed in slightly over-size drill holes which extend beyond the lower end of the casing.

b. The clearance between casing and drill hole in rock will be filled with sand from the strata above the rock, and the normal closure pressure around the casing will be very nominal. This closure stress is consistent with generally accepted engineering assumptions. See Terzaghi, Reference 6, page 202-205.

c. As a result of assumptions a and b the active value of the friction forces restraining the axial movement of the casing will be only sufficient to maintain the axial position of the casing under static conditions.

d. The casing will not be subjected to axial end loading from weapons effects.

e. A section of conductor pipe of larger diameter than the casing will house the upper end of the casing to possibly 30 feet below the surface so that the lateral component of the vertical foundation reaction of the well head housing (under weapons effects loading) will not appreciably affect the drag stresses on the casing near the surface.

6.2 LOAD AND STRESS ANALYSIS

The analysis used in the evaluation of the horizontal and vertical displacements, and stresses in the casing are given in detail in Appendix B.

In the evaluation of the axial stresses in the casing two concepts are used, from here on referred to as the friction method and the strain method. The two methods are outlined below.

6.2.1 Friction Method

The distribution of downdrag forces as assumed by the friction method is shown in Figure 6.1(b). In the friction method it is assumed that the maximum downdrag force F is developed all along the casing and is a function of the horizontal pressure distribution, indicated in Figure 6.1(a), and the cohesion of the soil.

$$F = C + \mu P_h$$

where F = downdrag force
C = cohesion of soil
P_h = horizontal pressure
μ = coefficient of friction.

This is correct for a fairly short or a very stiff structure depending on the ratio

$$n = \frac{E}{M_p}$$

where E is the modulus of elasticity of the structure and M_p is the soil modulus at peak stresses. If n is large the maximum downdrag force can be developed. If n is small or n = 1 the maximum downdrag force will never be developed. In other words, a soft structure will deflect with the surrounding soil and never develop internal forces large enough to produce maximum friction forces.

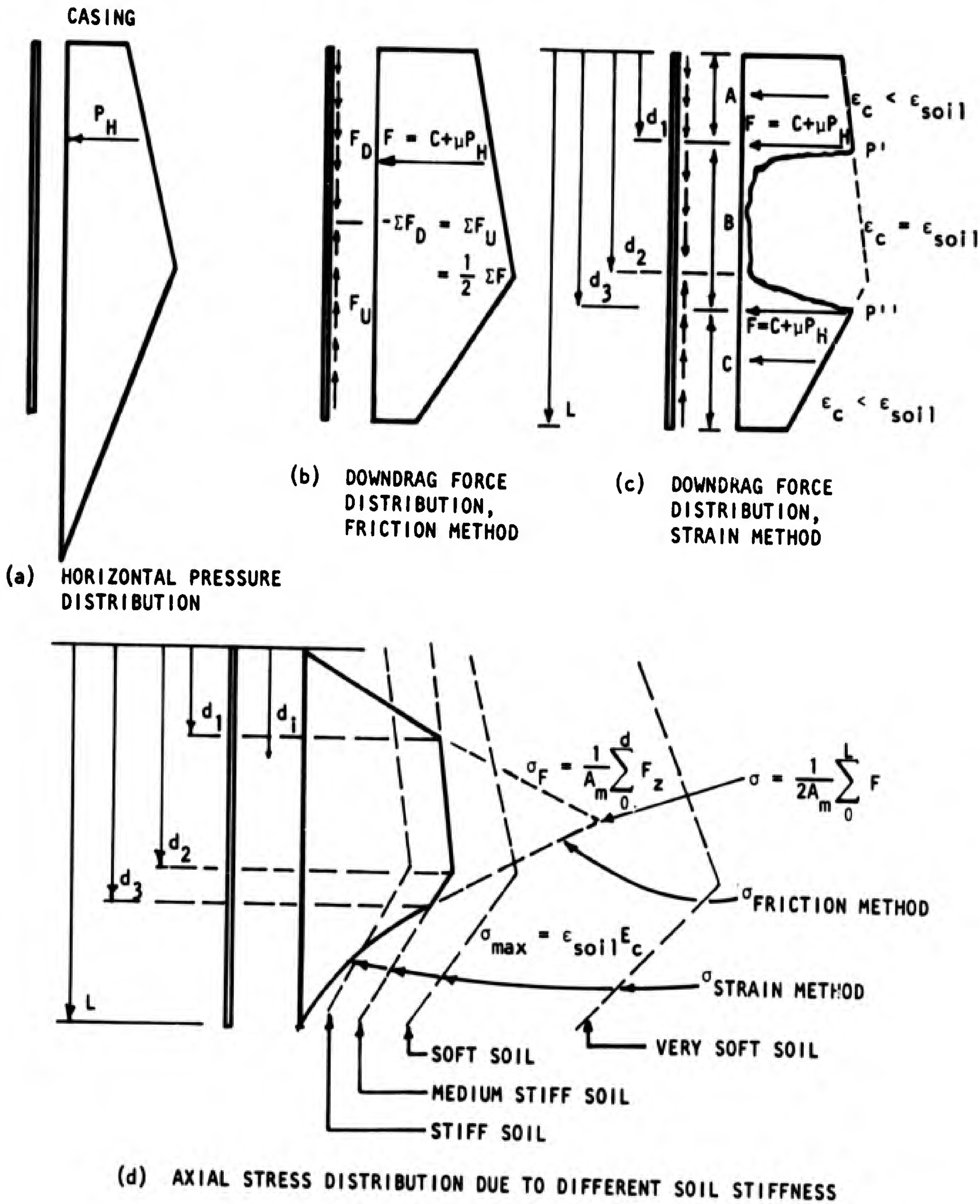

FIGURE 6.1 FORCES AND STRESSES IN A WELL CASING AT TIME, t (A HOMOGENEOUS MEDIUM IS ASSUMED)

The axial force in the casing is found by assuming one-half of the total downdrag force acting downwards and the other half acting upwards. The axial stress is given by the formula:

$$\sigma_{a_{max}} = \frac{1}{2A_m}\sum_{0}^{L} F_z$$

where F_z = downdrag force per incremental length in lbs.

A_m = area of casing in square inches.

At a point, i, at a depth, d, from the top of the casing and above the point of maximum stress the axial stress is

$$\sigma_{a_i} = \frac{1}{A_m}\sum_{0}^{d} F_z$$

For the 600 and 1,600 foot deep casing the friction method indicates extremely high axial stresses due to the assumption of an infinitely rigid structure. It is believed that the friction method greatly overestimates the axial stresses in long casings.

6.2.2 Strain Method

In the strain method the loading of the casing is a result of the deformation of the soil. It then follows that the deformation of the soil is the upper bound for the axial deformation of the casing. Thus the upper bound for the axial strain of the casing is equal to the vertical strain of the soil. Figure 6.1(c) shows the distribution of the downdrag-forces as assumed by the strain method. Maximum downdrag force is developed in the end Regions A and C. Going down from the top of the casing in Region A, or up from the bottom in Region C, the axial strain of the casing ε_c at a section n is equal to

$$\varepsilon_c = \frac{1}{A_m E} \sum_0^n F_z$$

In these regions the strain in the soil is larger than the strain in the casing therefore maximum downdrag force will be developed and slippage may occur at the interface soil-casing.

Coming down to point P' or up to point P'', the strain in the casing has reached the value of the strain in the soil, $\varepsilon_c = \varepsilon_{soil}$, and the casing is moving with the soil. Thus in Region B, between the points P' and P'', ε_c is equal to ε_{soil}, and here only sufficient downdrag forces are developed to insure that the two strains remain equal. At any point on the casing the equilibrium equation

$$\sum F_z = \varepsilon_c E A_m$$

must be satisfied.

The axial stress distribution as determined by the two methods is shown in Figure 6.1(d). The figure indicates that for stiff soils the maximum axial stress is governed by the displacement. However, for a very soft soil the maximum downdrag force may be developed all along the casing. This, of course, also depends on the length of the casing.

The strain in the soil ε_{soil_i} at the location i is equal to

$$\varepsilon_{soil_i} = \left(\frac{P_z}{M_p}\right)_i \qquad \text{(in/in)}$$

where P_{z_i} = the vertical soil stress at location i, (psi)

M_p = the soil modulus at peak stress (psi)

The axial stress distribution obtained for the cases D-600-20-100 and D-1600-20-50 by the two methods are shown in Figures 6.2 and 6.3. The stress σ_{af} and σ_{as} in the two figures is the axial stress in the well casing as obtained by the friction method and the strain method, respectively.

It is seen from Figures 6.2 and 6.3 that for a short casing ($L \approx 200$ ft) the axial stress is governed by the friction method. When the casing length exceeds 300 to 350 feet, the axial stresses are governed by the strain method. This means that the maximum axial stress developed in a 300 foot long casing will also be the maximum stress developed in a longer casing.

6.3 WELL HEAD SUPPORT CONCEPT

The well head for the integral concept is illustrated in Figure 6.4. The annulus between the well casing and the conductor casing (if needed) will be filled with drilling mud or sand. The upper part of the 6-inch well casing is reinforced with four 3-inch channels as shown in Figure 6.3. (The channels are not required for overpressures less than 50 psi). A 6-inch 300 lb "slip on" flange is welded to the top of the well casing. This flange serves as a mounting for the discharge pipe which is rigidly connected to a 300 lb blind flange and bolted to the "slip on" flange with six 7/8 inch high strength bolts. The welds should develop the full strength of the pipes.

A flexible hose connects the discharge pipe with the distribution pipes. In the annulus between the discharge pipe and the well casing rubber shock absorbers should be installed as described in Subsection 6.4 and illustrated in Figure 6.5.

(Text continued on Page 77)

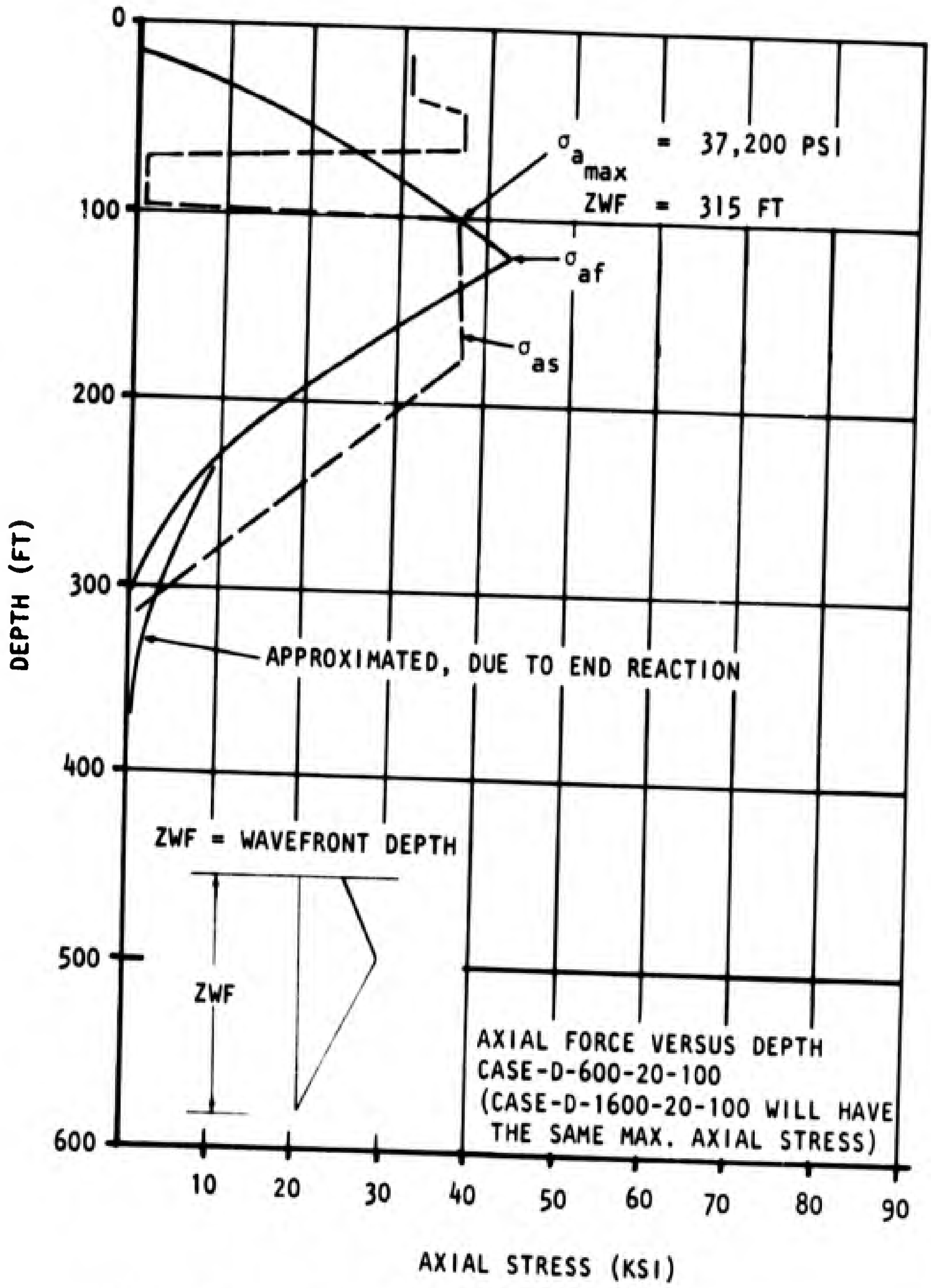

FIGURE 6.2 AXIAL STRESS DISTRIBUTION IN 600-FT CASING

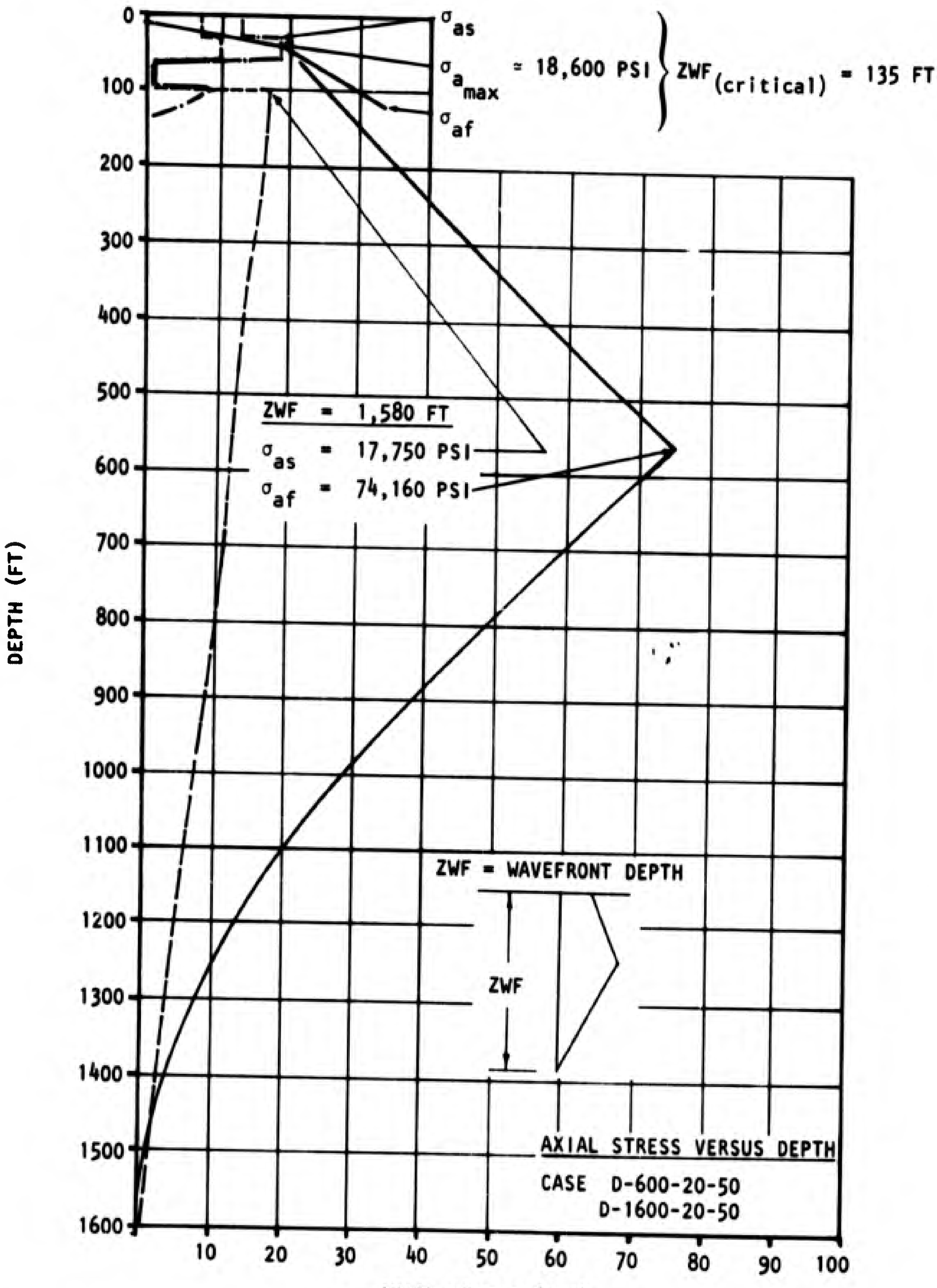

FIGURE 6.3 AXIAL STRESS DISTRIBUTION IN 600-FT AND 1,600-FT CASING

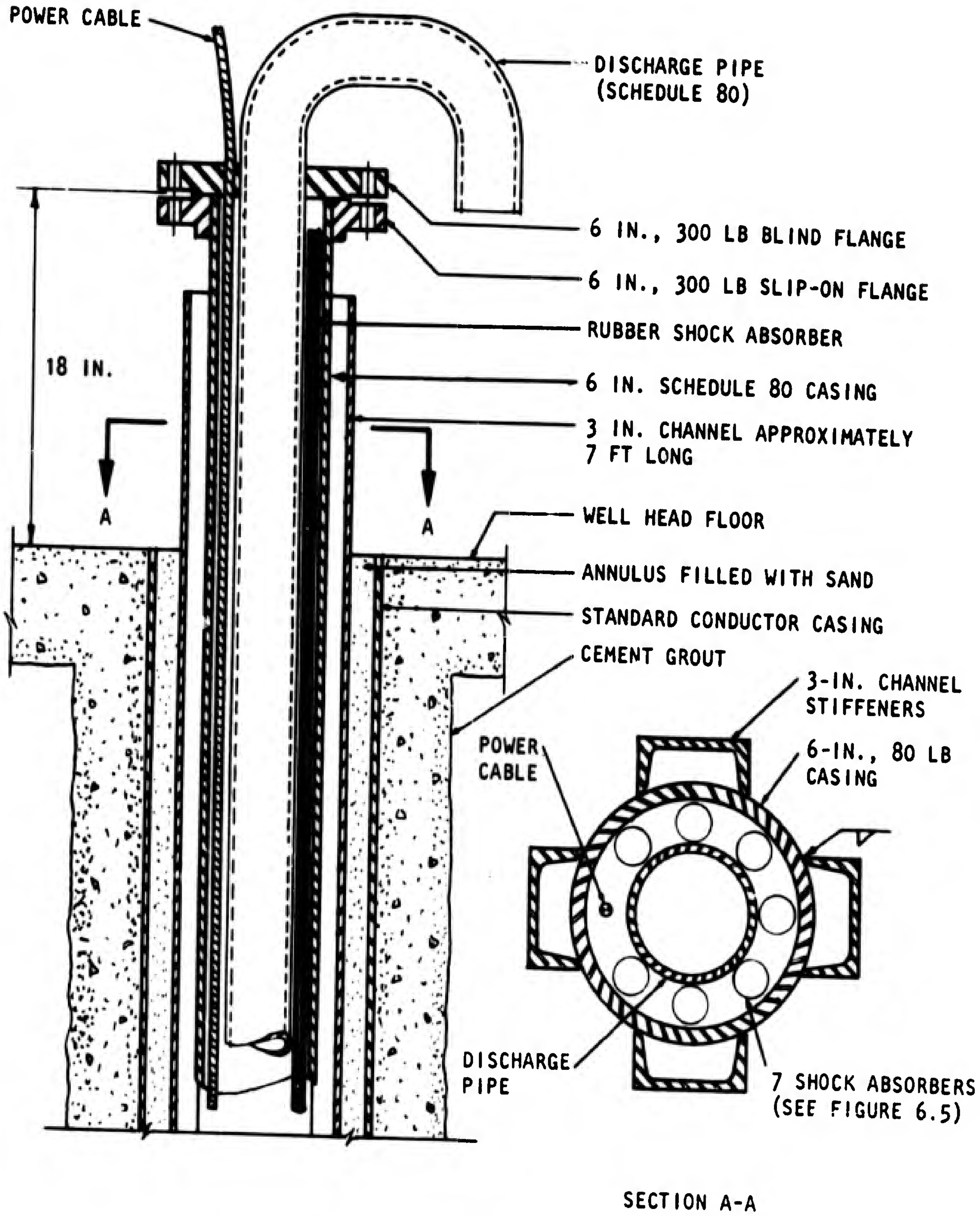

FIGURE 6.4 INTEGRAL WELL - CONCEPT A

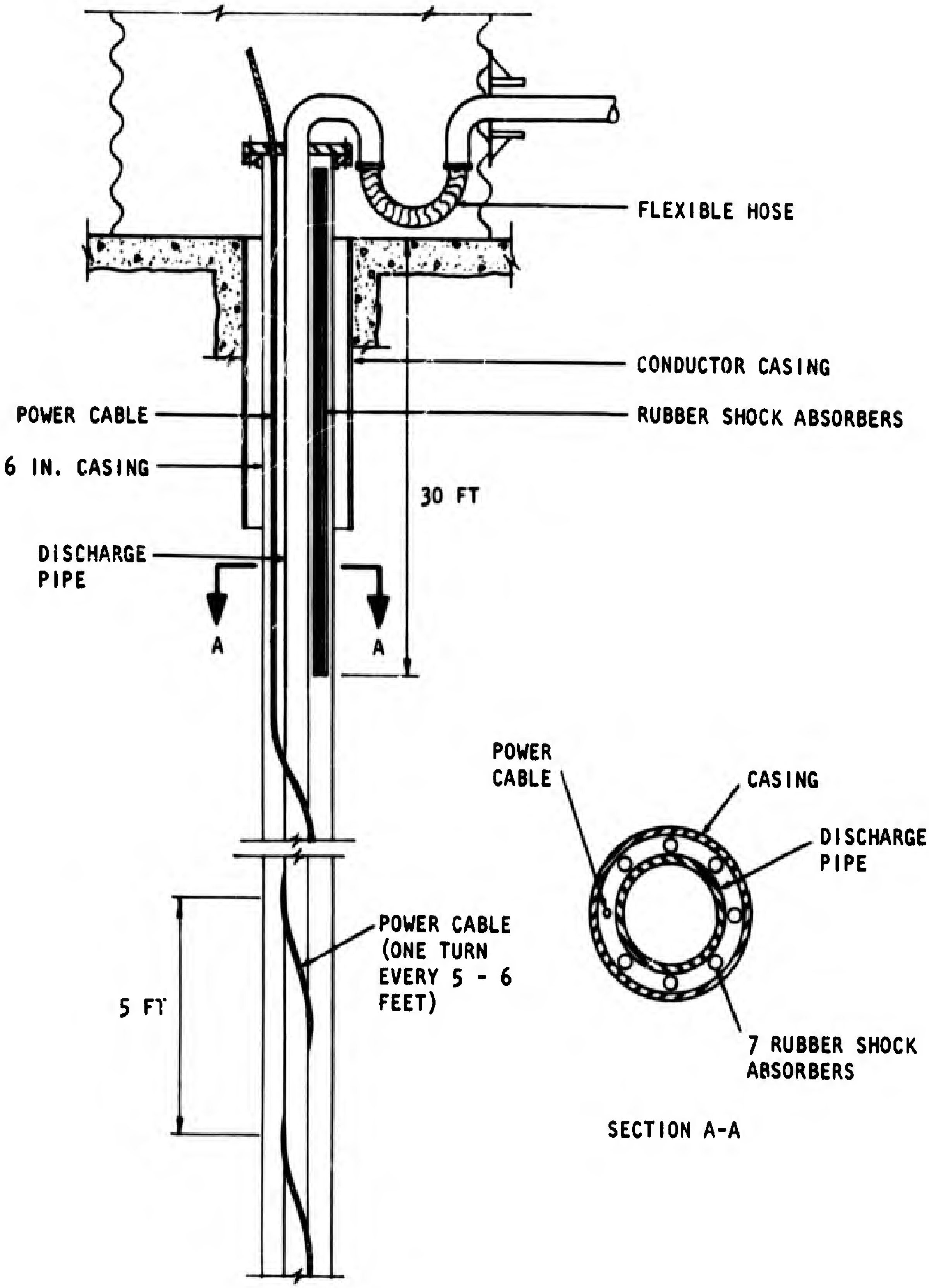

FIGURE 6.5 INSTALLATION OF POWER CABLE AND SHOCK ABSORBERS

6.4 INSTALLATION OF POWER CABLE

For all cases, integral and gel-isolated, it is recommended that the power cable be installed as shown in Figure 6.5 Seven shock isolators, consisting of rubber cables 30 feet long filling the annulus between the casing and the discharge pipe, plus the power cable should be attached to the discharge pipe from the casing top and down. From the 30-foot depth the power cable should be wound around the discharge pipe at a 5 foot pitch. The cable will act as a shock absorber and will prevent the discharge pipe from impacting the well casing. Steel bands or similar connectors that would cut the power cable should not be used to attach the power cable to the discharge pipe.

6.5 RESPONSE OF DISCHARGE PIPE

6.5.1 Horizontal Response

Due to the shock isolation provided by the power cable and the shock isolators between the discharge pipe and the well casing, the horizontal response of the discharge pipe will produce relatively small bending stresses in the discharge pipe; also the shear stresses at the blind flange welded to the pipe are well within allowable limits.

6.5.2 Vertical Response

The initial vertical motion of the casing head can be either upward or downward depending on whether the shock condition is outrunning or superseismic. In the analysis of the vertical response of the discharge pipe the friction forces between the pipe and the well casing are neglected, and it is assumed that the discharge pipe gets its initial vertical shock from the casing head. Treating the discharge pipe and the pump unit as a uniform cantilevered beam with a mass at the end, the axial dynamic stresses are computed (Appendix E) and tabulated in Table 6.1 for the most severe cases. The dynamic stresses control the design. Other soil profiles will cause stresses of the same magnitude for corresponding overpressures.

TABLE 6.1 AXIAL STRESSES FOR DISCHARGE PIPE*

CASE NO. SOIL-L-W-P_{so}	STATIC STRESS σ_{st} (ksi)	DYNAMIC STRESS σ_d (ksi)	COMBINED STRESS $\sigma_c = \sigma_{st} + \sigma_d$ (ksi)
A-50-20-300	0.35	43.5	43.9
B-200-20-300	1.0	66.0	67.0
B-1600-20-300	7.0	69.0	76.0
B-50-20-100	0.35	13.0	13.3
B-200-20-100	1.0	16.5	17.5
B-1600-20-100	7.0	17.2	24.2

*4-Inch Schedule 80

SECTION 7

DYNAMIC ANALYSIS OF GEL-ISOLATED CONCEPT

7.1 WELL CASING INSTALLATION ASSUMPTION

The analysis of the gel-isolated system is based on the use of free-field shock spectra. The following assumptions were made for the well casing installation.

a. The well casing will be installed in an oversized drill hole, or an outer casing if needed, so that an annulus of approximately one and one-half inch thickness is provided around the casing.

b. In order to minimize the downdrag forces on the well casing the annulus is filled with a low shear gel.

c. An outer casing will be used where it is needed in order to contain the gel and prevent it from dissipating into the surrounding soil.

d. The lower end of the casing will be grouted with cement grout to provide vertical support for the casing and also to provide an effective seal between the gel and the water bearing strata.

e. The top of the casing will be supported horizontally by a hinge joint, free to move vertically. For superseismic conditions the casing is spring supported vertically at the top. For outrunning conditions there is no vertical support at the top.

f. The discharge pipe and the pump unit will hang from the top of the casing with a bolted flange connection between the casing and the discharge pipe.

g. A section of conductor pipe of larger diameter than the casing will house the upper end of the casing to possibly 30 feet below well head floor so as to provide the necessary vertical support of the casing.

7.2 WELL HEAD SUPPORT CONCEPTS

This subsection uses the data obtained by the shock spectra analysis, Subsection 4.3 and Appendix C, to analyze the well head support for the gel-isolated concepts. The casing head support concepts, illustrated in Figures 7.1 and 7.2 for the superseismic and outrunning conditions respectively, are considered compatible with the maximum static loading and the maximum weapons effects parameters under consideration.

7.2.1 Well Head - Superseismic Condition

For superseismic conditions the design of the well head, Figure 7.1, is based on four postulations.

a. The vertical dead load of the discharge pipe and the water contained in the pipe, pump unit, and 3/4 of the well casing should be supported at the casing head.

b. Permanent vertical surface displacements due to weapons effects or natural settlement should not reduce the vertical support reaction by more than about 20 percent.

c. Although it is possible to do so, the added cost and complexity in casing head support assembly necessary to maintain a substantial part of the vertical support reaction during maximum transient vertical displacements is probably not justified.

d. Design of the casing head support assembly to insure casing head lateral movement with transient horizontal ground displacements is simpler than horizontal shock isolation and provision of adequate lateral rattlespace.

7.2.1.1 Basic Support Method. Although other methods of casing head support have been used, the most widely applied, where the loads are substantial, utilizes a conductor pipe flanged at the upper end. At least a temporary conductor pipe is very often required to prevent caving of the well in overburden material prior to casing. A conductor pipe will almost

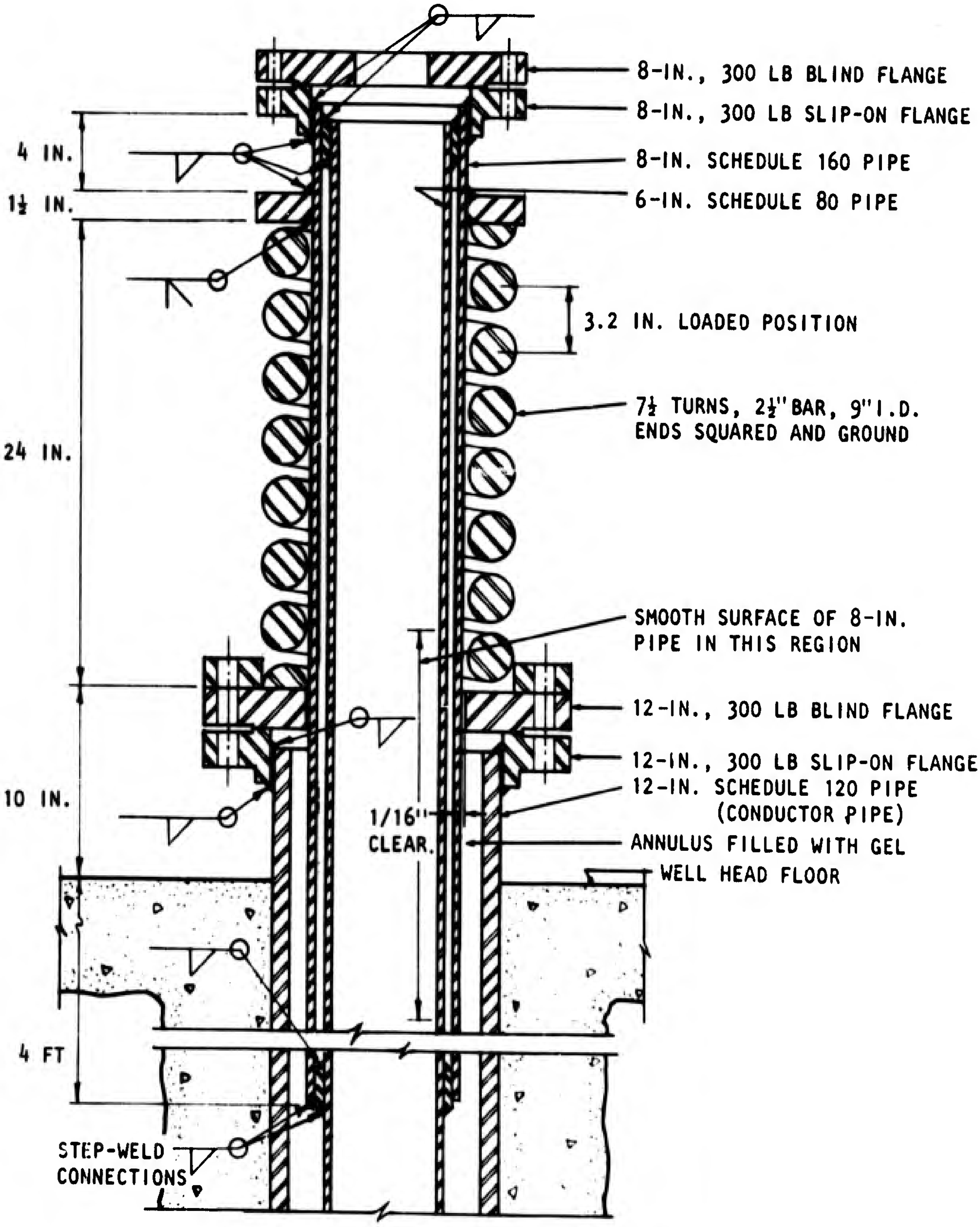

FIGURE 7.1 CASING HEAD SUPPORT - CONCEPT B FOR SUPERSEISMIC CONDITION

AGBABIAN-JACOBSEN ASSOCIATES

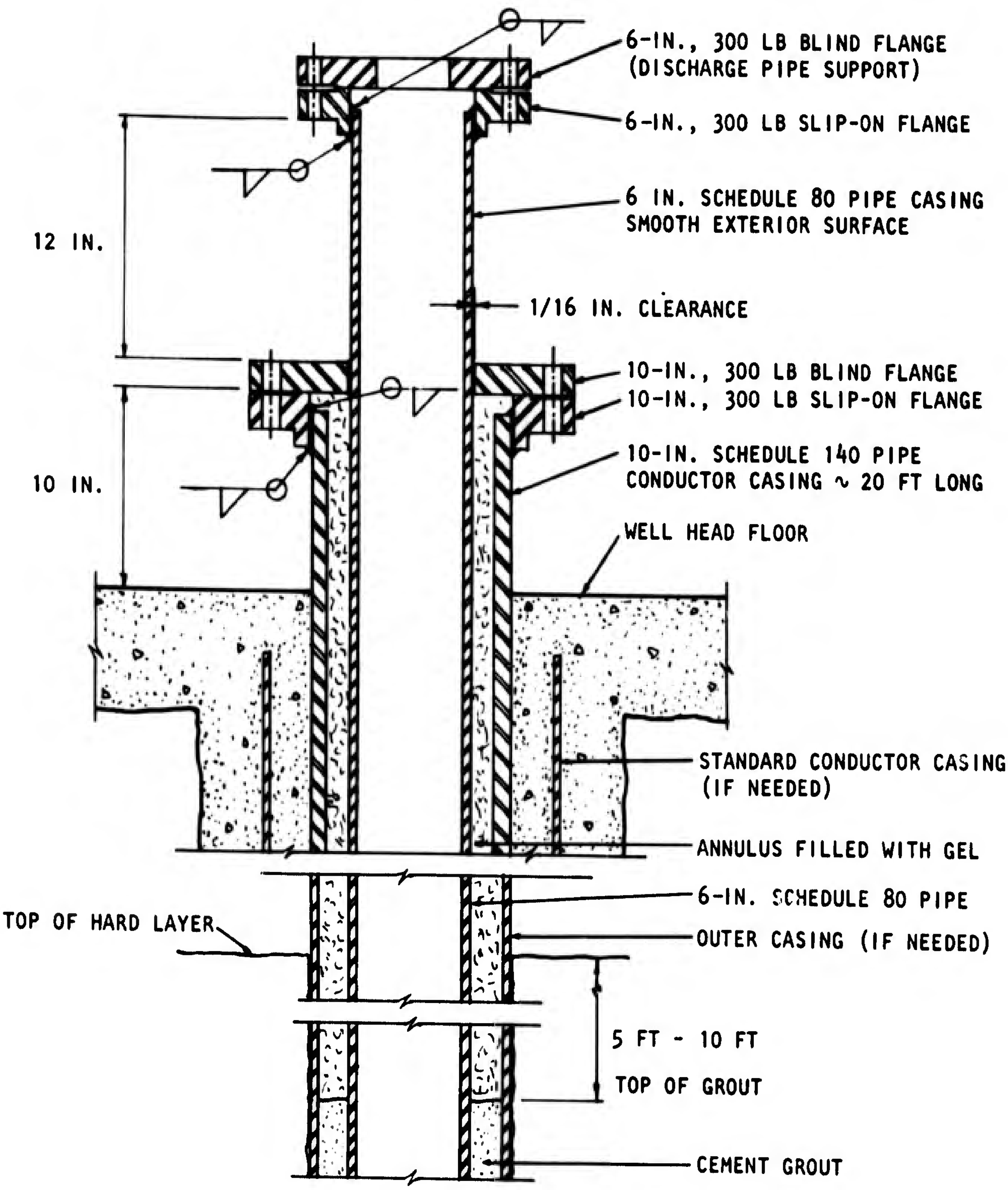

FIGURE 7.2 CASING HEAD SUPPORT - CONCEPT C FOR OUTRUNNING CONDITION

certainly be required in the gel-isolated well concept in order to stabilize the gel filled annulus around the well casing through the softer overburden materials. The concept illustrated uses a 12-inch conductor pipe having a thick (about 1-inch) wall at the upper end and terminated in a standard 300-lb "slip-on" flange. (If the conductor pipe is of considerable length, a reduction in wall thickness below the top 10 feet would be economical.) The concrete encasement serves to fix the conductor pipe in the soil for both static vertical and dynamic lateral load transfer. Depth and diameter of the concrete encasement would be determined on the basis of the soil conditions and design loads. The exposed, flanged end serves as a mounting for the actual casing head support assembly.

7.2.1.2 Lateral Support System. The lateral support and horizontal transient load transfer system illustrated in Figure 7.1 consists of a 12-inch 300-lb blind flange bolted to a 12-inch 300-lb slip-on flange which is welded to the conductor casing. A 1/16-inch clearance should be provided between the blind flange and the casing to permit vertical displacements. The casing should be ground smooth a distance 2 feet below the flange and a permanent lubricant should be applied to the casing surface. For the upper part of the well casing an 8-inch Schedule 160 pipe is used in order to provide extra strength. The assembly is planned to permit free vertical sliding or rotating motion of the casing head. Also some rotational motion of the casing about a horizontal axis is permitted.

7.2.1.3 Vertical Support System. The 1½-inch thick steel ring bolted to the 300-lb slip-on flange centralizes a heavy spring. The spring would be designated to suit each specific case with respect to well casing load. The spring illustrated (2½-inch bar diagram, 11½-inch pitch diameter, 6 active coils) is representative of what may be required for an approximately 500-ft depth gel-isolated well casing. The spring should be designated such that a 1-inch permanent downward displacement of the well head will not reduce the casing support by more than 10 percent. The casing head is supported and the spring centralized at the top by a special flange welded to the casing. A standard 8-inch slip-on flange terminates the casing head a few inches above the top support flange. Before the casing is installed the spring must be compressed. The casing end is closed, and the discharge pipe and pump unit supported by a standard 8-inch, 300-lb blind flange. The discharge pipe is secured to the lower end of the coupling, and an elbow to the flexible external discharge line enters the top of the coupling.

7.2.2 Well Head — Outrunning Condition

The well head support system for wells where outrunning conditions can be expected is somewhat similar to the previously described support system. An outrunning condition is caused by a hard layer in the soil profile causing an upward initial vertical deflection. As a deeper hard layer will not experience large strains, only moderate axial stresses will be developed in the well casing. Therefore, the casing can be grouted up to a few feet below the top of the hard layering. Above this point the casing is standing free in the gel supported vertically by the cement grout only. The casing is supported horizontally by the flanged connections at the top of the conductor casing as shown in Figure 7.2. In order to reduce the vertical shock in the well system the top of the cement grout should be at least 70 feet deep even though the top of the hard layer may be higher. For this case a 10-inch Schedule 140 pipe is used as the conductor casing. The well casing is made of 8-inch Schedule 80 pipe. The surface of the upper part of the casing should be ground smooth and a permanent lubricant applied in order to secure free vertical motion of the casing.

The connection between the well casing and the discharge pipe is the same as previously described.

7.3 INSTALLATION OF POWER CABLE

The power cable for the gel-isolated concept should be installed in the same manner as for the integral well concept, described in Subsection 6.4 and illustrated in Figure 6.5.

7.4 SYSTEM RESPONSE ANALYSIS

7.4.1 Introduction

In order to investigate the response of the well system to free-field ground motion, the free-field shock spectra for 20 selected cases (shown in Tables 4.5 to 4.9) were computed using a computer program previously developed by AJA. This program arrives at a shock spectra envelope using semi-empirical procedures based on one-dimensional wave propagation methods (see Reference 37). The peak intensities and resulting shock spectra due to the direct air blast slap motion and the peak intensities and shock spectra due to seismic (random) motion are calculated separately. The resultant response is combined either algebraically or by quadrature depending on the case and may be amplified over a narrow frequency range due to resonance with the direct air blast. The procedure and assumptions used in this analysis are given in Appendix C including a step-by-step derivation of the method.

The program compares the air blast arrival time at the target (well) range from ground zero (GZ) with the arrival time of the seismic waves. If the air blast wave, traveling in free air arrives at the ground surface of the target ahead of the GZ induced pulse, or the air blast seismic induced pulse, then the condition is noted as superseismic. If either of the seismic waves arrives first, the condition is noted as outrunning. These conditions are listed in Table 7.1, 4.8 and 4.9.

7.4.2 HORIZONTAL RESPONSE OF WELL CASING

In the analysis of the horizontal response of the casing, the model of the casing is taken as a single span vertical beam fixed at the bottom and hinged at the top. The horizontal support of the gel is neglected.

The maximum horizontal displacement of the casing is limited by the annulus between the outer and the inner casing. On this fact the following assumption is made. The effective length of the casing is taken equal to that of a beam whose maximum horizontal displacement due to maximum horizontal ground shock, is approximately equal to the annulus, or 1 to 1½ inches (see Figure 7.3). This is considered to be a conservative approach when compared to the actual problem in which the cushioning effect of the gel isolation provides some horizontal support to the casing. This effect was neglected in the analysis.

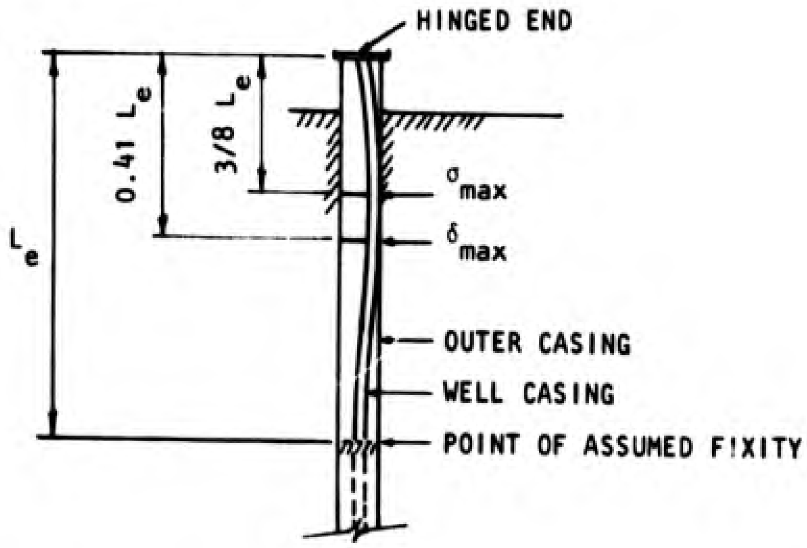

FIGURE 7.3 MODEL FOR HORIZONTAL RESPONSE ANALYSIS

The groundshock is taken as the average of the shock spectra at the 10 foot and the (10 + L_e) foot depth. The point of maximum horizontal displacement is taken at a distance 0.41 L_e, and the point of maximum bending stress at 3/8 L_e, from the hinged end of the casing. The bending stress at the fixed end is not considered to be the maximum bending stress as this is only an assumed point of fixity.

The model was analyzed as a discrete system with "n" lumped masses along the beam. The number "n" was from 10 to 20 depending on the length L_e. The normal mode method was employed in order to combine the effects of the higher modes. The procedure is shown in Appendix D.

In order to find the effective length L_e, six different beam lengths were analyzed using the most critical cases as indicated by the shock spectra analysis. The lengths, displacements and bending stresses for the different cases are given in Table 7.1. Using an annulus of approximately one inch, it is seen from Table 7.1 that the effective length L_e is somewhat less than 20 feet and the corresponding upper bound for the bending stresses is 48,000 psi.

TABLE 7.1 HORIZONTAL RESPONSE OF CASING

UPPERBOUND OF RELATIVE HORIZONTAL DISPLACEMENT
AND BENDING STRESSES IN THE WELL CASING

L_e (ft)	SOIL PROFILE	W (MT)	P_{so} (psi)	SHOCK VELOCITY CONDITION	δ_{max} (in.)	$\sigma_{b\,max}$ (ksi)	
						SUM	R.M.S.
10	E1	20	100	Outrunning	0.16	17.5	16.5
10	E1	20	300	Superseismic	0.30	27.3	25.8
13	A	20	300	Superseismic	0.67	44.0	42.0
13	E1	20	300	Superseismic	0.66	44.0	42.0
16	E1	20	300	Superseismic	1.09	40.0	36.8
16	E2	1	300	Superseismic	1.12	45.2	42.2
20	E1	20	100	Outrunning	0.43	16.6	11.4
20	A	20	100	Superseismic	0.53	15.8	13.9
20	B	20	300	Superseismic	1.63	48.6	44.9
20	DD2	20	300	Outrunning	1.27	44.9	41.1
20	E2	1	300	Superseismic	1.76	50.0	45.4
50	B	20	300	Superseismic	6.89	27.7	
50	DD2	20	300	Outrunning	4.56	25.8	
50	E1	20	300	Superseismic	5.44	34.7	

NOTE: The 100 ft model has a response similar to the 50 ft model and was not included.

Table 7.1 also shows that the shorter and stiffer 10 foot model, and the longer and more flixible 50 foot model develop less stress than the 16 to 20 foot models as would be expected. These stresses occur only in the upper 20 to 30 feet of the casing. Below a depth of 30 feet the bending stresses are believed to be much less. Therefore, only the axial stress due to the vertical response of the discharge pipe must be added to the bending stress. The axial stresses due to drag forces should be added to the axial dynamic stress of the casing only, which will reach a maximum at the bottom of the casing.

Due to the shock isolation provided between the casing and the discharge pipe the bending stresses in the discharge pipe will be nominal.

7.4.3 Vertical Response of Well System

The vertical response of the well system was investigated for the model shown in Figure 7.4(a). The discharge pipe and submersible pump are attached to the top of the well casing for vertical support. Cement grout is used in the annulus between the casing and bore hole at the bottom of the well to support the gel and seal it off from the water bearing stratum. Both well casing and discharge pipe will respond to the free-field motions transmitted to the well system through the grout seal. The damping effect of the gel is neglected in the analysis.

The well system was analyzed as a two-degree-of-freedom system using the dynamic model shown in Figure 7.4(b). The casing mass m_1 and the discharge pipe and pump represent mass m_2. A two mass modal analysis was used to investigate response amplification of the mass accelerations. Only fundamental frequencies were considered in the analysis. It is recognized that each mass will also respond in higher modes but the participation of the higher modes is usually small in the longitudinal response of a long bar and can normally be disregarded. The effect of higher modes on the transverse response of the well casing was considered in Paragraph 7.4.2, but the maximum bending stresses were not sufficiently different from the stresses predicted by using the fundamental mode only.

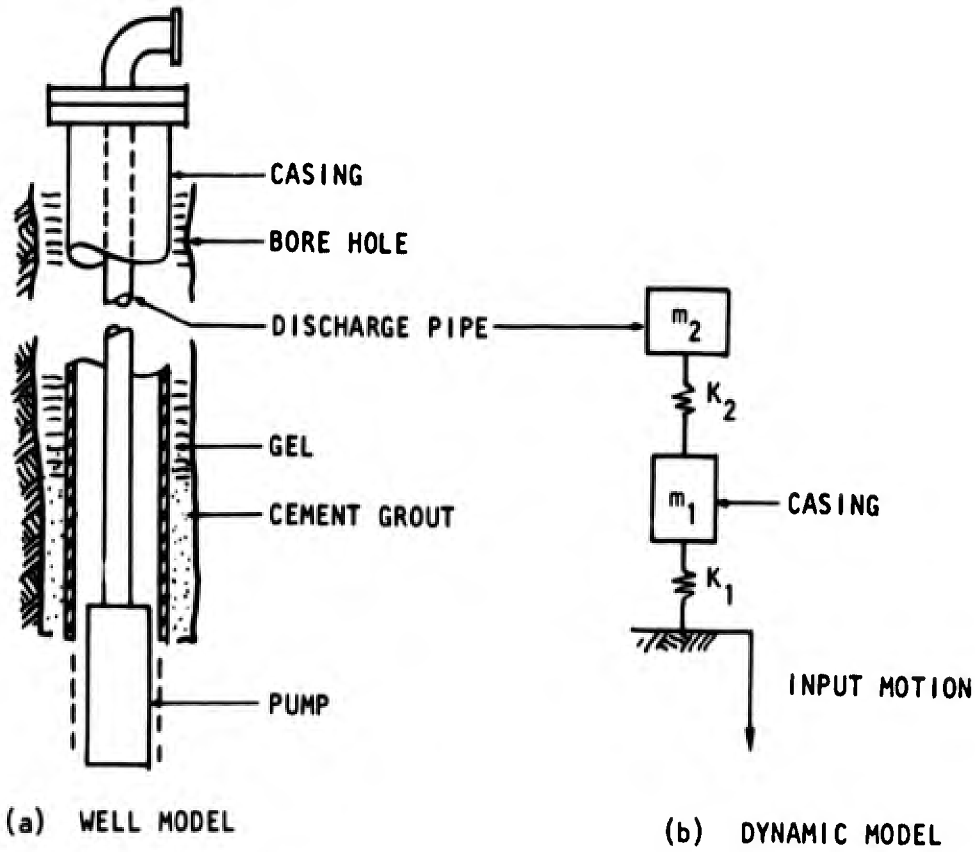

FIGURE 7.4 MODEL FOR AXIAL RESPONSE ANALYSIS

The derivation of the two mass response analysis is given in Appendix D. Calculations for the well system parameters and resulting dynamic axial stresses in the casing and discharge pipe can be found in Appendix E. Results of the analyses are shown in Table 7.2. Stresses for wells below a depth of 200 feet are not significant.

TABLE 7.2 VERTICAL RESPONSE STRESSES

CASING LENGTH	CASE NUMBER	CASING RESPONSE			DISCHARGE PIPE RESPONSE		
		Acceleration (g's)			Acceleration (g's)		
		Shock Spectra	Peak Response	Stress (psi)	Shock Spectra	Peak Response	Stress (psi)
50	B-50-20-300	34	57	9.0	34	47	13.7
100	B-100-20-300	25	42	13.3	25	38	17.5
200	B-200-20-300	4	7	4.9	4	7	6.6
50	A-50-20-100	12	20	3.4	12	17	4.8
50	A-50-20-300	30	50	8.1	30	41	12.3
50	E1-50-20-100	8	13	2.3	8	11	3.5
50	E1-50-20-300	12	20	3.4	12	17	4.8
50	E2-50-1-300	8	13	2.3	8	11	3.5
50	DD2-50-20-300	10	17	2.6	10	14	4.0

7.4.4 Downdrag Forces

A water based gel with low dynamic shear strength is believed to reduce the downdrag forces acting on the well casing to very small values. The dynamic shear strength of water based gels suitable for this purpose is little affected by pressure and velocity, however, acceleration might cause a considerable increase in the shear strength.

The ratio between the dynamic and static shear strength of the gel is defined as

$$R_d = \frac{\tau_d}{\tau_s}$$

As the shear strength of the gel is influenced primarily by the free-field acceleration, it will be assumed that the downdrag force is constant over the entire length of the casing. The incremental downdrag force on the casing is given by the formula

$$\Delta F = R_d \tau_s \pi D \Delta L$$

where τ_s = static shear strength of gel

D = casing diameter

ΔL = length increment

For a casing of length L and cross-sectional area A, the maximum axial stress due to downdrag is

$$\sigma_{a_{max}} = \frac{1}{A}\int_0^L R_d \tau_s \pi D dL = \frac{R_d \pi D \tau_s}{A} L$$

This stress will occur at the top of the cement grout at the bottom of the well casing. If it is assumed that the casing is grouted for one-fourth of its length, the axial stress in the casing becomes

$$\sigma_{a_{max}} = 0.75 \frac{R_d \pi D \tau_s}{A} L$$

The axial stress in the casing is also limited by the vertical strain in the soil as discussed for the integral well concept.

Table 7.3 lists maximum axial stresses due to downdrag for a 6-inch casing and assuming the following conditions:

$$R_d = 20 \text{ and } 40$$

$$\tau_s = 0.005 \text{ psi minimum}$$

$$\tau_s = 0.033 \text{ psi maximum}$$

$$\sigma_{a_{max}} = 22.3\tau_s R_d L$$

where L is in feet.

The values assumed for R_d are arbitrary and should be investigated by testing as discussed in Paragraph 5.2.6. The use of gel isolation to depths greater than 600 feet should not be necessary for any practical purposes.

TABLE 7.3 AXIAL STRESS DUE TO DOWNDRAG AT TOP OF GROUT OF GEL-ISOLATED CASING

CASING LENGTH (ft)	$\sigma_{a_{max}}$ (ksi) $R_d = 20$		$\sigma_{a_{max}}$ (ksi) $R_d = 40$	
	$\tau_s = 0.005$ (psi)	$\tau_s = 0.033$ (psi)	$\tau_s = 0.005$ (psi)	$\tau_s = 0.033$ (psi)
65	.14	.94	.28	1.88
115	.25	1.70	.51	3.40
215	.48	3.17	.96	6.34
615	1.39	9.20	2.78	18.40

7.4.5 Dynamic Analysis of Pump and Motor

A model of the submerged pump and motor is shown in Figure 7.5. The horizontal ground shock is transferred through the water, and the pump and motor unit is considered to act as a rigid body supported laterally by the surrounding water.

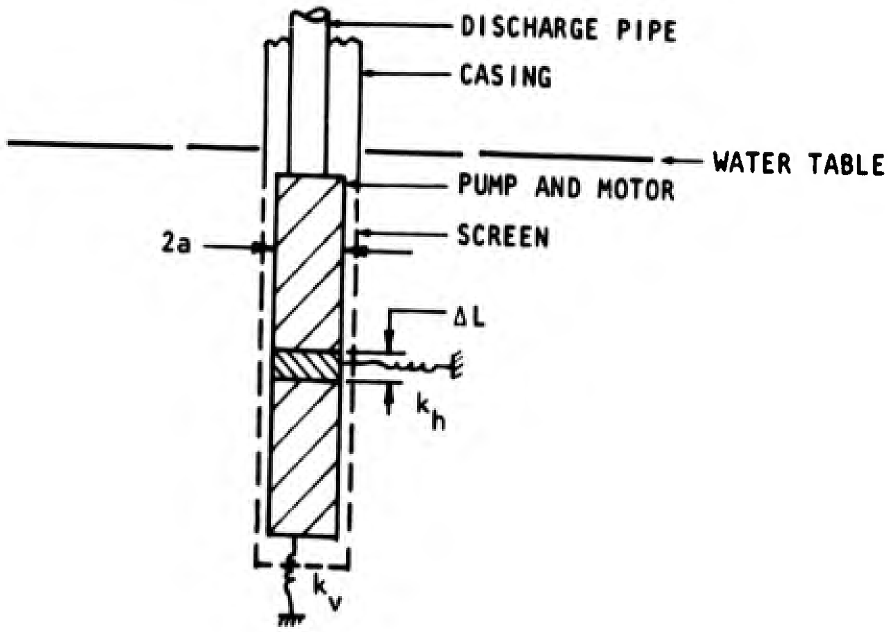

FIGURE 7.5 PUMP RESPONSE MODEL

The horizontal spring constant for a circular body submerged in water is taken as (Reference 16):

$$k = \frac{E_b}{2a} \qquad (lb/in^3)$$

where E_b = bulk modulus of water (psi) = 300,000 psi
a = radius of body (in.)

Assuming the water pressure to act over a segment spanning an angle ϕ, and over a length ΔL, the spring constant k_h for the mass covered by the length ΔL is

$$k_h = a\phi\Delta Lk \qquad (lb/in.)$$

Taking ϕ equals $\pi/2$ and ΔL equals one inch, the spring constant per unit length is:

$$k_h = \frac{\pi}{2} a \frac{E_b}{2a} = \frac{\pi}{4} E_b$$

The pump and motor units given in Table 5.2 have a weight approximately four to five pounds per inch of length, and the horizontal circular frequency of the unit is given by:

$$f = \frac{1}{2\pi}\sqrt{\frac{k_h}{m}}$$

$$f = \frac{1}{2\pi}\sqrt{\frac{(300{,}000)(386)}{5}\frac{\pi}{4}} = 680 \text{ cps}$$

From the shock spectra the maximum values for acceleration, velocity and displacement of the pump unit are found for Case B-50-20-300,

where A = 34 g's

V = 2.75 ips

D = .001 inches

The usefulness of these figures is a subject of engineering judgement. From Table 4.1 the maximum free-field horizontal displacement at 65 feet depth is found to be approximately 2 inches for Case DD1-200-20-300. With an annulus of 0.16 inches between the screen and the motor and 0.30 inches for the pump, an impact between the casing and the pump unit will occur. As the water occupying the annulus has a great "cushioning" effect, the magnitude of the impact is assumed to be within a tolerable range.

SECTION 8

CRITERIA FOR DESIGN

8.1 SCOPE

This section outlines the special considerations for the design of water wells intended for use with hardened facilities which must remain operational after exposure to the shock and ground displacements associated with nuclear weapons effects.

8.2 SITE SELECTION

In general well locations will be established by their proximity to the facilities to be served (with a minimum separation of twice the aggregate structure diameter), and many of the features desirable in sites for other hardened underground structures also apply to hardened wells. When available the following characteristics are desirable:

a. A high soil modulus from the surface downward (with the seismic velocity well in excess of criteria shock front velocities).

b. A low total dynamic shear strength (a function of the coefficient of internal friction) or a low ratio of lateral to vertical pressure where the lateral pressure is a function of the vertical pressure.

c. A gradual increase in modulus with depth without abrupt discontinuities.

d. A high rise of capillary water above the water table (to prevent an abrupt increase in modulus at the water table).

8.3 LOADING

The structural loadings that are used in the analysis of the well system will be influenced by the following considerations.

a. Static loading (dead load and active earth pressures) is usually a minor consideration in hardened design.

b. The weapons effects parameters producing the dynamic loadings will normally be specified in the general design criteria for the overall facility.

c. The well head housing will normally be close to the surface, and overpressure attenuation may be neglected. If the depth of burial of the top of the housing is at least one half of the housing diameter, consideration of increased loading due to unsymmetrical loading and other dynamic effects may be neglected in the head housing design. If the top of the housing is flush with the surface a dynamic loading increase factor should be used.

d. Casing loadings should be established by application of the methods outlined elsewhere in this report. For this purpose the dynamic characteristics of the actual soil media under consideration should be established by laboratory tests of undisturbed samples representative of the complete soil profile affecting the casing.

8.4 WELL CONCEPT

Major functional and technical details of the well are briefly mentioned here as they are considered to be important for design criteria.

8.4.1 Separation Distances from Shelter Structure

Separation distances are functions of interconnecting equipment and interdependent loading on both structural elements; usual recommendations are to provide two roof span lengths between structures.

8.4.2 Access

Access is required for maintenance and repair of the submersible pump and the electrical control box and circuit breakers. Since repairs to the pump or motor will require lifting the submersible pump to the surface, the access opening should be centered over the well casing.

8.4.3 Space

The well housing must provide sufficient space for the electrical equipment and for access to the equipment for maintenance. Consideration must be given to space for installation and replacement as well as shock isolators and rattlespace to protect the equipment.

8.4.4 Power

Power must be provided for operation of the pump and for convenience outlets and general lighting requirements.

8.4.5 Waterproofing

Waterproofing will be a stringent requirement to prevent entry of ground water during both the pre-attack and post-attack periods. This may dictate a need for a sump pump which would have to be protected from the weapons effects to insure its survivability.

8.5 CIVIL

Other than the site selection data previously mentioned, surface grading to carry surface water away fron the well head and access for four wheel drive vehicles are the major civil criteria considerations. It is assumed that all piping and power cables will be buried, and the usual criteria for such installations are applicable.

8.6 STRUCTURAL

8.6.1 Well Head Housing

From the standpoint of economical configurations the circular cylindrical housing is the most advantageous. The bending stress concentrations found at the corners of rectangular slabs are eliminated and maximum bending stresses in walls are materially less than those in the walls of a rectangular enclosure housing the same useful space. Performed corrugated culvert or tunnel liner plates may be used for the walls with a concrete roof slab and floor slab.

8.6.2 Well Casing

From the standpoint of both strength and corrosion resistance Schedule 80 (formerly called "extra strong") pipe should be used for the casing. Since bending stress increases directly with diameter (within limits) the minimum adequate casing diameter should be used where bending stress are likely to be critical. In the case of the more usual installations, critical for axial loading, the stresses vary inversely as the metal area divided by the diameter, i.e., $\sigma_a \sim D/A_m$, and increased wall thickness can be used directly to reduce stresses for any required casing diameter.

8.6.3 Discharge Pipe

The discharge pipe should be Schedule 80 pipe.

8.6.4 Design Stress Limitations

Dynamic stresses in the well casing and discharge pipe should be limited to the criteria given below:

Bending Stress:	to yield point
Axial Strain:	to four times yield stress
Combined Strain:	to four times yield strain

8.7 MECHANICAL

8.7.1 Submersible Pump

The type of submersible pump selected should house the motor and pump within a heavy-walled exterior seamless steel tubing. A shock test specification for use in the procurement specifications is given in Appendix F.

8.7.2 Shock Generated Pressure in Piping

Shock waves generated in the piping will travel through the piping system as pressure pulses. They will be modified and reflected at discontinuities in the system, such as bends, tees, crosses and changes in pipe diameter or material properties. A method for calculating maximum pressures in the system can be found in Reference 17. Calculations were made for the shock induced pressures in elbows, dead ends, and tees for a velocity pulse of 187 inches per second. This corresponds to the maximum horizontal free-field surface velocity as indicated by the response spectra contained in Appendix C.

Positive pressures are generated at points where the fluid is suddenly denied previously available space. Negative pressures result when additional space is made available (rarefaction wave). As the positive and negative pressure pulses travel through the system, being modified by discontinuities, they combine algebraically (superposition) when they meet.

Under horizontal motion, it was found that an internal pressure of 980 psi could be generated at a plugged connection. The pressure at 90° bends would be 490 psi, and for tee junctions, where all pipes are the same size, 330 psi would be generated. Since 980 psi is the peak initial pressure that is generated by the transient horizontal motion, it is felt that Schedule 80 pipe would be more than adequate for maximum pressure superpositions that may develop in the system. It has been found that a 3-inch Schedule 40 pipe system will have a burst pressure approaching 10,000 psi. The vertical velocity of the piping system is believed to be less than the horizontal, and therefore it will cause smaller pressures. The procedures outlined in Reference 17 can be followed to determine the acoustic wave pressure-time histories in the piping, but this is very tedious and is not required at the overpressure levels being considered.

8.7.3 Buried Piping

Piping between the well head housing and the shelter can be buried, but provisions must be made for relative motion where the pipe connects to the structures. A method that is in common usage for achieving flexibility at the interface passes the pipe through an oversized rigid sleeve that is attached to the wall and extends a short distance away fron the structure. The remaining space in the oversized sleeve is usually filled with a packing material to prevent soil from filling the space (see Reference 36). This detail is shown in Figure 8.1(a) and can be used at the shelter. However, at the well head housing the detail can be modified slightly to accommodate the corrugated steel construction as shown in Figure 8.1(b) and 8.1(c). The penetrations must be sealed to prevent ground water from entering the housing.

Another solution that could be considered if the distance between structures is short would be to place the piping within a corrugated metal pipe casing and then fill the casing with a plastic foam. This scheme provides excellent shock isolation for the piping and permits differential motion between piping and structures. This type of construction is expensive however, especially if the distance is great; it is not justified at the overpressures being considered.

Relative motion between the piping and the well head housing should be small since they would both tend to move with the same free-field depth. Maximum surface displacements can be large under special combinations of overpressure and site models, but the maximum relative displacements are estimated at 2 to 3 inches. These can be accommodated by the details shown in Figure 8.1. Relative motions at the shelter cannot be estimated since they are dependent on the structure configuration and depth of foundation below grade.

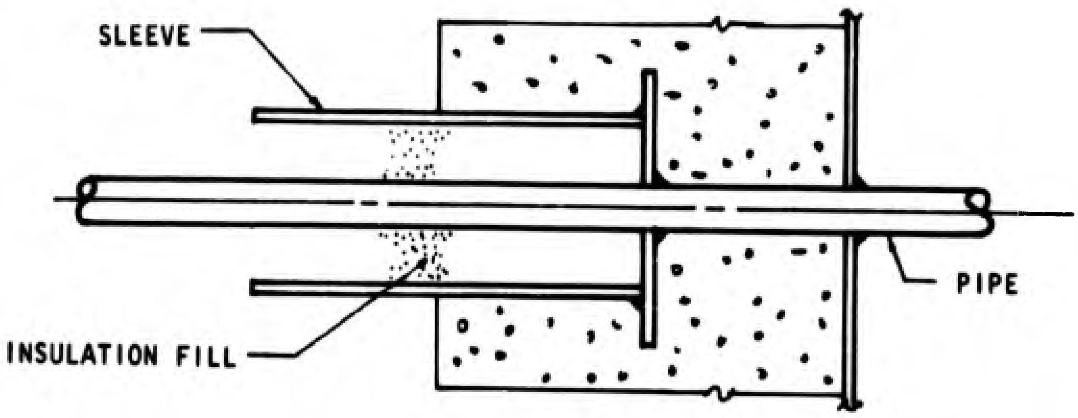

(a) CORRUGATED STEEL STRUCTURE

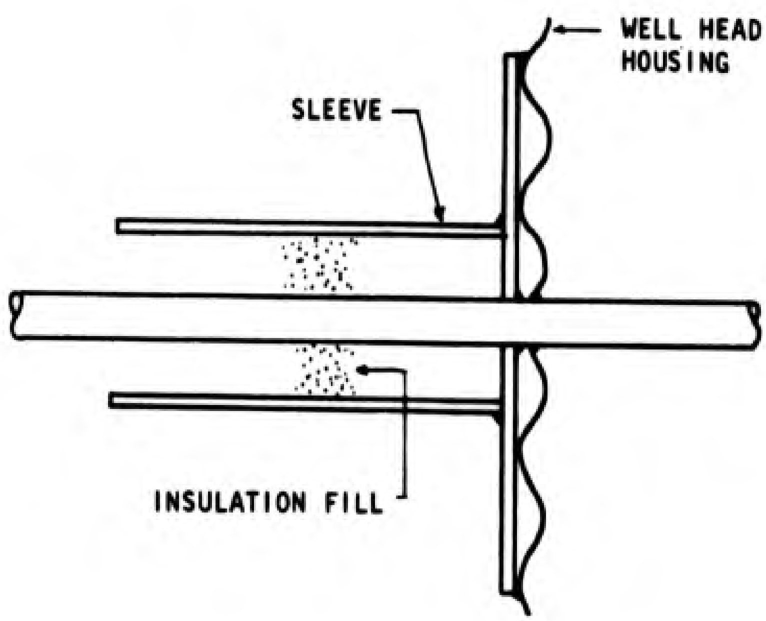

(b) CORRUGATED STEEL STRUCTURE

FIGURE 8.1 HARDENED PIPE PENETRATIONS

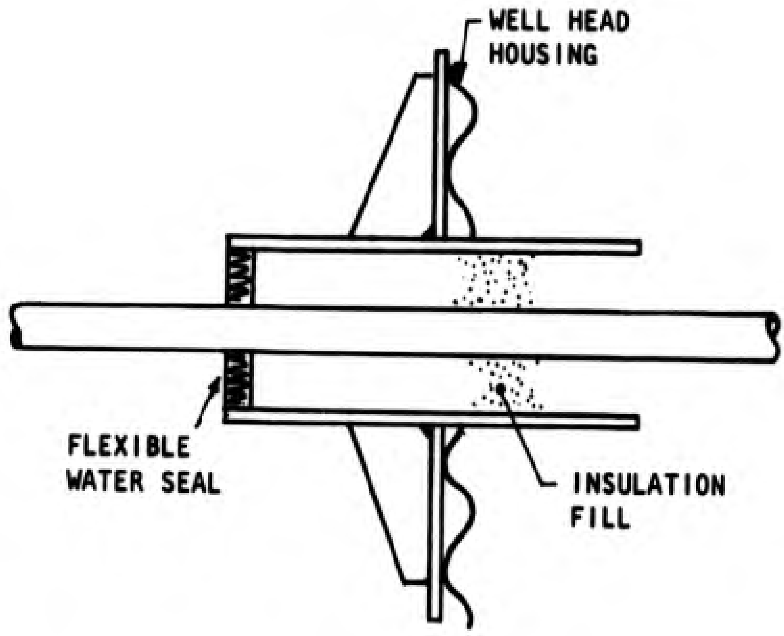

(c) CORRUGATED STEEL STRUCTURE

FIGURE 8.1 HARDENED PIPE PENETRATIONS (Continued)

The flexible connections described above are for vertical (or shearing) relative displacements. Differential horizontal displacements can be provided for by bends in the pipe routing to the shelter.

8.7.4 Well-to-Housing Connection

The connection between the discharge pipe and the housing structure must provide flexibility for relative vertical and horizontal motion. A flexible neoprene hose in the configuration shown in Figures 1.1 to 1.3 is recommended for the connection.

8.8 ELECTRICAL

All electrical cable and equipment (breakers, relays, etc.) should be completely water tight and all connections from supply cable to well head housing and from housing to pump motor should be flexible as discussed in Paragraph 8.7.3 for flexible pipe connections.

(This page intentionally left blank.)

SECTION 9

SIMULATED WELL CASING TESTS

9.1 INTRODUCTION

This section deals with the stress analysis of deep water well casings that are planned to be installed and tested at the scheduled 500 ton TNT test at the Watching Hill Blast Range of the Suffield Experiment Station, Ralston, Alberta, Canada.

Three cases were analyzed, one integral 200-foot well, subjected to a 50 psi overpressure, and one gel-isolated 200-foot well, subjected to a 50 psi, and a 100 psi overpressure. Any higher overpressures were not used in the analysis, as these occur close to the explosion where large direct ground disturbances are induced by the detonation, (see References 33 and 34). Thus the assumptions which these analyses are based on may not correspond to the actual field conditions in some respects.

Table 9.1, taken from Reference 33, lists the overpressure versus the distance from ground zero produced by a previous 500 ton TNT test, Operation Snowball. In the planning of the analysis it was suggested to use a 6-inch schedule 40 pipe for the well casing instead of a schedule 80 pipe as used for the other cases.

TABLE 9.1 OVERPRESSURE VERSUS DISTANCE FROM GROUND ZERO FOR OPERATION SNOWBALL

STATION	DISTANCE FROM GROUND ZERO (ft)	OVERPRESSURE (psi)	AIR WAVE SHOCK VELOCITY (ft/sec)
Estimated	200	300	8300
1	245	210	4300
2	280	150	3600
3	310	120	3300
4	370	82	2500

9.2 SOIL PROPERTIES

The soil profile illustrated in Figure 9.1 represents the soil layering at the site of the Operation Snowball test, and it is assumed that the site of the scheduled test has a similar soil layering. The soil profile was compiled from information given in References 33 to 35. The Tables A-2 and A-3, Appendix A, are used to obtain the other soil parameters required in the analysis.

9.3 INTEGRAL WELL CONCEPT

The procedure used for the stress analysis of the integral well is described in Section 6 and Appendix B. The overpressure used for this case is 50 psi, weapon yield 0.5 kilotons, and the positive phase duration is 0.053 seconds.

The axial stress in the 6-inch schedule 40 pipe caused by the wave front that produced the maximum combined stress (σ_c = 28,600 psi) in the casing is illustrated in Figure 9.2. The bending stress developed at the water table (σ_b = 22,100 psi) is the governing stress.

Figure 9.3 shows the free-field horizontal displacements caused by the 93-foot deep wave front. The Figures 9.4 and 9.5, taken from Reference 33, show the measured displacements at Station 4 of the Operation Snowball test.

At Station 4, where the overpressure was 82 psi, the measured horizontal displacement at the 15-foot depth was 2.4 inches, see Figure 9.5. Reference 33 shows that most of the ground displacement is due to the direct ground disturbance which is not accounted for by the computer solution of the integral well concept.

9.4 GEL-ISOLATED WELL CONCEPT

The free-field shock spectra for the two cases analyzed, 50 psi and 100 psi overpressure, are given in Appendix C, Figures C-43 to C-46.

(Text continued on Page 111)

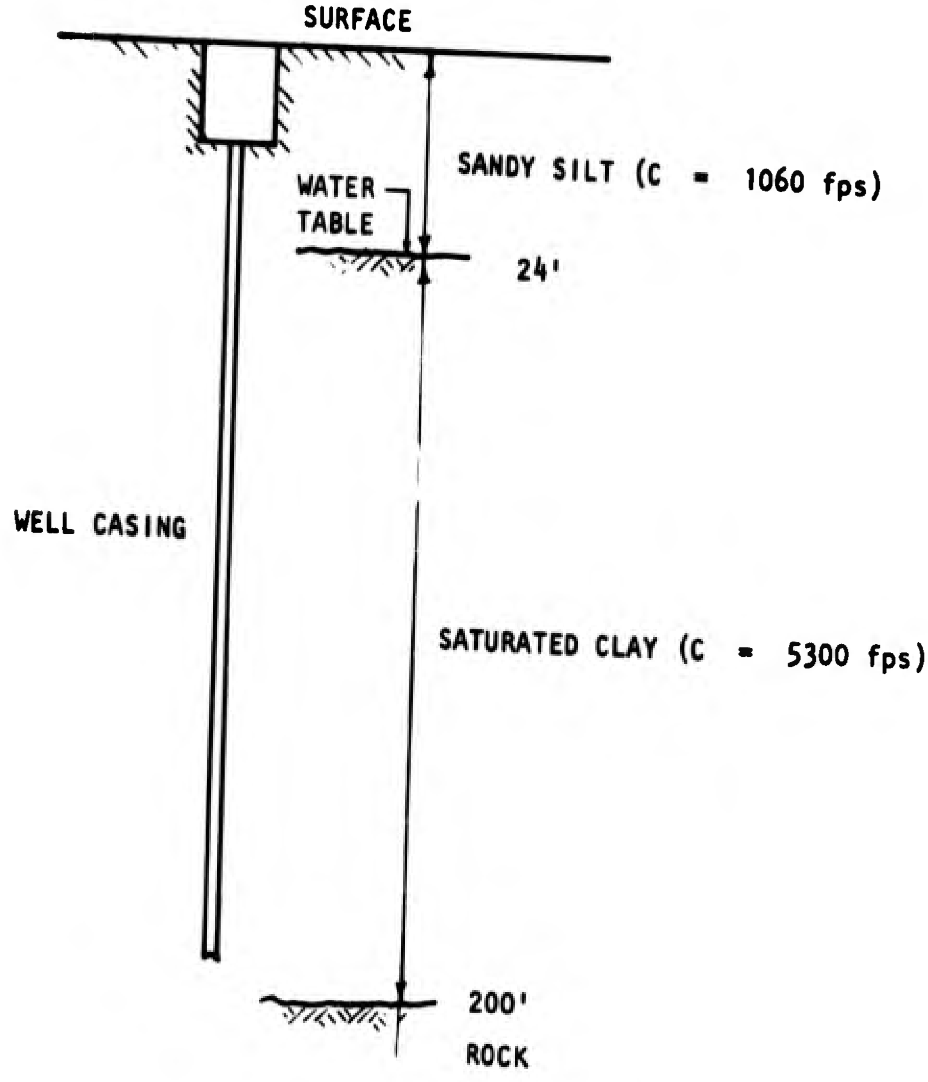

FIGURE 9.1 SOIL PROFILE FOR THE CANADIAN TEST SITE

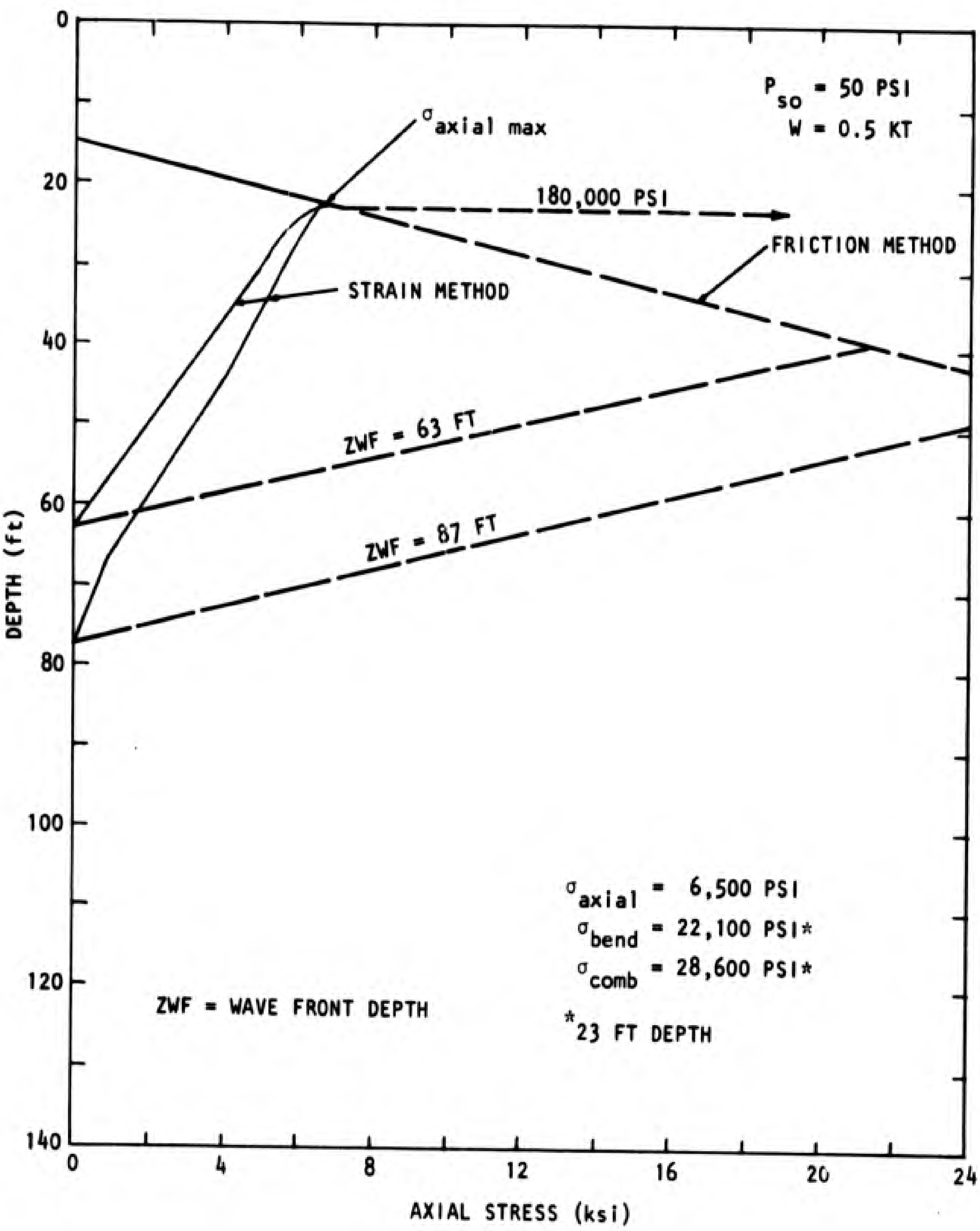

FIGURE 9.2 MAXIMUM AXIAL STRESS VERSUS DEPTH (CASE-CANADA)

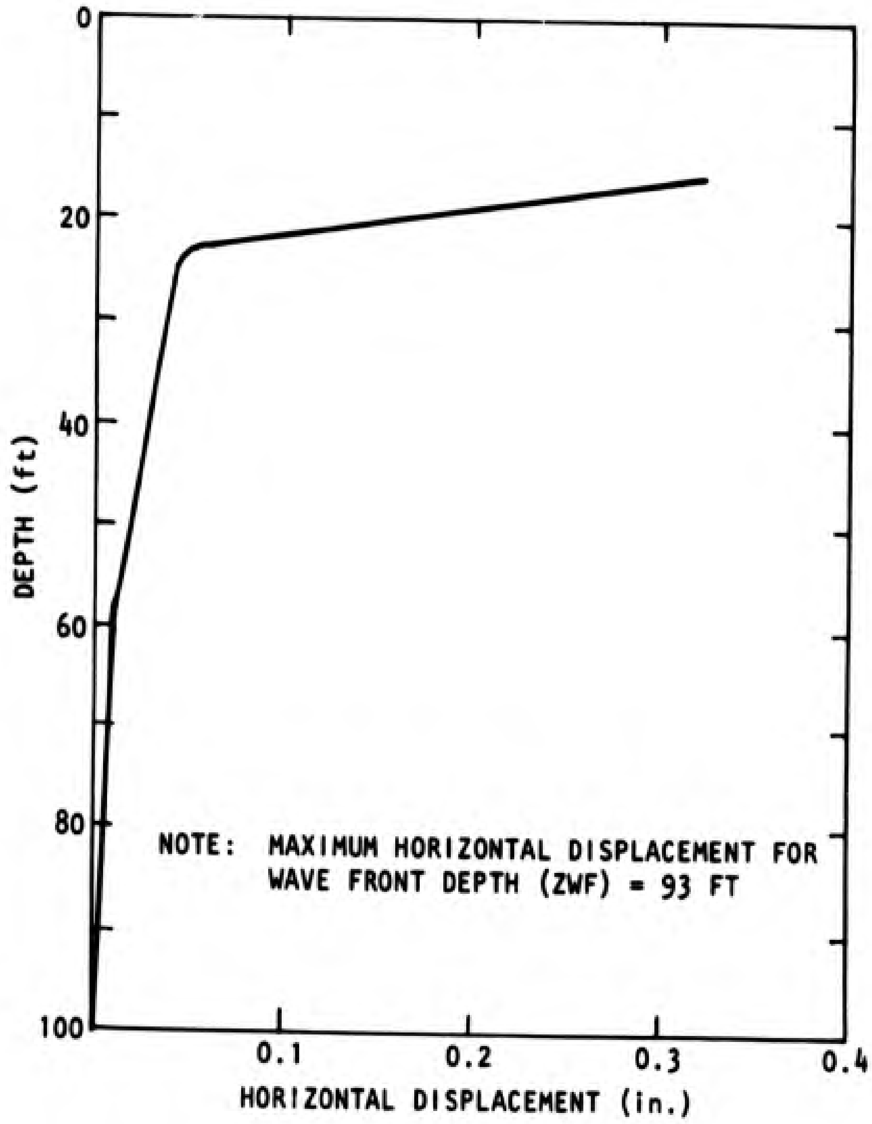

FIGURE 9.3 HORIZONTAL DISPLACEMENT VERSUS DEPTH (CASE-CANADA)

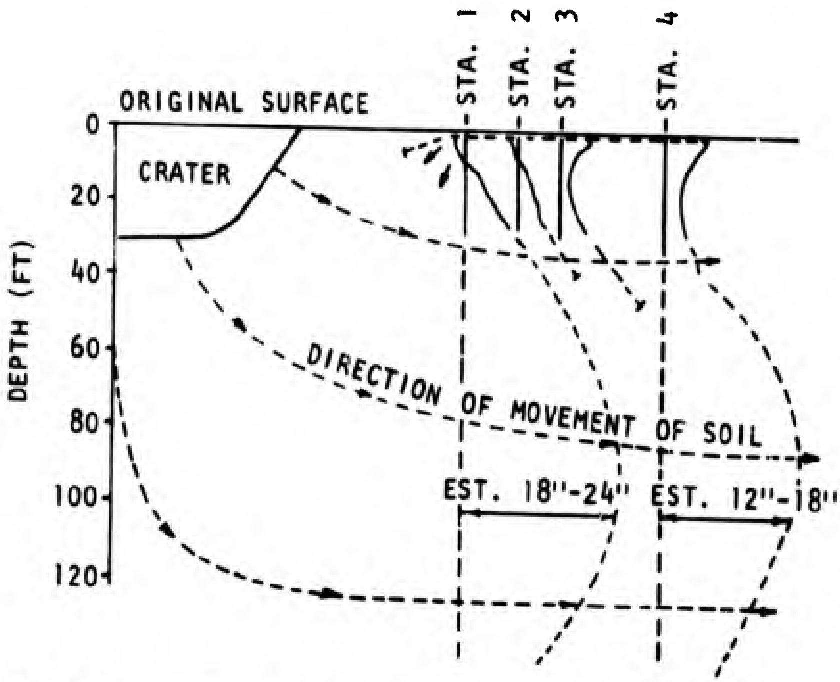

FIGURE 9.4 ESTIMATED RADIAL DISPLACEMENTS BELOW CASING (FROM REFERENCE 33)

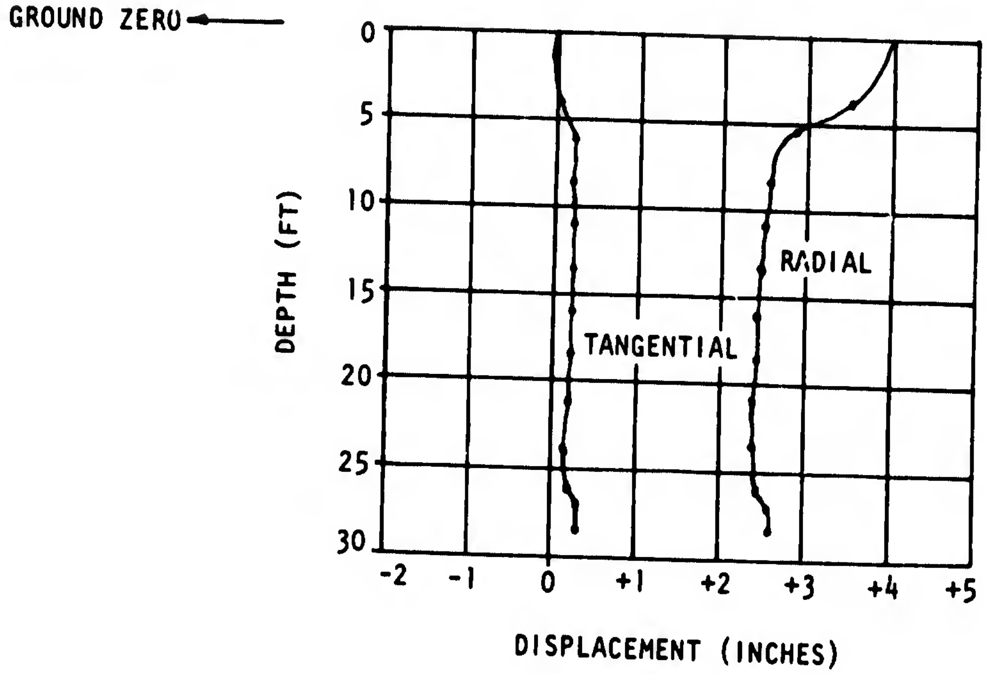

FIGURE 9.5 RADIAL AND TANGENTIAL MOVEMENT WITH DEPTH, STATION 4 (FROM REFERENCE 33)

The peak values of the accelerations, velocities and displacements are given in Table 3.11. The maximum acceleration and horizontal displacement at the 10-foot depth for the 50 psi and 100 psi overpressures are 20 and 19 g's, and 0.43 and 0.70 inches, respectively. The displacements are in the same range as the displacement indicated by the analysis of the integral well concept.

In calculating the stresses it was assumed that the casing would be gel isolated down to a depth of 100 feet. The stresses are listed in Table 4.10.

(This page intentionally left blank.)

SECTION 10

ALTERNATE WELL CONCEPTS

10.1 CHEMICAL GROUTING

10.1.1 Objective

In the case of the integral well concept, it was found that maximum axial stresses occur in well casings sited in soft soil layers such as dry sand. Chemical grouts are available which can be pumped into a soil to fill the voids and consolidate them into a continuous mass when the grout gels. The grouted soils will have increased stability and strength due to the shear strength of the gel matrix binding the soil particles together and will be more impervious to ground water.

Chemical grouting was investigated as a means of stiffening a cylindrical shaped soil-column around the well to reduce the vertical strain in the soil, and consequently reduce the axial stress in the well casing.

10.1.2. Chemical Grouts

The earliest chemical grouting was by the Joosten Process (now patented in the United States), consisting of a combination of sodium silicate and calcium chloride. The sodium silicate is diluted with water and the gelling agent, a 5 to 10 percent solution of calcium chloride, is added just before injection.

AM-9, a trademarked product of the American Cyanamid Company, uses a somewhat different combination of materials. The AM-9 is a mixture of two organic compounds, acrylamide and N-N'-methylene bisacrylamide, available as a water-soluble powder. Made up in solutions varying from 7 to 15 percent, the AM-9 is gelled by the use of two catalysts. By varying the relative quantities of these catalysts, the setting time can be controlled from a few minutes to 2 hours.

Another type of chemical grout uses lignin, a waste product resulting from paper manufacture. The lignin, combined with a dichromate, forms a soluble chrome-lignin powder which gels to a dark brown substance of rubbery consistency. The powder is mixed with 4 or 5 parts of water, the amount of water controlling the setting time. TERRA FIRMA, a chemical grouting compound manufactured by Intrusion-Prepakt, Inc. is an example of a lignin-type grout.

10.1.3 Other Types of Grout

Grouts containing suspended solids, such as cement and bentonite, are also used to grout soils for stability and dewatering, but these were not considered because the size of the voids that can be grouted is limited by the size of the suspended particles. Practically, in order to penetrate a formation, the size of the suspended particles cannot be greater than about one-third the size of the voids. This criterion determines the range of soils in which cement and bentonite grouts are effective. The minimum grain size for effective use of cement is 0.8 mm (coarse sand), and the minimum grain size for effective use of bentonite is 0.4 mm (medium sand), (Reference 21, 22).

10.1.4 Limitations on Chemical Grouting

The ability of a chemical grout to penetrate a formation at a pumping rate and pressure, consistent with good engineering practice, is limited by the viscosity of the solution. The sodium silicate-type chemical grouts can be used effectively down to a fine sand or similar soil classification. The chrome lignins can also be used for fine sands. The AM-9 chemical grout can be used for silts with a grain size down to 0.013 mm. Figure 10.1 taken from Reference 22 shows a comparison of the limitations of different grouts as determined by the grain size of the soil to be grouted.

10.1.5 Injection of Chemical Grout

Injection is performed through a pipe 1/2 to 3/4 inch in diameter which is driven into the ground to full depth and then retracted slightly. Pipes are spaced on 18 to 30-inch centers, generally staggered, since the area of dispersion is considered to be within a radius of about 2 feet (Reference 28).

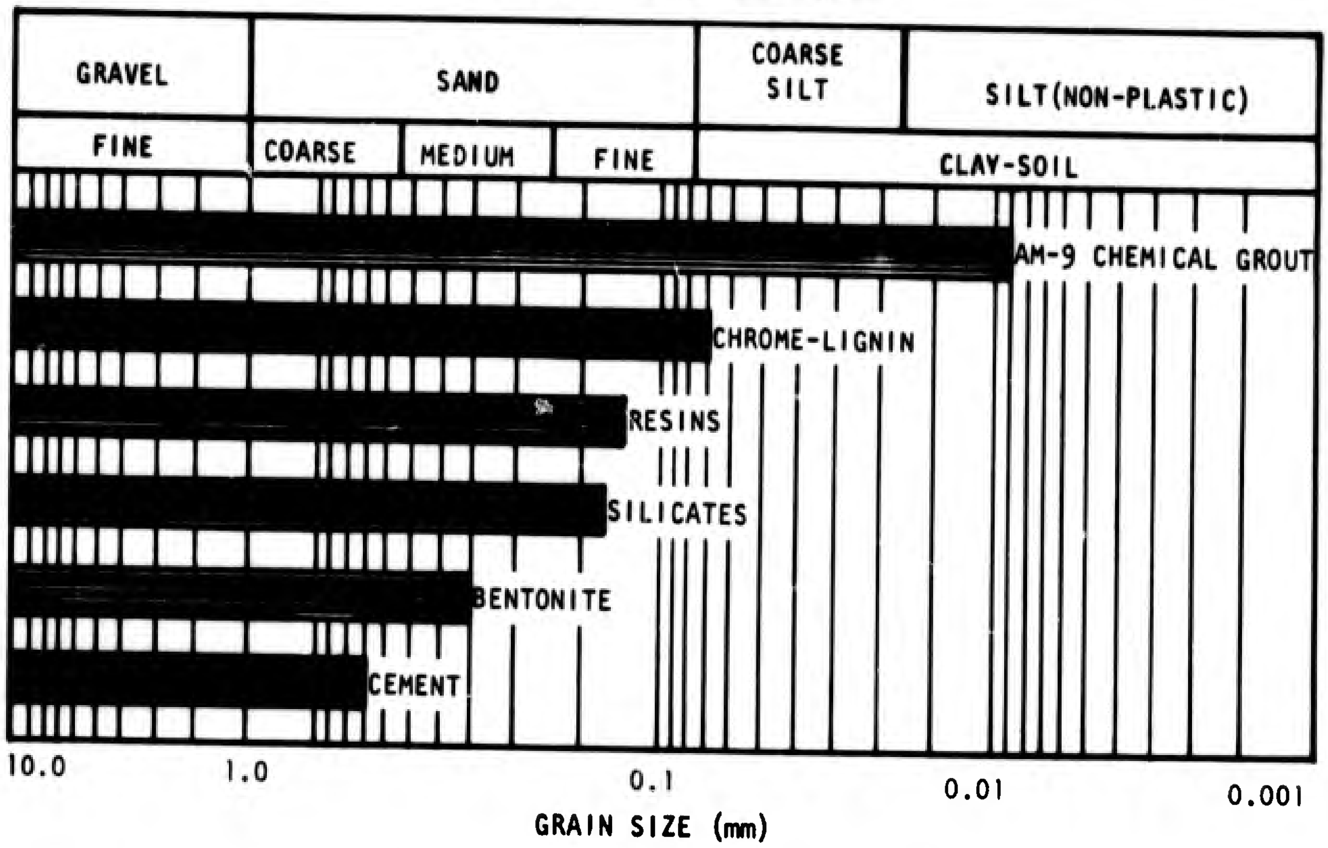

FIGURE 10.1 COMPARISON OF GROUT LIMITATIONS

Grouting is begun at the bottom of the layer to be grouted, the grout pipe being gradually withdrawn as an increase in the pressure required indicates that the maximum quantity of grout has been absorbed.

10.1.6 Analysis of Soil-Column

The following analysis is used to investigate a possible reduction in casing stress if the surrounding soil is stiffened by chemical grout.

It is assumed that the chemically grouted soil forms a cylindrical column with a radius R as shown in Figure 10.2

Where P_h = horizontal pressure in the soil (psi)
P_z = vertical pressure in the soil (psi)
F = downdrag force acting on the soil column (psi)
μ = coefficient of friction between grouted and ungrouted soil
k_o = ratio of vertical to horizontal pressure

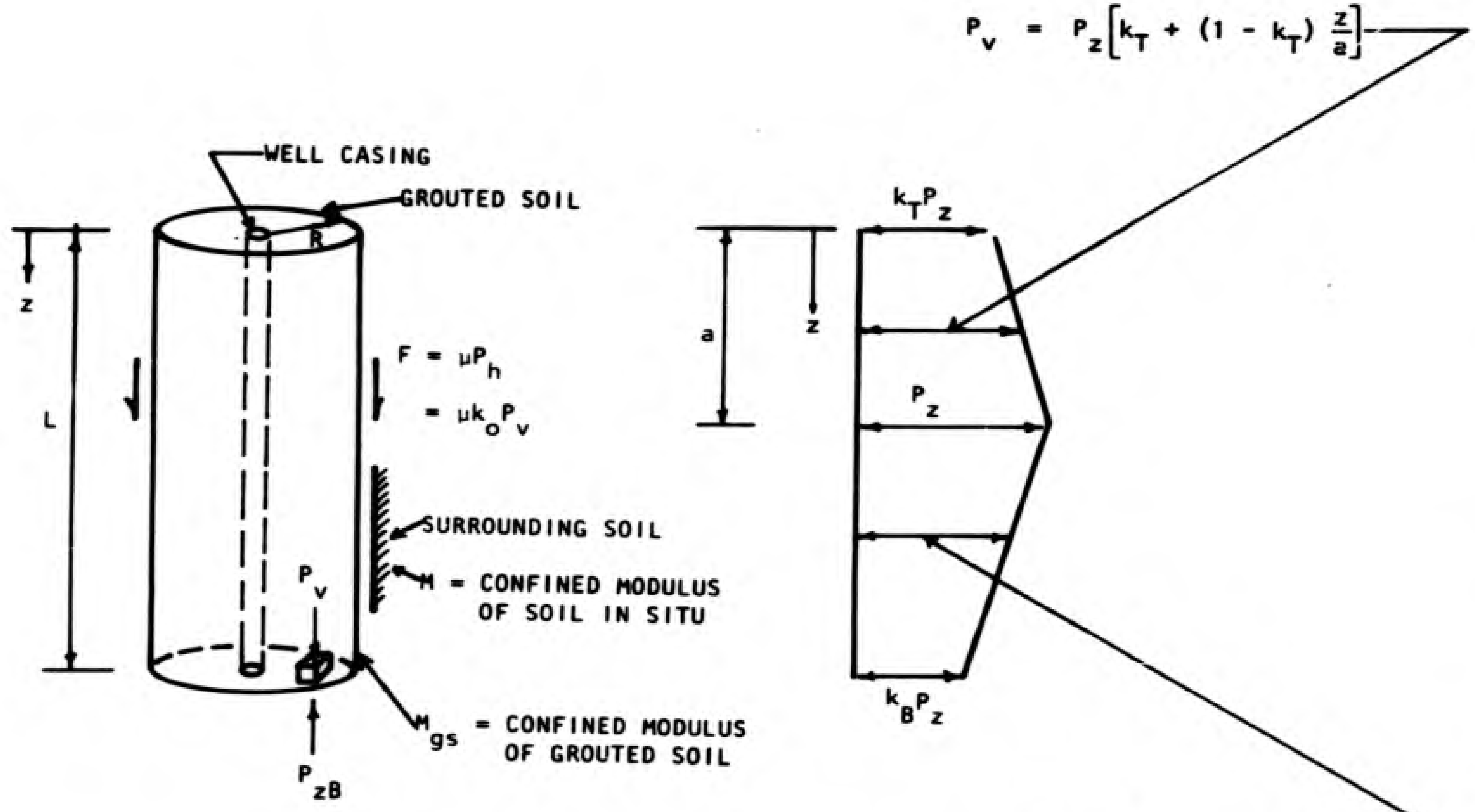

FIGURE 10.2 MODEL OF GROUTED SOIL COLUMN

Because of the increased strength of the grouted soil it is assumed that a shear failure will occur in the interface between the grouted soil and the natural soil. Further a uniform horizontal pressure distribution is assumed around the grouted soil-column. Using a vertical pressure distribution as shown in Figure 10.2 and summing up the static forces acting on the column and neglecting any dynamic response, the pressure at the bottom of the column is:

$$P_{zB} = k_B P_z + \frac{1}{\pi R^2} \int_0^L F 2\pi R dz$$

$$P_{zB} = P_z k_B + \frac{2\pi R}{\pi R^2} \left[\int_0^a \mu k_o P_z \left[k_T + \left(1 - k_T\right) \frac{z}{a} \right] dz \right.$$

$$\left. + \int_a^L \mu k_o P_z \left[1 - \left(1 - k_B\right) \left(\frac{z - a}{l - a}\right) \right] dz \right]$$

where k_T and k_B are the ratios of the vertical pressure at the top and at the bottom of the column to the maximum vertical pressure along the column respectively.

Performing the integration, the following formula is obtained:

$$P_{zB} = P_z \left[k_B + \frac{2\mu k_o}{R} \left(\left(k_T + 1\right) \frac{a}{2} + L \left[1 - \frac{1}{2}\left(1 - k_B\right)\left(\frac{L - 2a}{L - a}\right) \right] \right. \right.$$

$$\left. \left. - a \left[1 + \frac{a}{2} \left(\frac{1 - k_B}{L - a}\right) \right] \right) \right]$$

In the case of a rectangular vertical pressure distribution in which k_T and k_B equal one, the pressure at the lower end of the grouted column will be:

$$P_{zB} = P_z\left(1 + 0.8\,\frac{L}{R}\right)$$

for $\mu = 0.8$

$k_o = 0.5.$

For the case of a vertical pressure distribution in which k_T equals 0.9 and k_B equals 0.7, the pressure at the lower end of the grouted column will be:

$$P_{zB} = P_z\left(0.7 + 0.75\,\frac{L}{R}\right)$$

for $\mu = 0.8$

$k_o = 0.5$

$a = L/2.$

The coefficient 0.75 L/R is the contribution from the shear forces acting along the outside of the grouted soil.

Taking the depth of the layer L as 60 feet and the radius R of 5 feet, the bottom pressure will be:

$$P_{zB} = P_z\left(0.7 + 0.75\,\frac{60}{5}\right) \approx 10P_z$$

Thus in order to have the same strain in the grouted soil as in the surrounding soil at the 60 foot depth, the effective modulus of the grouted soil must be 10 times larger than the effective modulus of the surrounding soil. This would of course produce the same stress in the well casing as if no grouting was used. In order to reduce the axial stress in the casing by one-half, assuming that there is no major reduction in the coefficient of internal friction, the constrained modulus of the grouted soil should be 20 times that of the surrounding soil. Any such increase in the stiffness of the soil would be difficult to obtain by the use of chemical grouting as discussed below.

10.1.7 Strength of Chemically Grouted Soils

Most chemical grout compounds are composed of about 90 to 95 percent water, by weight and by volume. Upon gellation, this water becomes integrated into the space lattice of the gel structure. When the gel is stored under conditions of low humidity, such as dry soil, water will evaporate slowly, and the gel will shrink. Reference 22 reports that in medium to dense soils, shrinkage of the soil mass as a whole does not occur, although the solid gel in the soil pores will shrink under non-saturated conditions, as would be the case if the water table was lowered. This results in capillary tensile forces which will increase the apparent unconfined compression strength. Upon drying of the gel, internal tensile forces are developed and the intergranular pressure is increased, and so is the resistance to shear failure. In a completely dry, gelled soil, internal tensile forces are large, and it is reported (Reference 22) that the unconfined compressive strength may approach that of weak cement mortar, with an elastic modulus of approximately E_c equals 100,000 psi, but even this is inadequate for the stiffness requirement of a soil-column surrounding the well casing. The chemical grout itself is a rubbery elastic material and its strength and stiffness is negligible.

The use of chemical grouts for stiffening of dry soils, as would be the case for most of the well sites, has been discouraged in the past due to poor results (see Reference 22, 23 and 24). The use of AM-9 in dry sands, with the same techniques as would be used below the water table, results in poor stabilization and strength. The low viscosity of the compound permits gravitational and capillary forces to act so rapidly, that dispersion of the fluid occurs prior to gellation. In addition, there is evidence of catalyst absorption on the dry sand grains, lengthening and even inhibiting completely the formation of a gel.

One possible solution is an additive to increase the solution viscosity. This, however, would restrict the penetration of the grout and require either higher pumping pressures or lower pumping rates for field work. None of these side effects are desirable. Another possible solution to the dispersion part of the problem is to use shorter gel times. This requires the use of higher catalyst concentrations, which would also solve the problem of catalyst absorption. This possibility has been investigated by laboratory tests (see Reference 24). A third solution would be, prior to grouting, to saturate the soil that is to be grouted with water, and thus create the same conditions as for grouting under the water table. However, any dependable and successful stiffening of dry soil by this method is not reported.

Since it is uncertain that a proper gellation may occur in grouting of a dry soil, as would be the case for any well site application, the necessary increase in the constrained modulus of the grouted soil may not be obtained.

10.1.8 Permanence

In the case of AM-9 chemical grout, experience only dates back to the early fifties and there are no long-term data to illustrate its permanence in the ground. On the basis of field experience, however, it is known that stabilized soils retain their properties for a minimum of ten years. Reference 22 states that there is no reason to believe that AM-9 gels in place are not permanent.

Laboratory tests indicate that repeated freeze-thaw and complete wet-dry cycles will cause eventual deterioration of stabilized soil masses due to the rupture of gel-soil bonds but not to deterioration of the gel itself.

10.1.9 Cost of Grouting

In addition to meeting all of the technological requirements dictated by specific field conditions, any grout must be economically feasible. This includes weighing the overall benefits against the costs, comparison with other methods of solving the problem, and comparison with other grouts.

The in-place cost of grouting seems to be about the same for both cement and chemical grout. Reference 25 gives an in-place cost of $5 to $10 per cubic foot of grout. Assuming a ten foot diameter grouted soil-column around the well casing and a 30 percent void space, the cost of grouting would be in the range of $120 to $240 per foot of casing. The in-place cost of a 15 foot diameter grouted soil-column would range from $260 to $520 per foot of casing.

10.1.10 Toxicity

Most chemical grouting compounds contain toxic compounds. In gel form, AM-9 chemical grout contains some acrylamide. The gel produced when a 10 percent solution AM-9 is properly catalyzed contains approximately 0.3 percent acrylamide. Poor gellation may increase this percentage. It is recommended that an application of chemical grouting near a water supply which may be used for drinking water or recreational purposes should be undertaken only when conditions indicate that no appreciable quantity of toxic components will find its way into such water. Approval for the use of chemical grouting should be obtained from health authorities for each such case (see Reference 23).

10.1.11 Conclusions and Recommendations

In order to obtain, by chemical grouting, a significant reduction of the axial stresses in a "hard" well casing installed in a soft soil layer like Sand III or similar material, the constrained modulus of the soil around the casing must be increased from 15 to 20 times, depending on the depth of the layer and the area grouted. It is very unlikely that such an increase in the constrained modulus can be obtained by present methods of chemical grouting. By grouting a large area around the well the required increase in the soil stiffness may be obtained; however, this would prove extremely costly compared to the gel-isolated well concept.

10.2 COATED CASINGS

In connection with the design of protective structures, studies have been made on the feasibility of coating the outside surface of the structure with a lubricant to reduce downdrag shear stresses caused by relative movement between the structure and the surrounding medium. Reference 27 reports on one such laboratory investigation in which the coefficient of friction between sand and cement mortar and steel bars coated with teflon and graphite were measured under both static and dynamic loading conditions.

Graphite is classified as a solid lubricant because of its laminar molecular structure which allows the layers to slide over each other easily. Plastics such as teflon offer good antifriction characteristics and can be used in sliding bearings, without lubrication, where loads or reaction forces are transmitted to a shaft rotating relative to the bearing.

Results of the tests indicated that both graphite and teflon serve as friction reducers compared to uncoated surfaces, especially under static or slow rates of loading. A comparison of static and dynamic coefficients of friction as reported in Reference 27 is shown in Table 10.1.

TABLE 10.1 COMPARISON OF STATIC AND DYNAMIC COEFFICIENTS OF FRICTION IN SAND

BAR SURFACE	COEFFICIENT OF FRICTION	
	Static μ_s	Dynamic μ_d
Plain Steel	0.50	0.63
Plain Smooth Mortar	0.59	0.67
Plain Rough Mortar	0.74	0.82
Teflon Coated Smooth Mortar	0.33	0.58
Teflon Coated Steel	0.33	0.56
Graphite Coated Smooth Mortar	0.32	0.44

It is seen from the table that the static coefficients of friction for the coated bars are approximately 50 percent of those for the plain smooth surfaces. However, under dynamic loading conditions the coefficient of friction for the coated surfaces averages about 80 percent of those for the teflon coated specimens. Graphite appears to be somewhat more effective than teflon at high rates of loading due, perhaps, to viscosity effects. Reference 27 also concludes that once slip has been initiated, the dynamic coefficient of friction increases slightly with increasing velocity (about 10 percent for velocities up to 30 inches per second).

In Section 6 the skin friction stresses determined for the integral well casing located in sandy material assumed a coefficient of friction of 0.60 for dry sand. Therefore, downdrag forces under dynamic loading conditions cannot be reduced significantly by coating the casings.

It is noted that the coefficient of friction between teflon and teflon is very small. This might be used effectively to reduce skin friction if a teflon sleeve, or equivalent covering, would be placed over the teflon-coated casing to provide a teflon-to-teflon sliding surface. However, the difficulties in constructing an inner face of this type would have to be investigated and tested.

10.3 FOAM-ISOLATED WELL CASING

The use of a plastic foam backfill to isolate the casing from the soil was also considered. The foam would be used in place of the liquid gel and would have to exhibit some of the same characteristics; i.e., minimum transfer of downdrag shear to the well casing and support of soil or rock that might slough off the boring wall.

Polyurethane foams are available in two formulations which could be used in this application. These are the rigid and semi-rigid foams which have the density and stress-strain properties that would be required (see Reference 30). Flexible polyurethane foams would not be applicable because of their softness (low bearing strength) and inability to support sloughing from the cavity wall. The foams would have to be placed in the annulus by grouting from the outside of the casing and in layers, since the material rises (expands) when curing.

The principal disadvantage of using a foam material is cost. The material itself is expensive and a large volume would be required to fill the annulus. Since the material is not normally used in a field application nor placed underground, special provisions would have to adapt the mixing equipment to field usage and, in addition, special techniques would have to be developed and tested for placing the foam. It has been estimated (Reference 31) that the cost of foam plastics in-place is more expensive than cement grouts by a factor of 10 or more. However, research into and development of the capability of casting large volumes of foamed plastics ground tunnel liners is currently being undertaken, and, if successful, will undoubtedly influence their in-place cost.

The use of foam to isolate the casing is not recommended because of ecomony.

SECTION 11

REFERENCES

1. Newmark, M.M., Haltiwanger, J.D., Air Force Design Manual - Principals and Practices for Design of Hardened Structures, AFSWC-TDR-62-138 (AD 295 408), University of Illinois, December 1962.

2. Whitman, R.V., "Effects of Viscosity and Inelasticity Upon Stress Waves Through Confined Soil", Shock, Vibration and Associated Environments, Protective Construction, Part II, Bulletin No. 32, August 1963, p. 107-123.

3. Whitman, R.V., Clark, G.B., Nuclear Geoplosics, Part II - Mechanical Properties of Earth Materials, DASA-1285(II), MIT, May 1964.

4. Elswick, W.R., Pressure Response Within an Enclosure Subject to a Blast Wave, RM-2660, Rand Corp., March 1961.

5. Sauer, F.M., Nuclear Geoplosics, Part IV - Empirical Analysis of Ground Motion and Cratering, DASA-1285(IV), SRI, May 1964.

6. Terzaghi, K., Theoretical Soil Mechanics, Wiley, New York, 1943.

7. Salvadori, M.G., and Baron, M.L., Numerical Methods in Engineering, Prentice-Hall, Englewood Cliffs, N. J., 1961.

8. Allen, D., "Wilmington Subsidence Problems", World Oil, August 1959, p. 86-87.

9. Agbabian-Jacobsen Associates, Design of Shock Proof Wells for Shelter Cooling, AJA-6625, Report for USNCEL, July 1966, (Unpublished).

10. Jastrzebski, Z.D., Nature and Properties of Engineering Materials, Wiley, New York, 1959.

11. Mitchell, J.K., "Fundamental Aspects of Thixotropy in Soils," Trans. ASCE, 126, Part I, 1961, p. 1586-1620.

12. Jackson, G.L., "Oil-System Packer Fluid Insures Maximum Casing Recovery", Oil and Gas Journal, February 24, 1964.

13. Lloyd, D.D., Casing Recovery Economics, Paper Presented at Los Angeles, March 18, 1963, American Petroleum Institute Meeting.

14. Chemical Engineers' Handbook, McGraw-Hill, New York, 1950, p. 1195-1202.

15. Todd, M.B., "How to Complete Water Source Wells", World Oil, March 1967, p. 86-91.

16. Costantino, C.J., Automated Design of Advanced Hardened Facilities Study, BSD TR-66-256 Volume 1 (AD 801 237 L), IIT Res. Inst. September 1966.

17. Lipner, N., Fay, F.B., "Acoustic Waves Generated by the Motion of Piping Containing a Fluid", Shock and Vibration Bulletin, Bulletin 35, Part 3, (AD 628 600), January 1966, p. 161-167.

18. Wang, C.K., Matrix Methods of Structural Analysis, International Textbook Company, Scranton, Pa., 1966.

19. Young, D., "Response of Structural Systems to Ground Shock," "Shock and Structural Response", Papers Presented at the Annual Meeting of ASME, November 1960.

20. Archer, J.S., "Consistent Mass Matrix for Distributed Mass Systems," ASCE - Structural Journal, 89 ST4, August 1963, p. 161-178.

21. King, J.C., Bush, E.G.W., "Symposium on Grouting: Grouting of Granular Material," Trans. ASCE 128, Part 1, 1963, p. 1279-1310.

22. AM-9 Chemical Grout, Engineering Chemical Research Center, American Cyanamid Company.

23. Chemical Grout Field Manual, Engineering Chemical Research Center, American Cyanamid Company, April 1966.

24. Karol, R.H., Grouting in Dry Sands, Soils Engineering Research Center, American Cyanamid Company, October 2, 1962.

25. Karol, R.H., Grout Costs, Soils Engineering Research Center, American Cyanamid Company, November 18, 1963.

26. Wahl, A.M., Mechanical Springs, Second Edition, McGraw-Hill, New York, 1963.

27. Leonards, G.A., Experimental Study of Static and Dynamic Friction Between Soil and Typical Construction Materials, AFWL-TR-65-161 (AD 627 138), Purdue University, December 1965.

28. Carson, A.B., Foundation Construction, McGraw-Hill, New York, 1965, p. 110-113.

29. Agbabian-Jacobsen Associates, Study of Shock Isolation for Hardened Structures, (AD 639 303), June 1966.

30. Dombrow, B.A., Polyurethanes, Reinhold, New York, 1965.

31. Hoff, G.C., Shock-Absorbing Materials, Report 1 - Backpacking Materials for Deeply Buried Protective Structures, TR 6-763 (AD 654 511), WES, March 1967.

32. Kingery, C.N., Pannill, B.F., Peak Overpressure versus Scaled Distance for TNT Surface Burst - Hemispherical Charge, BRL Memo Number 1518, (AD 443 102), April 1964.

33. DASA Data Center, Operation Snowball, Symposium Proceedings, (AD 470 321), DASA 1642-1, August 1965.

34. Seknicka, J.E., Druebert, H.H., Operation Snowball Ground Displacement Study, WL TR-64-175 (AD 471 182), AFWL, August 1965.

35. Hendron, A.J., Jr., Correlation of Operation Snowball Ground Motions with Dynamic Properties of Test Site Soils; Paper 1-745 (AD 474 046), WES, October 1965.

36. Tomita, H., Flexible Utility Connections for Underground Protective Shelters, Technical Note N-678 (AD 454 794), NCEL, January 1965.

37. Newmark, N.M., (U) Computations of Free-Field Motions and Shock Spectra for Linear and Nonlinear Systems, Prepared Under Contract AF 04(694)-503, July 1964 (SECRET).

38. Jacobsen, L. S. Ayre, R. S. Engineering Vibrations, McGraw-Hill, New York, 1958.

39. Timoshenko, S., Theory of Elastic Stability, McGraw-Hill, New York, 1936.

(This page intentionally left blank.)

APPENDIX A

PHYSICAL CONSTANTS AND SOIL PROPERTIES

A number of assumptions or derivations are necessary to provide complete working data for use with the analytical procedures outlined in the report. These additional data requirements fall into three classifications.

a. Those related to the overpressure wave form, free air and sub-surface wave velocities, and peak pressure attenuation versus depth.

b. Those related to the otherwise undefined soil properties such as: the variation of stress sensitive properties, including assumptions as to the variation of the horizontal to vertical soil displacement coefficient β; the variation in the ratio of the seismic velocity in the soil to the free air shock velocity C/U.

c. Assumptions implicit in the method of installation of the casings and the effects of soil properties on axially directed forces induced by vertical soil displacement.

OVERPRESSURE WAVE CHARACTERISTICS

Free air shock wave characteristics as related to overpressure and weapon yield are well established. There is less complete agreement on sub-surface peak pressure attenuation. However, the most generally accepted approach is that defined in the Air Force Design Manual, (Reference 1). This source has been used in this study to establish the free air shock front velocities U and positive phase durations D_p^+ tabulated in Table A-1.

TABLE A-1 D_p^+ AND U VERSUS YIELD AND P_{so}

PEAK SURFACE OVERPRESSURE (psi)	POSITIVE D_p^+ PHASE DURATION		FREE AIR SHOCK FRONT VELOCITY U (fps)
	1 M.T. (sec)	20 M.T. (sec)	
15	1.40	3.80	1520
50	.90	2.44	2200
100	.84	2.28	2900
300	.96	2.62	4800

For the purposes of computing pressure sensitive soil parameters and the attenuated peak stress values used in the computer program the peak vertical soil stress P_z at any depth Z is computed from the formula (Reference 1) as:

$$P_z = \alpha_z P_{so}$$

where α_z is the attenuation factor at depth Z for a specific yield and overpressure as:

$$\alpha_z = \frac{1}{1 + Z/L_w}$$

where

$$L_w = \frac{2300W^{1/3}}{\left(P_{so}\right)^{1/2}}$$

where W is yield in megatons, Z is in feet and P_z and P_{so} are in psi.

The determination of surface overpressure P_s versus time after arrival of the shock front utilizes a two term exponential approximation developed by H. L. Brode and reduced by W. R. Elswick (Reference 4) in which:

$$P_s = P_{so}\left(1 - \tau\right)\left(Ae^{-a\tau} + Be^{-a\tau}\right)$$

where

$$\tau = \frac{t}{D_p^+}$$

and

$$A = \frac{2.28(8 + P_a)}{\left(27.66 + P_a + 1.2P_a^2 + .007P_a^3\right)}$$

$$B = 1 - A$$

$$a = \left[\frac{P_a}{1 + .1P_a}\right]^{\frac{1}{2}} + \frac{1.5P_a^2}{1500 + P_a^{1.5}}$$

$$b = 9 + 1.4P_a$$

$$P_a = \frac{P_{so}}{14.7}$$

The time after arrival of the shock front directly above the well is denoted as t.

SOIL PROPERTIES

The work statement provided the nominal seisimic velocity C and the general description of the various soils under consideration shown in Figures 2.1 to 2.3. However, eight soil properties are required to be either assumed or computed numerically.

For the purpose of this study six variables have been considered. These necessary characteristics are:

a. The seismic velocity C both above and below the water table where applicable, ft/sec.

b. The weight density γ both above and below the water table, lb/ft^3, (the seismic modulus M_c is expressed as $M_c = \rho C^2 = \gamma C^2/4.64 \times 10^3$, psi).

c. The ratio of lateral to vertical displacement, under overpressure stress, for each stratum and loading condition (a variable), β.

d. The dynamic cohesive strength C_o (psi).

e. The tangent of the angle of internal friction, $\tan\phi$.

f. The ratio of lateral to vertical dynamic stress, $k_o = P_h/P_z$. (The downdrag coefficient f_z (psi) is expressed as $f_z = C_o + k_o P_z \tan\phi$.)

g. The ratio k_p of permanent to peak vertical strain under dynamic loading (a variable).

h. The ratio k_m of soil modulus under overpressure loading to the seismic modulus, (a variable).

In a design study for a specific well installation the best available field and laboratory test methods should be applied to determine the actual static and dynamic characteristics of each soil type involved in order to provide a sound basis for the analysis. In the case at hand, however, most of the soil properties are established by engineering experience and judgement with the resulting soil profile characteristics notably idealized. The controlling consideration in making the necessary assumptions is that the assigned properties be consistent with the specified soil description within each soil type as well as among the different types. Available test data on the dynamic properties of soils are inadequate for purposes of generalization, however the properties assigned and listed in Table A-2 are, for the most part, based on reference to actual test data for specific soils and are believed to be reasonably representative.

In sandy material, the drag stress was computed as the lateral pressure times a coefficient of friction between the sand and the steel casing. The coefficient was taken as equal to the tangent of the angle of internal friction. No increase was made for dynamic loading conditions. Research carried out at Purdue University investigated static and dynamic friction between sand and various construction materials (Reference 27). Results indicated that the dynamic coefficient of friction was greater than the static coefficient of friction by about 25 percent in the case of steel or cement mortar unless the static coefficient was such that sand/sand slip was approached. Thus the angle of shearing resistance for the sand provides an upper limit to the coefficient of wall friction at all rates of loading.

It will be noted that the assumed values for C_o and $\tan\phi$ for sand are also used in the rock strata. This is based on the assumption that the casings will be installed in slightly oversized holes through the rock and that the clearance between the casing and the inside of the drill hole will be filled with sand from the strata above or with rock cuttings of similar properties. Except for the "sandy clay", clays are assumed to have no true angle of internal friction (i.e., $\tan\phi = 0$), the sands are assumed to be cohesionless. The constant C_o is sensitive to rate of load application, and the values used are based on dynamic loading. However, no attempt is made to carry the loading rate (pressure wave rise time) as a variable beyond the initial cons[illegible]ation in evaluating C_o. The coefficient k_o is similarly carried as a constant since it does not influence the down-drag coefficient in clay; it is believed to be relatively insensitive to loading rate and stress level in sand and rock.

TABLE A-2 BASIC SOIL PROPERTIES

CRITERIA		ASSUMED								COMPUTED	
Soil Description	Seismic Velocity C (fps)	Soil[1] Type	Weight Density γ (pcf)	Seismic[1] Velocity C_w (fps)	Vertical[2] Strain Ratio k_p At 300 psi	Modulus[3] Ratio k_m At 300 psi	Dynamic Cohesive Strength C_o (psi)	Horizontal to Vertical Stress Ratio k_o	Coefficient of Friction $\tan\phi$	Downdrag Coefficient f_z (psi)	Seismic Modulus M_c (psi)
Clay	6,000	I	100		.5	.05	21	.30	0	21	780,000
Sand Clay	3,000	II	100		.4	.1	12	.30	.20	$12 + 0.06P_z$	190,000
Sand	2,000	III	100		.3	.2	0	.25	.60	$0.15P_z$	86,000
		III_w	125	3,100	0	.2	0	.25	.80	$0.2P_z$	260,000
Sand	3,000	IV	110		.3	.2	0	.25	.60	$0.15P_z$	210,000
		IV_w	130	4,200	0	.2	0	.25	.80	$0.2P_z$	490,000
Water Bearing Sand	6,000	V	120		.2	.2	0	.25	.80	$0.2P_z$	930,000
		V_w	135	7,600	0	.2	0	.25	.80	$0.2P_z$	1,680,000
Water Bearing Rock	10,000	VI	140		.1	.5	0[4]	.05	.6[4]	$0.03P_z$	3,020,000
		VI_w	150	11,300	0	.5	0[4]	.05	.8[4]	$0.04P_z$	4,140,000
Rock	15,000	VII	160		.1	.5	0[4]	.05	.6[4]	$0.03P_z$	7,800,000

[1]Subscript w indicates "below water table".

[2]Reducing to 0.01 on a log scale at 1 psi.

[3]Increasing to 1.0 on a log scale at 1 psi.

[4]Based on sand filled annulus between rock and casing.

The coefficients k_p and k_m are sensitive to both stress and stress rate, but the two effects are usually in opposition. Within the range of rise times of interest the stress effect is dominant. For this reason k_p and k_m have been varied by engineering judgment for each of the cases under consideration, but since these values are approximations it did not appear justifiable to assume that k_p and k_m are continuous variables. Accordingly, a series of values of k_m, k_p, and C_p, corresponding to average peak attenuated pressure at each layer (including the artificial layers) are introduced as step functions in the analysis. The method gives conservative results in terms of soil displacement, since the values so introduced give peak pressure velocities, effective soil moduli M_p and residual deformation ratios corresponding to the simultaneous occurrence of peak attenuated overpressure at all levels. (The analysis, however, considers realistically attenuated pressures for each level in computing displacements.) Since pressure attenuation varies with depth at a much lower rate for the 20 MT than for the 1 MT yield, the degree of conservatism could be sufficiently large to cloud the comparisons. To minimize this effect, for case combinations based on the 20 MT yield; values of k_p and k_m employed for attenuated peak pressure profile are estimated on a somewhat increased attenuation with depth.

The values of the coefficient β, the ratio of horizontal to vertical soil displacement, are assumed for each of the various loading and soil profile combinations. Although limited experimental data have indicated isolated cases of apparent β values as high as one, for more typical conditions and for any of the soil profiles considered, the value of β does not exceed .75. It should be noted that the coefficient β, under weapons effects blast loading, has never been evaluated in a satisfactory manner. However, the concensus appears to be that, at soil layer seismic velocities less than, but approaching shock front velocity (i.e., $C \leq U$), β increases rapidly from about 1/3 to 1/2 and to values which may, in isolated cases, reach 1, at C/U equals 1; and that at values of $C/U > 1$ (i.e., outrunning condition) β drops rapidly to a value of about 1/2 (Reference 5). The problem is further complicated in layered media by the amplification effects in the "softer" strata and by refraction from harder underlying strata. Consideration of the effect of the water table in the otherwise homogeneous, single layered sand (Profile A) sufficiently affects the properties so that it is necessary to treat it as a two layered profile. Any extension of the knowledge of this particular subject is beyond the scope of this study. However, reasonable upper bounds for the specific cases under investigation may be estimated by applying engineering judgement.

Specific values established for each stratum of the profiles are listed in Table A-3.

TABLE A-3 DISPLACEMENT RATIO, β, VERSUS SOIL STRATA AND PROFILE

PROFILE AND WELL DEPTH	STRATUM NO.	SOIL TYPE NO.	SEISMIC VELOCITY, C (ft/sec)	RATIOS	OVERPRESSURE (psi) 15 / AIR SHOCK VELOCITY, U (ft/sec) 1520	50 / 2200	100 / 2900	300 / 4600
A-100 A-200	1	III	2,000	C/U	1.3	.91	.69	.42
				β	.50	.75	.75	.42
	2	III_w	3,100	C/U	2.0	1.4	1.1	.65
				β	.33	.33	.33	.33
B-100	1	II	3,000	C/U	2.0	1.4	1.0	.63
				β	.50	.50	.75	.75
	2	V_w	7,600	C/U	5.0	3.5	2.6	1.6
				β	.33	.33	.33	.33
B-200	1	II	3,000	C/U	2.0	1.4	1.0	.63
				β	.50	.50	.75	.63
	2	V	6,000	C/U	4.0	2.7	2.1	1.3
				β	.50	.50	.50	.50
	3	V_w	7,600	C/U	>1	>1	>1	>1
				β	.33	.33	.33	.33
C-100 C-200	1	I	6,000	C/U	4.0	2.7	2.1	1.3
				β	.50	.50	.50	.50
	2	IV	3,000	C/U	2.0	1.4	1.0	.63
				β	.50	.50	.75	.75
	3	VI_w VI	11,300 10,000	C/U	>1	>1	>1	>1
				β	.33	.33	.33	.33
D-100 D-200	1	I	6,000	C/U	4.0	2.7	1.0	1.3
				β	.50	.50	.50	.50
	2	IV	3,000	C/U	2.0	1.4	1.0	.63
				β	.50	.50	.75	.75
	3	VII	15,000	C/U	>1	>1	>1	>1
				β	.33	.33	.33	.33

APPENDIX B

STRESS ANALYSIS OF INTEGRAL CONCEPT

PROBLEM FORMULATION

The solutions of the problem as previously discussed are based on generally accepted principles of one dimensional wave front propagation in a soil medium. The two basic phases involved in the description and solution of the problem are:

a. An integration process in which the axial, bending and shear loadings along the lengths of the casing are determined at a series of discrete times for each of the 84 combinations of input data previously defined.

b. The locations and magnitudes of the maximum combined stresses for each set of parameters are computed for the casing sizes specified.

The formulation of the first phase of the solution is in turn subdivided into three steps which may be conveniently outlined by defining the procedure used to complete a single representative series of calculations. The major steps are:

1. Calculate the vertical stress-versus-depth profile in the soil at specific time instants.

2. Calculate the downdrag load for a vertical strip of unit width and for a length equal to the casing length.

3. Calculate the horizontal displacement-bending stress-versus-depth profile of the casing.

VERTICAL STRESS PROFILE IN SOIL

The vertical stress profile or stress wave form for any specific loading condition and specific time t_n after shock front arrival is idealized as shown in Figure B-1. This form is approximated by a linear

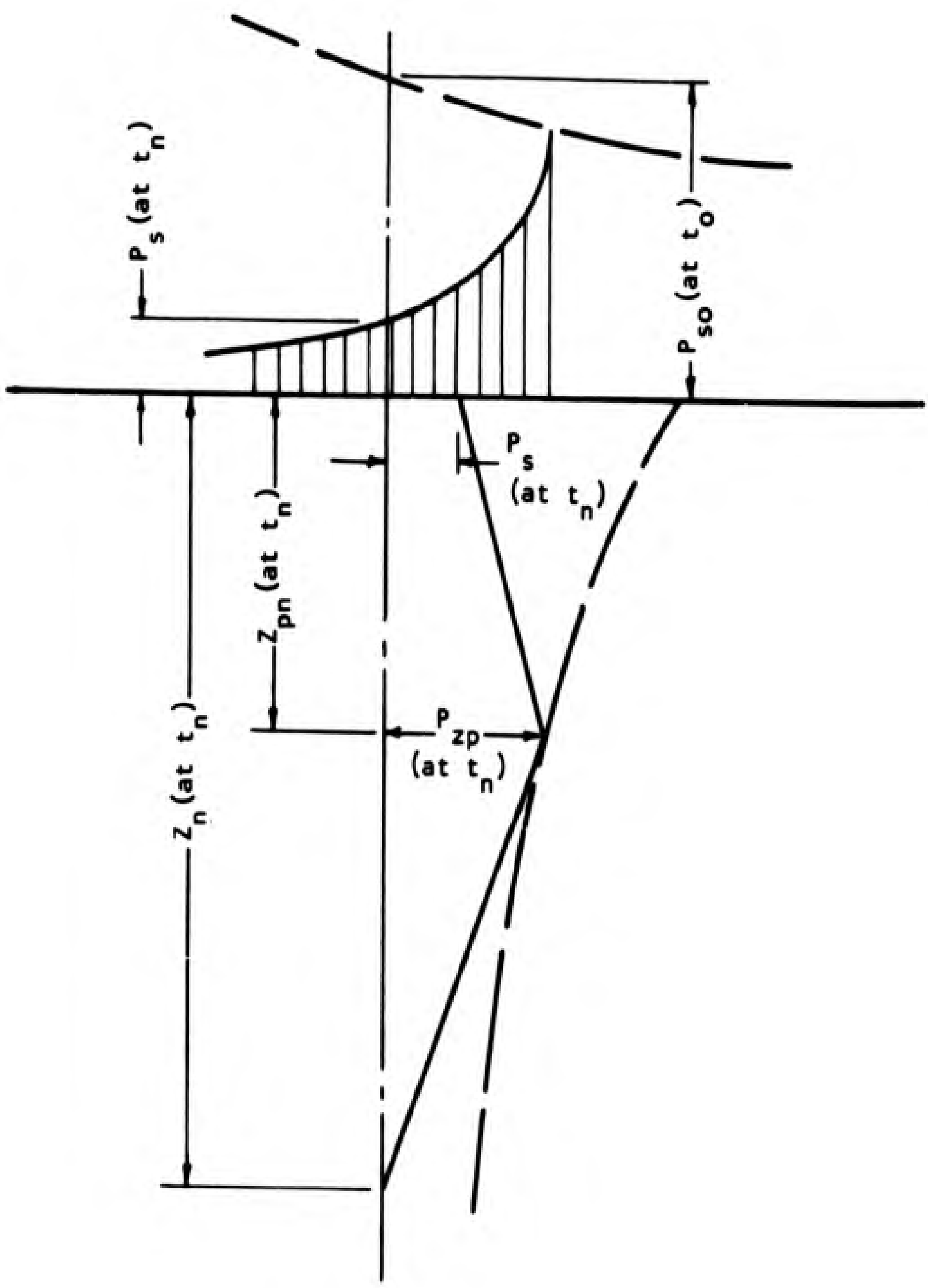

FIGURE B-1 SUBSURFACE STRESS VERSUS DEPTH BELOW SURFACE AT TIME $t_o + t_n$

rise in stress from the toe to the peak and a linear decay from the peak to the surface overpressure at the time considered. The definition of the stress profile is a procedure based on the calculation of:

a. The time t_n (after surface shock front arrival time) required for the stress wave toe to reach the depth Z_n is computed by summing the surface downward transit time of the wave front at seismic velocities C through the intervening layers, as:

$$t_n = \frac{\Delta Z_1}{C_1} + \frac{\Delta Z_2}{C_2} + \cdots + \frac{\Delta Z_n}{C_n}$$

b. The depth Z_{pn} of the stress wave peak at time t_n is calculated by summing the surface downward transit distances which the stress wave peak traverses at the pertinent peak stress wave velocities C_p through the intervening layers during time t_n. This is a logical step and involves the summation

$$Z_{pT} = \Delta Z_1 + \Delta Z_2 + \cdots + \Delta Z'$$

of the layer thicknesses traversed by the peak pressure, where $\Delta Z'$ is the distance in the last layer of peak travel. The corresponding travel time of the peak pressure at the appropriate peak stress wave velocities C_p is:

$$t_{pT} = \Delta t_1 + \Delta t_2 + \cdots + \Delta t'$$

$$t_{pT} = \frac{\Delta Z_1}{C_{p1}} + \frac{\Delta Z_2}{C_{p2}} + \cdots + \frac{\Delta Z'}{C'_p}$$

until a cumulative travel time t_{pT} is reached such that $t_{pT} \geq t_n$. If, at this point, $t_{pT} > t_n$ then $Z_{pT} > Z_{pn}$, and it is necessary to reduce both depth and travel time by the values in the last layer, i.e., by $\Delta Z'$ and $\Delta t'$ respectively. The unused travel time $\delta t'$ available in this layer can be expressed as:

$$\delta t' = t_n - (t_{pT} - \Delta t') = t_n - t_{pT} + \Delta t'$$

The corresponding remaining peak pressure travel distance, $\delta Z'$ in this layer is:

$$\delta Z' = \delta t' C'_p = C'_p (t_n - t_{pT} + \Delta t')$$

and the required depth Z_{pn} of the peak pressure at time t_n can be found as:

$$Z_{pn} = Z_{pT} - Z' + C'_p (t_n - t_{pT} + \Delta t')$$

c. The third step is the evaluation of magnitude of the attenuated peak pressure P_{zp} at time t_n and depth Z_{pn}. P_{zp} is assumed independent of soil properties, and its evaluation has been defined in Reference 1 as:

$$P_{zp} = \alpha P_{so} = \frac{P_{so}}{1 + Z/L_W}$$

where αP_{so} = peak attenuated stress and the other terms defined in Appendix A.

d. The final step in establishing the wave form profile is the determination of the decayed surface overpressure P_s at time t_n. This term is evaluated as:

$$P_s = P_{so}(1 - \tau)(Ae^{-a\tau} + Be^{-b\tau})$$

where the values of the terms are as defined in Appendix A.

The above procedure permits the definition of all magnitudes and locations of vertical stress at any depth in the soil.

DOWNDRAG COMPRESSIVE STRESSES

In calculating the axial drag forces applied to a casing, as a result of relative vertical soil displacement, the unit drag stress f_z at a specific depth Z below the surface, is evaluated as:

$$f_Z = C_o + k_o P_z \tan\phi$$

where C_o = cohesive strength under dynamic stress
k_o = ratio of lateral to vertical pressure
ϕ = angle of soil's internal friction in the stratum under consideration
P_z = vertical soil stress at depth Z

At each specific time t_n after arrival of the free air shock front, the position of the subsurface pressure front, the "toe" of the pressure wave, will be at Z_n. The complete vertical pressure-versus-depth profile can be computed as described earlier, from which the corresponding unit drag stress f_z can be determined for any point above the toe of the pressure wave. The summation of the drag stresses can be expressed as:

$$Q = \sum_{0}^{Z_n} (f_z \Delta_z)$$

where Δ_z = finite increment of depth

This represents a fictitious total drag force on the profile of a vertical strip of unit circumferential width extending from the top to the bottom of the casing. The static soil pressure resistance is neglected in the P_z relationship, since it can be shown that for an 8 inch cased hole in a granular material the dead load radial pressure at the bottom of a 200 foot lined cavity is a maximum of 0.31 psi (see calculations Appendix E). The total force Q is divided into two equal and opposite forces, one tending to displace the casing downward, and the other resisting this displacement. The maximum drag force acting on the casing therefore is Q/2.

The maximum compressive stress $(\sigma_a)_{max}$ in the casing due to the downdrag force is then:

$$(\sigma_a)_{max} \doteq \frac{Q\pi D}{2A_m} \approx \frac{Q}{2t_m}$$

where D = diameter

t_m = metal thickness of the casing

If Q is plotted against Z up to Q/2 and then as $Q/2 - f_z$ it is apparent that $(\sigma_c)_{max}$ will usually occur near the midpoint for casing of uniform diameter in homogeneous media. Once the location of the maximum stress has been established, the stress at any other vertical depth of the loaded area is obtained for that specific loading by summing the stress obtained with the following expression:

$$\sigma_a = \frac{D\pi}{A_m} \sum f_z \Delta Z$$

from the top end of the casing downward, or from the bottom end of the casing upward, toward the point where the strain in the casing is equal to the strain in the soil. The axial stress $(\sigma_a)_{max}$ equals $(P_z/M_p)E$, if the strain method governs the stresses.

HORIZONTAL DISPLACEMENT

The determination of the horizontal displacement is dependent upon the method of defining the vertical stress profile. The procedure requires the determination of vertical displacement in the soil media. The incremental vertical displacement when the applied stress is increasing can be expressed as:

$$\delta V = P_z \frac{\Delta Z}{M_p}$$

where P_z = vertical pressure in the soil medium at the depth of interest (z)
M_p = soil modulus at peak stress
ΔZ = incremental depth considered

For decreasing stress, as defined by the stress profile, the residual stress ratio of the soil k_p must be considered so that

$$\delta V = P_z \frac{\Delta Z}{M_p} (1 - k_p) + P_{zp} \frac{\Delta Z}{M_p} k_p$$

where P_{zp} = attenuated pressure at the depth of peak pressure.

From the above relationships the total vertical displacements at any time t_n or depth Z_n may be determined by summation procedures.

The conversion of the vertical displacement to horizontal displacement is based on an assumed proportionality of the two terms, expressed as $H = \beta V$ where β is a factor based on the soil properties and the magnitude and direction of the stress wave in the soil (determination of this factor is discussed in Appendix A.

The horizontal displacement-versus-depth profile along the casing is accomplished by a four-step procedure. Each step is carried out for each of the selected cases, for each soil stress wave front location, and for targets located at one-foot increment of the casing length. The wave front locations used are adjusted to provide data point spacing to permit interpolation and to insure that the peak stress will reach depths well below the end of the casings. Twenty wave front locations were considered in all cases. The four basic steps are:

a. Compute the absolute vertical and horizontal displacements V_B and H_B at the bottom target point T_B.

b. Compute the relative vertical and horizontal displacements $(V)_i - (V)_{i+1}$ and $(H_z)_i - (H_z)_{i+1}$, of each successive target point with respect to the next lower point, from the bottom to the top target point.

c. Compute the summations,

$$\sum_{T_B}^{T_N} \delta V \quad \text{and} \quad \sum_{T_B}^{T_N} \delta H,$$

for each successive target point T_N.

d. Compute the bending stress in the casing.

The absolute vertical displacement referred to the toe of the stress wave is used as a check information for computer output, and absolute hori-aontal displacement from the same reference point is used as a base line for the computation of bending stresses.

The bottom target is used as an initiation point for the computation of the incremental displacements used to establish the horizontal-displacement-versus-depth profile. In all cases under consideration, for any single set of input data conditions, the soil properties below the water table and hence below the bottom target point, have been assumed as constants and k_p equals zero. This simplification is based on the fact that displacements below the bottom target change the absolute, but not the relative, displacements above that level and hence do not influence casing stresses. Since all soil properties within any layer are constant, the only variable factors influencing the absolute displacement at the bottom target are the stress wave form and stress values between the bottom target and the toe of the stress wave. Three conditions are possible:

a. the peak soil stress is above the target,

b. the peak soil stress is at the target,

c. the peak soil stress is below the target.

For the first condition (Figure B-2) the average vertical stress, P' below the bottom target T_B is:

$$P' = \frac{P_{zp}}{2}\left(\frac{Z_n - Z_B}{Z_n - Z_{pn}}\right)$$

and the absolute vertical displacement V_B at T_B is:

$$V_B = \frac{P'(Z_n - Z_B)}{M_p}$$

$$= \frac{P_{zp}}{2M_p}\left(\frac{Z_n - Z_B}{Z_n - Z_{pn}}\right)^2$$

where M_p is the applicable soil modulus below the water table.

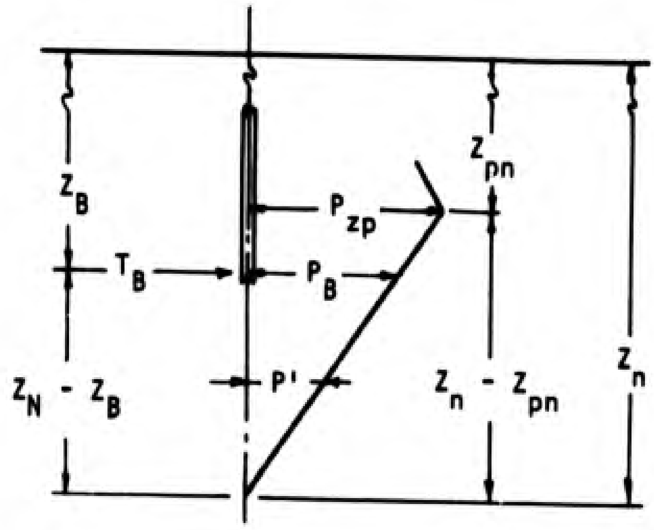

FIGURE B-2 PEAK SOIL STRESS ABOVE TARGET

For the second condition, referring to Figure B-2, $(Z_B = Z_{pn}$ and $P_B = P_{ap})$ the expression for displacement at T_B becomes:

$$V_B = \frac{P_{zp}(Z_n - Z_{pn})}{2M_p}$$

The third condition is shown in Figure B-3. Since k_p equals zero, the basic expressions for strain under increasing and decreasing stress are identical:

$$\varepsilon = \frac{P_z}{M_p}$$

and the incremental vertical deformation is:

$$\delta V = \sum \varepsilon \Delta Z = \sum \frac{P_z \Delta Z}{M_p}$$

For this condition, the stress at T_B is:

$$P_B = P_s + \frac{Z_B}{Z_{pn}} (P_{zp} - P_s)$$

and the absolute vertical displacement at T_B is:

$$V_B = \frac{P_{zp}}{2M_p}(Z_n - Z_{pn}) + \left[\frac{Z_{pn} - Z_B}{2M_p}\right]\left[P_s + \frac{Z_B}{Z_{pn}}(P_{zp} - P_s) + P_{zp}\right]$$

For each of the above conditions the absolute horizontal displacement is taken as:

$$H_B = V_B\beta = .33V_B$$

since β equals .33 below the water table in all cases.

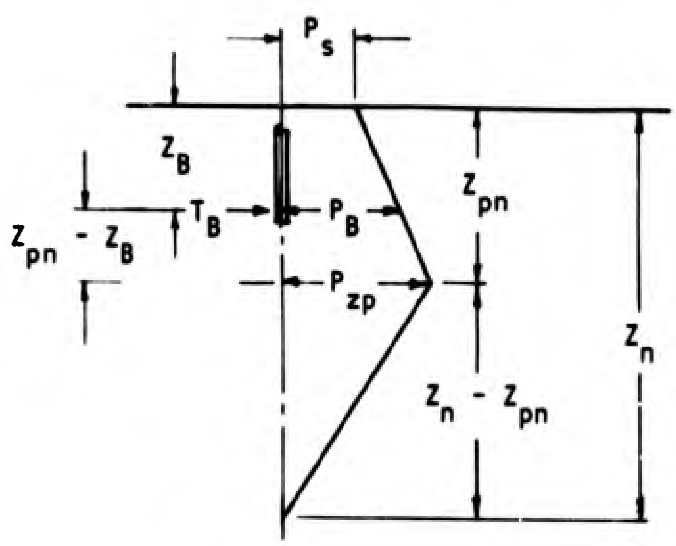

FIGURE B-3 PEAK SOIL STRESS BELOW TARGET

The relative vertical and horizontal displacements of successive target points are computed in that order. The interval ΔZ between target points is two feet (with the exception of the one foot interval between points 60 and 61 on the 200-foot casing). Consequently, the arithmetical average vertical stress P'_{TN} between the top and bottom of each two foot interval is:

$$P'_{TN} = \frac{P_{TN} + P_{T(N+1)}}{2}$$

where P_{TN} and $P_{T(N+1)}$ are the stresses at the top and bottom respectively, of the interval; this may be considered as the true mean stress, with little error, for all intervals. In each case, (starting with the bottom target at Z_B) the stress $P_{T(N+1)}$ at the lower face of the interval is available from the previous computation.

For any target point T_N between the toe and peak of the stress wave, i.e., increasing stress area, Figure B-4, the vertical stress at the top of the interval is:

$$P_{TN} = \left(\frac{Z_n - Z_{TN}}{Z_n - Z_{pn}}\right) P_{zp}$$

the average stress in ΔZ_N is:

$$P'_{TN} = \frac{1}{2}\left[P_{T(N+1)} + P_{zp}\left(\frac{Z_n - Z_{TN}}{Z_n - Z_{pn}}\right)\right]$$

and δV_{TN}, the incremental vertical displacement in ΔZ_N, is:

$$\delta V_{TN} = \frac{\Delta Z_n}{2M_p}\left[P_{T(N+1)} + P_{zp}\left(\frac{Z_n - Z_{TN}}{Z_n - Z_{pN}}\right)\right]$$

where M_p is the applicable soil modulus for the layer containing the interval ΔZ_N.

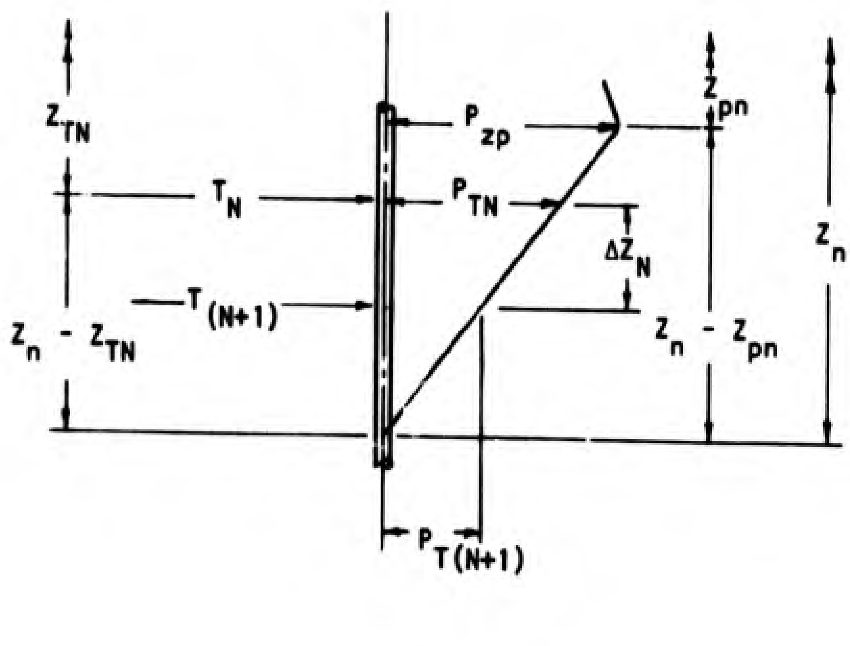

FIGURE B-4 TARGET WITHIN INCREASING STRESS AREA

When the target point in question lies above the peak pressure, i.e., in the decreasing pressure area, Figure B-5, the vertical stress P_{TN} at the target level is:

$$P_{TN} = P_s + \frac{Z_{TN}}{Z_{pn}}\left(P_{zp} - P_s\right)$$

and the incremental vertical displacement is:

$$\delta V_{TN} = \left[\frac{\Delta Z_N(1 - k_p)}{2M_p}\right]\left[P_{(N+1)} + P_s + \frac{Z_{TN}}{Z_{pn}}\left(P_{zp} - P_s\right)\right] + \frac{k_p P_{zp} \Delta Z_N}{M_p}$$

In each case the incremental horizontal displacement between $T_{(N+1)}$ and T_N is:

$$\delta H_{TN} = \delta V_{TN}\beta$$

where β is the applicable value for the layer containing ΔZ_N.

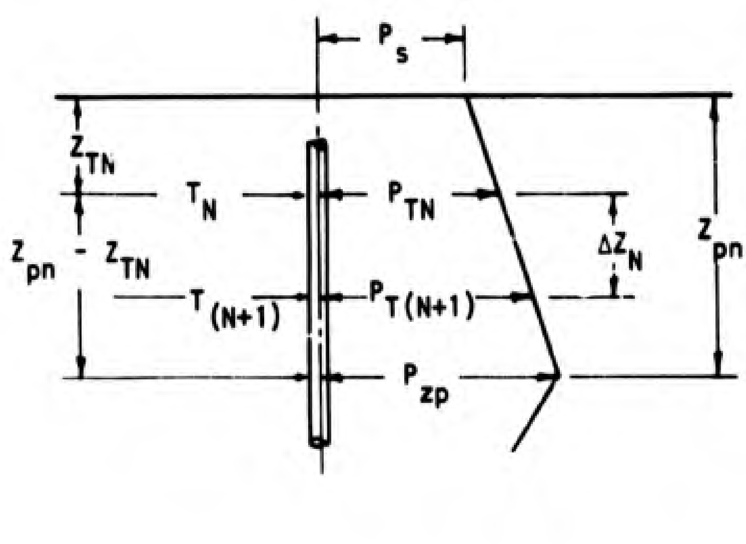

FIGURE B-5 TARGET WITHIN DECREASING STRESS AREA

BENDING AND SHEAR STRESSES

Bending Stresses

Bending stresses in the casing can be computed as direct functions of casing stiffness and horizontal deformation. Where d^2H/dZ^2 is the second derivative of the horizontal displacement-versus-depth curve, the bending moment in the casing is:

$$M = \frac{d^2H}{dZ^2} EI$$

and the approximate maximum bending stress is:

$$\sigma_b = \frac{MR}{I} = \frac{d^2H}{dZ^2}\frac{EID}{2I} = \frac{1}{2}\frac{d^2H}{dZ^2} ED$$

where D is the diameter of the casing. Substituting the value of E for steel, 3×10^7 psi, the above equation becomes:

$$\sigma_b = \frac{d^2H}{dZ^2}\left(1.5 \times 10^7\right)D$$

Shear Stresses

In general, shear stresses may not be of sufficient magnitude to be significant. However, where rapid changes or reversal of bending stress indicate high shear stress, the approximate shear between any two points on the casing may be obtained as the algebraic summation of the moments at the two points divided by the distance between the points, i.e.:

$$V = \frac{M_1 - M_2}{\Delta Z} = 2\,\frac{(\sigma_{b1} - \sigma_{b2})I}{D\Delta Z}$$

and the corresponding shear stress for a thin walled cylindrical shell is approximately:

$$\sigma_v \cong \frac{.16D}{\Delta Z}(\sigma_{b1} - \sigma_{b2})$$

where σ_{b1} and σ_{b2} are the bending stresses at the two points and ΔZ is the intervening distance.

COMBINED STRESSES

Due to the variations in the properties and layering of the soils under consideration, there is a very limited probability of maximum bending and downdrag compressive stresses occurring at the same specific time. The probability of the simultaneous occurrence of these maxima at the same position on the casing is negligible. Maximum tensile stress will always occur at the time and point of maximum bending stress. Maximum combined compressive stress may occur at the location of maximum downdrag stress, or at an intermediate location or time. The computer solution of downdrag stress at the same time intervals as bending stress permits direct comparisons with respect to both time and location of stress on the casing. The computer program used, first computed bending and downdrag stresses (for each target point on the casing and each of the twenty soil stress profiles) as functions independent of casing dimensions, i.e.:

$$\sigma_b' = \frac{d^2H}{dZ^2}\left(3 \times 10^7\right)D$$

and

$$\sigma_a' = \frac{Q\pi}{2}$$

For the four casing sizes (4-in., 5-in., 6-in., and 8-in.) and for schedule 80 casing the computer then calculated all actual combined stresses as:

$$\sigma_c = \frac{D}{A_m}\sigma'_a \pm \frac{D}{2}\sigma'_b$$

All values of σ_c were then scanned and the maximum combined compressive and tensile stresses were printed out for each of the four combinations of pipe size and schedule (i.e., wall thickness) for each of the 64 basic input conditions. For the other 20 conditions only a 6 inch Schedule 80 pipe was studied.

OTHER CONSIDERATIONS

In addition to the investigation for maximum stresses, an investigation of the buckling stability of the casing structure is required.

Limited investigation indicated that critical buckling stresses will be well above yield stresses for the four modes of buckling listed below:

1. Column (Euler)
2. Circumferential
3. Radial
4. Axial

This result primarily from the restraints provided by the soil and to the ratios of diameter to wall thickness (see Appendix E).

SAMPLE PROBLEM

A sample problem (Case B-400-20-300) is shown in the following pages. The computer input is shown in full. Only the peak values of the displacements and stresses are shown for the print-out.

AGBABIAN-JACOBSEN ASSOCIATES

SHOCK LOADING ON WELL CASING

JOB NO. 6712-1

CASE-B-400-20-300

INPUT PARAMETERS

WEAPON PARAMETERS

P_{so} = 300. psi

W = 20. MT

D_p^+ = 2.62 sec

SOIL PARAMETERS

LAYER	DEPTH (ft)	C_i (fps)	C_p (fps)	M_p (psi)	k_p	β	C_o (psi)	μk_o
1	0	3,000	948	19,400	0.400	0.63	12	0.07
2	50	3,000	976	20,600	0.368	0.63	12	0.07
3	80	6,000	2,768	198,000	0.250	0.50	0	0.15
4	200	6,000	2,858	211,000	0	0.50	0	0.15
5	300	6,000	2,926	221,000	0	0.50	0	0.15
6	400	7,600	3,776	415,000	0	0.33	0	0.20

NO. OF TARGETS = 200

NO. OF WAVEFRONTS = 20

AGBABIAN-JACOBSEN ASSOCIATES

SHOCK LOADING ON WELL CASING

JOB NO. 6712-1

CASE-B-400-20-300

DISPLACEMENTS

MAXIMUM RELATIVE VERTICAL DISPLACEMENT = 10.60 in.

MAXIMUM RELATIVE HORIZONTAL DISPLACEMENT = 6.26 in.

MAXIMUM ABSOLUTE VERTICAL DISPLACEMENT = 10.60 in.

MAXIMUM ABSOLUTE HORIZONTAL DISPLACEMENT = 6.26 in.

RESIDUAL HORIZONTAL DISPLACEMENT = 0.23 in.

AGBABIAN-JACOBSEN ASSOCIATES

JOB NO. 6712.W.E. SHOCK LOADING ON WELL CASINGS

JOB NO. 6712-1

CASE-B-400-20-300

MAXIMUM COMBINED TENSILE STRESS(+)

PIPE DIAMETER IN.	AREA IN.**2	H(I) (ft)	I	ZWF(K) (ft)	K	COMBINED STRESS (psi)
6.625	8.400	81.0	34	9.7000+001	2	5.7654+003

MAXIMUM COMBINED COMPRESSIVE STRESS(-)

PIPE DIAMETER IN.	AREA IN.**2	H(I) (ft)	I	ZWF(K) (ft)	K	COMBINED STRESS (psi)
6.625	8.400	201.0	94	6.7500+002	19	-1.4253+005*

*Maximum Combined Stress $\left(\sigma_{aF_{max}}\right)$ = 142,530 psi (See Table 4.2)

JOB NO. 6712, W.E. SHOCK LOADING ON WELL CASINGS

JOB NO. 6712-1 CASE-B-400-20-300

MAXIMUM STRESSES

- BENDING STRESSES, FB = STPESS/R, IN-LB/IN**3
- AXIAL STRESSES, FA = STRESS* A/D, IN-LB/IN
- SHEAR STRESSES, FV = STRESS/R**2, IN-LB/IN**4

K	ZWF(K) = FT	FB(MAX)	AT H = FT	FA(MAX)	AT H = FT	FV(MAX)	AT H = FT
1	6.3000+001	7.0263+002	51.0	2.0092+004	33.0	1.6438+001	21.0
2	9.7000+001	2.4356+003	81.0	3.2234+004	45.0	1.9004+002	81.0
3	1.3100+002	5.0589+003	81.0	4.3795+004	55.0	4.1404+002	81.0
4	1.6500+002	6.4233+003	81.0	5.6346+004	67.0	5.3066+002	81.0
5	1.9900+002	7.2290+003	81.0	6.9478+004	79.0	5.9962+002	81.0
6	2.3300+002	7.7392+003	81.0	8.1948+004	91.0	6.4337+002	81.0
7	2.6700+002	8.0778+003	81.0	9.5353+004	101.0	6.7246+002	81.0
8	3.0100+002	8.3045+003	81.0	1.0722+005	111.0	6.9201+002	81.0
9	3.3500+002	8.4558+003	81.0	1.1980+005	123.0	7.0512+002	81.0
10	3.6900+002	8.5543+003	81.0	1.3253+005	133.0	7.1372+002	81.0
11	4.0300+002	8.6139+003*	81.0	1.4387+005	143.0	7.1900+002	81.0
12	4.3700+002	8.4771+003	81.0	1.5471+005	153.0	7.1201+002	81.0
13	4.7100+002	8.0814+003	81.0	1.6394+005	163.0	6.7853+002	81.0
14	5.0500+002	7.7617+003	81.0	1.7002+005	171.0	6.5145+002	81.0
15	5.3900+002	7.4957+003	81.0	1.7439+005	179.0	6.2893+002	81.0
16	5.7300+002	7.2694+003	81.0	1.7784+005	185.0	6.0979+002	81.0
17	6.0700+002	7.0735+003	81.0	1.7943+005	191.0	5.9322+002	81.0
18	6.4100+002	6.9015+003	81.0	1.7954+005	195.0	5.7868+002	81.0
19	6.7500+002	6.7487+003	81.0	1.8055+005	201.0	5.6576+002	81.0
20	7.0900+002	6.6117+003	81.0	1.7998+005	205.0	5.5419+002	81.0

*Maximum Bending Stress $\left(\sigma_{b_{max}}\right) = 8613.9 \times \frac{6.625}{2} = 28.5$ psi (see Table 4.2)

AXIAL STRESSES IN PSI

JOB NO. 6712-1

	K = 5		K = 6		K = 7		K = 8	
	ZSP(5) = 44.1		ZSP(6) = 49.5		ZSP(7) = 55.0		ZSP(8) = 60.5	
H	FAF (psi)	FAS (psi)	FAF (psi)	FAS (psi)	FAF (psi)	FAS (psi)	FAF (psi)	FAS (psi)
15.0	0	-369918	0	-360956	0	-352552	0	-344748
17.0	1634	-371975	1592	-362884	1553	-354349	1517	-346421
19.0	3281	-374041	3197	-364822	3119	-356155	3046	-348104
21.0	4942	-376116	4816	-366769	4697	-357970	4586	-349796
23.0	6617	-378201	6447	-368725	6287	-359795	6139	-351498
25.0	8306	-380294	8092	-370691	7890	-361629	7704	-353208
27.0	10008	-382397	9749	-372665	9506	-363472	9280	-354928
29.0	11724	-384508	11420	-374648	11135	-365324	10869	-356656
31.0	13454	-386629	13105	-376640	12775	-367184	12470	-358393
33.0	15198	-388757	14802	-378641	14429	-369053	14082	-360139
35.0	16955	-390894	16512	-380650	16095	-370931	15707	-361893
37.0	18726	-393040	18236	-382667	17773	-372816	17343	-363655
39.0	20511	-395194	19973	-384692	19464	-374710	18992	-365425
41.0	22310	-397355	21723	-386725	21168	-376612	20652	-367204
43.0	24123	-398786	23486	-388767	22884	-378522	22325	-368990
45.0	25946	-394740	25262	-390816	24613	-380440	24009	-370785
47.0	27759	-389580	27052	-392873	26354	-382365	25706	-372587
49.0	29558	-384420	28854	-393092	28108	-384298	27414	-374396
51.0	31343	-357793	30663	-366957	29875	-364087	29135	-354125
53.0	33113	-352925	32460	-362902	31654	-366118	30867	-356033
55.0	34869	-348057	34245	-358847	33445	-365390	32612	-357947
57.0	36610	-343189	36019	-354793	35238	-361926	34368	-359868
59.0	38337	-338321	37780	-350738	37020	-358463	36137	-361658
61.0	40050	-333453	39530	-346683	38792	-355000	37916	-360087
63.0	41749	-328585	41267	-342628	40554	-351536	39693	-357074
65.0	43432	-323717	42992	-338574	42306	-348073	41461	-354061
67.0	45102	-318849	44706	-334519	44048	-344609	43221	-351047
69.0	46757	-313981	46407	-330464	45779	-341146	44971	-348034
71.0	48398	-309114	48097	-326409	47500	-337682	46712	-345021
73.0	50025	-304246	49774	-322354	49211	-334219	48445	-342008
75.0	51637	-299378	51440	-318300	50911	-330756	50168	-338994
77.0	53234	-294510	53094	-314245	52602	-327292	51883	-335981
79.0	54818*	-289642	54735	-310190	54282	-323829	53589	-332968
81.0	53602	-29525	56365	-31739	55952	-33215	55286	-34209
83.0	51800	-29020	58302	-31319	57979	-32856	57373	-33896
85.0	50029	-28515	60213	-30899	59983	-32497	59442	-33584
87.0	48289	-28011	62098	-30478	61966	-32137	61491	-33272
89.0	46580	-27506	63958	-30058	63927	-31778	63521	-32959
91.0	44902	-27001	64657	-29637	65867	-31419	65532	-32647
93.0	43254	-26497	62848	-29217	67784	-31060	67524	-32334
95.0	41637	-25992	61066	-28797	69679	-30701	69498	-32022
97.0	40051	-25487	59308	-28376	71552	-30342	71452	-31710
99.0	38496	-24982	57577	-27956	73404	-29983	73386	-31397
101.0	36972	-24478	55871	-27535	75234	-29624	75302	-31085

* Maximum Axial Stress $\left(F_{a_{max}}\right)$ = 54818 psi (See Table 4.2)

APPENDIX C

FREE-FIELD SHOCK SPECTRA ANALYSIS

INTRODUCTION

The procedures and assumptions that were used in the development of a computer program for determining shock spectra envelopes are described below. The method is based on the procedures given in References 1 and 37.

METHOD

Following is a step-by-step procedure for determining the free-field shock spectra.

Step 1

Compute peak free-field ground motion intensities due to direct air blast slap. The soil profile is assumed to be layered with uniform properties in each increment as shown in Figure C-1. This gives a stepwise linear approximation to the soil characteristics considered.

a. Displacement

The displacement at a specified target depth Z is determined by summing the displacement in each layer below the target at small time intervals until a maximum displacement d_{max} is determined (see Reference 37 for complete description of procedure).

Figure C-1 shows a typical stress pattern with depth at a particular time. A linear rise distance and decay is assumed. The toe of the stress wave is assumed to travel with the nominal seismic velocity C_i and the peak stress is assumed to travel with velocity C_p as given by:

$$C_p = 68.1\left(\frac{M_p}{\rho}\right)^{1/2}$$

where M_p = modulus under peak stress, psi

ρ = density, lb/ft^3

An idealized stress-strain wave is assumed as shown in Figure C-2.

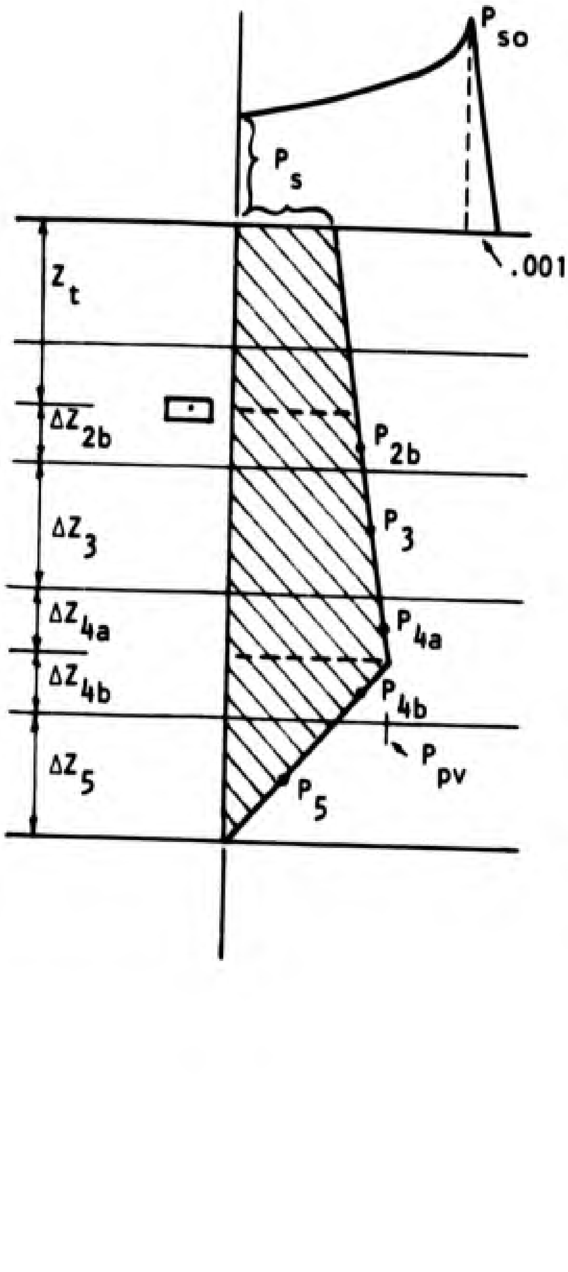

FIGURE C-1 TYPICAL STRESS VARIATION WITH DEPTH AT ONE TIME INTERVAL

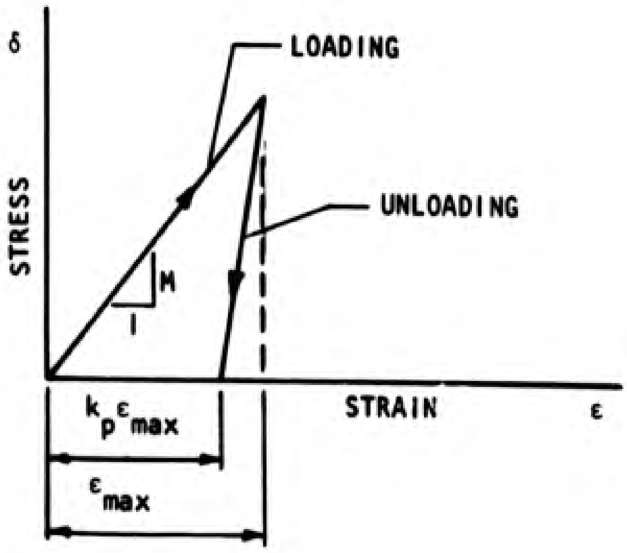

FIGURE C-2 IDEALIZED STRESS-STRAIN WAVE

The degree of plasticity is specified by k_p, which is the ratio of residual strain to peak strain, and is a function of overpressure, weapon yield, and soil properties. It varies from 0.3 for soft layers at the surface to zero for rock and firm materials at large (200 ft) depths (for rock $k_p = 0$). When the stress is increasing on the stress-strain curve the displacement per increment is given by:

$$\Delta d = P_{zi} \frac{\Delta Z}{M_i}$$

where P_{zi} is the average stress and M_i the modulus under peak stress in the increment. Similarly when the stress is in the unloading portion of the stress-strain curve the displacement per increment is given by:

$$\Delta d = \left[P_{zi}\left(1 - k_p\right) + k_p P_{pv}\right] \frac{\Delta Z}{M_i}$$

where the terms have the meaning given in Figure C-1 and C-2.

For the stress pattern shown in Figure C-1, the vertical displacement at target depth Z is:

$$d = \frac{P_5 \Delta Z_5}{M_5} + \frac{P_{4b} \Delta Z_{4b}}{M_4} + \left[P_{4a}\left(1 - k_p\right) + k_p P_{pv}\right] \frac{\Delta Z_{4a}}{M_4}$$

$$+ \left[P_3 \left(1 - k_p\right) + k_p P_{pv}\right] \frac{\Delta Z_3}{M_3} + \left[P_{2b} \left(1 - k_p\right)\right.$$

$$\left. + k_p P_{pv}\right] \frac{\Delta Z_{2b}}{M_2}$$

The horizontal displacement is assumed to be 1/3 of the vertical displacement.

b. Velocity

The peak vertical velocity is computed from the peak attenuated stress at the target depth.

$$v = \frac{P_z}{(C_p)_z (\gamma)_z}$$

where P_z = attenuated pressure at target depth Z

$$P_z = P_{so} \alpha$$

$$\alpha = \frac{1}{1 + Z/L_W}$$

$$L_W = \frac{2,300 (W)^{1/3}}{\sqrt{P_{so}}}$$

$(C_p)_z$ = peak stress seismic velocity at target depth Z
$(\gamma)_z$ = mass density at target depth Z

The horizontal velocity is assumed to be 2/3 of the vertical velocity.

c. Acceleration

The peak vertical acceleration a is assumed to occur during the initial rise of the velocity pulse. The acceleration is given by:

$$a = \frac{v}{t_r}$$

where

$$t_r = .001 + \sum \frac{Z}{C_p} - \sum \frac{Z}{C_i}$$

The horizontal acceleration is assumed to be euqal to the vertical acceleration.

Step 2

Compute critical arrival times at ground surface at target distances from ground zero. Figure C-3 shows the postulated 2 layer model and the paths through which critical motions may arrive at the target location.

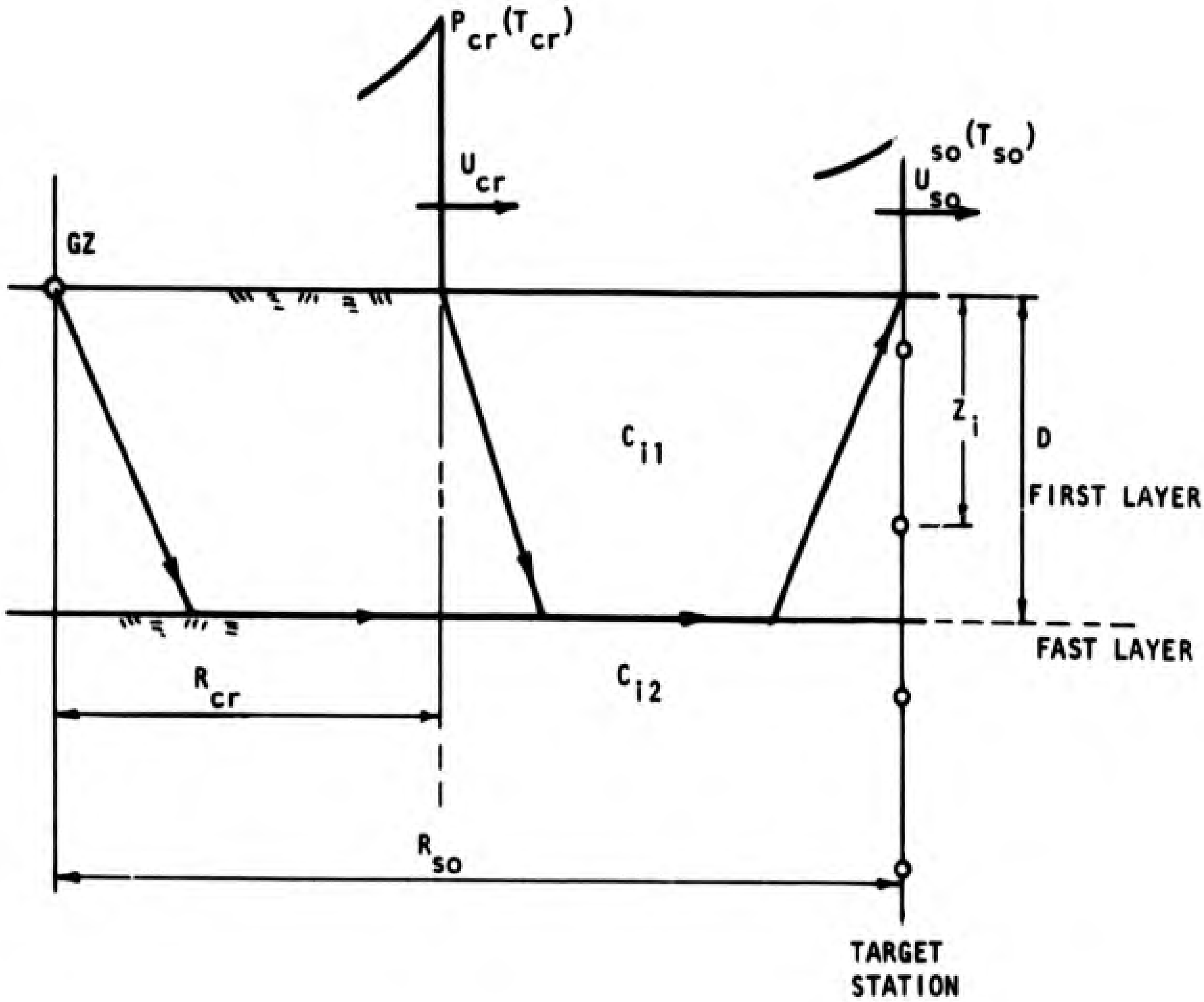

FIGURE C-3   GROUND MOTION PROPAGATION PATHS

The semi-empirical equations which are used to calculate the arrival times are given below:

a. The distance (ft) to target station from ground zero R_{so} can be approximated as:

$$R_{so} = \left[\frac{(36 \times 10^{11})(W)}{(P_{so})(1MT)}\right]^{1/3}$$

where W = weapon yield, MT

P_{so} = peak surface overpressure, psi

b. The arrival time (sec) of the surface overpressure wave at the target station from GZ, T_{so}, is assumed as:

$$T_{so} = 0.024\left(\frac{1MT}{W}\right)^{1/2}\left(\frac{R_{so}}{1,000}\right)^{2.5}$$

c. A critical condition will occur when the velocity (ft/sec) of the air blast shock front $U(t)$ is equal to the nominal seismic velocity in the lower layer C_{12}. At this instant in time, the air shock front velocity is critical (U_{cr}) and identifies a critical location as shown in Figure C-3, defined by the following relationships:

$$U(t) = C_{12} = U_{cr}$$

P_{cr} = surface overpressure at critical location, psi

$$P_{cr} = \left(U_{cr}/280\right)^2$$

R_{cr} = distance to critical location from GZ, ft

$$R_{cr} = \left[\frac{(36 \times 10^{11})(W)}{(P_{cr})(1MT)}\right]^{1/3}$$

T'_{cr} = arrival time of surface overpressure wave at critical location, sec

$$T'_{cr} = 0.024\left(\frac{1MT}{W}\right)^{\frac{1}{2}}\left(\frac{R_{cr}}{1,000}\right)^{2.5}$$

d. The time (sec) for the seismic wave to travel from the critical location to the target location is defined as T''_{cr}

$$T''_{cr} = \frac{2D}{C_{11}C_{12}}\sqrt{C_{12}^2 - C_{11}^2} + \frac{R_{so} - R_{cr}}{C_{12}}$$

where D = depth of top layer, ft

C_{11} = nominal seismic velocity in top layer, ft/sec

C_{12} = nominal seismic velocity in lower layer, ft/sec

e. The total arrival time (sec) of the air blast induced seismic motion is T_{cr} and is equal to:

$$T_{cr} = T'_{cr} + T''_{cr}$$

f. The time (sec) for the seismic wave to travel from GZ to the target location is defined as T_{GZ}

$$T_{GZ} = \frac{2D}{C_{11}C_{12}}\sqrt{C_{12}^2 - C_{11}^2} + \frac{R_{so}}{C_{12}}$$

The three arrival times (T_{so}, T_{cr}, T_{GZ}) are then compared to determine whether the air blast is superseismic at the ground surface target location. Superseismic conditions will occur if the air blast shock front arrives before the seismic motion as determined by the following criteria:

If $T_{so} < T_{GZ}$ and T_{cr}, superseismic conditions exist.

If $T_{so} \geq T_{GZ}$ or T_{cr}, outrunning conditions exist.

These two conditions establish the magnitude of the random motion intensities in the following section.

Step 3

The random motion is assumed to be the result of seismic waves reflected or refracted in layered media due to the air blast slap or seismic waves induced from ground zero (GZ). The peak vertical intensities are empirically related to the motions calcualted in Step 1 based on the recommended factors in Reference 16, see Table C-1. It can be noted that the values d', v' and a' (peak random motion displacement, velocity, and acceleration) have larger intensities for the outrunning condition.

TABLE C-1 FACTORS RELATING FREE-FIELD MOTIONS TO PEAK RANDOM MOTIONS

SUPERSEISMIC CONDITION	OUTRUNNING CONDITION
$d' = 0.1d$	$d' = 0.3d$
$v' = 0.2v$	$v' = 0.6v$
$a' = 0.4a$	$a' = 1.0a$

The horizontal components of the random motion are related to the vertical components by the following factors.

$$\frac{a'_h}{a'_v} = 1.0; \qquad \frac{v'_h}{v'_v} = 2.3; \qquad \frac{d'_h}{d'_v} = 1.0$$

Step 4

Compute separately the shock spectra bound for the direct air blast induced motion (Step 1) and the shock spectra bound for the random motion. The soil near the surface is assumed to have 5 to 10 percent equivalent viscous damping. Therefore, amplification response factors for plotting the typical shock spectra envelope on a 4-log coordinate system are:

Air Blast Induced:

$$\frac{D}{d} = 1.0; \quad \frac{V}{v} = 1.5; \quad \frac{A}{a} = 2.0$$

Random Motion:

$$\frac{D'}{d'} = 1.0; \quad \frac{V'}{v'} = 1.7; \quad \frac{A'}{a'} = 3.0$$

where the capital designation indicates the response spectra envelope boundary as three straight intersecting lines.

Step 5

Obtain the resultant shock spectra by combining the two separate shock spectras calculated in Step 4. The response displacements are added algebraically and the velocity and acceleration are added by quadrature.

$$D_r = D + D', \quad V_r = \sqrt{V^2 + V'^2}, \quad A_r = \sqrt{A^2 + A'^2}$$

Step 6

Estimate the frequency range where resonance may occur. The bump on the shock spectra will occur in the frequency region where the period of a single degree of freedom system is nearly the same as the duration of a ground return velocity pulse. Assuming an idealized velocity pulse as shown in Figure C-4, the critical frequency region is estimated to lie between the limits:

$$\frac{2}{t_d} \geq f \geq \frac{1}{2t_d}$$

where t_d is defined by the velocity time-history represented by Figure C-4.

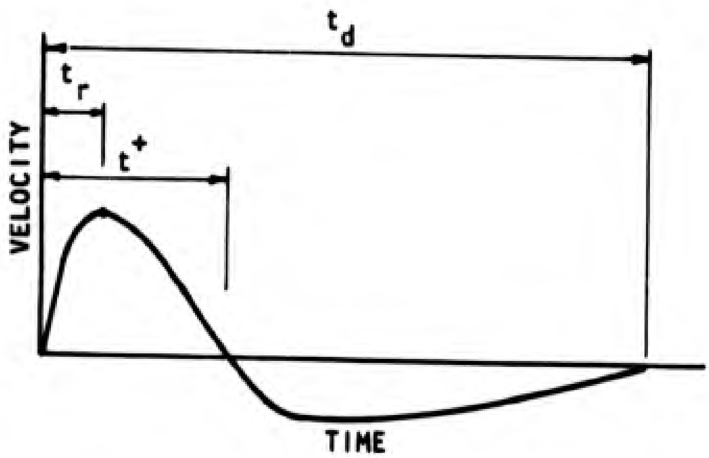

t_d = $4t^+$ Assumed Velocity Pulse Duration

t^+ = $\frac{2d}{v}$

t_r = Rise Time to Peak Velocity

FIGURE C-4 VELOCITY PULSE

SHOCK SPECTRA CONFIGURATION

The shock spectra configuration shown in Figure C-5 is obtained as a result of the above six steps. In the figure, the notations D and A represent maximum response displacement and acceleration respectively, and V indicates the maximum pseudo velocity. The lower and upper bound frequency where a resonance condition exists is identified by F_1 and F_2 respectively. The amplified displacement due to the resonance with the input velocity pulse is shown as D_{12}. The D_{12} displacement may not be applicable in some cases when the frequency band F_1 to F_2 is not in the constant displacement region. The results are summarized in Section 4.3 in table form.

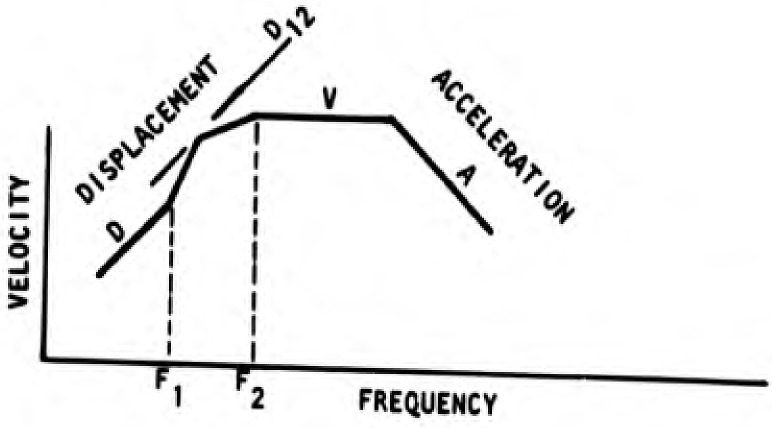

FIGURE C-5 SHOCK SPECTRA

RESULTS

Shock spectra graphs for vertical and horizontal motion are shown in Figures C-6 to C-45 for the twenty cases analyzed. The designation TD appearing on the shock spectra refers to the target depth. Peak intensities and resulting shock spectra due to the direct air blast slap motion and the peak intensities and resulting shock spectra due to seismic (random) motions are calculated separately. As an example problem the computer data from the CASE-B-200-20-300 is shown. The notations WT and RL following the case numbers refer to water table depth and depth to rock layer, respectively.

AGBABIAN-JACOBSEN ASSOCIATES

SHOCK SPECTRA BY PHASE I METHOD

JOB NO.6712-1

CASE SERIAL NO B28
B-200-20-300

INPUT PARAMETERS

OVERPRESSURE = 3.0000+002 (PSIG)
WEAPON YIELD = 2.0000+001 (MT)
DURATION = 2.6200+000 (SEC.)
NO. OF TARGETS = 3
NO. OF LAYERS = 25

SOIL PARAMETERS

Z (FT.)	C I (FPS)	C P (FPS)	M (PSI)	GAMMA (PCF)	K P	DAMPING (PERCENT)
0.000+000	3.000+003	9.485+002	1.940+004	1.000+002	4.000-001	5.000+000
1.000+001	3.000+003	9.607+002	1.990+004	1.000+002	3.900-001	5.000+000
2.000+001	3.000+003	9.679+002	2.020+004	1.000+002	3.800-001	5.000+000
3.000+001	3.000+003	9.750+002	2.050+004	1.000+002	3.770-001	5.000+000
4.000+001	3.000+003	9.750+002	2.050+004	1.000+002	3.730-001	5.000+000
5.000+001	3.000+003	9.798+002	2.070+004	1.000+002	3.690-001	5.000+000
6.000+001	3.000+003	9.798+002	2.070+004	1.000+002	3.660-001	5.000+000
7.000+001	3.000+003	9.845+002	2.090+004	1.000+002	3.640-001	5.000+000
8.000+001	6.000+003	2.773+003	1.990+005	1.200+002	2.600-001	1.000+000
9.000+001	6.000+003	2.773+003	1.990+005	1.200+002	2.570-001	1.000+000
1.000+002	6.000+003	2.780+003	2.000+005	1.200+002	2.540-001	1.000+000
1.100+002	6.000+003	2.787+003	2.010+005	1.200+002	2.500-001	1.000+000
1.200+002	6.000+003	2.794+003	2.020+005	1.200+002	2.480-001	1.000+000
1.300+002	6.000+003	2.808+003	2.040+005	1.200+002	2.460-001	1.000+000
1.400+002	6.000+003	2.815+003	2.050+005	1.200+002	2.450-001	1.000+000
1.500+002	6.000+003	2.815+003	2.050+005	1.200+002	0.000+000	1.000+000
1.600+002	6.000+003	2.815+003	2.050+00	1.200+002	0.000+000	1.000+000
1.700+002	6.000+003	2.815+003	2.050+005	1.200+002	0.000+000	1.000+000
1.800+002	6.000+003	2.815+003	2.050+005	1.200+002	0.000+000	1.000+000
1.950+002	7.600+003	6.579+003	1.260+006	1.350+002	0.000+000	1.000+000
2.000+002	7.600+003	6.579+003	1.260+006	1.350+002	0.000+000	1.000+000
2.500+002	7.600+003	6.579+003	1.260+006	1.350+002	0.000+000	1.000+000
3.000+002	7.600+003	6.579+003	1.260+006	1.350+002	0.000+000	1.000+000
4.000+002	7.600+003	6.579+003	1.260+006	1.350+002	0.000+000	1.000+000
5.000+002	7.600+003	6.579+003	1.260+006	1.350+002	0.000+000	1.000+000

AGBABIAN-JACOBSEN ASSOCIATES

SHOCK SPECTRA BY PHASE I METHOD

JOB NO. 6712-1

CASE SERIAL NO. B28
B-200-20-300

SHOCK SPECTRA RESULTS

DEPTH (ft)	DESCRIPTION	A (g's)	V (ips)	D (in.)	D(12) (in.)	F(1) (cps)	F(2) (cps)
10	AIR INDUCED						
	VERTICAL	107	225	11.17	14.52	1	4
	HORIZONTAL	107	170	3.72	4.84	2	8
	AIR INDUCED PLUS RANDOM						
	VERTICAL	125	262	12.29	15.64	1	4
	HORIZONTAL	125	175	4.84	5.95	2	8
70	AIR INDUCED						
	VERTICAL	15	213	3.03	3.94	3	12
	HORIZONTAL	15	142	1.01	1.31	6	23
	AIR INDUCED PLUS RANDOM						
	VERTICAL	17	219	3.33	4.24	3	12
	HORIZONTAL	17	146	1.31	1.61	6	23
194	AIR INDUCED						
	VERTICAL	4	58	0.68	0.89	3	12
	HORIZONTAL	4	39	0.23	0.30	6	24
	AIR INDUCED PLUS RANDOM						
	VERTICAL	4	60	0.78	0.99	3	12
	HORIZONTAL	4	40	0.33	0.40	6	24

SUPERSEISMIC CONDITION AT TARGET STATION

ARRIVAL TIMES (msec)

T(SO) = 517
T(GZ) = 2340
T(CR) = 0

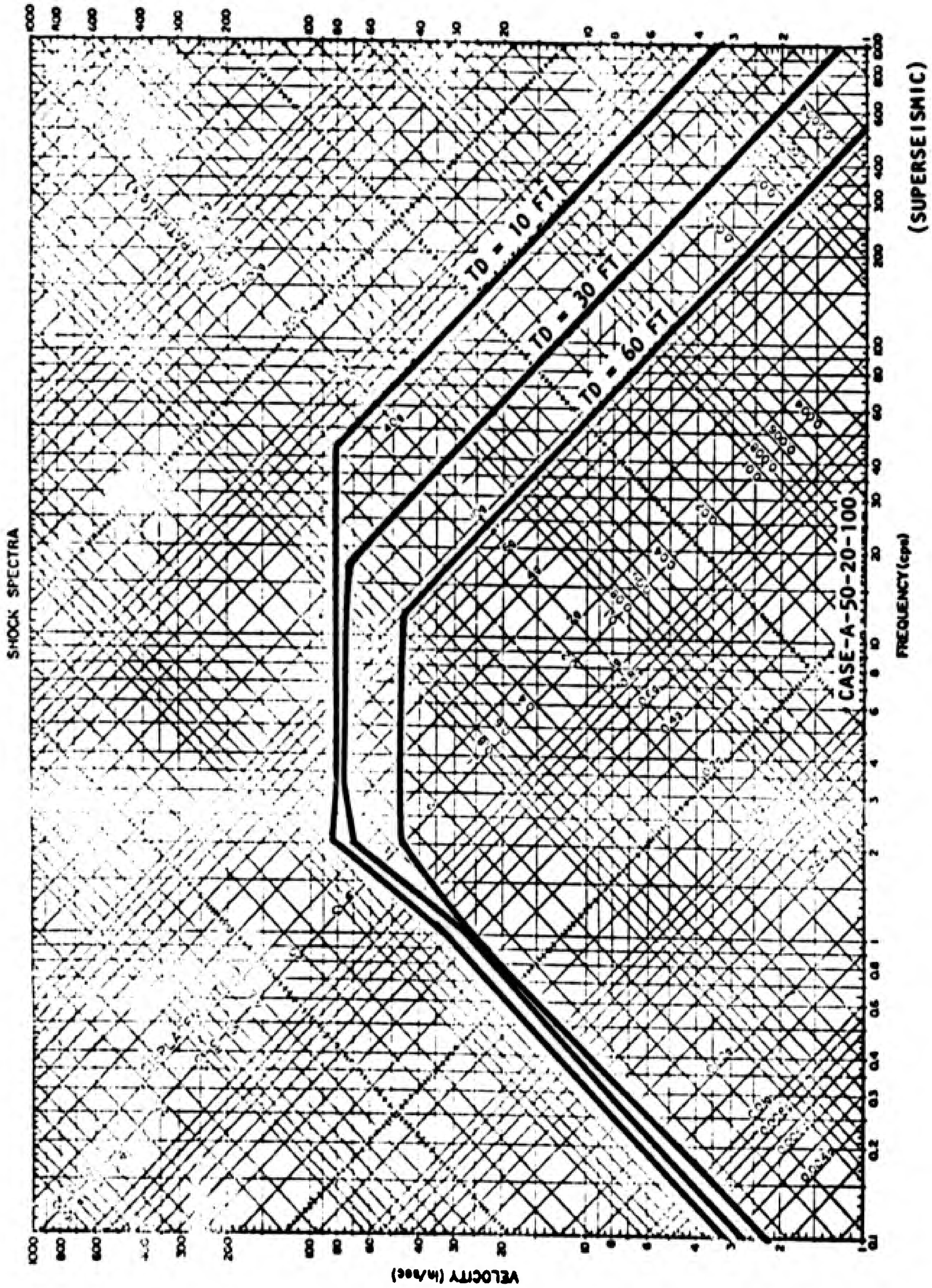

FIGURE C-6 SHOCK SPECTRA FOR VERTICAL MOTION

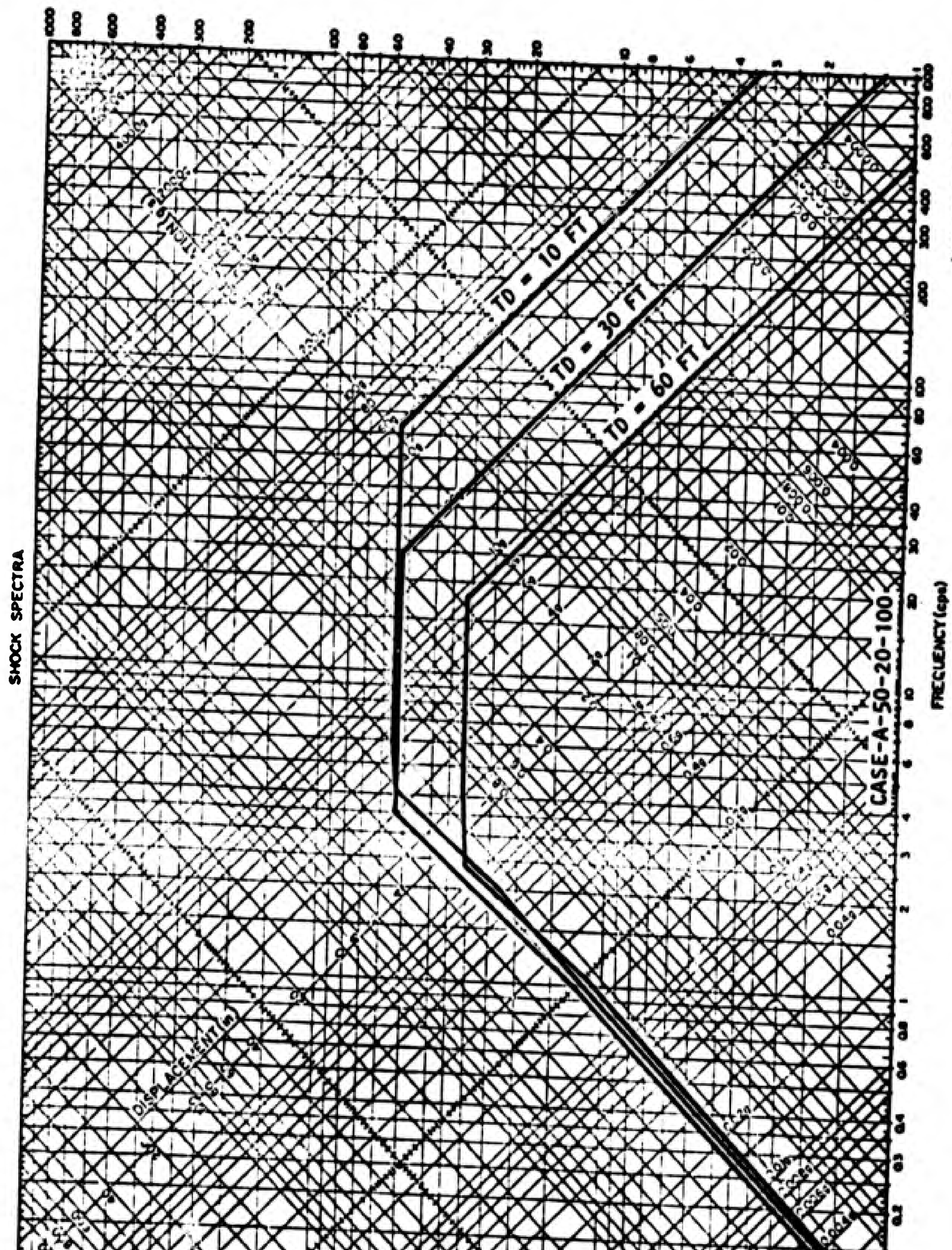

FIGURE C-7 SHOCK SPECTRA FOR HORIZONTAL MOTION

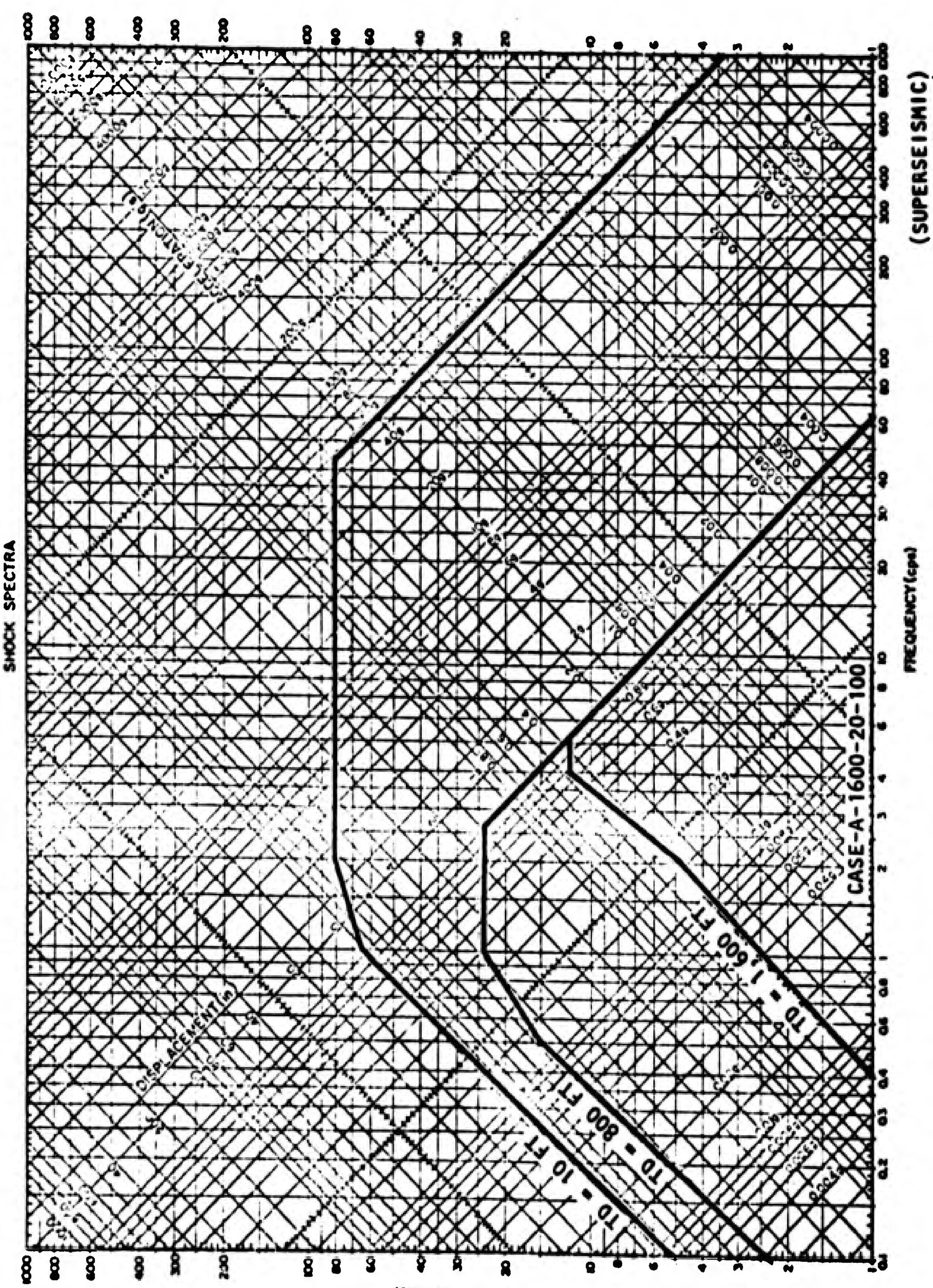

FIGURE C-8 SHOCK SPECTRA FOR VERTICAL MOTION

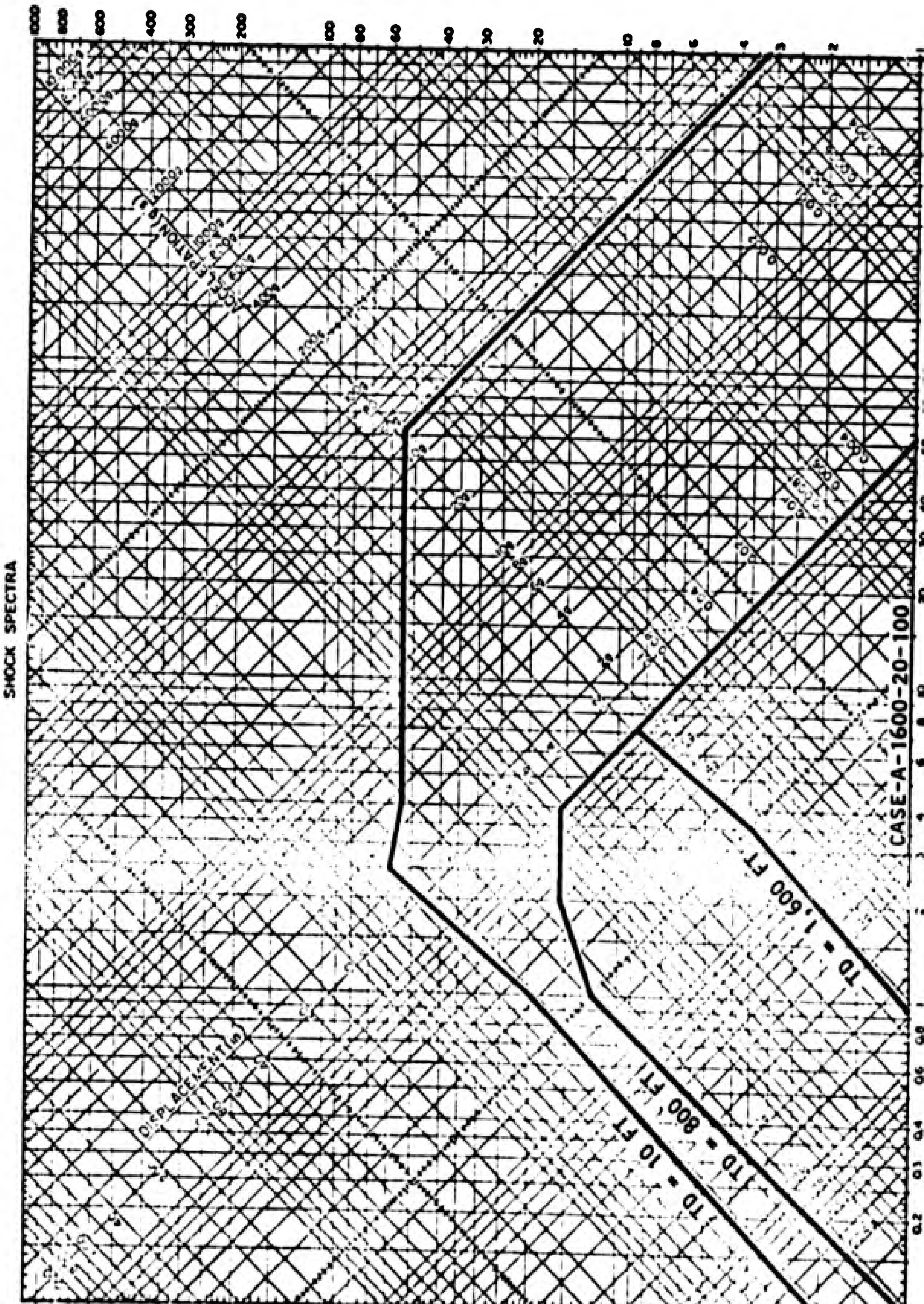

FIGURE C-9 SHOCK SPECTRA FOR HORIZONTAL MOTION (SUPERSEISMIC)

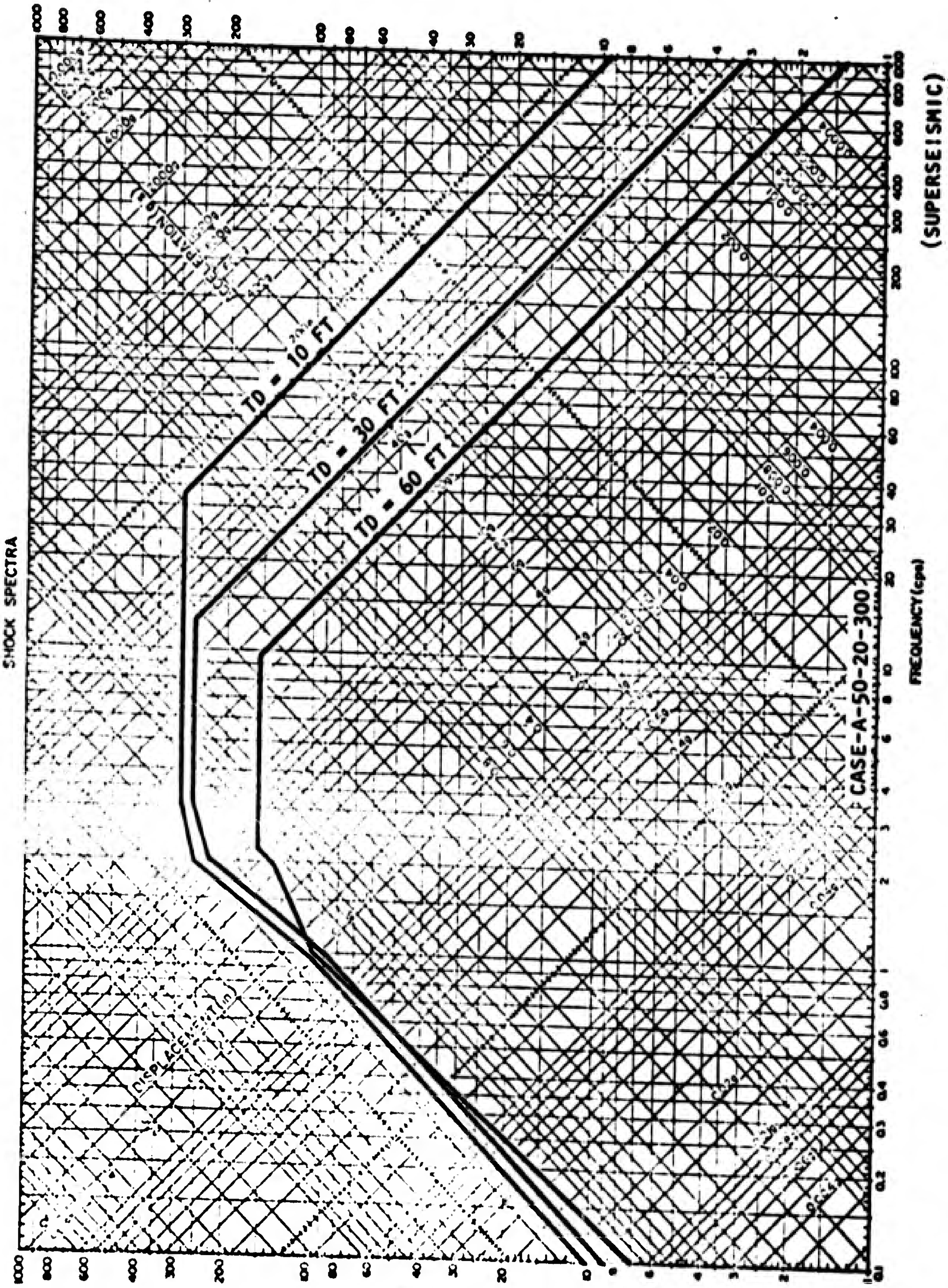

FIGURE C-10 SHOCK SPECTRA FOR VERTICAL MOTION

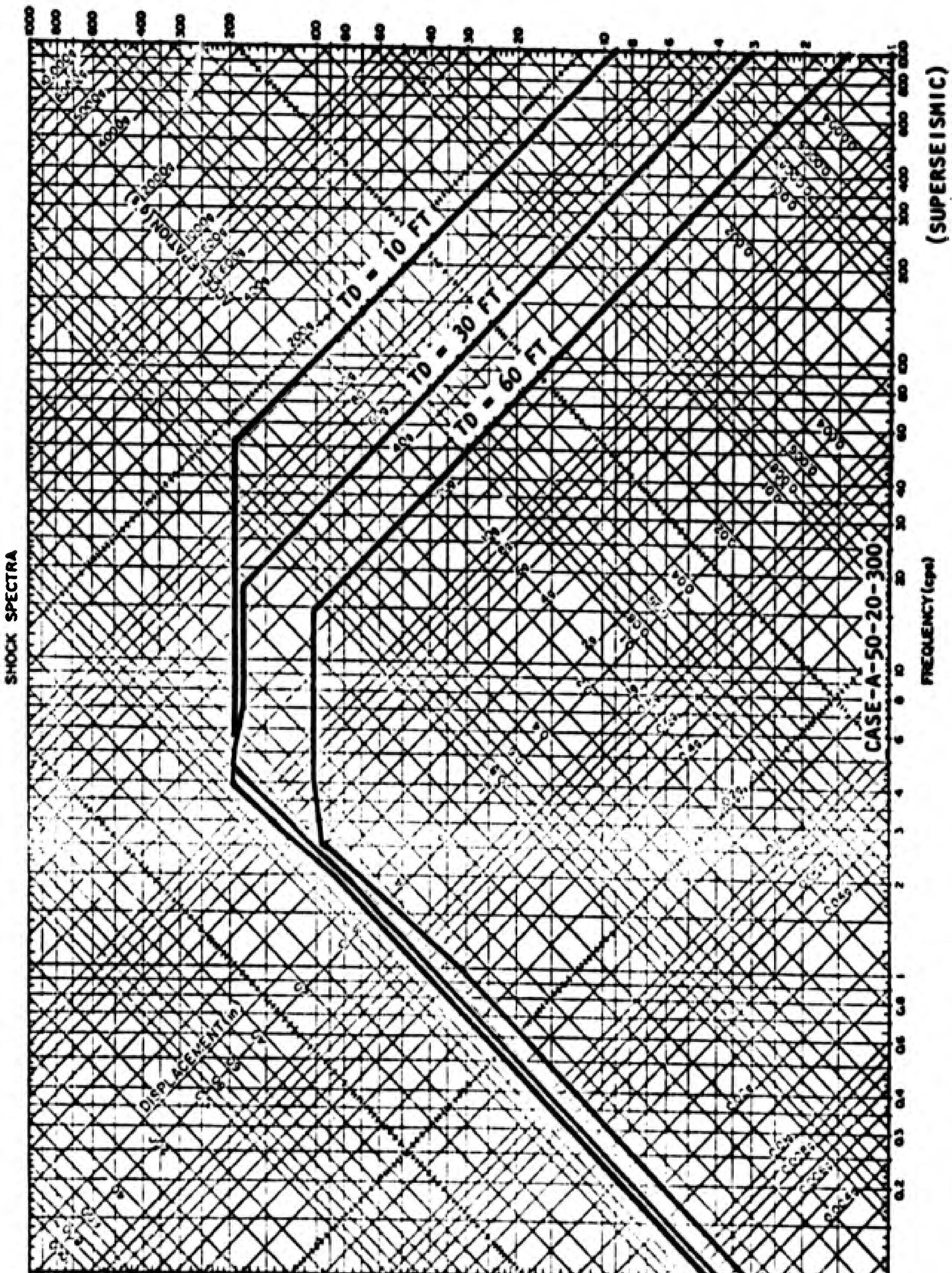

FIGURE C-11 SHOCK SPECTRA FOR HORIZONTAL MOTION

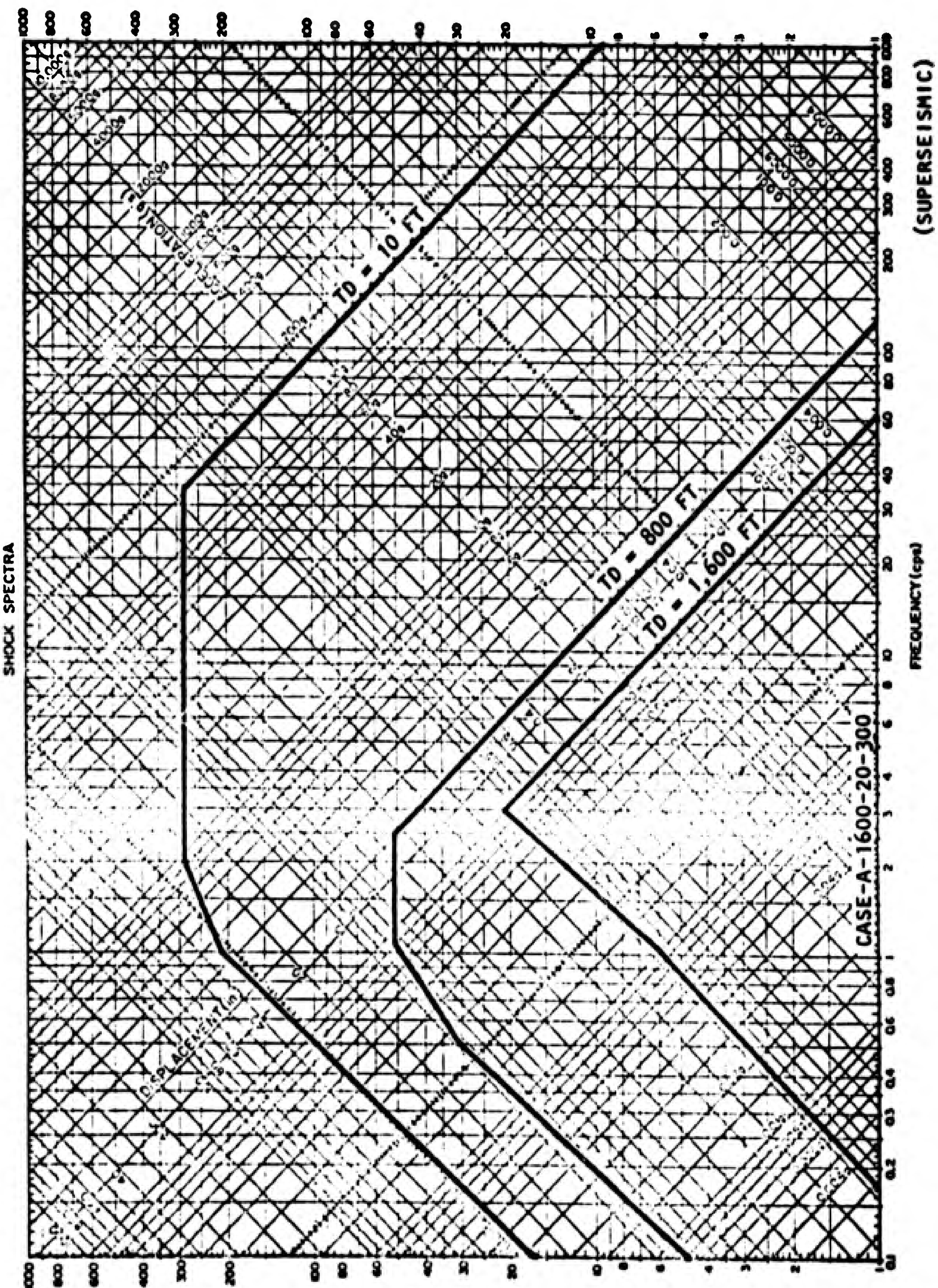

FIGURE C-12 SHOCK SPECTRA FOR VERTICAL MOTION

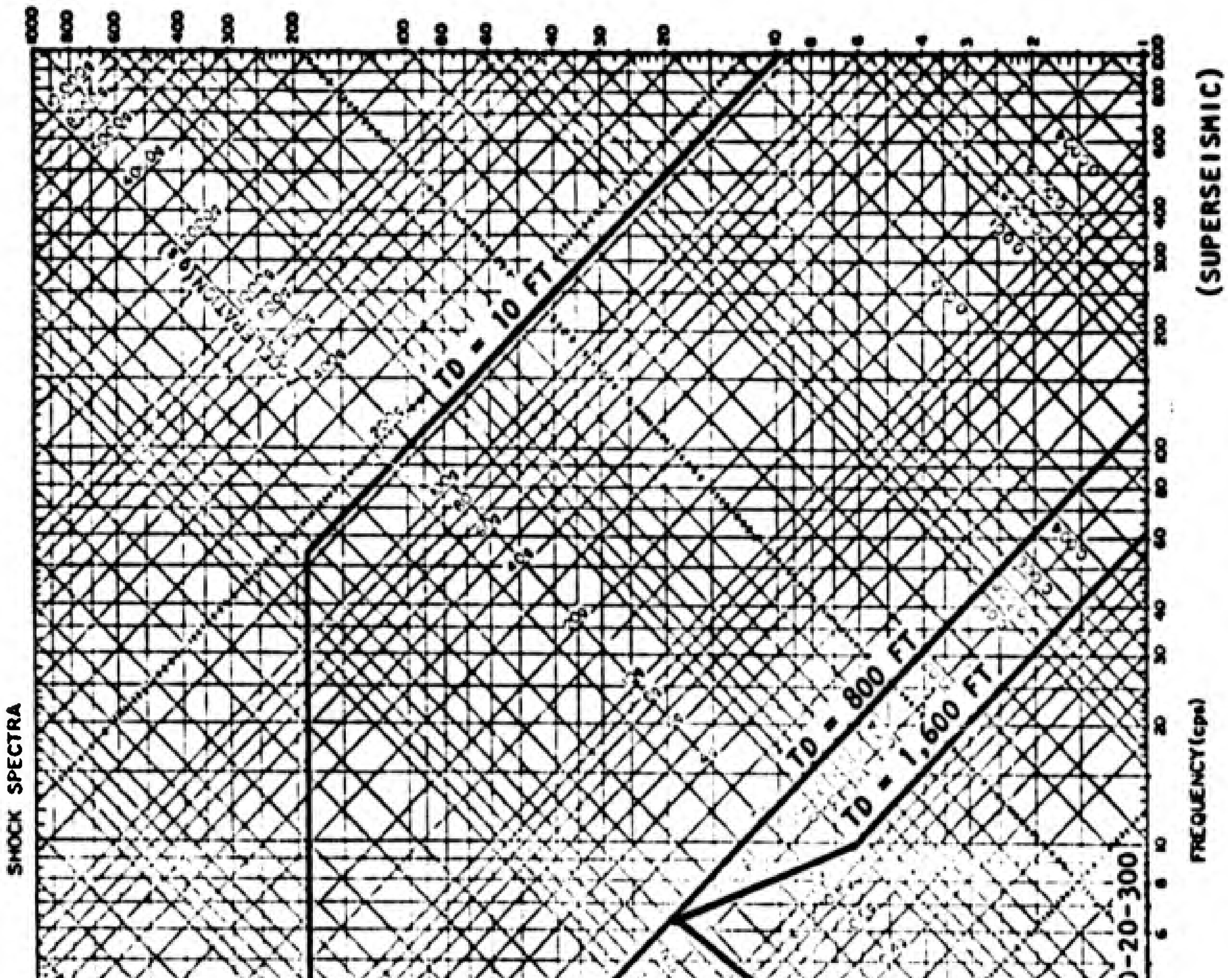

FIGURE C-13 SHOCK SPECTRA FOR HORIZONTAL MOTION

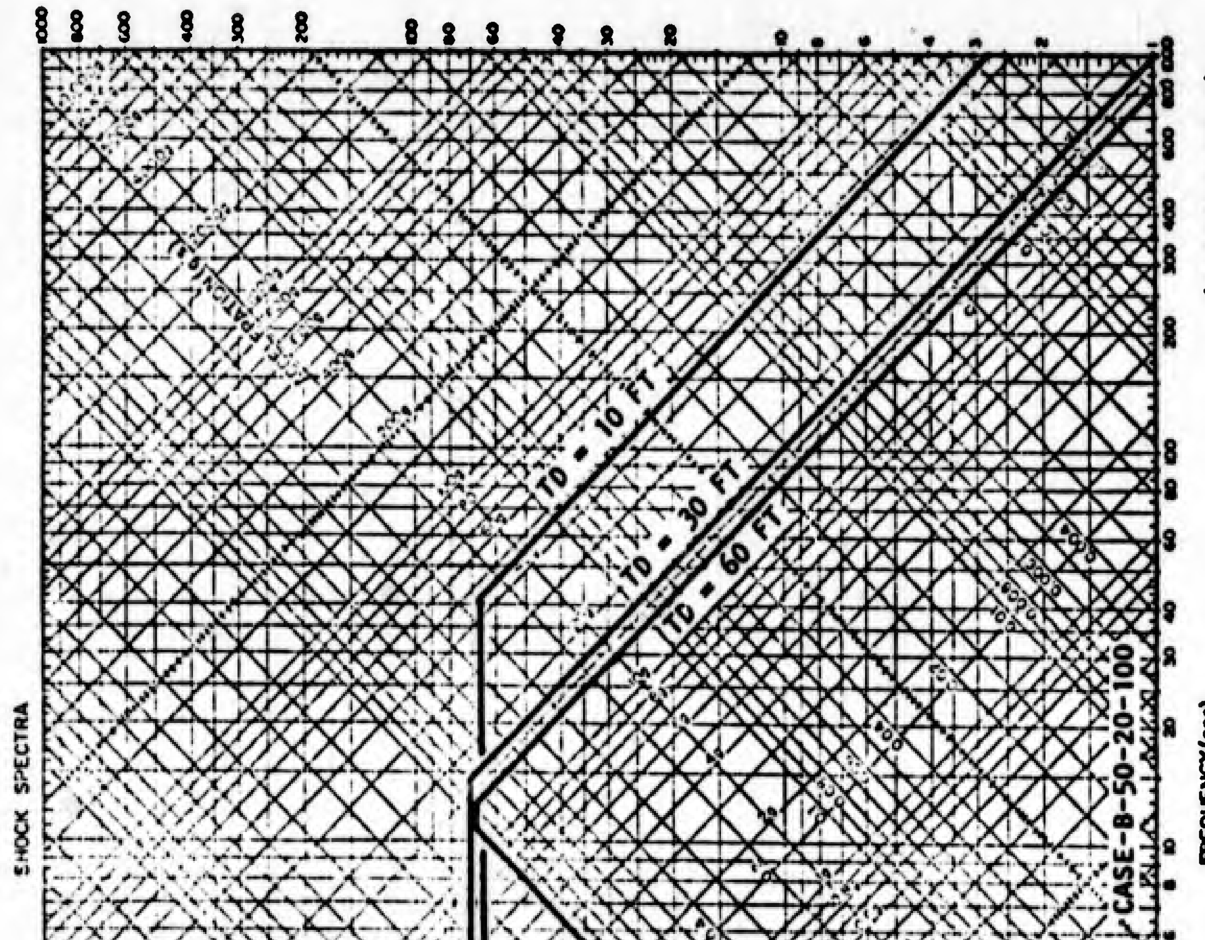

(SUPERSEISMIC)

FIGURE C-14 SHOCK SPECTRA FOR VERTICAL MOTION

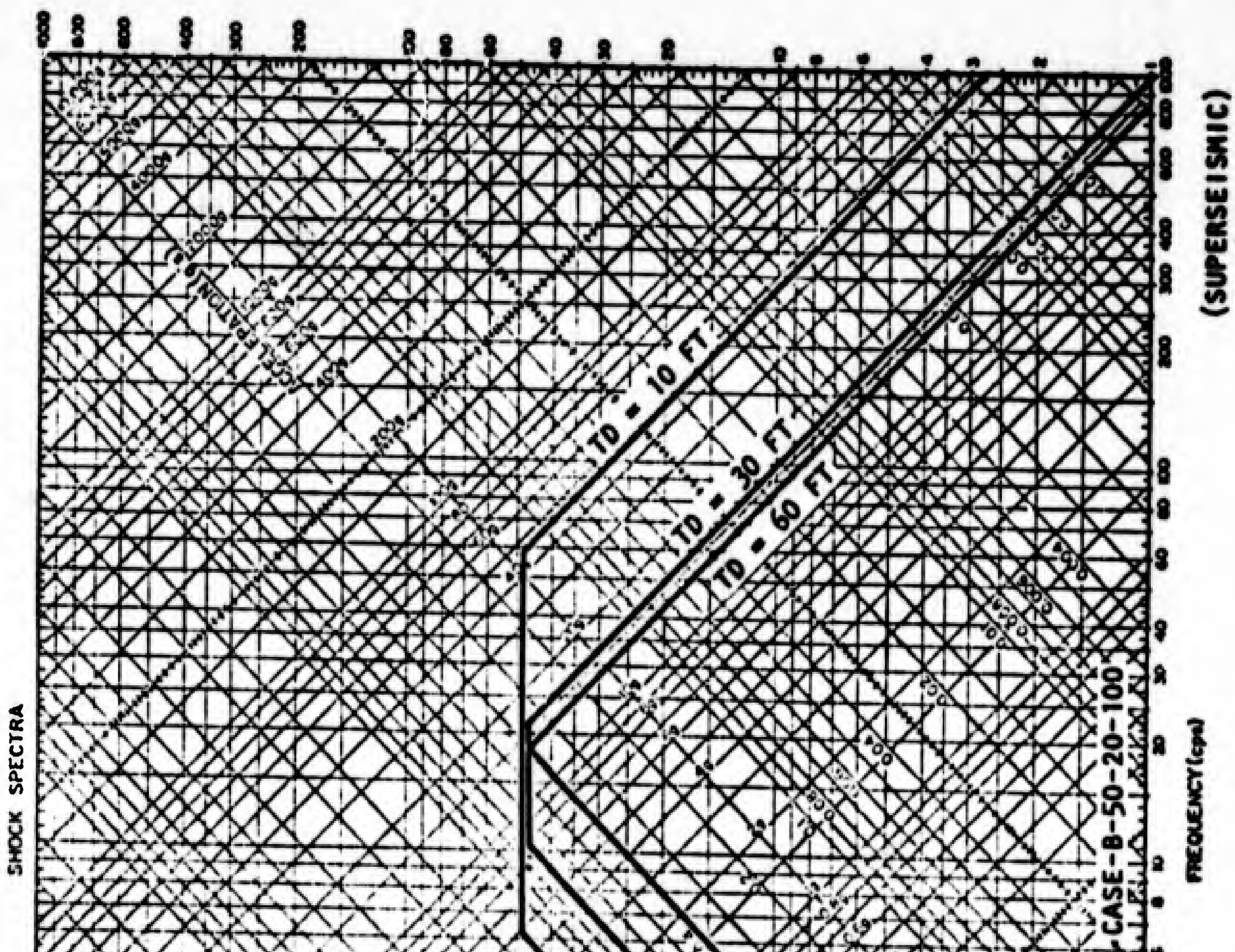

FIGURE C-15 SHOCK SPECTRA FOR HORIZONTAL MOTION

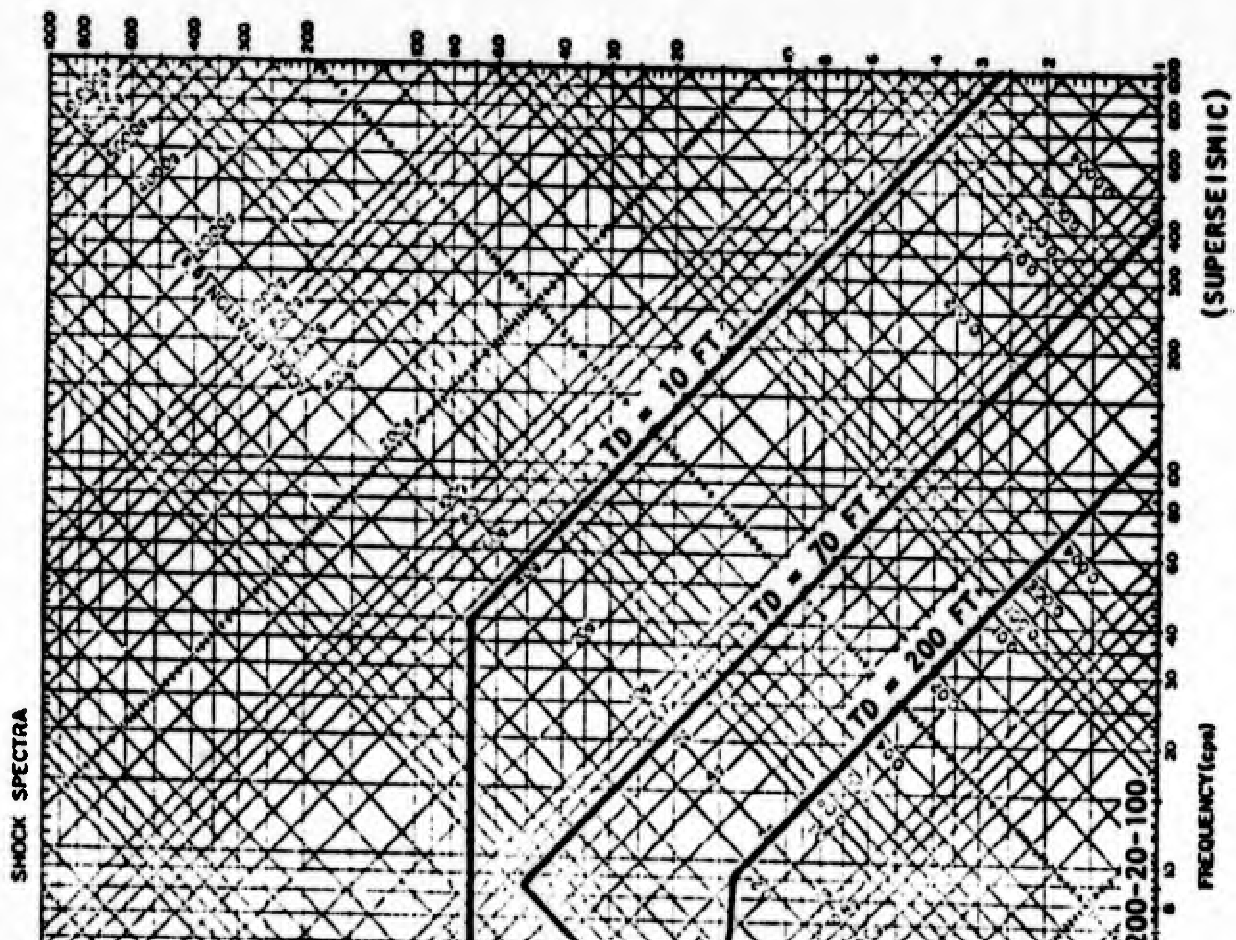

FIGURE C-16 SHOCK SPECTRA FOR VERTICAL MOTION

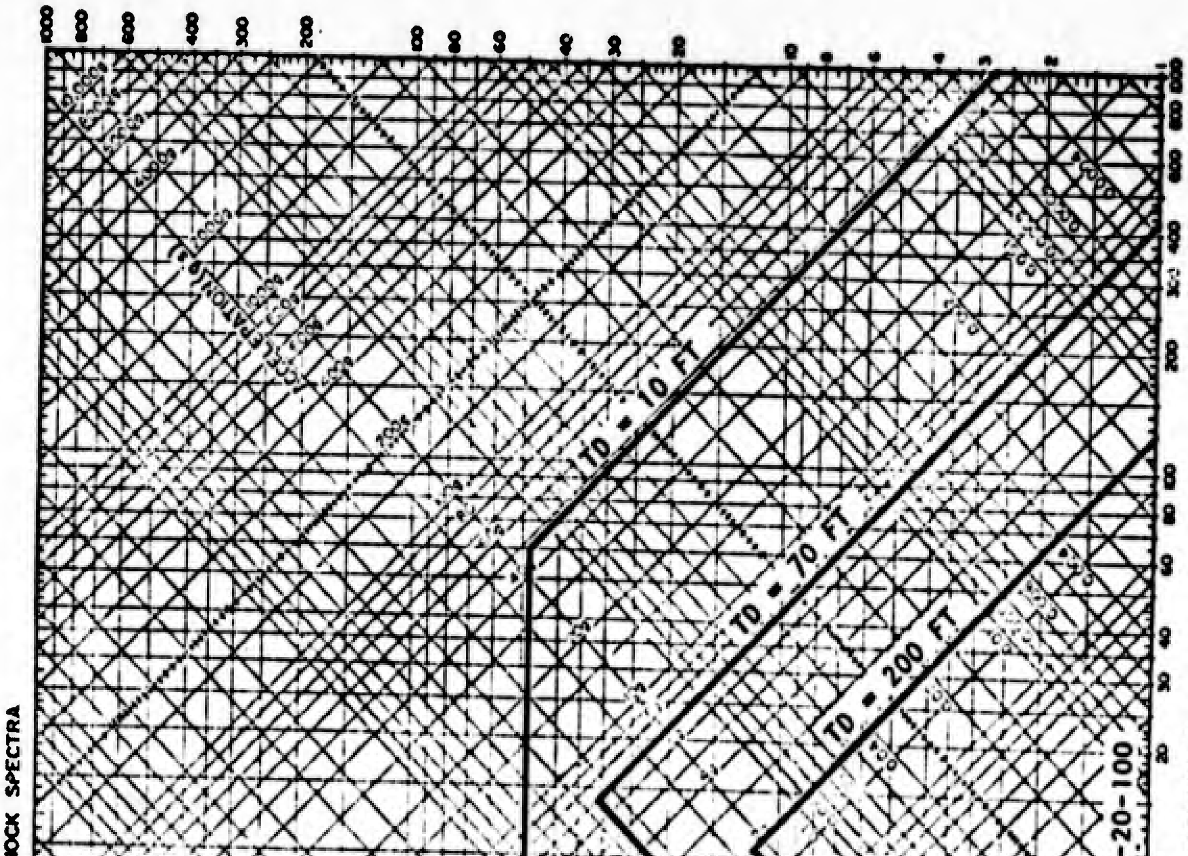

(SUPERSEISMIC)

FIGURE C-17 SHOCK SPECTRA FOR HORIZONTAL MOTION

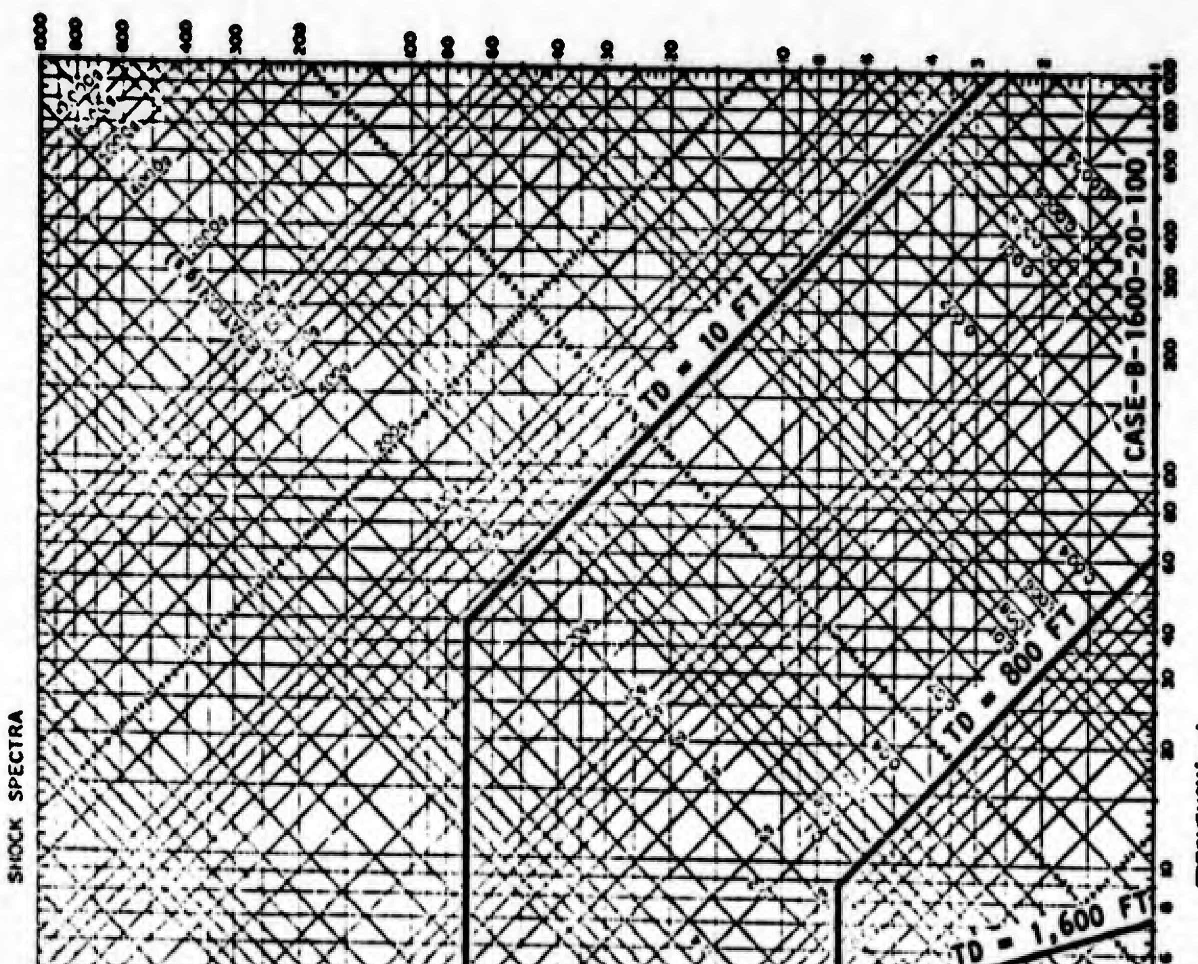

(SUPERSEISMIC)

FIGURE C-18 SHOCK SPECTRA FOR VERTICAL MOTION

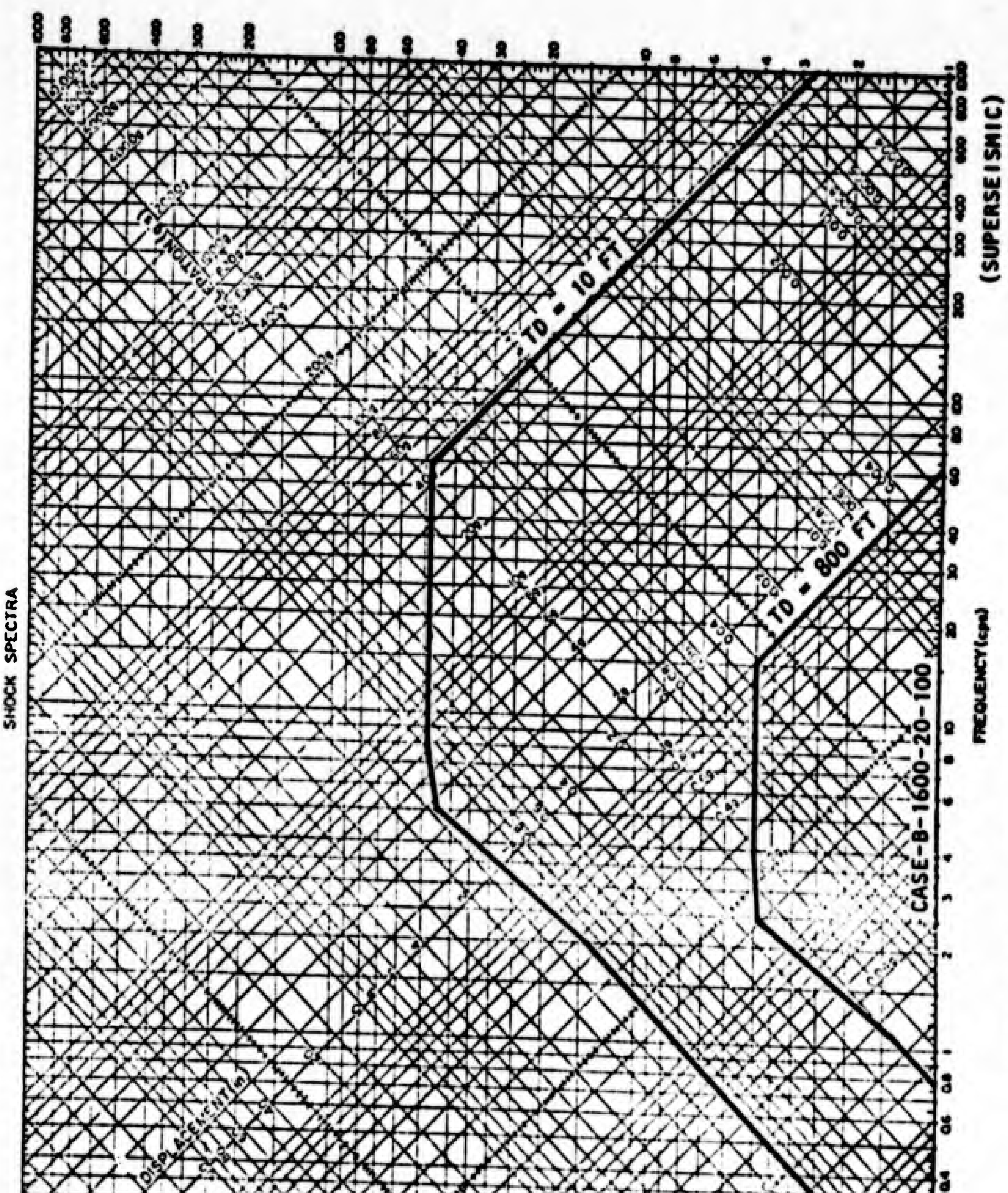

FIGURE C-19 SHOCK SPECTRA FOR HORIZONTAL MOTION

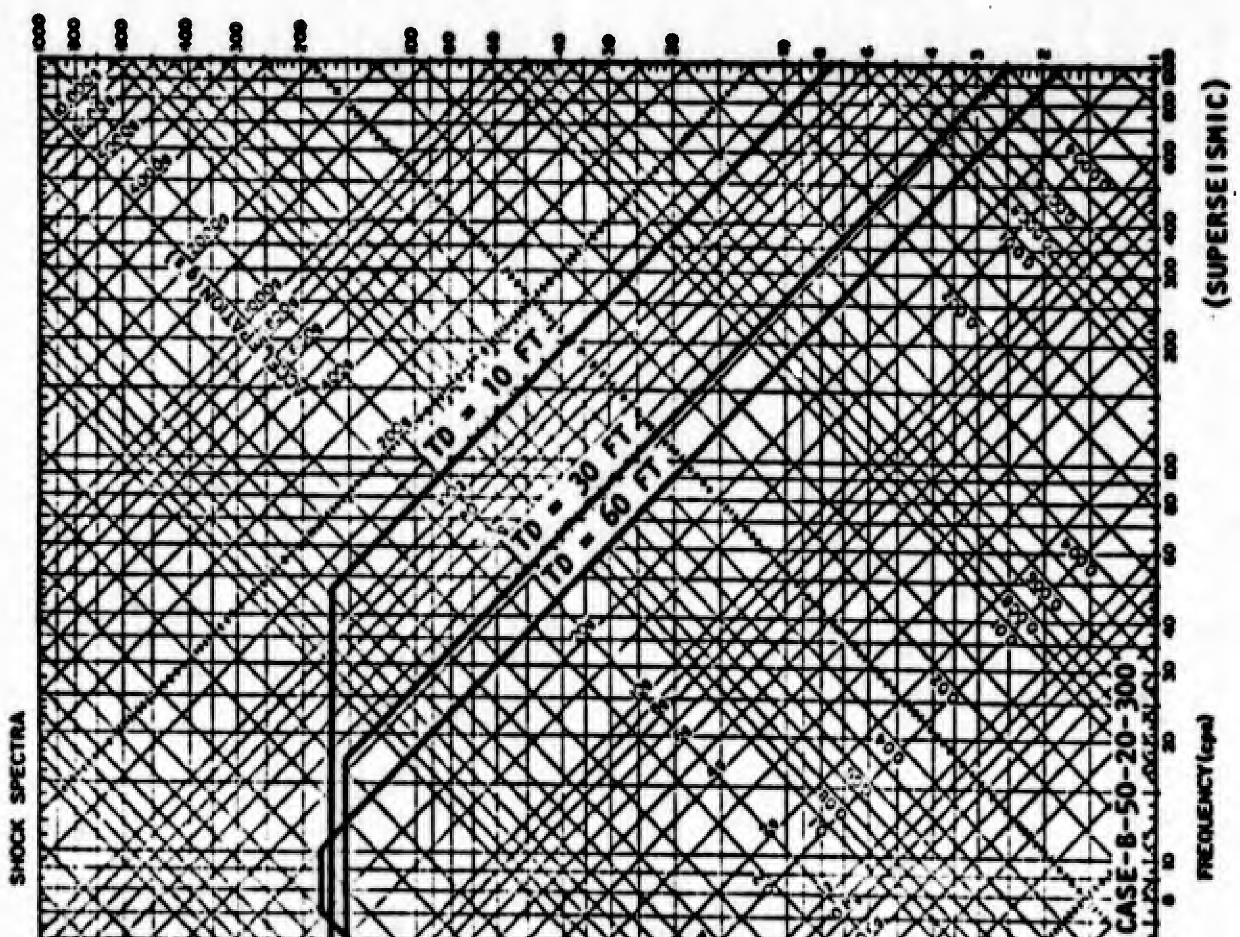

FIGURE C-20 SHOCK SPECTRA FOR VERTICAL MOTION

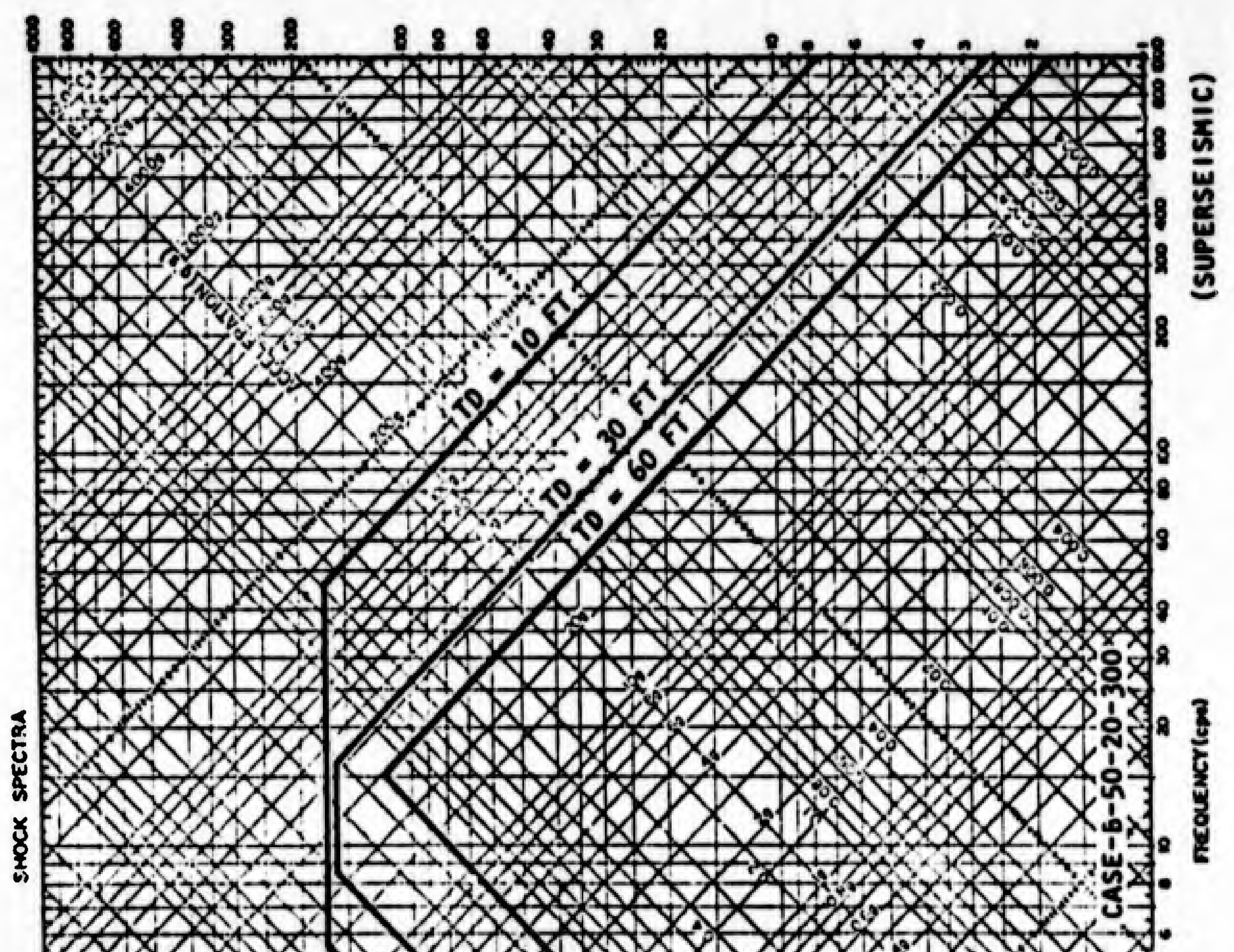

FIGURE C-21 SHOCK SPECTRA FOR HORIZONTAL MOTION

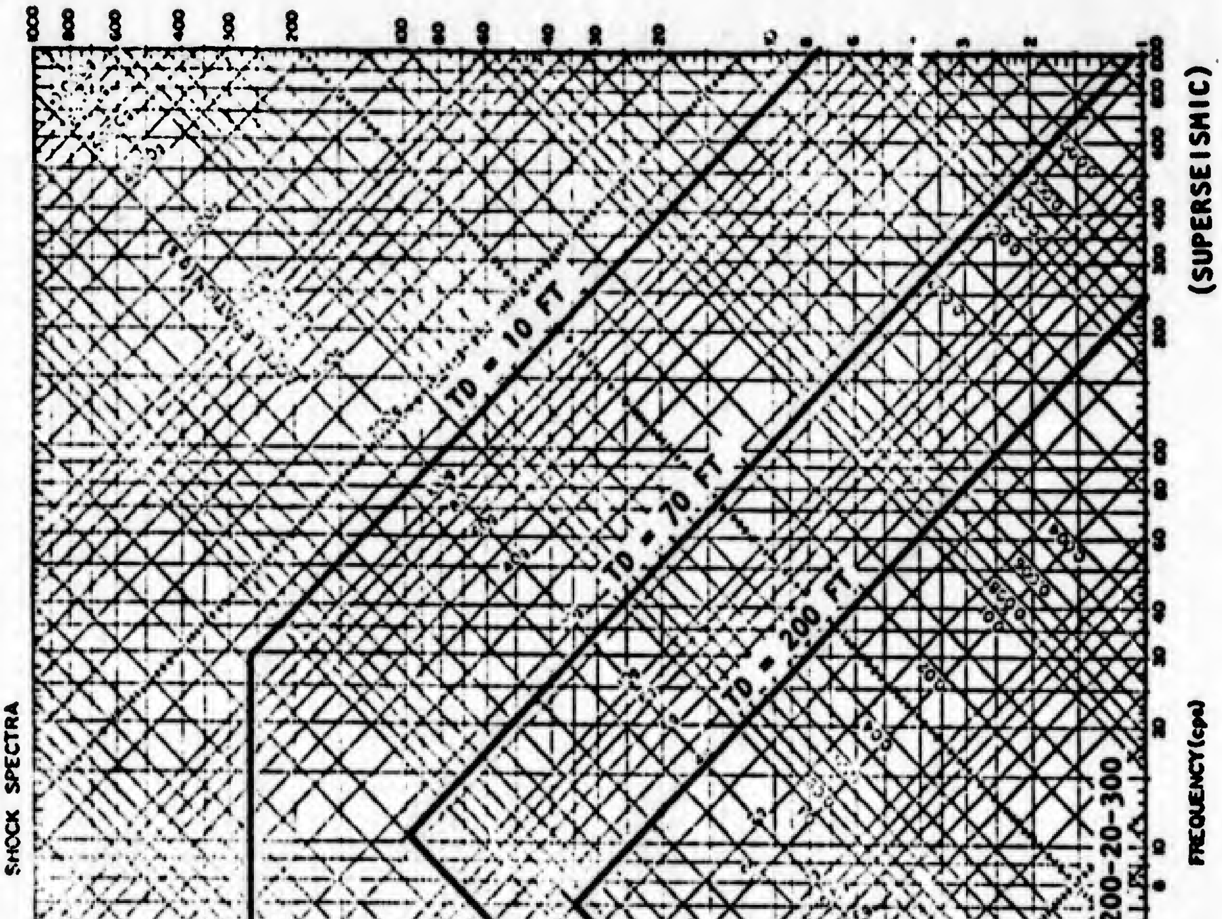

FIGURE C-22 SHOCK SPECTRA FOR VERTICAL MOTION

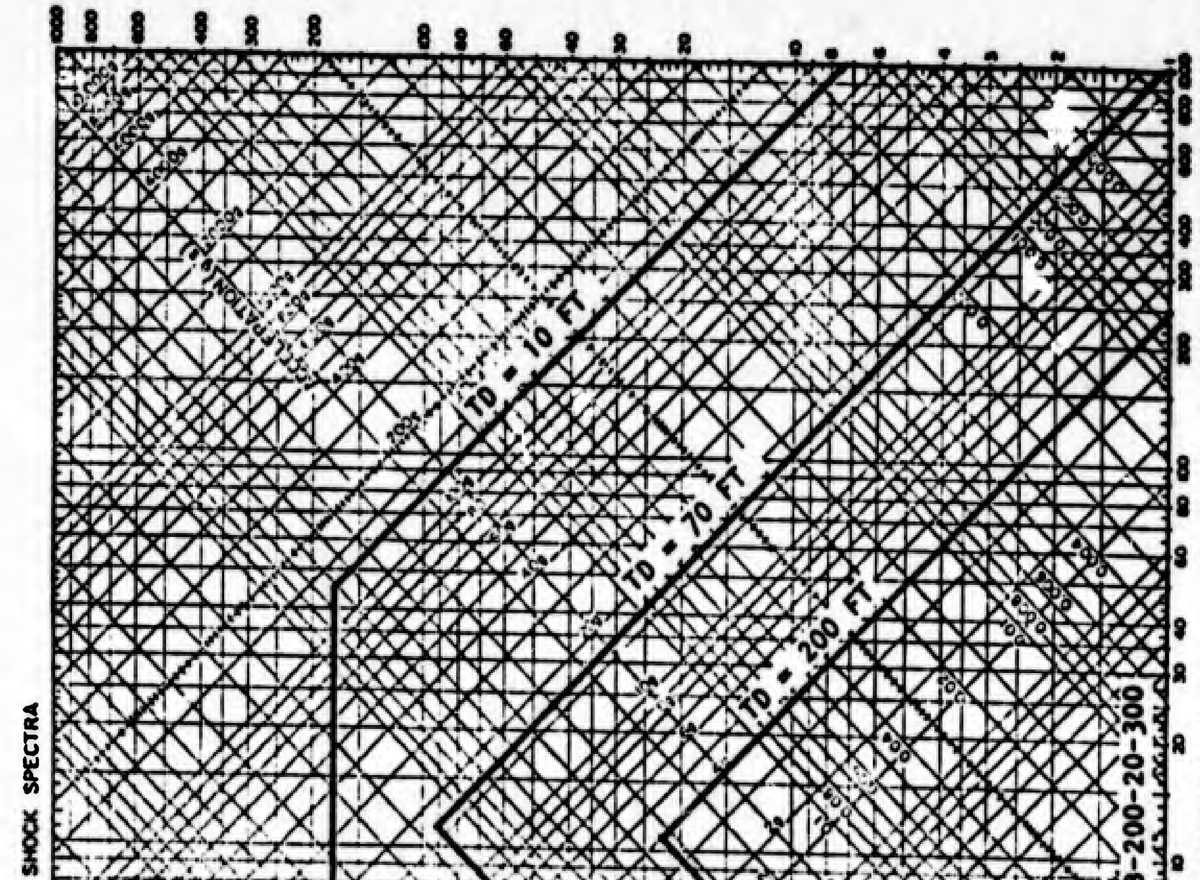

(SUPERSEISMIC)

FIGURE C-23 SHOCK SPECTRA FOR HORIZONTAL MOTION

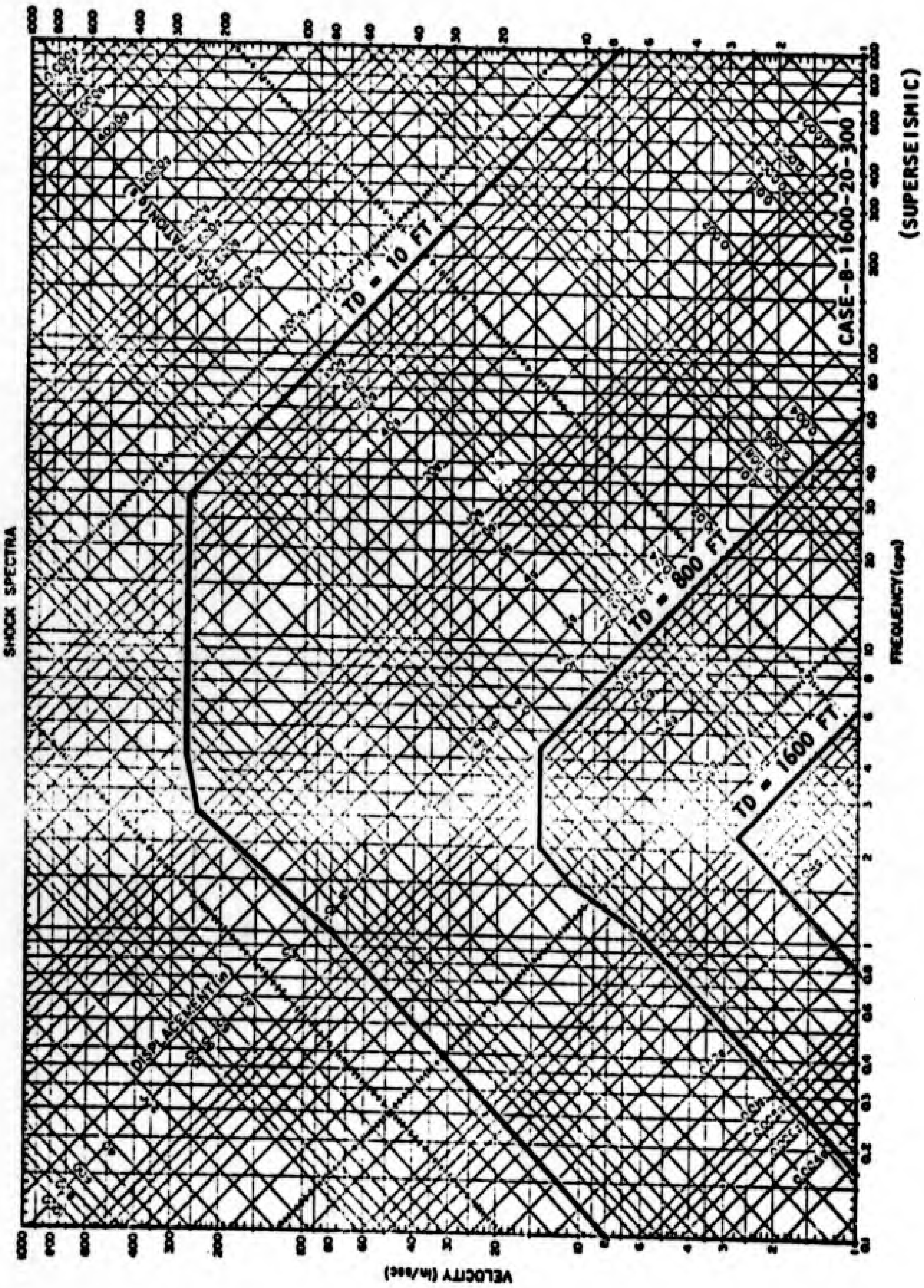

FIGURE C-24 SHOCK SPECTRA FOR VERTICAL MOTION

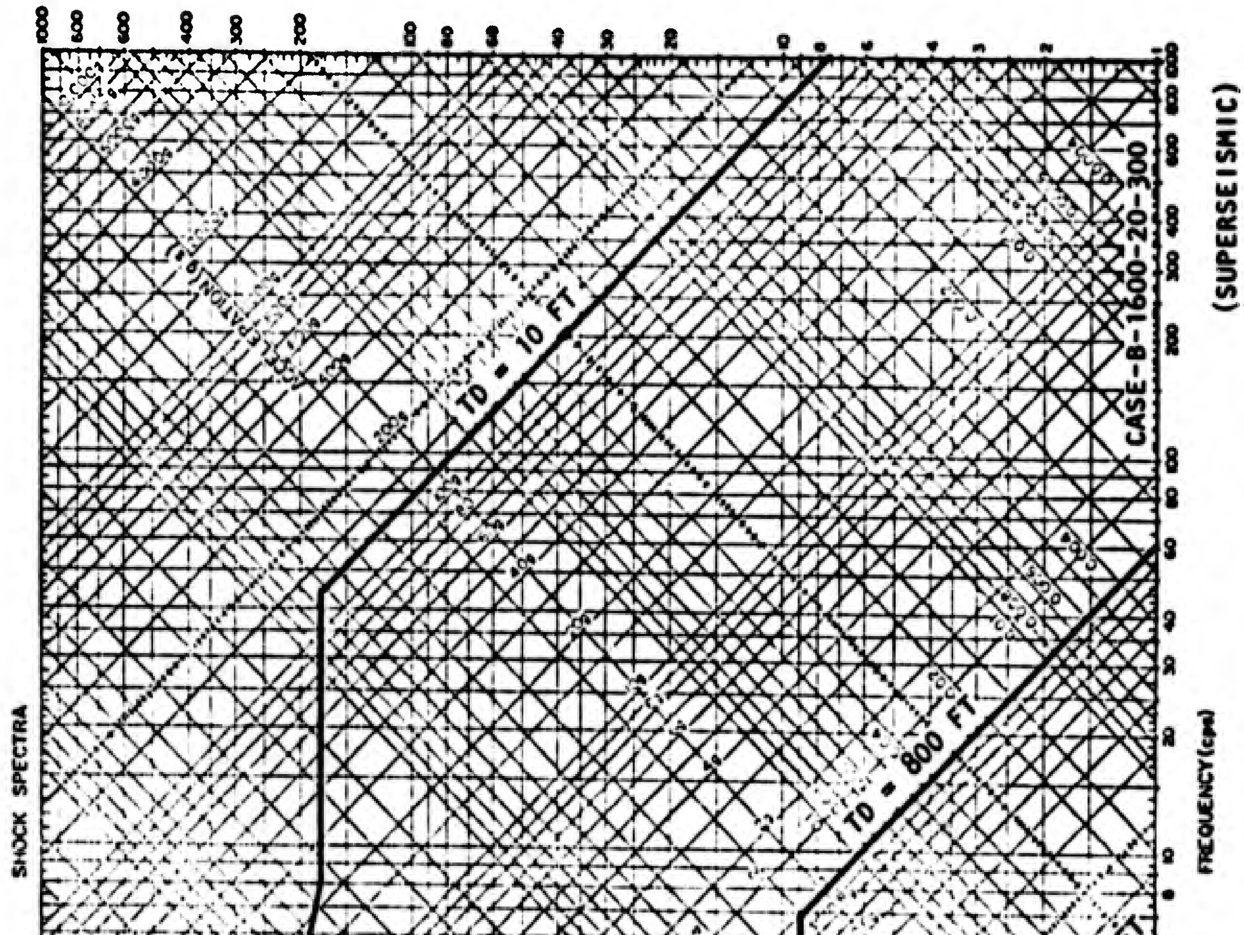

FIGURE C-25 SHOCK SPECTRA FOR HORIZONTAL MOTION

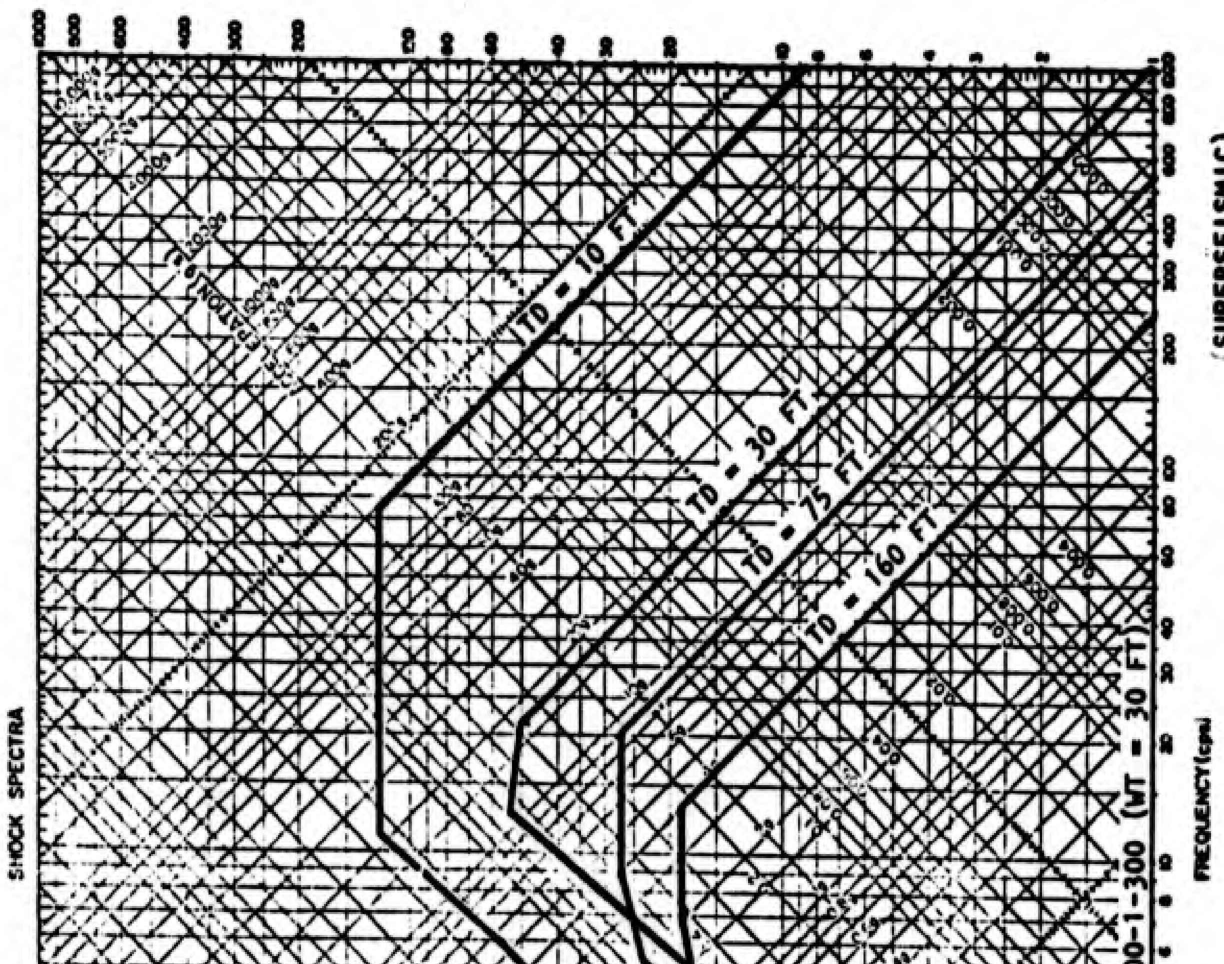

FIGURE C-26 SHOCK SPECTRA FOR HORIZONTAL MOTION

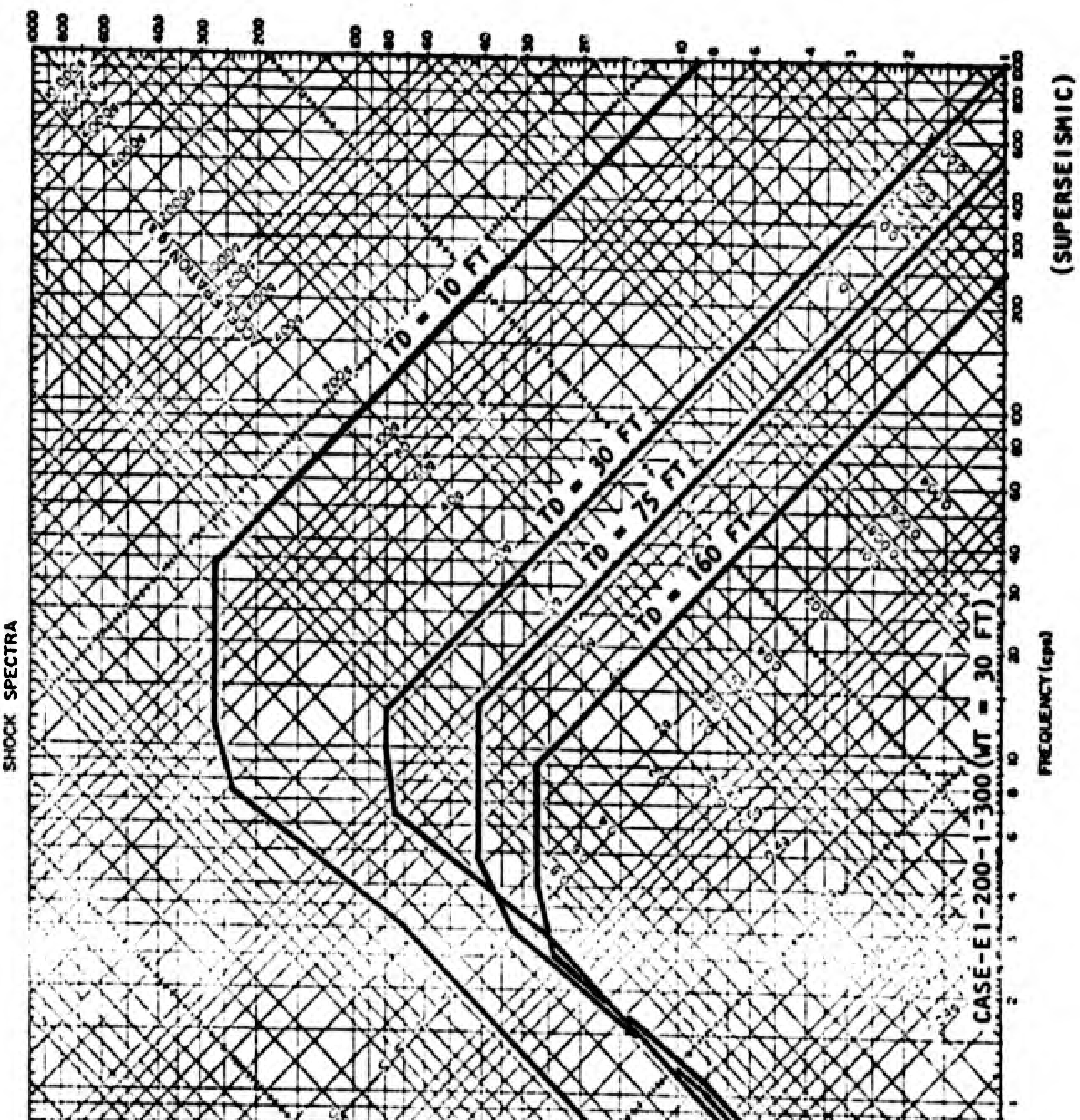

FIGURE C-27 SHOCK SPECTRA FOR VERTICAL MOTION

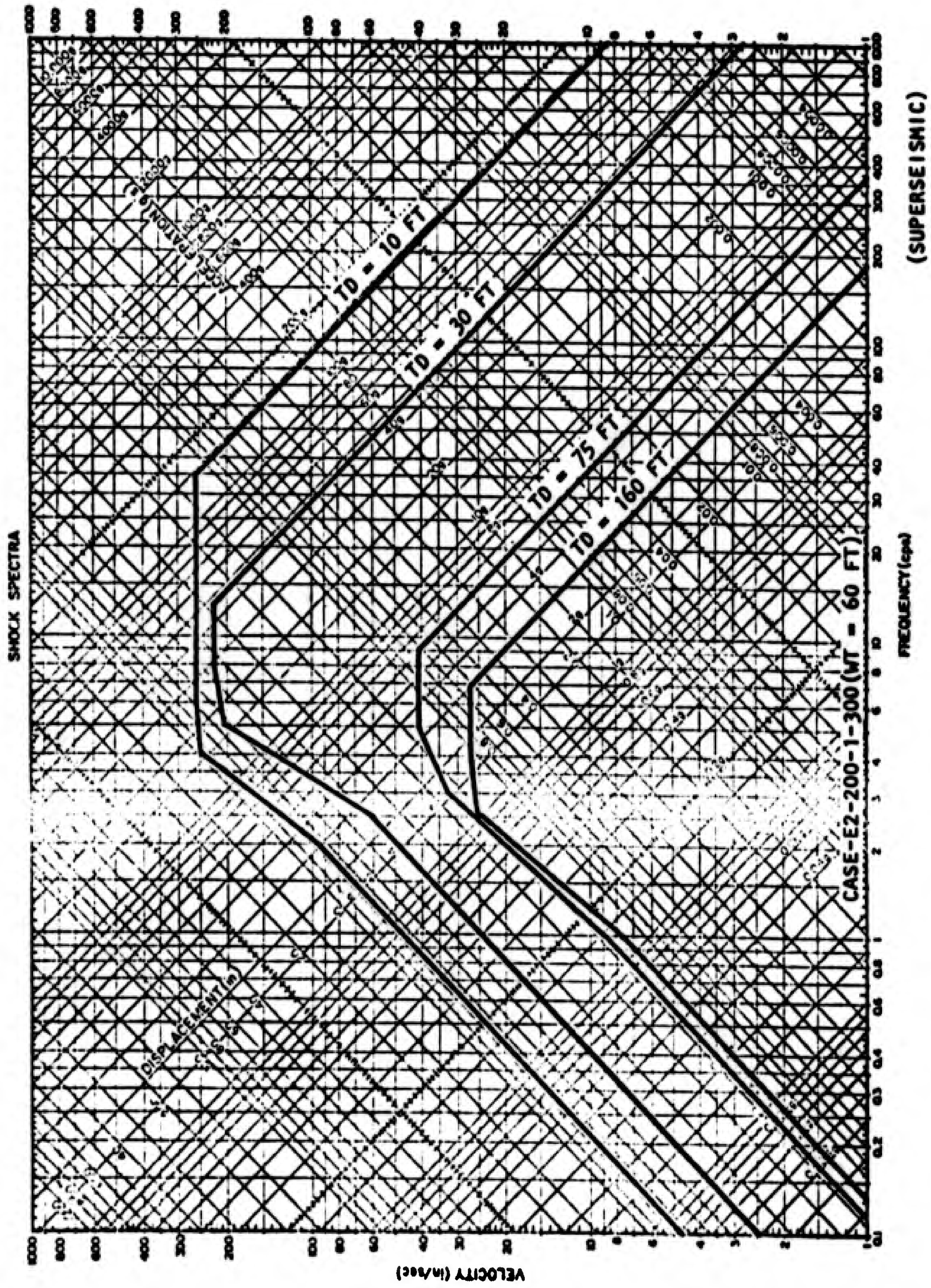

FIGURE C-28 SHOCK SPECTRA FOR VERTICAL MOTION

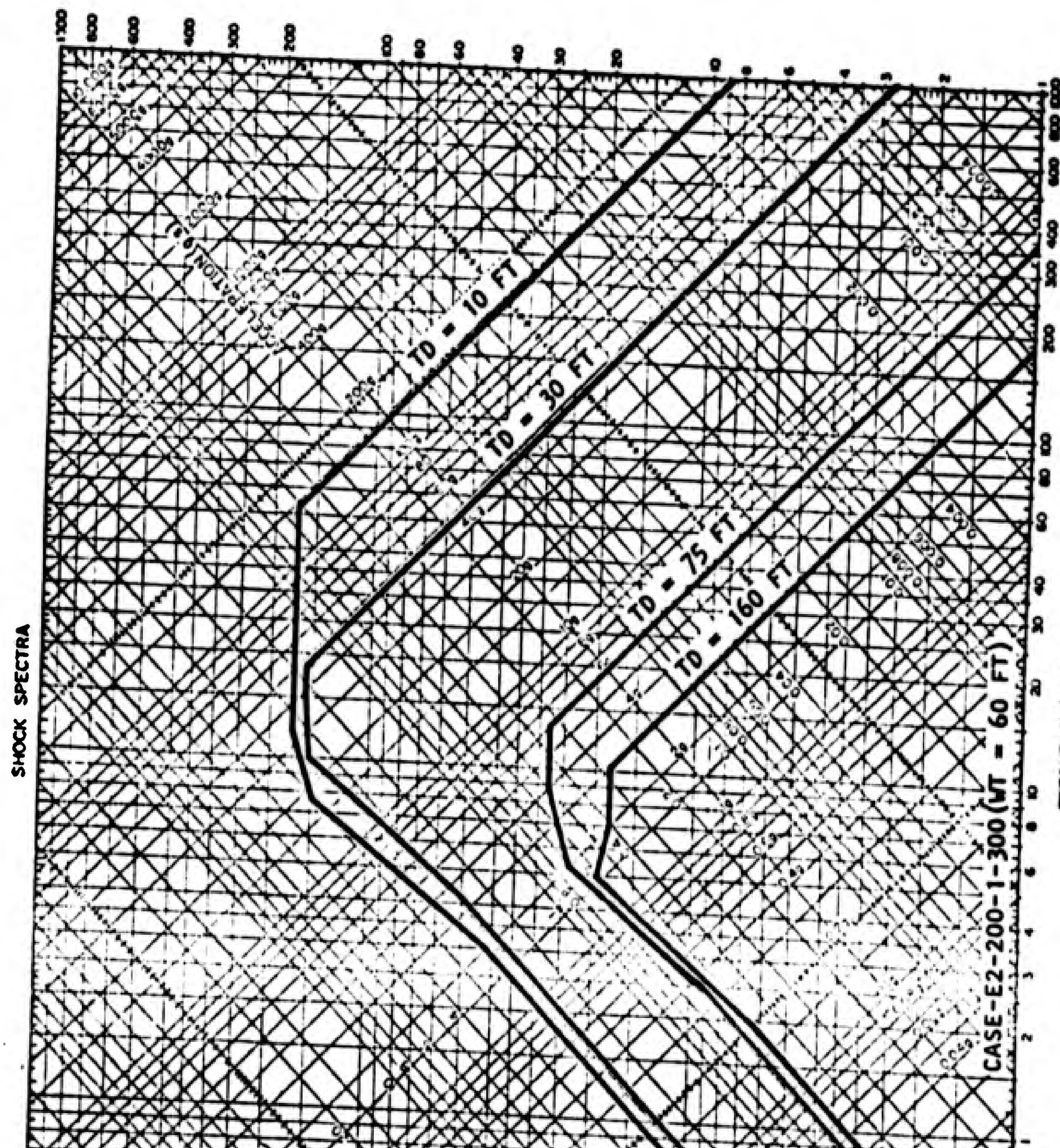

FIGURE C-29 SHOCK SPECTRA FOR HORIZONTAL MOTION (SUPERSEISMIC)

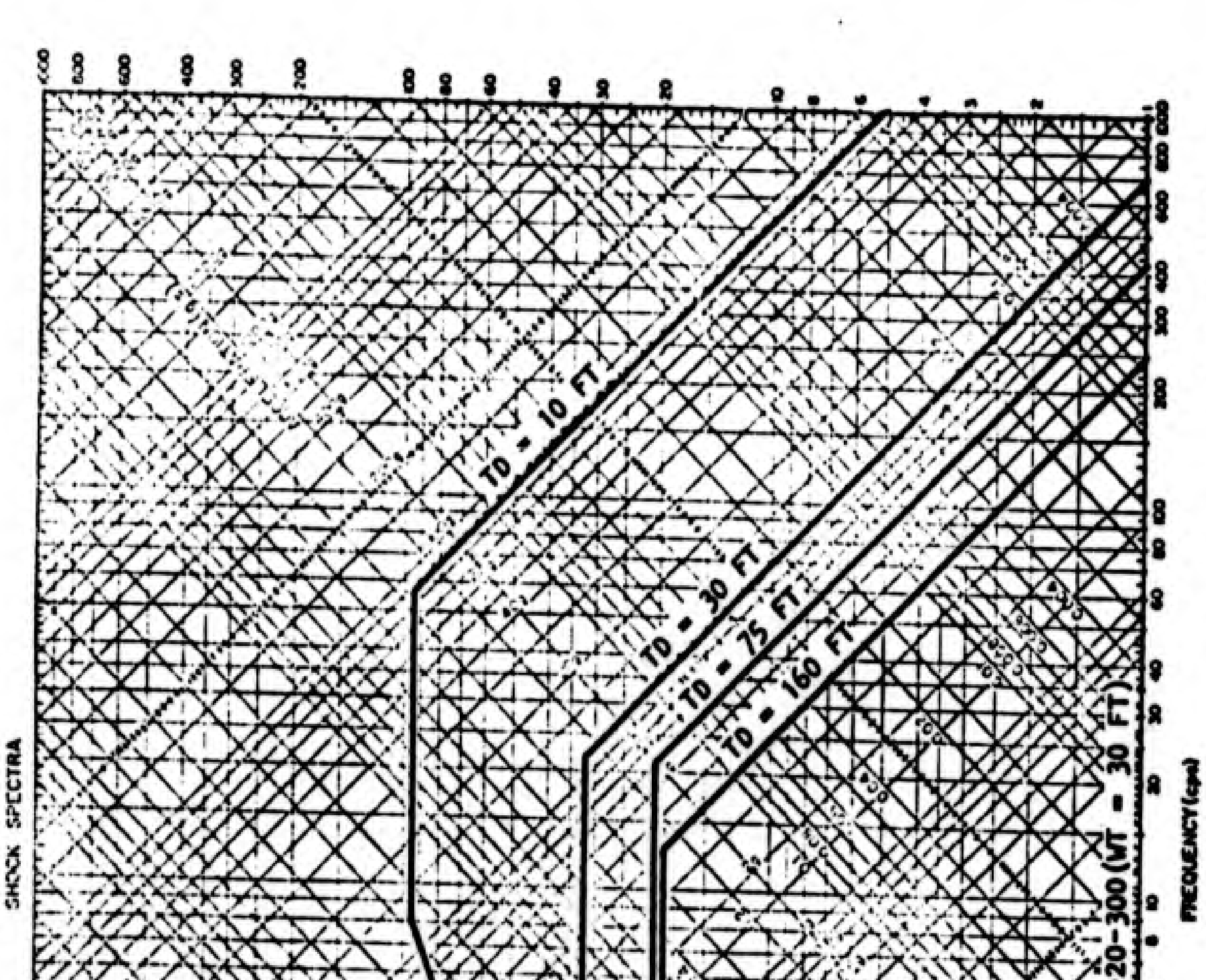

(OUTRUNNING)

FIGURE C-30 SHOCK SPECTRA FOR VERTICAL MOTION

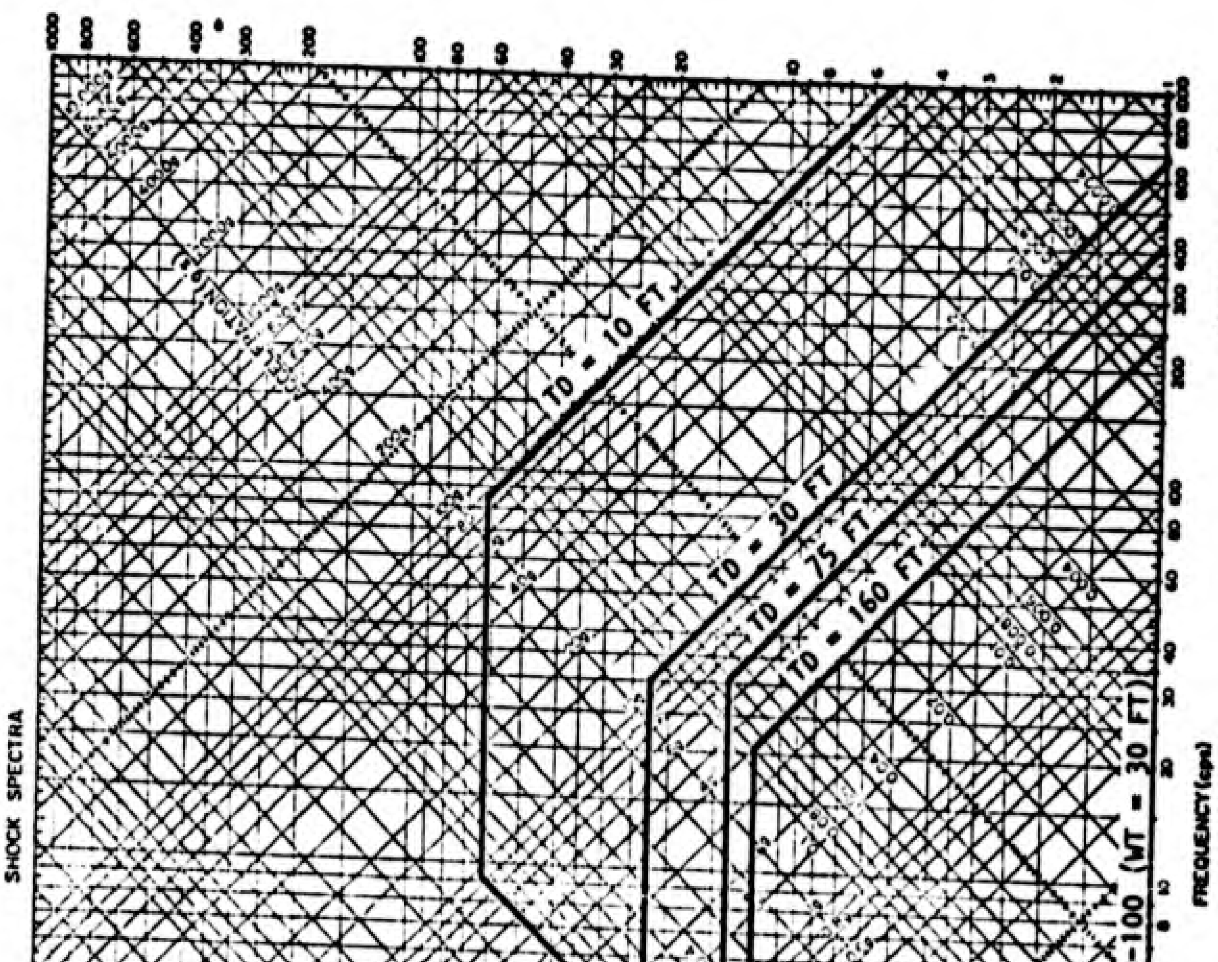

(OUTRUNNING)

FIGURE C-31 SHOCK SPECTRA FOR HORIZONTAL MOTION

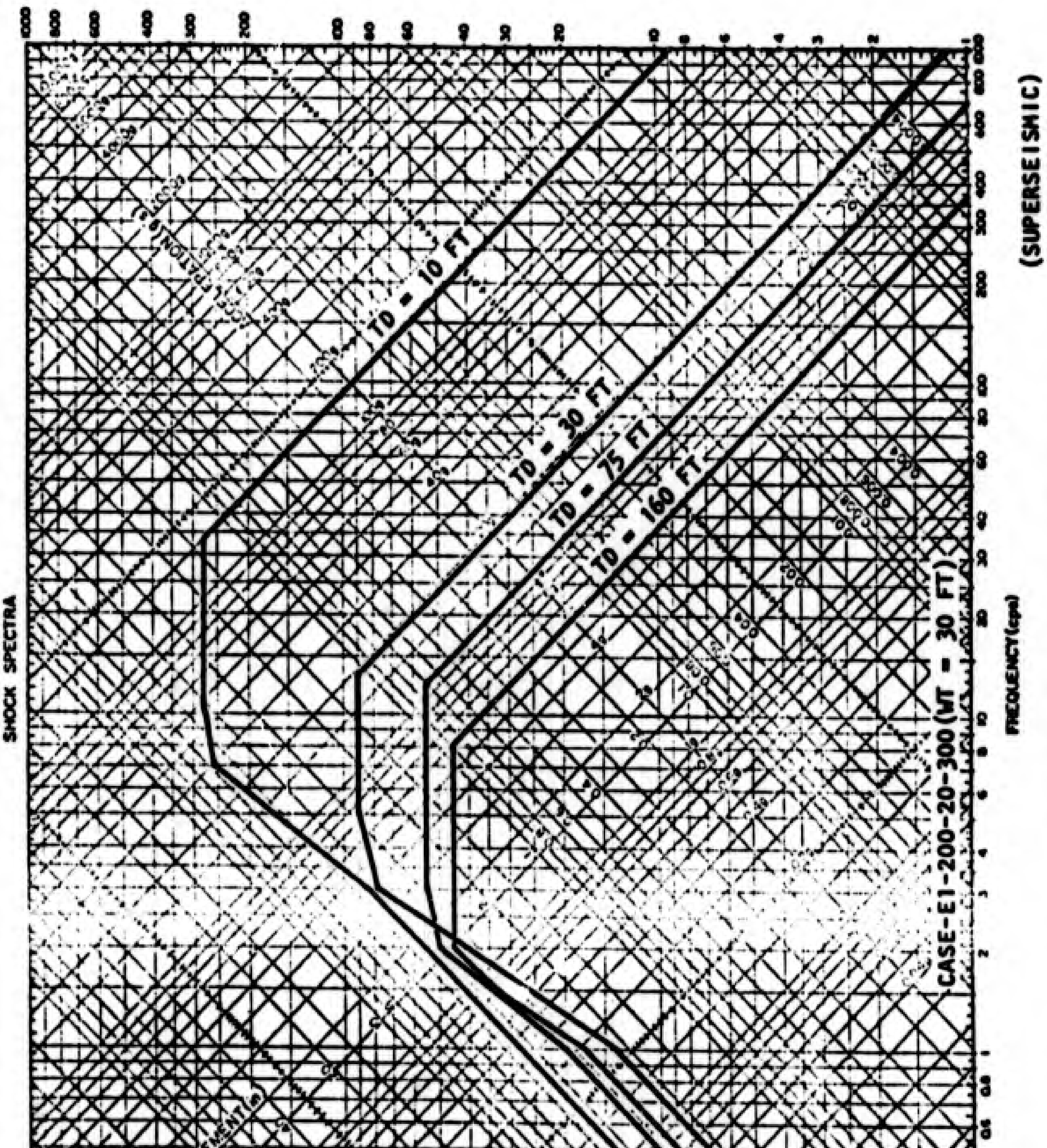

FIGURE C-32 SHOCK SPECTRA FOR VERTICAL MOTION

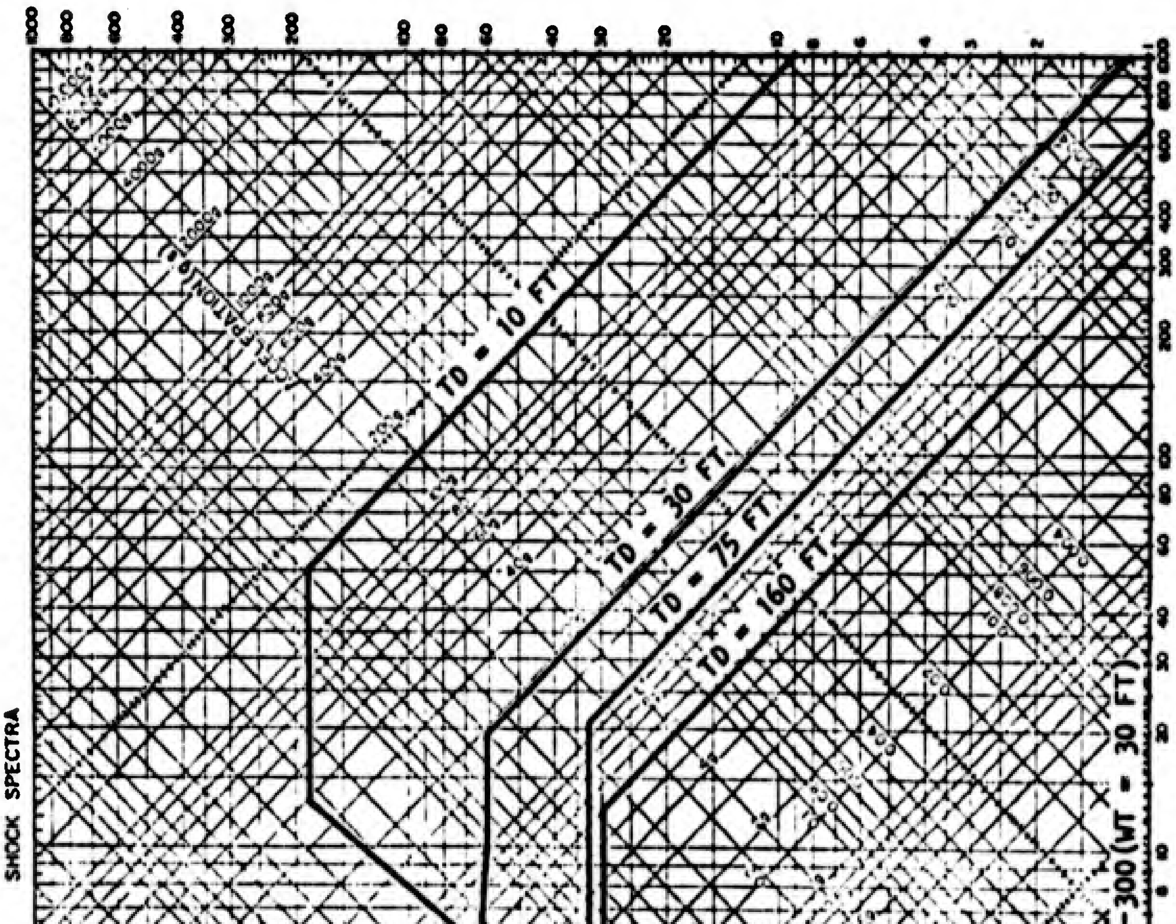

FIGURE C-33 SHOCK SPECTRA FOR HORIZONTAL MOTION (SUPERSEISMIC)

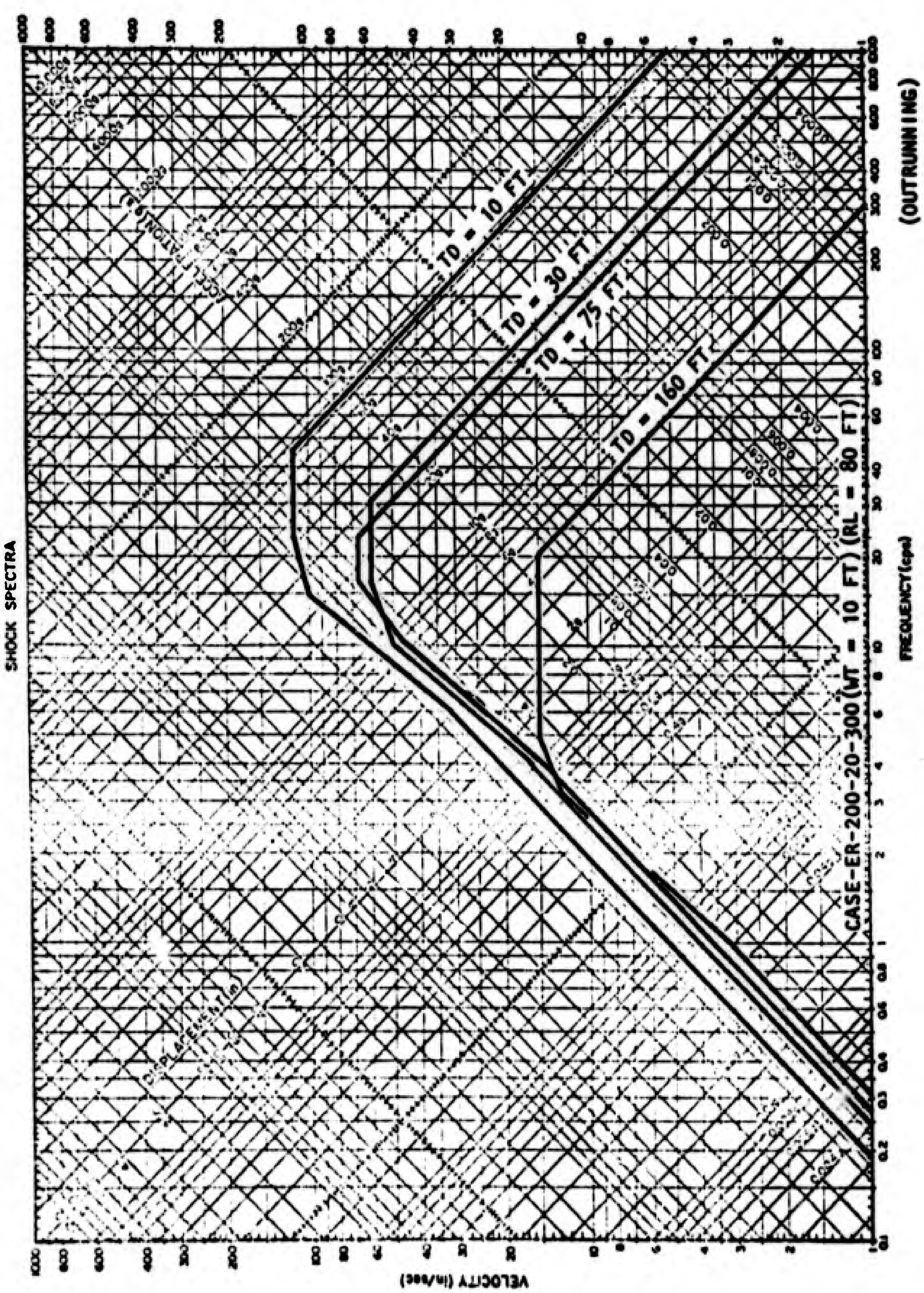

FIGURE C-34 SHOCK SPECTRA FOR VERTICAL MOTION

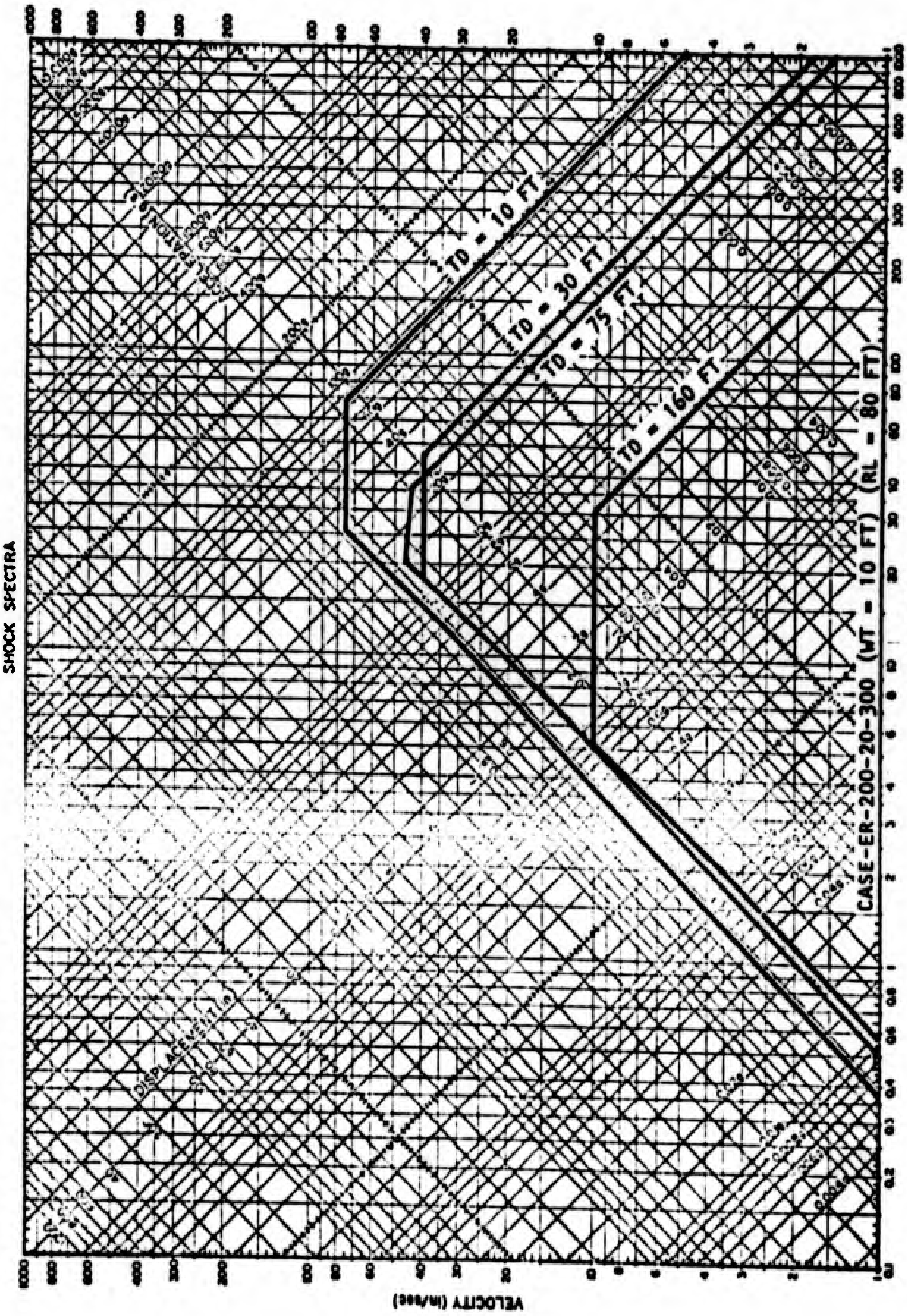

(OUTRUNNING)

FIGURE C-35 SHOCK SPECTRA FOR HORIZONTAL MOTION

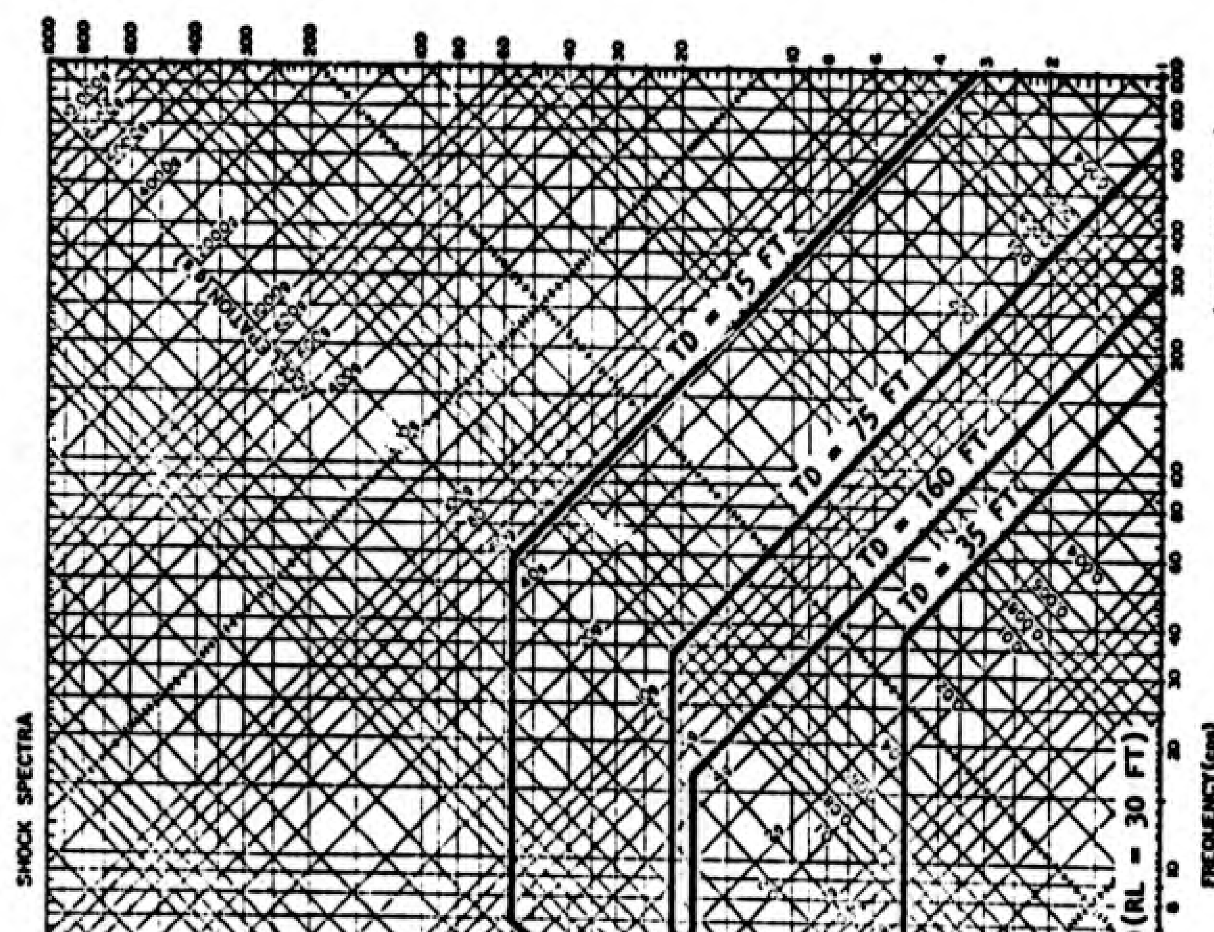

(OUTRUNNING)

FIGURE C-36 SHOCK SPECTRA FOR VERTICAL MOTION

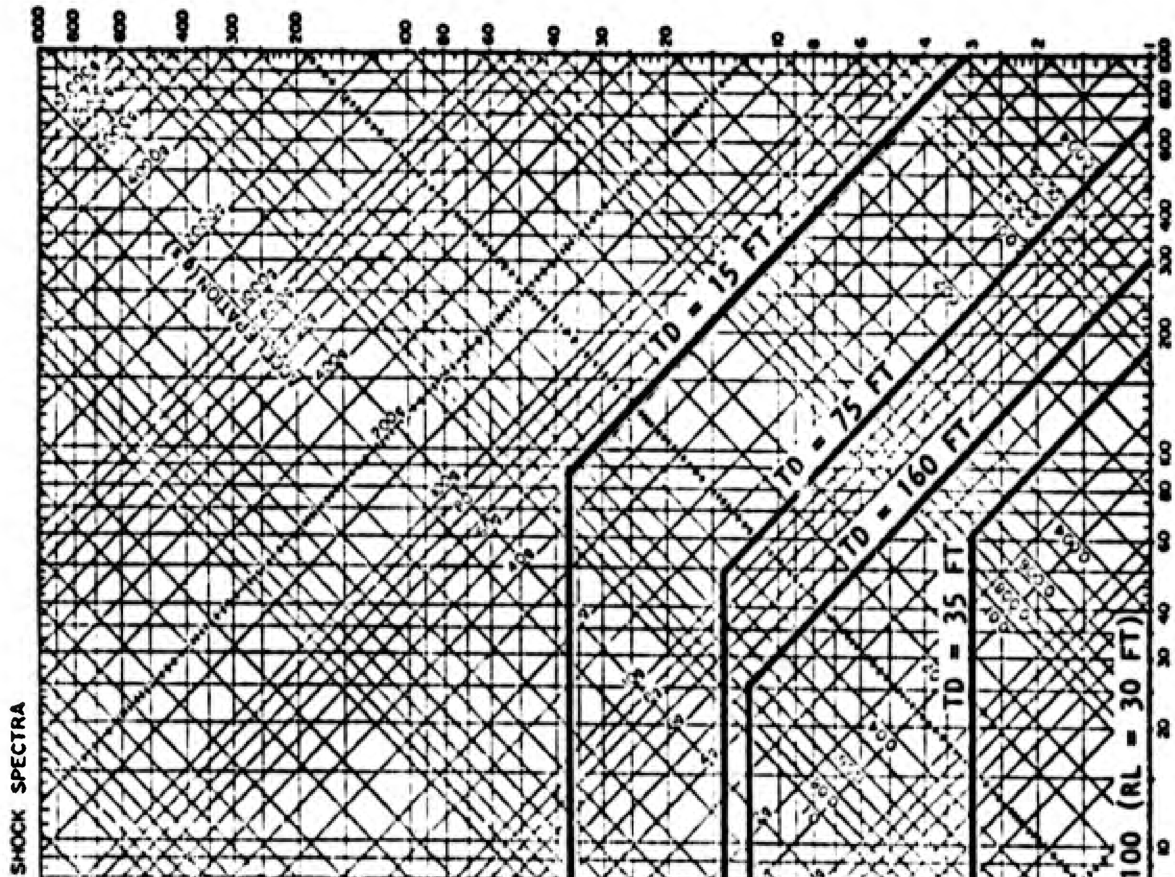

FIGURE C-37 SHOCK SPECTRA FOR HORIZONTAL MOTION (OUTRUNNING)

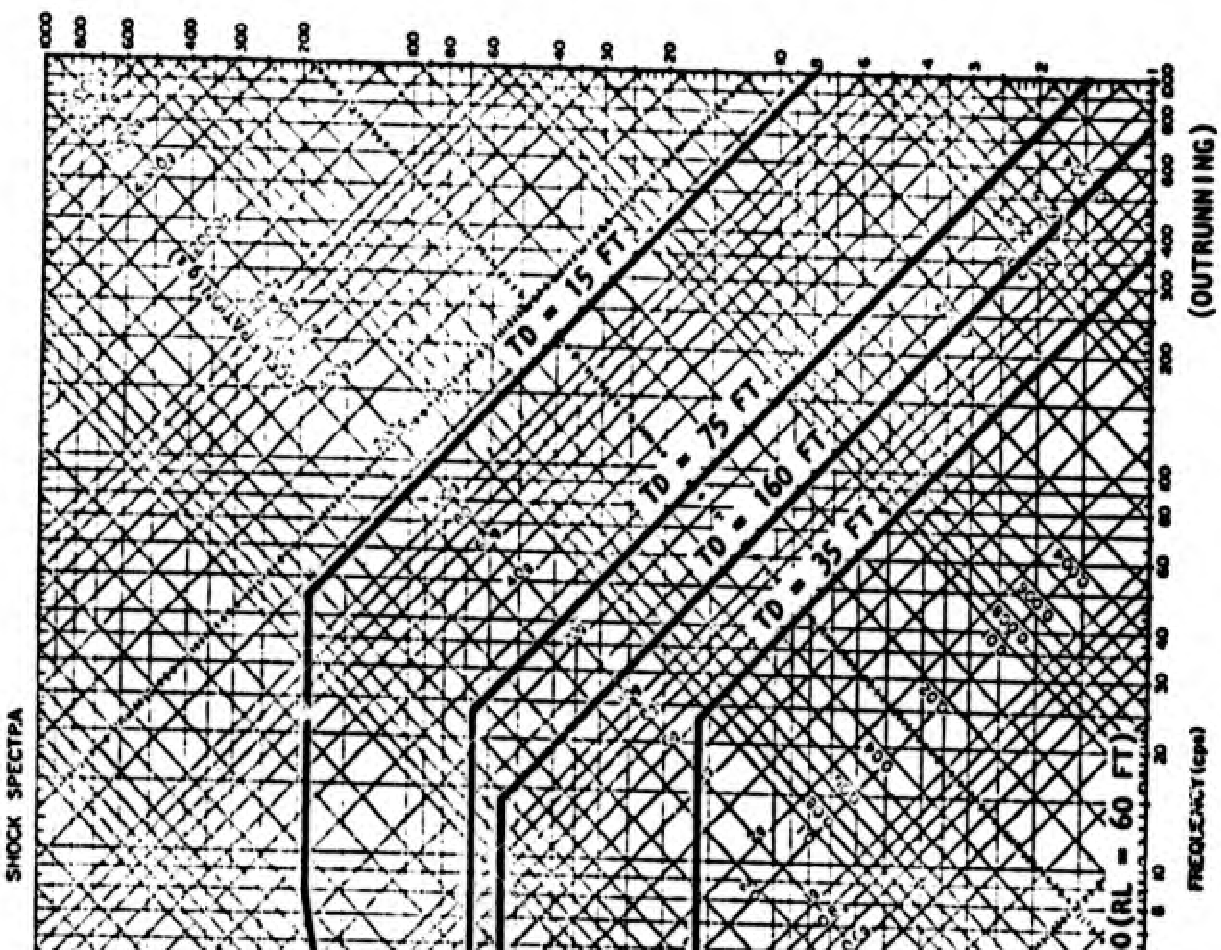

FIGURE C-38 SHOCK SPECTRA FOR VERTICAL MOTION

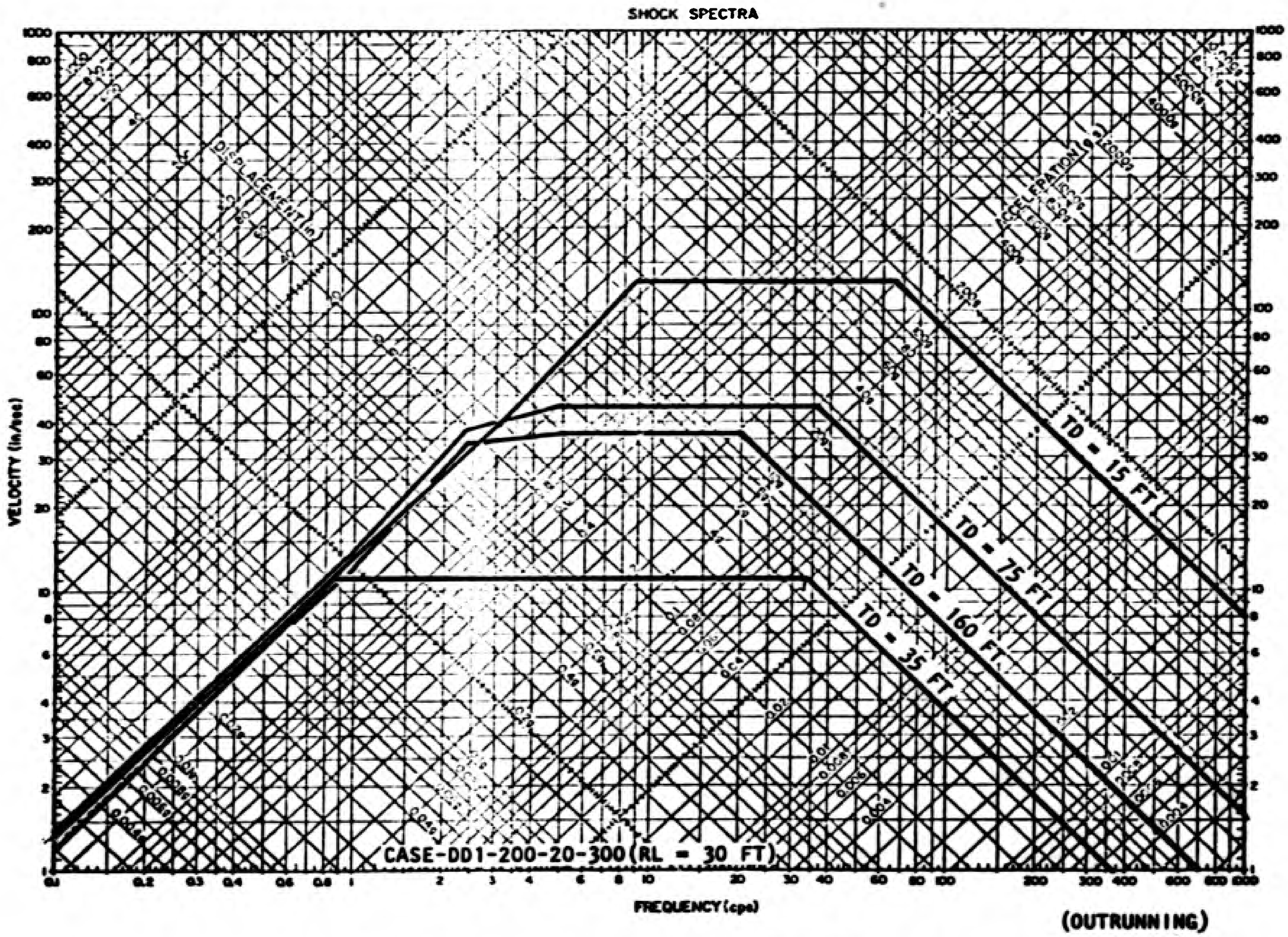

FIGURE C-39 SHOCK SPECTRA FOR HORIZONTAL MOTION

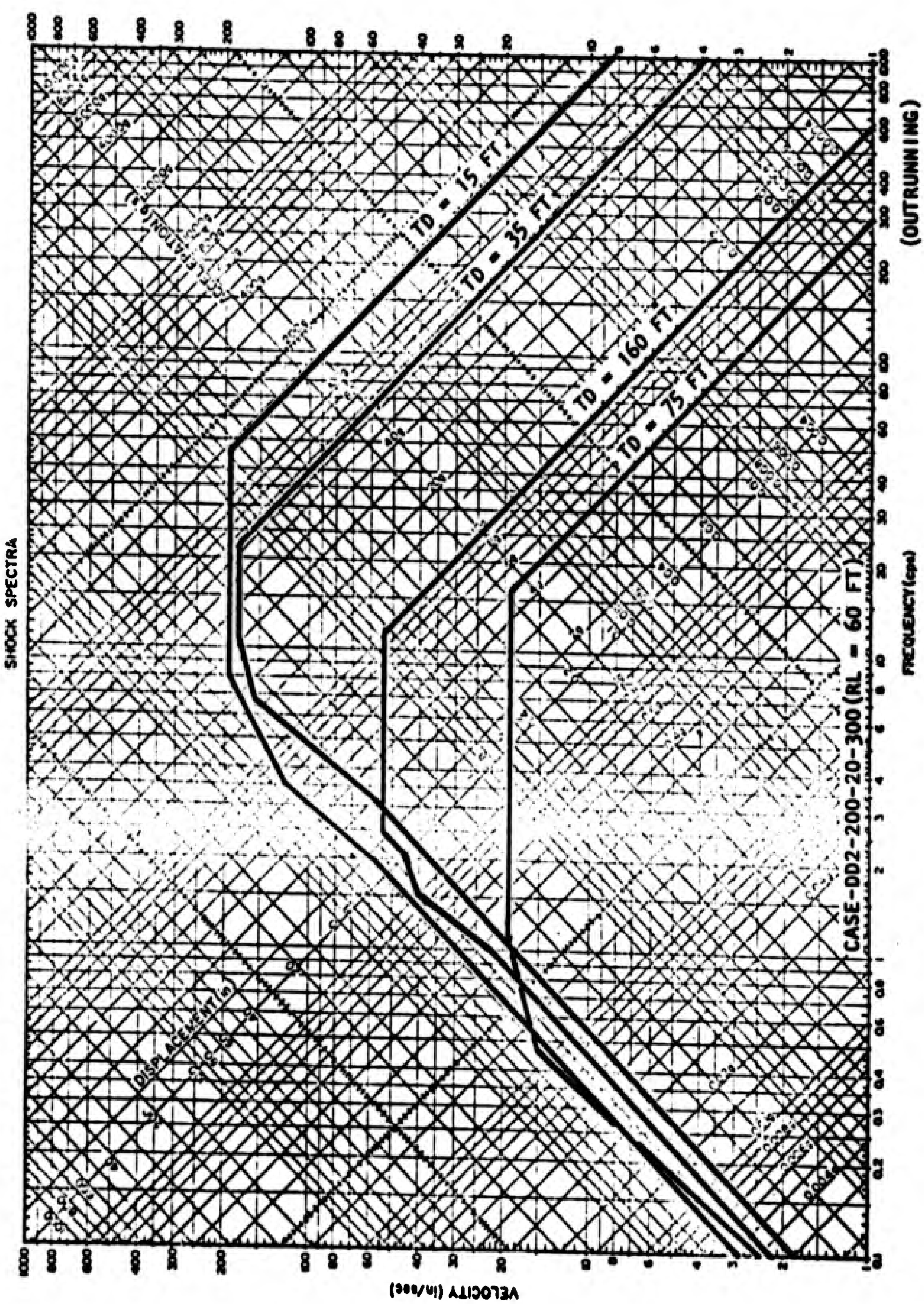

FIGURE C-40 SHOCK SPECTRA FOR VERTICAL MOTION

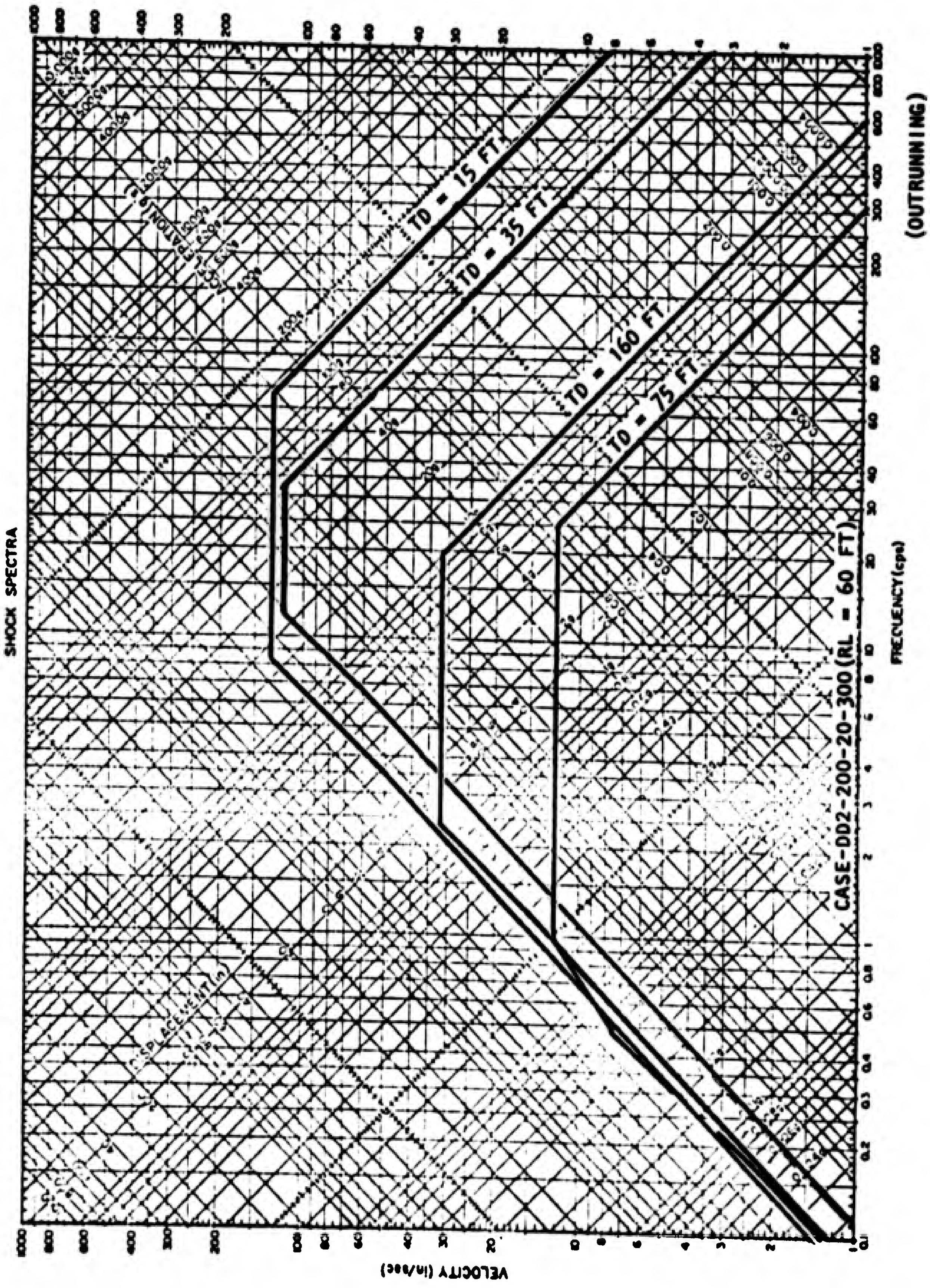

FIGURE C-41 SHOCK SPECTRA FOR HORIZONTAL MOTION

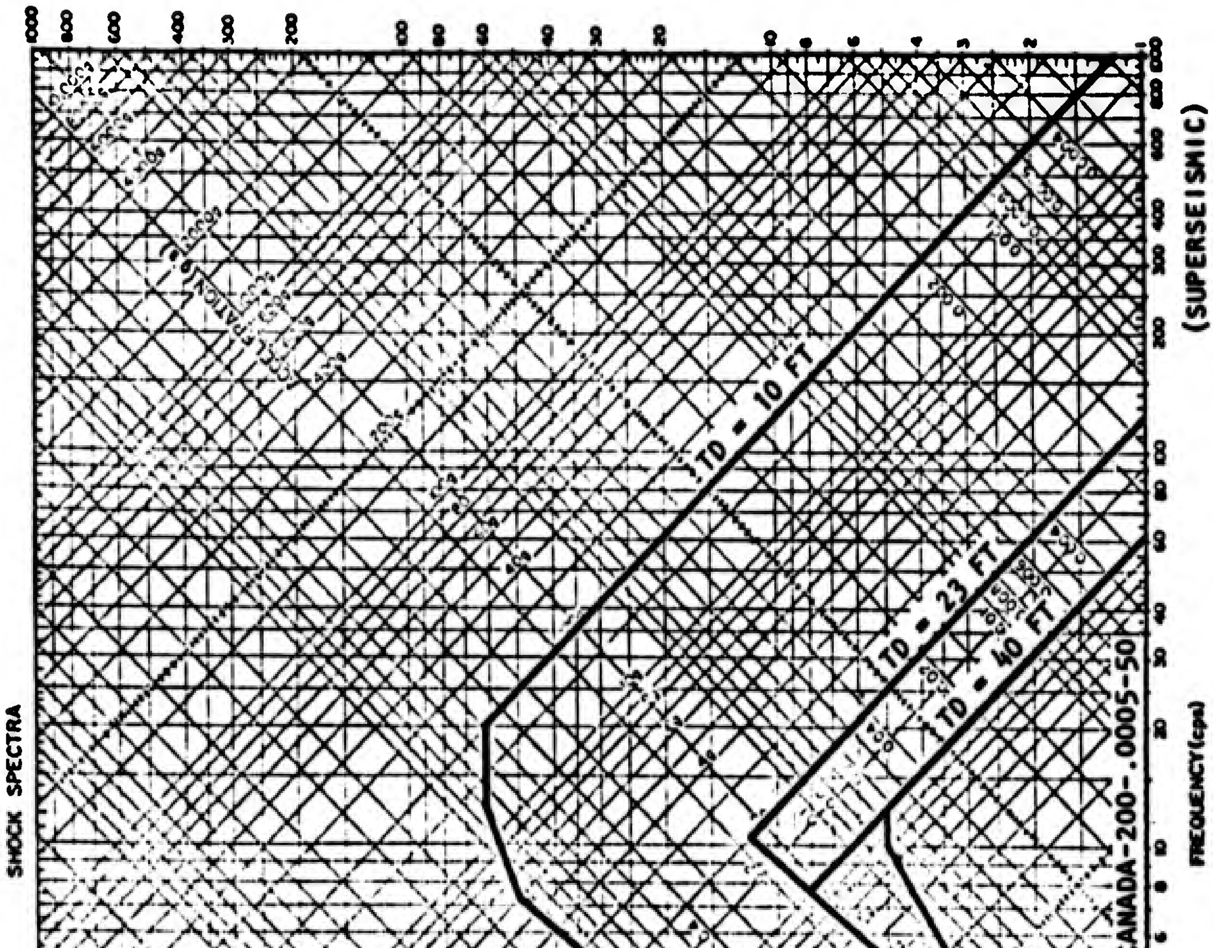

FIGURE C-42 SHOCK SPECTRA FOR VERTICAL MOTION

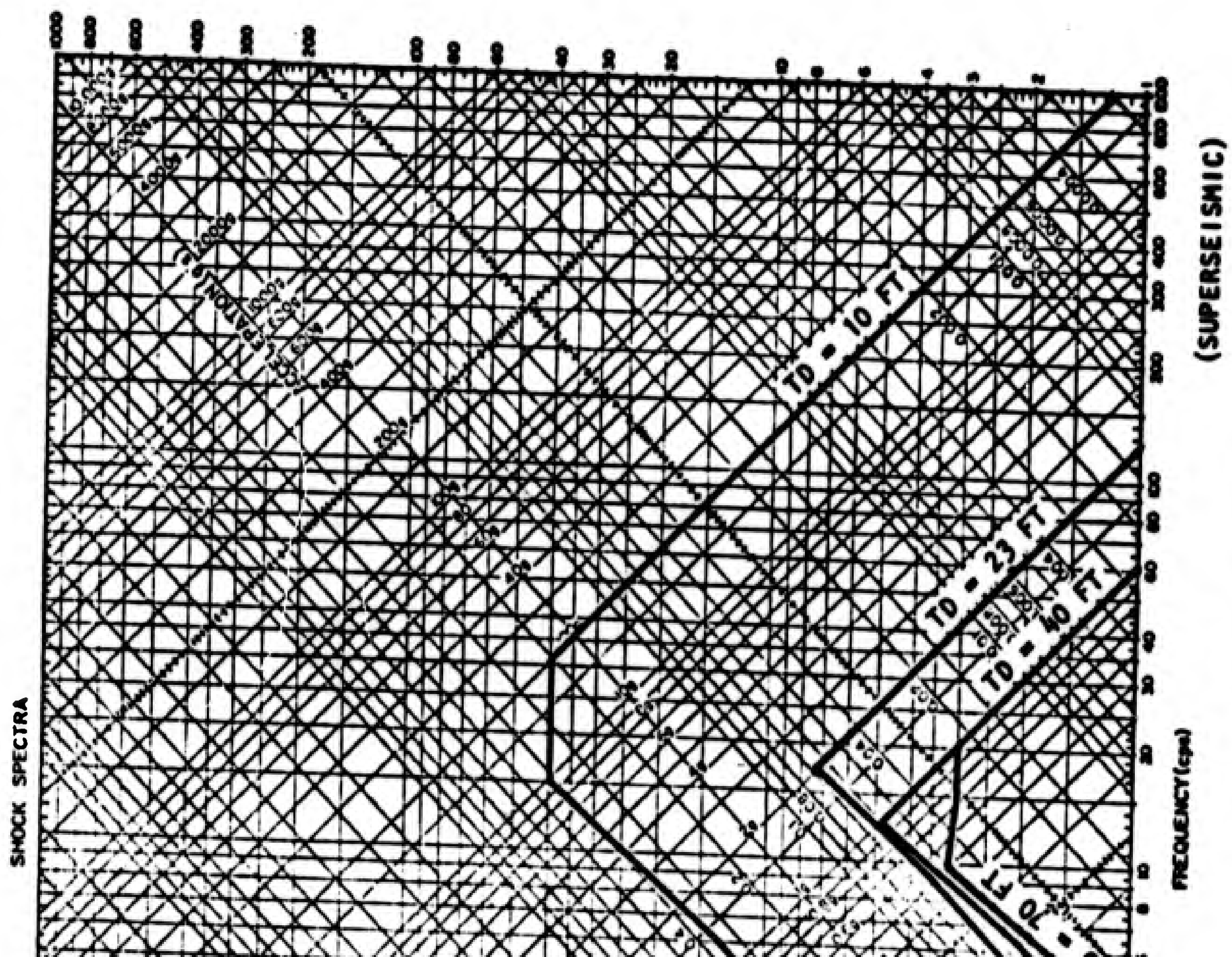

FIGURE C-43 SHOCK SPECTRA FOR HORIZONTAL MOTION

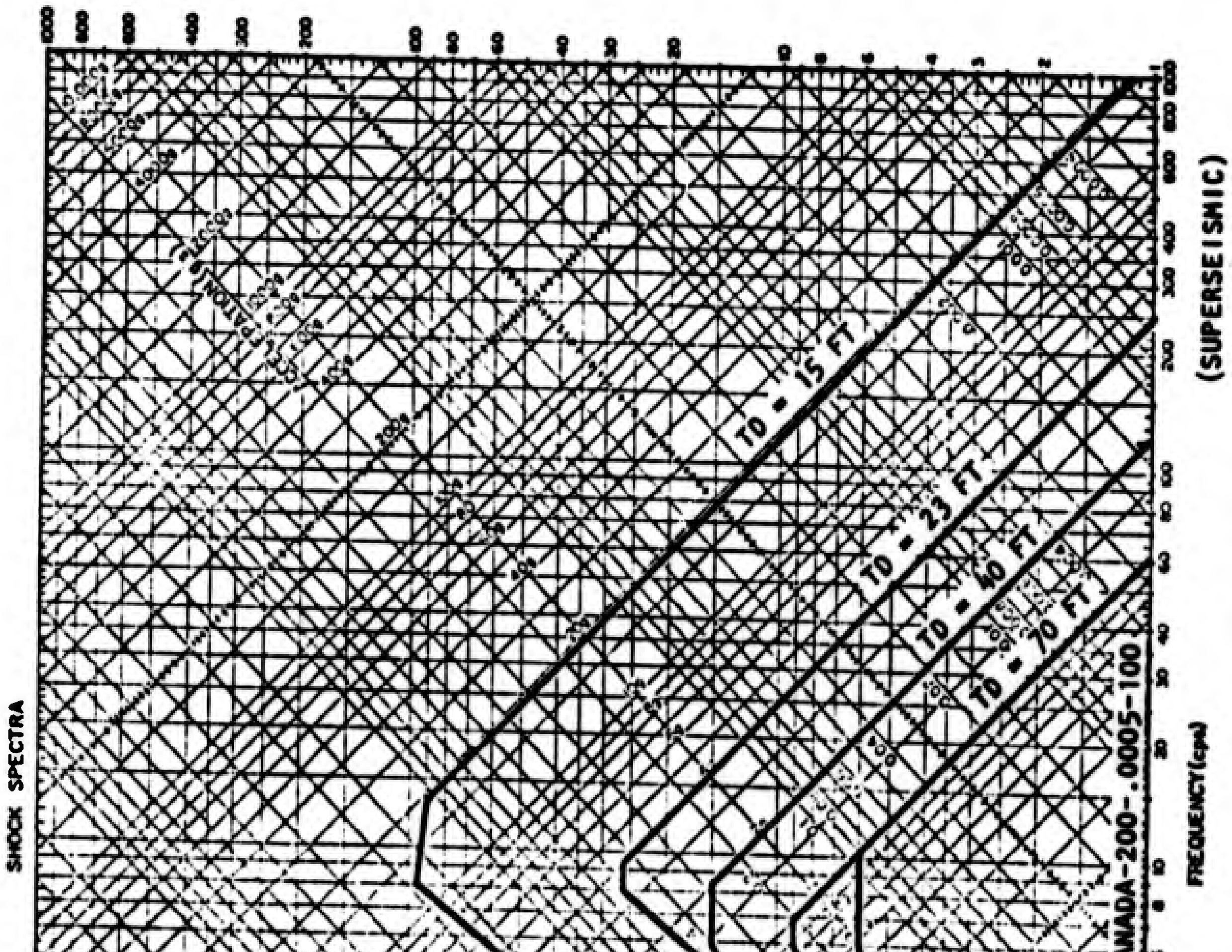

FIGURE C-44 SHOCK SPECTRA FOR VERTICAL MOTION

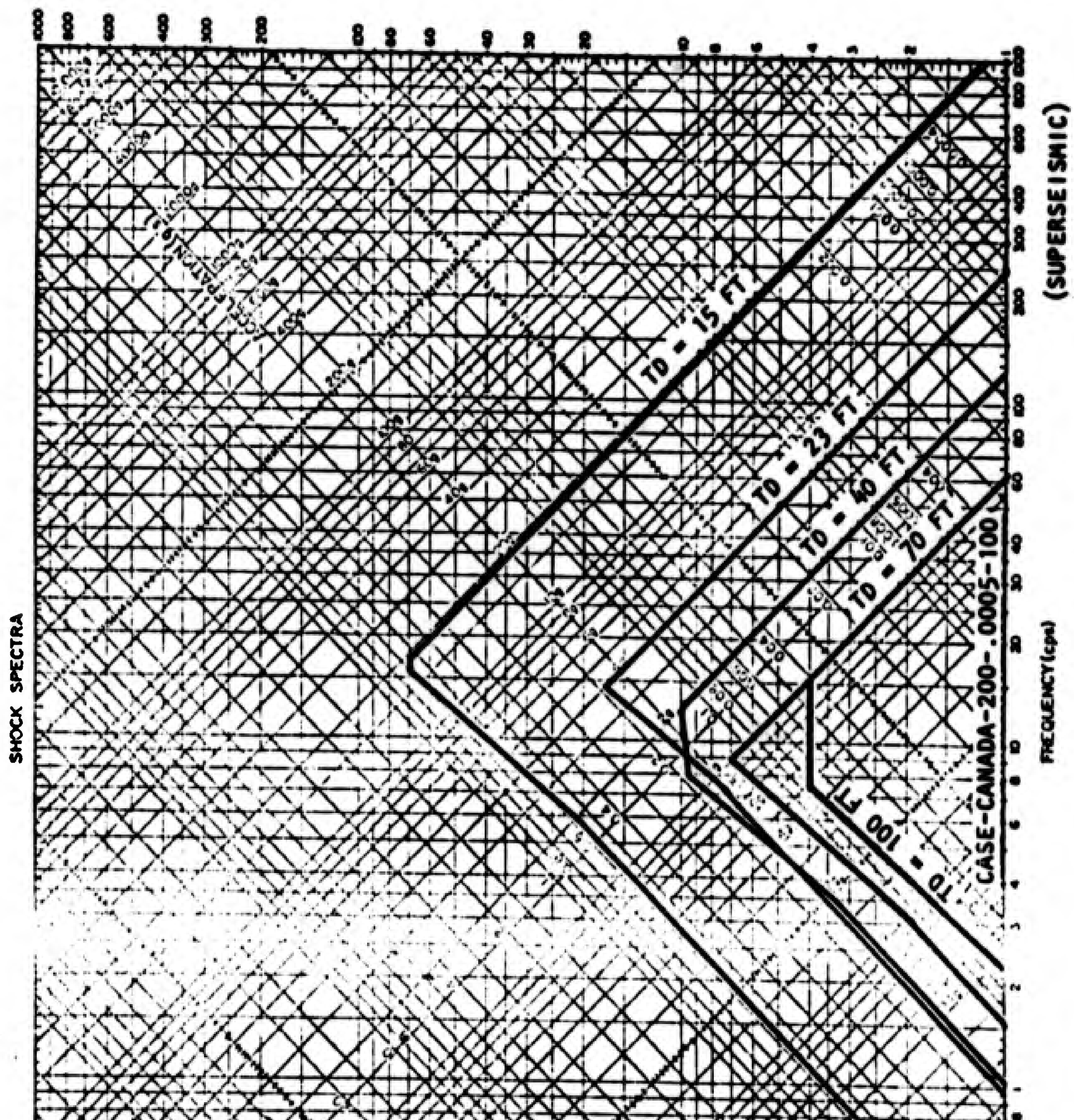

FIGURE C-45 SHOCK SPECTRA FOR HORIZONTAL MOTION

APPENDIX D

CASING RESPONSE ANALYSIS

HORIZONTAL RESPONSE ANALYSIS

The model used in the horizontal response analyses of the casing is a vertical beam fixed at the bottom and hinged at the top as shown in Figure D-1.

Treating the beam as an elastic system with its mass lumped at (ns) discrete stations, its number of degrees of freedom in rotation are nr, and its number of degrees of freedom in side sway are ns. The total degrees of freedom are nr + ns = np. Neglecting the effects of the rotational moments of inertia of the lumped masses the first (ns) natural modes of vibrations can be found.

The stiffness matrix [K] of the system is obtained by the use of transfer matrices,

$$[K] = [A][S][A^T] = [ASA^T]$$

where [A] = the transformation between external and internal forces, $P = AF$

[S] = the member stiffness matrix which expresses all the internal forces in terms of the internal displacements, $F = Se$.

From Figures D-1(b) and D-1(c) the matrices [A] and [S] are developed as shown in Figure D-2 and Figure D-3 respectively.

(For the purpose of illustration only 3 discrete masses are shown)

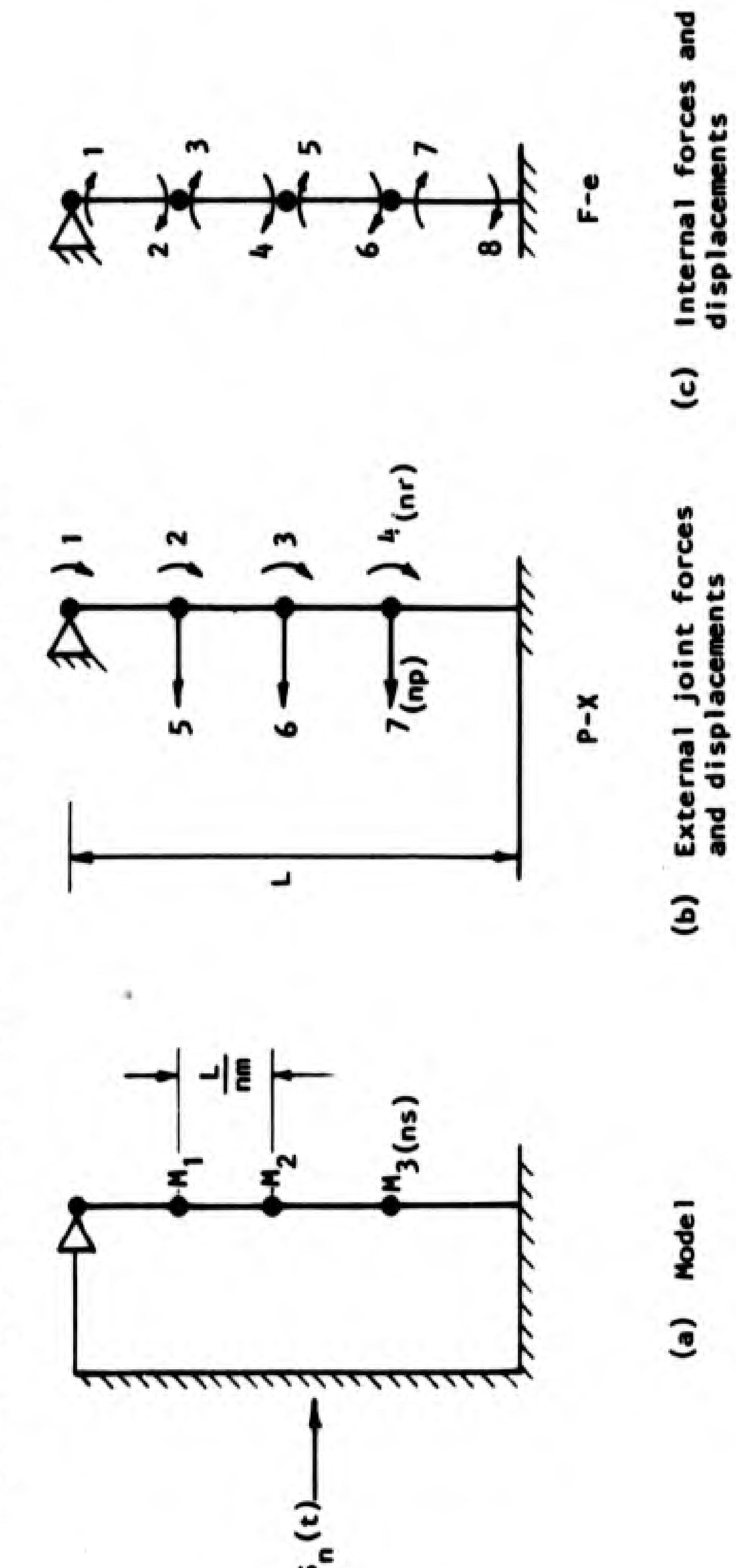

FIGURE D-1 LUMPED BEAM SUBJECTED TO A HORIZONTAL SHOCK DISPLACEMENT

[A] = (np x 2nm)

	P \ F	1	2	3	4	5	6	7	8
nr	1	1							
nr	2		1	1					
nr	3				1	1			
nr	4						1	1	
ns	5	-a	-a	a	a				
ns	6			-a	-a	a	a		
ns	7					-a	-a	a	a

where a = 1/(L/nm)

L = length of beam

nm = number of elements

FIGURE D-2 THE STATICS MATRIX

[S] = (2nm x 2nm)

F \ e	1	2	3	4	5	6	7	8
1	4b	2b						
2	2b	4b						
3			4b	2b				
4			2b	4b				
5					4b	2b		
6					2b	4b		
7							4b	2b
8							2b	4b

where b = EI/(L/nm)

E = modulus of elasticity

I = moment of inertia

FIGURE D-3 THE MEMBER STIFFNESS MATRIX

The flexibility matrix of the system is the inverse of the stiffness matrix.

$$[\delta]_{np \times np} = [K]^{-1}$$

The mass matrix [M] is a diagonal matrix. Neglecting the rotational moments of inertia of the masses it is seen that the matrix:

$$[\delta M]_{ns \times ns} = [\delta] \times [M]$$

will have the dimension (ns x ns). From the matrix [δM] the natural frequencies and the modal matrix [ϕ] are found by matrix interation. The consistant mass matrix method is employed for improved accuracy of the higher modes, (see Reference 20).

In order to evaluate the effects of the higher modes on the displacements and the bending stresses the normal mode method is employed (see Reference 19).

The normal mode method defines the participation factor for mode n as:

$$\gamma_n = \frac{\sum_{i=1}^{ns} m_i \phi_{in}}{\sum_{i=1}^{ns} m_i \phi_{in}^2}$$

where m_i = the i^{th} lumped mass

ϕ_{in} = the i^{th} element of the n^{th} eigenvector

Using the shock spectra the upper bound for the displacement of a point (i) is equal to

$$|u_i|_{max} \leq \sum_{n=1}^{ns} |\phi_{in}\gamma_n D_n|$$

where D_n is the displacement as given by the shock spectra at the frequency of the mode n.

The upper bound of the bending moment at a point (i) is equal to

$$|B_i|_{max} \leq \sum_{n=1}^{ns} |b_{in}\gamma_n A_n| \qquad \left(\frac{\text{moment}}{g}\right)$$

where A_n is the acceleration as given by the shock spectra at the frequency of the mode n. And b_{in} is the element of the i^{th} row and the n^{th} column of a matrix b which is defined as

$$[b] = [FI][M][\phi]$$

where [FI] is the moment influence matrix where an element FI_{ij} is the moment at point (i) due to a unit load at point (j).

The upper bound for the bending stresses at point (i) is thus

$$|\sigma_i|_{max} = \frac{|B_i|_{max}}{S} g$$

where S = section modulus

g = acceleration of gravity

Sometimes the upper bound is defined as the root mean square of the different mode contributions instead of the sum.

The matrix [FI] is found as follows:

a. By equilibrium the relation between the external joint forces P and the internal end moments F is:

$$[P] = [A][F]$$

b. By compatibility the relation between the internal end displacement e and the external joint displacement X is written as:

$$[e] = [A^T][X]$$

c. The relation between the internal end moments F and displacements e is:

$$[F] = [S][e]$$

d. The following relationships are derived from the equations in a, b, and c by matrix operations

$$[F] = [SA^T][X]$$

$$[P] = [ASA^T][X]$$

$$[X] = [ASA^T]^{-1}[P]$$

$$[F] = [SA^T][ASA^T]^{-1}[P]$$

In this case the external force matrix P is a diagonal matrix where the diagonal elements for rotation is equal to zero and the diagonal elements for side sway is equal to one.

$$P = \begin{bmatrix} 0 & & & & & & \\ & 0 & & & 0 & & \\ & & \ddots & & & & \\ & & & 1 & & & \\ & & & & 1 & & \\ & 0 & & & & 1 & \\ & & & & & & 1 \\ & & & & & & & 1 \end{bmatrix}_{np \times np}$$

$$\underbrace{\qquad\qquad\qquad}_{ns}$$

Thus, the matrix [X] is identical to the last ns column of the matrix $[ASA^T]^{-1}$. The [FI] for this problem is found by taking the rows 3, 5, 7 . . . . n of the matrix [F].

A computer program was developed for the computation of the natural frequencies and for the normal mode analysis. The cases analyzed and the resulting upperbound relative horizontal displacements and bending stresses are summarized in Table 7.1.

A sample calculation is shown on the following pages for determining the upperbound bending stresses and horizontal displacements of a 16-foot model using the shock spectra of CASE-E1-200-20-300.

SAMPLE CALCULATION OF PEAK BENDING STRESS AND PEAK
DISPLACEMENT OF GEL-ISOLATED CASING

Case No. E1-200-20-300 (Superseismic Condition) - Water Table at 30 feet

16-Foot Model

The natural frequencies and normal mode contribution factors for determining peak bending stresses and peak displacements are found by a computer solution. The values are given in Tables D-1 and D-2.

Two basis for calculating bending stresses are considered. One is based on the sum of the contributions from each mode. This gives a maximum or upper bound value. The other method uses a root-mean-square (R.M.S.) averaging of the mode contributions

TABLE D-1 FREQUENCY AND NORMAL MODE ANALYSIS

n	f (cps)	$B\gamma$	A	$B\gamma A$ $\left(\frac{lb/ft}{g}\right)$	$(B\gamma A)^2$
1	29.5	16.48	70	1150.0	1,322,000
2	95.7	0.125	110	13.7	187
3	199.0	0.511	110	56.1	3,150
4	340.0	0.073	110	8.0	64
5	518.0	0.077	110	8.4	70
6	727.0	0.039	110	4.3	18
7	960.0	0.141	110	15.0	225
8	1197.0		110		
9	1408.0		110		
10	1555.0	0.0187	110	2.1	
			TOTAL	1257.6	1,325,714

Bending stress σ is found from the following formula

$$\sigma = \frac{\Sigma B\gamma A}{S} g$$

where S = section modulus = 12.1 in^3 for 6-inch Schedule 80 pipe

Method 1 - Sum of Mode Contributions

$$\sigma_{sum} = \frac{(1257.6)(12)(32.2)}{12.1} = 40,200 \text{ psi}$$

Method 2 - R.M.S. of Mode Contributions

$$\sqrt{\Sigma(B\gamma A)^2} = 1,151$$

$$\sigma_{RMS} = \frac{(1,151)(12)(32.2)}{12.1} = 36,800 \text{ psi}$$

Peak displacements are found from Table D-2.

TABLE D-2 PEAK DISPLACEMENT

n	f (cps)	$\phi\gamma$	D (in.)	$\phi\gamma D$ (in.)
1	29.5	1.199	0.90	1.080
2	95.7	0.004	0.10	
3	199.0	0.461	0.023	0.011
4	340.0	0.012	0.008	
5	518.0	0.250	0.003	0.001
6	727.0	0.032	0.001	
			σ_{max} =	1.092 in.

VERTICAL RESPONSE ANALYSIS

The gel-isolated well concept was modeled as a two-degree-of-freedom system and the method of analysis is presented here in detail. The derivation of the response equations and the analysis was taken from Reference 29 and was reproduced in this section for the benefit of the reader.

Derivation of Response Equation for a Two-Degree-of-Freedom System

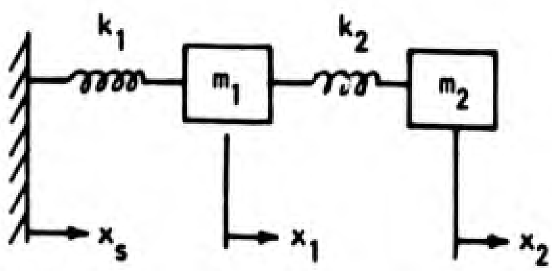

The equations of motion are:

$$m_1\ddot{x}_1 + (k_1 + k_2)x_1 - k_2x_2 = k_1x_s \qquad \text{(D-1)}$$

$$m_2\ddot{x}_2 + k_2x_2 - k_2x_1 = 0 \qquad \text{(D-2)}$$

where $\ddot{x}_1$, x_1, $\ddot{x}_2$, x_2 are the absolute coordinates of the two masses.

Introducing a coordinate transformation,

$$y_1 = x_1 - x_s \qquad \ddot{y}_1 = \ddot{x}_1 - \ddot{x}_s$$

$$y_2 = x_2 - x_s \qquad \ddot{y}_2 = \ddot{x}_2 \quad \ddot{x}_s$$

equations (D-1) and (D-2) can be rewritten in terms of the relative displacements y_1 and y_2, the relative accelerations $\ddot{y}_1$ and $\ddot{y}_2$, and the support acceleration $\ddot{x}_s$.

Accordingly,

$$m_1\ddot{y}_1 + (k_1 + k_2)y_1 - k_2y_2 = -m_1\ddot{x}_s \tag{D-3a}$$

$$m_2\ddot{y}_2 + k_2y_2 - k_2y_1 = -m_2\ddot{x}_s \tag{D-3b}$$

or simply,

$$[m](\ddot{y}) + [k](y) = -[m](\ddot{x}_s) \tag{D-4}$$

in matrix notation.

Normal Mode Vibrations

Free vibrations of the two-mass system are obtained from the homogeneous solution of Equation (D-4) by postulating harmonic response:

$$y_1 = y_{1_{max}} \sin\omega t$$

$$y_2 = y_{2_{max}} \sin\omega t \tag{D-5}$$

and substituting into Equations (D-3a) and (D-3b) we obtain

$$\omega_1^2 m_1 y_1 - (k_1 + k_2)y_1 + k_2y_2 = 0 \tag{D-6}$$

$$\omega_2^2 m_2 y_2 - k_2y_2 + k_2y_1 = 0$$

The natural frequencies (eigenvalues) can be determined by solving the determinant of Equation (D-6).

$$\begin{vmatrix} \omega^2 m_1 - (k_1 + k_2) & k_2 \\ k_2 & (\omega^2 m_2 - k_2) \end{vmatrix} = 0 \tag{D-7}$$

or

$$\omega^4 - \left(\frac{k_1 + k_2}{m_1} + \frac{k_2}{m_2}\right)\omega^2 + \frac{k_1 k_2}{m_1 m_2} = 0$$

Discarding the negative results, we obtain two positive natural frequencies which we denote as ω_1 and ω_2.

The amplitude ratios y_2/y_1 may be found from Equation (D-6) as

$$\frac{y_2}{y_1} = \frac{-k_2}{\omega^2 m_2 - k_2}$$

or

$$\frac{y_2}{y_1} = \frac{k_1 + k_2 - \omega^2 m_1}{k_2} \qquad \text{(D-8)}$$

Substituting the two frequencies ω_1^2 , ω_2^2 into either of Equation (D-8) results in the amplitude ratios in the two modes ω_1 and ω_2.

Thus, normalizing $y_1 = 1$ and at natural frequency ω_1, y_2 is solved from Equation (D-6)

$$y_2 = \frac{-k_2}{\omega_1^2 m_2 - k_2} = \frac{k_1 + k_2 - \omega_1^2 m_1}{k_2} = \beta_{21} \qquad \text{(D-9)}$$

At natural frequency ω_2

$$y_2 = \frac{k_2}{\omega_2^2 m_2 - k_2} = \frac{k_1 + k_2 - \omega_2^2 m_1}{k_2} = \beta_{22} \qquad \text{(D-10)}$$

Either of the two terms defining y_2 in Equations (D-9) and (D-10) may be used to calculate the amplitude ratio, where

β_{21} = amplitude of mass 2 in frequency mode ω_1 if $y_1 = 1$

β_{22} = amplitude of mass 2 in frequency mode ω_2 if $y_1 = 1$

The above amplitude ratios define an orthogonal set of coordinates that is called the modal matrix $[\beta]$

$$[\beta] = \begin{bmatrix} 1 & 1 \\ \beta_{21} & \beta_{22} \end{bmatrix} \tag{D-11}$$

With the use of the modal matrix it is possible to express the equations of motion in a coordinate system that will uncouple the original Equations (D-3 and D-4). Let η be the new coordinate system such that

$$(y) = [\beta](\eta) \text{ and } (\ddot{y}) = [\beta](\ddot{\eta}) \tag{D-12}$$

Substitute into Equation (D-4) and pre-multiply by $[\beta]$

$$[\beta]^T[m][\beta](\ddot{\eta}) + [\beta]^T[k][\beta](\eta) = -[\beta]^T \begin{pmatrix} m_1 \ddot{x}_s \\ m_2 \ddot{x}_s \end{pmatrix} \tag{D-13}$$

where the new set of coordinates (η) are orthogonal and are called the normal mode coördinates.

Let

$$\left.\begin{aligned}
[M] &= [\beta]^T[m][\beta] &&: \text{ Generalized Mass (Diagonal)} \\
[K] &= [\beta]^T[k][\beta] &&: \text{ Generalized Stiffness (Diagonal)} \\
[\beta]^T(m) &= (N) &&: \text{ Generalized Forcing Function} \\
\frac{K_r}{M_r} &= \omega_r^{\,2} &&: \text{ Normal mode frequency} \\
\frac{N_r}{M_r} &= \Gamma_r &&: \text{ Mode participation factor}
\end{aligned}\right\} \tag{D-14}$$

Substitution into Equation (D-13) yields the following

$$\begin{bmatrix} M_1 & 0 \\ 0 & M_2 \end{bmatrix} \begin{pmatrix} \ddot{\eta}_1 \\ \ddot{\eta}_2 \end{pmatrix} + \begin{bmatrix} K_1 & 0 \\ 0 & K_2 \end{bmatrix} \begin{pmatrix} \eta_1 \\ \eta_2 \end{pmatrix} = \begin{pmatrix} N_1 \\ N_2 \end{pmatrix} \ddot{x}_s$$

where

$$M_1 = m_1 + m_2 \beta_{21}^2$$

$$M_2 = m_1 + m_2 \beta_{22}^2$$

$$K_1 = k_1 + k_2 (1 - \beta_{21})^2$$

$$K_2 = k_1 + k_2 (1 - \beta_{22})^2$$

$$N_1 = m_1 + m_2 \beta_{21}$$

$$N_2 = m_1 + m_2 \beta_{22}$$

Equation (D-13) can now be written in the normal mode coordinates system:

$$\ddot{\eta}_1 + \omega_1^2 \eta_1 = -\Gamma_1 \ddot{x}_s$$

$$\ddot{\eta}_2 + \omega_2^2 \eta_2 = -\Gamma_2 \ddot{x}_s$$

or

$$(\ddot{\eta}) + (\omega^2 \eta) = -(\Gamma \ddot{x}_s) \qquad \text{(D-15)}$$

The displacement response in each mode to the generalized forcing function can then be determined from the convolution integral:

$$D_r(t) = -\frac{1}{\omega_r}\int_0^t \ddot{x}_s(\tau)\ \sin\omega_r(t-\tau)d\tau$$

$$D_r(t) = -\int_0^t \dot{x}_s(\tau)\ \cos\omega_r(t-\tau)d\tau \qquad \text{(D-16)}$$

$$D_r(t) = -\frac{d}{dt}\int_0^t x_s(\tau)\ \cos\omega_r(t-\tau)d\tau$$

$$D_r(t) = \text{Dynamic Response Factor}$$

where τ is a dummy variable of integration and the initial conditions are all zero.

The general solution to Equation (D-16) is then the sum of two harmonic motion components (in terms of ω_1 and ω_2) and $D_r(t)$.

Once the normal mode response is known the transformation back to the coupled coordinate system is made through the relationships:

$$(\ddot{y}) = [\beta](\ddot{\eta})$$

$$(\ddot{x}) = (\ddot{y}) + (\ddot{x}_s) \qquad \text{(D-17)}$$

The maximum acceleration of each mass can now be determined in each normal mode:

$$(\ddot{\eta}_1)_{max} = A_1$$

$$(\ddot{\eta}_2)_{max} = A_2$$

and it can be shown (see Equations 23 through 25 page 58 of Reference 19)

$$\ddot{x}_1 = |\beta_{11}\Gamma_1 A_1| + |\beta_{12}\Gamma_2 A_2|$$

$$\ddot{x}_2 = |\beta_{21}\Gamma_1 A_1| + |\beta_{22}\Gamma_2 A_2|$$

where A_1 = shock spectra response at Frequency 1
A_2 = shock spectra response at Frequency 2

and participation factors are:

$$\Gamma_1 = \frac{m_1 + m_2\beta_{21}}{m_1 + m_2\beta_{21}^2}$$

$$\Gamma_2 = \frac{m_1 + m_2\beta_{22}}{m_1 + m_2\beta_{22}^2}$$

$$\omega^2 = \frac{\left(\dfrac{k_1 + k_2}{m_1} + \dfrac{k_2}{m_2}\right) \pm \sqrt{\left(\dfrac{k_1 + k_2}{m_1} + \dfrac{k_2}{m_2}\right)^2 - \dfrac{4k_1k_2}{m_1m_2}}}{2}$$

<u>SAMPLE PROBLEM</u>

As an example problem, take constants for 65 feet well depth (see Calculations, Appendix E, for derivation of constants)

$$m_1 = 1.14 \text{ lb-sec}^2\text{/in.}$$
$$m_2 = 2.02 \text{ lb-sec}^2\text{/in.}$$
$$\left.\begin{array}{l} k_1 = 466 \times 10^3 \text{ lb/in.} \\ k_2 = 220 \times 10^3 \text{ lb/in.} \end{array}\right\} \frac{k_1 + k_2}{m_1} = 600 \times 10^3$$
$$k_2/m_2 = 109 \times 10^3$$
$$4k_1k_2/m_1m_2 = 17.8 \times 10^{10}$$

$$\omega^2 = \frac{709 \times 10^3 \pm \sqrt{50.2 \times 10^{10} - 17.8 \times 10^{10}}}{2}$$

$$\omega^2 = \frac{709 \times 10^3 \pm 568 \times 10^3}{2}$$

$$\omega_1^2 = \frac{141 \times 10^3}{2} = 7.05 \times 10^4 \quad (f_1 = 42 \text{ cps})$$

$$\omega_2^2 = \frac{1277 \times 10^3}{2} = 63.8 \times 10^4 \quad (f_2 = 127 \text{ cps})$$

$$\beta_{21} = \frac{k_1 + k_2 - \omega_1^2 m_1}{k_2} = \frac{686 \times 10^3 - 7.05 \times 10^4 \ (1.14)}{220 \times 10^3} = 2.75$$

$$\beta_{22} = \frac{k_2}{\omega_2^2 m_2 - k_2} = \frac{220 \times 10^3}{63.8 \times 10^4 \ (2.02) - 220 \times 10^3} = 0.206$$

$$\Gamma_1 = \frac{1.14 + 2.02(2.75)}{1.14 + 2.02(2.75)^2} = 0.406$$

$$\Gamma_2 = \frac{1.14 + 2.02(.206)}{1.14 + 2.02(.206)^2} = 1.27$$

$$\ddot{x}_1 = |0.406 \ A_1| + |1.27 \ A_2|$$

$$\ddot{x}_2 = |(2.75)(.406) \ A_1| + |(.206)(1.27) \ A_2|$$

$$\ddot{x}_2 = |1.12 \ A_1| + |0.262 \ A_2|$$

$$\left.\begin{array}{l} \text{at } f_1 = 42 \text{ cps}; A_1 = 34 \text{ g} \\ \text{at } f_2 = 127 \text{ cps}; A_2 = 34 \text{ g} \end{array}\right\} \begin{array}{l} \text{Vertical Shock Spectra for} \\ \text{Case B-50-20-300 (Figure C-20)} \end{array}$$

$$\ddot{x}_1 = 1.68 \ (34) = 57 \text{ g}$$

$$\ddot{x}_2 = 1.38 \ (34) = 47 \text{ g}$$

APPENDIX E

CALCULATIONS

VERTICAL RESPONSE ANALYSIS

Gel-Isolated Well Concept

The gel-isolated well system can be represented by the model shown in Figure E-1.

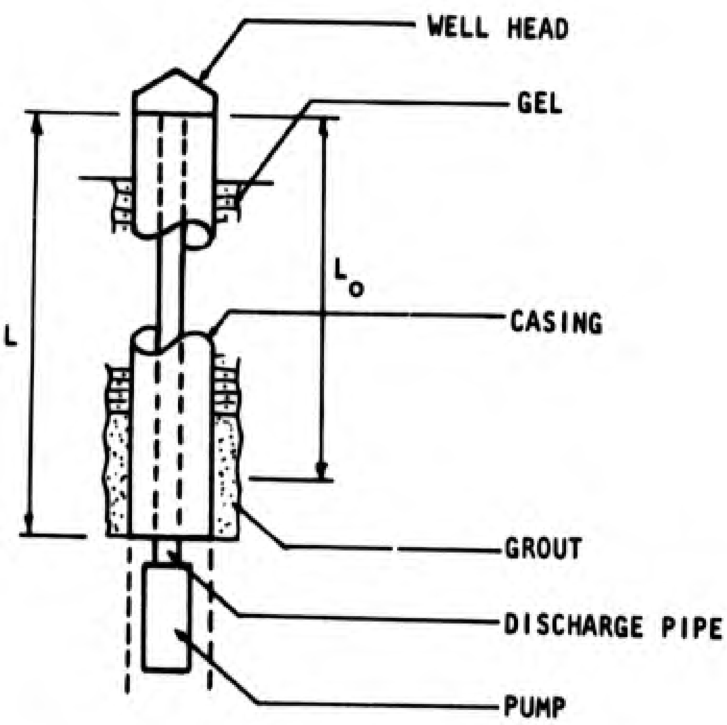

FIGURE E-1 GEL-ISOLATED WELL CONCEPT

The vertical response analysis is discussed in Appendix D. The dynamic response model for the well is shown in Figure E-2 for the condition in which the ground motion is initially downward. Since the casing is grouted at the bottom of the well, the initial ground displacement transmits a downward motion to the well system.

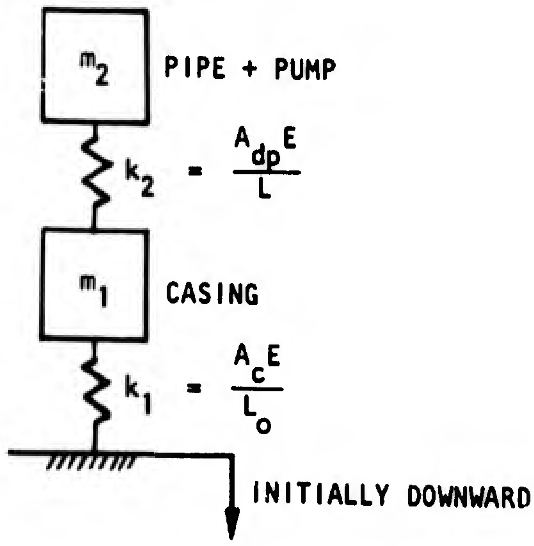

FIGURE E-2 RESPONSE MODEL

In Figure E-2 the symbols are defined as follows

where A_c = Area of casing, in^2

A_{dp} = Area of discharge pipe, in^2

E = Modulus of Elasticity psi

L = Well depth, ft

L_o = Effective casing length, assumed as 0.9L, ft

$m_1 = m_{casing/3}$

$m_2 = m_{pump} + m_{pipe}/3$

$$k_1 = \frac{A_cE}{12L_o} = \frac{8.4 \times 30 \times 10^6}{12 \times 0.9L} = \frac{23.4 \times 10^6}{L} \text{ lb/in.}$$

$$k_2 = \frac{A_{dp}E}{12L} = \frac{A_{dp} \times 30 \times 10^6}{12L} = \frac{2.5 \times 10^6}{L} A_{dp} \text{ lb/in.}$$

Properties for the casing, discharge pipe and pump are given in Tables E-1 and E-2.

TABLE E-1 CASING PROPERTIES

LENGTH L (ft)	SPRING CONSTANT k_1 (lbs/in.)	WEIGHT W (lbs)	TOTAL MASS M_c (lb-sec^2/in.)	EFFECTIVE MASS M_1 (lb-sec^2/in.)
50	466×10^3	1,320	3.42	1.14
100	233×10^3	2,640	6.85	2.28
200	117×10^3	5,270	13.65	4.55
600	38.9×10^3	15,800	41.0	13.7
1,600	14.6×10^3	42,200	109.5	36.5

Sample calculations for the vertical response of a 65 feet well depth are given in Appendix D for Case B-50-20-300. The maximum acceleration experienced by the two masses is:

$$\ddot{x}_1 = 57 \text{ g}$$

$$\ddot{x}_2 = 47$$

The resulting stresses are as follows:

For the Casing: Force $=$ Weight times $(\ddot{x}_1 + 1)$

$$= 1{,}320(57 + 1) = 75{,}500 \text{ lbs}$$

$$\text{Stress} = \frac{75{,}500}{8.4} = 9{,}000 \text{ psi}$$

For the Discharge Pipe: Force $=$ Weight of Pipe plus Pump $(\ddot{x}_2 + 1)$

$$= (750 + 530)(47 + 1) = 60{,}200 \text{ lbs}$$

$$\text{Stress} = \frac{60{,}200}{4.41} = 13{,}650 \text{ psi}$$

Casing and discharge pipe dynamic axial stresses are given in Table E-3 for the cases shown.

TABLE E-2 DISCHARGE PIPE AND PUMP PROPERTIES

LENGTH	DISCHARGE PIPE						PUMP		
	Diameter	Area	Spring Constant	Weight/ Foot	Weight	Mass	Weight	Mass	Effective Mass
L	D	A_{dp}	k_2	w	W_{dp}	m_{dp}	W_p	m_p	m_2
(ft)	(in.)	(in^2)	(lb/in.)	(lb/ft)	(lb)	($lb\text{-}sec^2/in$)	(lb)	($lb\text{-}sec^2/in$)	($lb\text{-}sec^2/in$)
50	4	4.41	220×10^3	15.0	750	1.94	530	1.37	2.02
100	4	4.41	110×10^3	15.0	1,500	3.89	530	1.37	2.66
200	4	4.41	55×10^3	15.0	3,000	7.78	640	1.66	4.26
600	3	3.02	12.6×10^3	10.25	6,150	15.95	1,050	2.72	8.04
1,600	3	3.02	4.71×10^3	10.25	16,400	42.5	980	2.54	16.71

TABLE E-3 AXIAL DYNAMIC STRESSES - GEL-ISOLATED WELL CONCEPT

CASE NO.	CASING			DISCHARGE PIPE		
	$\ddot{x}_1$ (g)	Force (lb)	Stress (psi)	$\ddot{x}_2$ (g)	Force (lb)	Stress (psi)
A-50-20-100	20.3	28,100	3,350	16.5	21,100	4,800
A-50-20-300	50.5	68,000	8,100	41.4	54,300	12,300
B-50-20-300	57.1	75,500	9,000	47.0	60,200	13,650
B-100-20-300	41.5	112,000	13,300	37.0	77,300	17,500
B-200-20-300	6.8	29,000	6,580	7.0	40,900	4,860
E1-50-20-100	13.4	19,000	2,260	11.0	15,400	3,500
E1-50-20-300	20.3	28,000	3,350	16.5	21,100	4,800
E2-50-1-300	13.4	19,000	2,260	11.0	15,400	3,500
DD2-50-20-300	16.8	22,200	2,640	13.8	17,600	4,000

The vertical response of initially upward ground motion is represented by the model shown in Figure E-3. The upward displacement of the ground will transmit a force to the casing through the spring. This spring will equal the relative ground displacement between the top and bottom of the well times the spring stiffness.

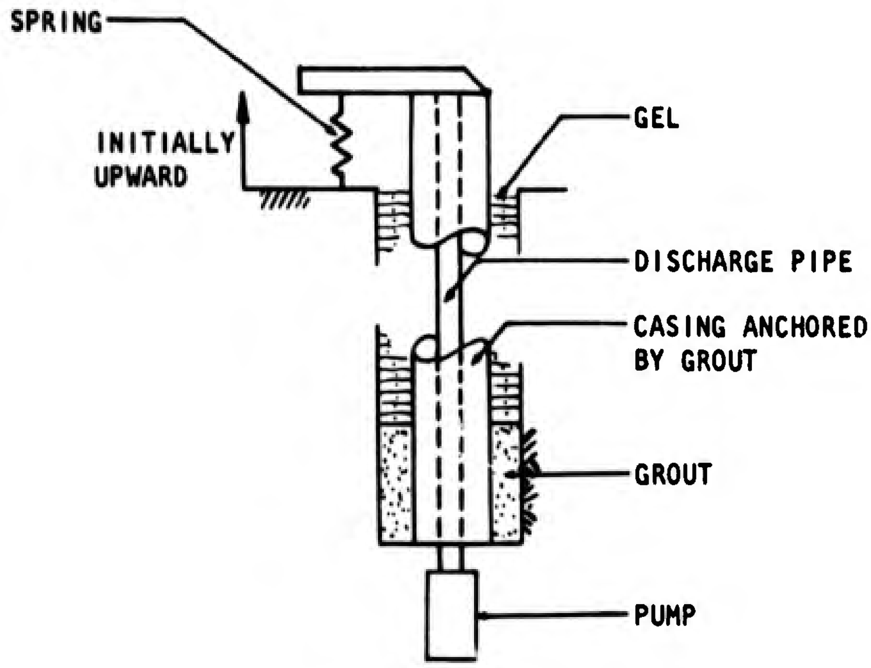

FIGURE E-3 GEL-ISOLATED WELL-INITIALLY UPWARD GROUND MOTION

Spring Characteristics

The spring design is described in Section 7.2.1.3. For maximum well depth, the spring design based on the dead load support load is shown below.

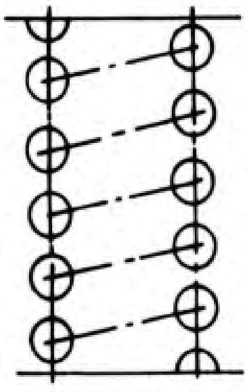

$7\frac{1}{2}$ TURNS
$2\frac{1}{2}$-IN. BAR STOCK DIAMETER
9-IN. COIL DIAMETER

$$\text{Spring Constant} = k = \frac{Gd^4}{8D^3n} \text{ (lb/in)} \quad \text{(Reference 26)}$$

where G = shear modulus = 10.5×10^6 psi

d = bar diameter = 2.5 in.

D = coil diameter = 9 in.

n = number of active coils = $7\frac{1}{2}$

$$k = \frac{10.5 \times 10^6 (2.5)^4}{8(9)^3(7.5)} = 9{,}370 \text{ (lb/in)}$$

Maximum vertical upward displacement at top of well under outrunning conditions is 5.5 inches.

Assuming this represents an upper bound for the maximum relative displacement between the top and bottom of the casing, the force transmitted to the casing can be estimated as:

$$5.5(9{,}370) = 51{,}500 \text{ lb}$$

The stress in the casing will be:

$$\frac{51{,}500}{8.4} = 6{,}130 \text{ psi}$$

Integral Well Concept

In the integral well concept, the well casing is anchored to the medium over its entire length and the shock input to the discharge pipe and pump will be through the casing head. The vertical dynamic response of the discharge pipe and pump can be represented by the model shown in Figure E-4.

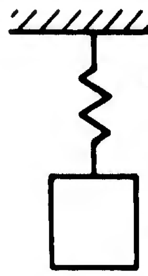

FIGURE E-4 RESPONSE MODEL

$$p \approx \left(\frac{k}{m + m_o/3}\right)^{1/2}$$ (Reference 38, page 70)

where p = circular frequency
k = spring constant
m = pump mass
m_o = discharge pipe mass

The frequency of the discharge pipe and pump subsystem for various well depths are given in Table E-4.

TABLE E-4 FREQUENCIES OF DISCHARGE PIPE AND PUMP ELEMENT

WELL DEPTH (ft)	DISCHARGE PIPE MASS m_o (lb-sec^2/in)	PUMP MASS m (lb-sec^2/in)	EFFECTIVE MASS $m + m_o/3$ (lb-sec^2/in)	SPRING CONST. k (lb/in)	CIRC. FREQ. p (cps)	FREQ. f (cps)
50	1.94	1.37	2.02	220×10^3	330	53
100	3.89	1.37	2.66	110×10^3	203	32
200	7.78	1.66	4.25	55×10^3	114	18
600	15.95	2.72	8.04	12.6×10^3	39.4	6
1,600	42.5	2.54	16.71	4.71×10^3	17	3

The dynamic axial stresses in the discharge pipe due to vertical ground shock effects are summarized in Table E-5 for various cases.

TABLE E-5 AXIAL STRESSES IN FOUR-INCH DIAMETER SCHEDULE 80 DISCHARGE PIPE

DEPTH (ft)	CASE NO.	ACCELERATION (g)	WEIGHT (lb)	FORCE (lb)	STRESS (psi)
50	A50-20-300	150	1,280	192,000	43,500
200	B200-20-300	80	3,640	291,000	66,000
1,600	B1600-20-300	12	17,380	209,000	69,000
50	B50-20-100	45	1,280	57,500	13,000
200	B200-20-100	20	3,640	72,800	16,500
1,600	B1600-20-100	3	17,380	52,000	17,200

WELL CASING BUCKLING STABILITY

Column (Euler) Buckling

The criterion for the buckling stability of the well casing when loaded by vertical drag forces can be related to the expressions for the critical buckling load of axially load piles as shown below (see Reference 6 Article 129).

$$m^2(m + 1)^2 = \frac{dk_h D^4}{\pi^4 EI}$$

and

$$Q_b = \frac{\pi^2 EI}{D^2}(2m^2 + 2m + 1)$$

where Q_b = buckling load, lb

m = number of half waves of the sinusoidal curve into which the pile tends to buckle

D = depth of casing over which buckling can occur

d = diameter of casing = 8 inches

E = casing modulus of elasticity = 3×10^7 psi

I = casing moment of inertia

k_h = coefficient of horizontal soil reaction = 2,000 psi

For casing with ¼-inch wall thickness:

$$I = 0.0491(8^4 - \overline{7.5}^4) = 46 \text{ in}^4$$

For depth D equal to 200 feet or 2,400 inches:

$$m^2(m+1)^2 = \frac{8(2{,}000)(2.4 \times 10^3)^4}{\pi^4(3 \times 10^7)(46)} = 39.7 \times 10^5$$

If it is assumed that $(m + 1) = m$, since m is a large number, then:

$$m^2(m+1)^2 = m^4 = 397 \times 10^4$$

and m = 45 half waves. Then

$$2m^2 + 2m + 1 = 2(45)^2 + 2(45) + 1 = 4{,}141$$

and

$$Q_b = \frac{\pi^2(3 \times 10^7)(46)}{(2{,}400)^2}(4{,}141)$$

$$Q_b = 9.78 \times 10^6 \text{ lb}$$

and

$$\sigma_a = \frac{Q_b}{A} = \frac{9.78 \times 10^6}{8.40} = 1.16 \times 10^6 \text{ psi} > 100{,}000 \text{ psi}$$

Therefore, column buckling can be neglected for well casing where depth is greater than 200 feet.

Buckling (Local) Due to Axial Compression

Check minimum axial stress in casing neglecting soil restraint (see Reference 39, Article 81).

$$\sigma_{cr} = \frac{Eh}{a\sqrt{3(1 - \nu^2)}}$$

where E = casing modulus of elasticity = 3×10^7 psi

h = casing wall thickness = 0.25 in.

a = casing radius = 4 in.

ν = Poisson's ratio = 0.3

$$\sigma_{cr} = \frac{3 \times 10^7(0.25)}{4\sqrt{3(1 - .09)}} = 1.2 \times 10^6 \text{ psi} << 100{,}000 \text{ psi}$$

Therefore, local buckling under axial compression can be neglected.

Hoop Buckling (Circumferential)

Check minimum uniform external lateral pressure (see Reference 39, Article 83).

$$q_{cr} = \frac{Eh^3(n^2 - 1)}{12a^3(1 - \nu^2}$$

where E = casing modulus of elasticity = 3×10^7

h = casing wall thickness = 0.25

n = number of waves into which ring buckles = 2(for flattening)

a = casing radius = 4 inches

ν = Poisson's ratio = 0.3

$$q_{cr} = \frac{3 \times 10^7 (0.25)^3 (4 - 1)}{12(4)^3 (1 - 0.09)}$$

$$q_{cr} = 2,000 \text{ psi}$$

Hoop buckling stability can be neglected since lateral pressures will be well below the critical pressure.

Maximum Lateral Soil Pressure

The maximum lateral static soil pressure acting on the casing as a radial load can be determined from the following equations (see Reference 6, Article 74).

$$\sigma_{ro} = \gamma r_o m_\sigma$$

$$m_\sigma = \frac{z}{r_o}\left(\frac{a + 1}{2a}\right)\left(\frac{a - (a - 2)n_1^2}{a}\right)$$

where
- γ = soil density = 100 lb per ft^3
- r_o = casing radius = 4 inches
- z = depth
- a = $\tan^2(45 + \phi/2)$ = σ_θ/σ_r
- n_1 = r/r_o
- r = soil diameter of peak stress

For a granular material, $\phi = 30^\circ$ and cohesion = 0.

From plots on page 212 of Reference 6, (for $\phi = 30^\circ$, $\phi - \phi = 5^\circ$, and $z = \infty$).

$$\sigma_{ro} = \frac{100(4)(1.2)}{1728} = 0.3 \text{ psi}$$

Static soil pressures can be neglected in the well analyses.

APPENDIX F

SHOCK TEST SPECIFICATION FOR SUBMERSIBLE PUMP

SCOPE

This section defines the shock environments to which the submersible pumps will be subjected to in their final installation, and specifics the procedure for certifying that they can withstand this environment. Shock or vibration associated with transportation or installation, or caused by operation of the equipment is not covered in this specification.

APPLICABLE PUBLICATION

The following Military Specifications, referred to hereafter by basic designation only, form a part of this specification to the extent indicated by the reference thereto:

MIL-S-4456 (USAF)	Shock, Variable Designation, Method and Apparatus for
MIL-S-901B (NAVY)	Military Specification for Shock Proof Equipment

SHOCK ENVIRONMENT

The shock environment that the pumps will experience are equivalent to the shock motions described in Table F-1. The wave type to be simulated is a half-sinusoidal acceleration pulse with the durations indicated. The shock shall be assumed to occur three times. In the case of the gel-isolated well concept, shock testing of pumps located below a depth of 300 feet is not required.

TABLE F-1 SHOCK ENVIRONMENT

WELL CONCEPT	OVERPRESSURE (psi)	DEPTH OF PUMP (ft)	MAXIMUM VERTICAL MOTION		MAXIMUM HORIZONTAL MOTION	
			ACCELERATION (g's)	DURATION (ms)	ACCELERATION (g's)	DURATION (ms)
Integral	100	50	45	20	15	1.5
		200	20	50	12	
		1600	4	300	3	
	300	50	150	20	35	1.5
		200	80	50	5	
		1600	12	300	3	
Gel-Isolated	100	50	20	8	15	1.5
		200	4	30	12	
	300	50	45	8	35	1.5
		200	7	30	5	

CERTIFICATION REQUIRED

The submersible pumps shall be certified for the shock environment in which they will be installed as indicated in the specifications. The contractor shall certify the pumps by one of the following procedures:

a. Certification by Previous Acceptance

Equipment qualified by a Government agency as meeting a shock environment equal to or more severe than that specified herein may be certified under this specification. The contractor shall submit for approval complete documentation of the previous qualification; if the qualification was based on tests, certificates of such tests shall be submitted. Approval of this certification shall be granted only if the documentation of the previous qualification establishes that all of the requirements for this previous qualification were equal to or more severe than the requirements of this specification.

b. Certification by Test

Equipment may be certified after having successfully passed a shock test environment as specified in Table F-1.

TEST REQUIREMENTS

All tests shall be performed in accordance with MIL-S-4456 or MIL-S-901B and subject to the conditions outlined below.

a. Testing Agency

All tests shall be performed by a qualified testing laboratory approved by the Contracting Officer.

b. Witnessing of Tests

Tests shall be scheduled so as to enable Government inspectors to witness any or all phases. Ten days advance notice and 24 hours advance confirmation shall be given to the contracting officer of all test operations.

c. Test Conditions

The pumps shall be tested as a complete unit, i.e., pump and motor combined in a single unit. They shall be mounted to the platform of the test machine.

d. Post-Shock Examination

After completion of the shock test, it shall first be determined if the motor and pump are still operative, then the specimens shall be dismantled and examined for damage.

e. Requirements for Certification

The pump may be certified as having passed the test if its capability of performing its design function has not been impaired by the tests.

f. Use of Test Specimens

Test specimens may be supplied in partial fulfillment of this contract only if they have suffered no damage or if any damaged parts have been restored to their original condition. Test specimens which have failed the test may not be used in partial fulfillment of this contract or used for further test purposes unless such use is authorized by the Contracting Officer.

g. Certification of Tests

The testing agency shall fully document the test, and shall certify that it has been performed in accordance with this specification and has produced the desired results.

h. Certification of Post-Shock Examination

The testing agency shall fully document the post-shock examination, and shall certify that the equipment is acceptable in accordance with this specification.

UNCLASSIFIED
Security Classification

DOCUMENT CONTROL DATA - R&D

(Security classification of title, body of abstract and indexing annotation must be entered when the overall report is classified)

1. ORIGINATING ACTIVITY (Corporate author)
Agbabian-Jacobsen Associates
Engineering Consultants
Los Angeles, California 90045

2a. REPORT SECURITY CLASSIFICATION
Unclassified

2b. GROUP

3. REPORT TITLE
SHOCK-RESISTANT WELLS

4. DESCRIPTIVE NOTES (Type of report and inclusive dates)
Final Report - 16 June 1966 - 14 August 1967

5. AUTHOR(S) (Last name, first name, initial)
Anderson, R. W.
Hove, K.

6. REPORT DATE	7a. TOTAL NO. OF PAGES	7b. NO. OF REFS
14 August 1967	246	39

8a. CONTRACT OR GRANT NO.
NBy-62212 and N62399-67-C-0017

b. PROJECT NO.
Y-F011-05-02-353

c.

d.

9a. ORIGINATOR'S REPORT NUMBER(S)
AJA 6712-2

9b. OTHER REPORT NO(S) (Any other numbers that may be assigned this report)
CR 68.007

10. AVAILABILITY/LIMITATION NOTICES
Distribution of this Document is Unlimited

11. SUPPLEMENTARY NOTES

12. SPONSORING MILITARY ACTIVITY
Naval Civil Engineering Laboratory
Port Hueneme, California 93041

13. ABSTRACT

A study is presented of water wells for shelter facilities, which will functionally survive the critical effects associated with the detonation of nuclear weapons. Overpressure, weapon yield, well depth, and soil properties are varied in order to determine siting and hardness limitations of the well concepts studied.

Two basic well casing environments are investigated: (1) direct encasement in soil (integral concept), and (2) encasement in a gel medium for shock isolation (gel-isolated concept). Well depths of 50 to 1,600 ft, overpressures up to 300 psi, and weapon yields up to 20 megatons are used in the study. The dynamic behavior of the well casing, the discharge pipe, and the pump unit is investigated for the different well concepts and weapon effects.

The integral well concept is analyzed as an equivalent static problem by using propagating wave fronts. Shock spectra analysis and the normal mode method are used to analyze the gel-isolated concepts.

DD FORM 1 JAN 64 1473 0101-807-6800

UNCLASSIFIED
Security Classification

UNCLASSIFIED
Security Classification

14. KEY WORDS	LINK A		LINK B		LINK C	
	ROLE	WT	ROLE	WT	ROLE	WT
wells weapon effects ground shock shock isolation gels						

INSTRUCTIONS

1. ORIGINATING ACTIVITY: Enter the name and address of the contractor, subcontractor, grantee, Department of Defense activity or other organization *(corporate author)* issuing the report.

2*a*. REPORT SECURITY CLASSIFICATION: Enter the overall security classification of the report. Indicate whether "Restricted Data" is included. Marking is to be in accordance with appropriate security regulations.

2*b*. GROUP: Automatic downgrading is specified in DoD Directive 5200.10 and Armed Forces Industrial Manual. Enter the group number. Also, when applicable, show that optional markings have been used for Group 3 and Group 4 as authorized.

3. REPORT TITLE: Enter the complete report title in all capital letters. Titles in all cases should be unclassified. If a meaningful title cannot be selected without classification, show title classification in all capitals in parenthesis immediately following the title.

4. DESCRIPTIVE NOTES: If appropriate, enter the type of report, e.g., interim, progress, summary, annual, or final. Give the inclusive dates when a specific reporting period is covered.

5. AUTHOR(S): Enter the name(s) of author(s) as shown on or in the report. Enter last name, first name, middle initial. If military, show rank and branch of service. The name of the principal author is an absolute minimum requirement.

6. REPORT DATE: Enter the date of the report as day, month, year; or month, year. If more than one date appears on the report, use date of publication.

7*a*. TOTAL NUMBER OF PAGES: The total page count should follow normal pagination procedures, i.e., enter the number of pages containing information.

7*b*. NUMBER OF REFERENCES: Enter the total number of references cited in the report.

8*a*. CONTRACT OR GRANT NUMBER: If appropriate, enter the applicable number of the contract or grant under which the report was written.

8*b*, 8*c*, & 8*d*. PROJECT NUMBER: Enter the appropriate military department identification, such as project number, subproject number, system numbers, task number, etc.

9*a*. ORIGINATOR'S REPORT NUMBER(S): Enter the official report number by which the document will be identified and controlled by the originating activity. This number must be unique to this report.

9*b*. OTHER REPORT NUMBER(S): If the report has been assigned any other report numbers *(either by the originator or by the sponsor)*, also enter this number(s).

10. AVAILABILITY/LIMITATION NOTICES: Enter any limitations on further dissemination of the report, other than those imposed by security classification, using standard statements such as:

(1) "Qualified requesters may obtain copies of this report from DDC."

(2) "Foreign announcement and dissemination of this report by DDC is not authorized."

(3) "U. S. Government agencies may obtain copies of this report directly from DDC. Other qualified DDC users shall request through ________________."

(4) "U. S. military agencies may obtain copies of this report directly from DDC. Other qualified users shall request through ________________."

(5) "All distribution of this report is controlled. Qualified DDC users shall request through ________________."

If the report has been furnished to the Office of Technical Services, Department of Commerce, for sale to the public, indicate this fact and enter the price, if known.

11. SUPPLEMENTARY NOTES: Use for additional explanatory notes.

12. SPONSORING MILITARY ACTIVITY: Enter the name of the departmental project office or laboratory sponsoring *(paying for)* the research and development. Include address.

13. ABSTRACT: Enter an abstract giving a brief and factual summary of the document indicative of the report, even though it may also appear elsewhere in the body of the technical report. If additional space is required, a continuation sheet shall be attached.

It is highly desirable that the abstract of classified reports be unclassified. Each paragraph of the abstract shall end with an indication of the military security classification of the information in the paragraph, represented as *(TS)*, *(S)*, *(C)*, or *(U)*.

There is no limitation on the length of the abstract. However, the suggested length is from 150 to 225 words.

14. KEY WORDS: Key words are technically meaningful terms or short phrases that characterize a report and may be used as index entries for cataloging the report. Key words must be selected so that no security classification is required. Identifiers, such as equipment model designation, trade name, military project code name, geographic location, may be used as key words but will be followed by an indication of technical context. The assignment of links, roles, and weights is optional.

UNCLASSIFIED
Security Classification